Exploitation of Biomaterials in Construction: Keratin Feather Fibres in Cement-Based Materials

Elizabeth-Rose Grima Delia Spiteri Cornish

Dissertation submitted to the Faculty for the Built Environment, University of Malta, in part fulfilment of the requirements for the attainment of the degree of Master of Science

August 2024

I dedicate this dissertation to my Mum, James,

and Casper, for always supporting me.

L-Università ta' Malta

FACULTY/~~INSTITUTE/CENTRE/SCHOOL~~ for the Built Environment

DECLARATIONS BY POSTGRADUATE STUDENTS

(a) Authenticity of Dissertation

I hereby declare that I am the legitimate author of this Dissertation and that it is my original work.

No portion of this work has been submitted in support of an application for another degree or qualification of this or any other university or institution of higher education.

I hold the University of Malta harmless against any third party claims with regard to copyright violation, breach of confidentiality, defamation and any other third party right infringement.

(b) Research Code of Practice and Ethics Review Procedures

I declare that I have abided by the University's Research Ethics Review Procedures. Research Ethics & Data Protection form code BEN-2024-00094.

As a Master's student, as per Regulation 77 of the General Regulations for University Postgraduate Awards 2021, I accept that should my dissertation be awarded a Grade A, it will be made publicly available on the University of Malta Institutional Repository.

Acknowledgements

I would like to extend my gratitude to the following people, without whom this research and dissertation would not have been possible.

Firstly, I would like to thank Professor Ruben Paul Borg B.E.&A. (Hons)(Melit.), Spec.Struct.Eng. (Milan), Ph.D. (Sheff.) for his role as a supervisor, for conceiving the project, and securing the funding. I also appreciate the acquisition of equipment over the years, establishing protocols used by previous students and myself, and the support with reviewing my dissertation while giving me the freedom to work on this project independently. I would also like to thank Professor Reuben Grima B.A. (Melit.), M.A. (R'dg), Ph.D. (Lond.), F.S.A., for his support and understanding in my writing.

Moreover, I would like to thank the management and teaching staff at De La Salle College, Birgu, for their patience, support, and understanding during this time.

I would like to extend my gratitude to *Xjenza* Malta, Mr J. Sammut and the staff at Central Cement Ltd., Philip A. Tabone Ltd., and SMINA Poultry Products Ltd.; for their generous funding, support and provision of all the cement, dolomite aggregate, superplasticiser and fibres needed for the SCC and SCM.

I would also like to thank the Built Environment Assistant Laboratory Manager Mr Nicholas Azzopardi M.Sc. (Q.U.B.), M.I.C.T. (UK), A.I.A.T. for his guidance in the laboratory, and to Mr Quentin Chevalier for being there to assist me in the laboratory, it would not have been possible to complete the experimental program without them.

Last, but certainly not least, I extend my sincere gratitude to my closest family and friends. To my parents, for supporting me throughout this entire endeavour; to my brother, James, for endlessly believing in me; to my boyfriend, Shaun, for always motivating me; and to my beloved cat, Casper, for never leaving my side, not just in my writing. Without all their constant support and encouragement, I would never have been able to see this dissertation to completion.

Project Funding

This research was conducted within the frame of the RECP Research Project: "Circular Economy through Recycling Poultry Waste for value-added products in Construction & Agriculture" REP-2022-020 (RECP) at the Faculty for the Built Environment, University of Malta, funded through the *Xjenza* Malta (Malta Council for Science & Technology) Research Excellence Programme (Project Principal Investigator: Prof. Ruben Paul Borg, Faculty for the Built Environment, with the collaboration of Prof. Everaldo Attard, Institute for Earth Systems). The funding received is gratefully acknowledged.

Abstract

Utilising chicken feathers in concrete materials has been attracting the attention of researchers due to the environmental benefits of reducing waste from the poultry industry, where large volumes of waste are generated with every slaughter. Local poultry processors produce over 7×10^4 metric tonnes of waste each month, and the keratin rich feather fibres, together with other waste, are incinerated at a waste processing plant. The process of extracting fibres was studied from start to finish, where the fibre would have been disposed of as a by-product of poultry for food consumption. The inclusion of feathers as fibre reinforcement in concrete was found to have different effects on the fresh, early-stage, and hardened properties of concrete, depending on fibre length and percentage volume fraction.

An experimental investigation assessed the fresh properties of concrete with added fibres, focusing on workability, self-compacting characteristics, and rheology, with note that fibre incorporation reduced workability and self-compacting properties. Early-stage characteristics were examined in a controlled environment, revealing that fibres delayed and narrowed plastic shrinkage cracks. Restraining concrete ring tests and Kraai mortar test panels showed that fibre-reinforced specimens did not crack during the test. Fibres also affected the concrete's density and ultrasonic pulse velocity, and improved the compressive strength, ductility, and tensile splitting strength. However, the inclusion of fibres negatively affected the overall flexural strength and toughness. Improvements in durability were evaluated through vacuum saturation porosity and chloride ion penetration testing.

Therefore, this research confirmed the potential for the exploitation of waste feather fibres as reinforcement in concrete, supporting circularity in the agricultural and construction sectors.

Keywords: fibre-reinforced concrete, feather fibres, self-compacting concrete, early-stage cracking, and concrete shrinkage

Table of Contents

List of Figures

List of Tables

List of Abbreviations

CMOD	Crack Mouth Opening Displacement
FTIR	Fourier-Transform Infrared Spectroscopy
LCA	Life Cycle Analysis
RCPT	Rapid Chloride Penetration Test
SCC	Self-Compacting Concrete
SCM	Self-Compacting Mortar
SDG	Sustainable Development Goal
SEM	Scanning Electron Microscope
TGA	Thermogravimetric Analysis
UPV	Ultrasonic Pulse Velocity
XRD	X-Ray Diffraction

Chapter 1

Introduction

1 Introduction

This research addresses circularity in the construction industry and in the agriculture sector, with a focus on the exploitation of waste generated as a resource, thereby reducing both waste disposal and also the use of natural resources as opposed to synthetic materials. This chapter provides an introduction to the construction and poultry industries; two essential, yet highly wasteful, industries on a global scale, and provides an overview of the research and development of this dissertation.

The introductory chapter is intended to set the scene for the research work, based on a by-product from the poultry industry, keratin-rich chicken feathers, which are applied as a key component in fibre-reinforced self-compacting mortar and concrete as new construction materials.

The innovation of the work lies in the careful understanding of the poultry industry process and exploiting a by-product in order to improve key performance characteristics of concrete. Whilst the research addresses fresh properties and rheology, mechanical properties, and durability properties, it also explores the early-stage cracking behaviour of the material.

1.1 Topic Overview

1.1.1 The Construction Industry

It is well known that the construction industry is one of the most wasteful industries on a global scale (Ajayi et al., 2016), accounting for 35% of the waste generation, and for about 50% of all extracted material in the European Union (European Commission, 2020). Concrete is one of the most widely used building materials in the construction industry, known for its versatility, durability, and strength. It is a composite material composed of fine and coarse aggregate with cement used as a binder. The widespread use of concrete dates back to ancient times, with notable structures such as the Roman Pantheon and Roman aqueducts exemplifying its historical significance. In the modern era, concrete remains fundamental to infrastructure development, including roads,

bridges, buildings, and dams. Its application spans residential, commercial, and industrial construction, making it indispensable to urbanisation and development. Innovations in materials engineering, such as the development of self-compacting concrete (SCC), which will be discussed in the following chapters, have enabled the use of concrete in specialist applications with requirements for high performance, allowing for the wider use of such materials.

However, the extensive use of concrete is accompanied by significant environmental concerns, particularly regarding its production and disposal. The manufacturing of cement, a primary ingredient in concrete, is highly energy-intensive and contributes substantially to global carbon dioxide (CO_2) emissions. The cement industry alone is responsible for approximately 8% of global CO_2 emissions (European Commission, 2019), highlighting the need for more sustainable practices within the sector.

The production and use of concrete generate substantial waste, primarily during the manufacturing process, construction activities, and demolition of structures at their end of life.

One particular type of concrete, known as fibre-reinforced concrete, is a composite material that utilises short, discrete fibres in the matrix which serve as a bridge during the formation of cracks, thereby enhancing the tensile properties of concrete and its toughness. Typical fibre reinforcing materials used in concrete production include glass fibres, polypropylene fibres, and steel fibres, among others. The use of such synthetic fibres is problematic as they are generally not biodegradable and often are costly to procure. These fibres are not sustainable and often not widely accessible to underdeveloped countries, making their implementation challenging for those who have limited resources.

The incorporation of natural fibres into concrete is emerging as a promising strategy in addressing the environmental concerns associated with traditional fibre-reinforced concrete production and disposal. Such initiatives support the global drive for decarbonisation in construction materials production and the exploitation of biomaterials. This innovative approach leverages the sustainable characteristics of

natural fibres to enhance the properties of concrete, thereby contributing to waste reduction and promoting the circular economy in the construction industry. This concept is being promoted internationally as in recent years, the European Commission has "propose[d] to revise the Construction Product Regulation, which may include recycled content requirements for certain construction products." (European Commission, 2020). Natural fibres such as those derived from agricultural by-products, such as chicken feathers, hemp, flax, coconut coir, etc., transform waste into valuable resources. Instead of being discarded or incinerated, which contributes to environmental pollution, these fibres can be repurposed as reinforcement materials in concrete.

By replacing synthetic fibres with natural fibres, the construction industry can reduce its reliance on non-renewable resources. This substitution helps conserve natural resources and reduces the ecological footprint of concrete production. Consequently, natural fibres are often locally sourced, which minimises the need for transportation and further reduces the carbon footprint associated with material procurement. Also, unlike synthetic fibres, natural fibres are biodegradable and pose less environmental risk at the end of their lifecycle. Their use in concrete can lead to more environmentally friendly demolition and disposal processes at the end of life of buildings or infrastructure.

The use of natural fibres in concrete represents a significant step towards more sustainable construction practices. By repurposing natural waste materials as reinforcement in concrete, the industry can reduce waste disposal, conserve natural resources, and overall lower its environmental impact. While challenges remain, ongoing research and innovation are paving the way for wider adoption of natural fibre-reinforced concrete, contributing to a greener and more sustainable future for the construction sector.

1.1.2 The Poultry Production Industry

One of the main objectives of this research was to understand the possibility of exploiting waste from the poultry production industry to be used as fibre reinforcement for cement-based construction materials. Therefore, prior to commencing the research, it was necessary to investigate the current state of the poultry production industry, to assess the possibility of using waste feather fibres in the construction industry.

Poultry meat is amongst the most consumed meat product globally (Food and Agriculture Organization of the United Nations, 2013) and is produced in most parts of the world, as shown in Figure 1.1. In Malta, it is estimated that the total poultry production is around 4,250 tonnes per year (Food and Agriculture Organization of the United Nations, 2023). While the chickens are bred on various approved farms, poultry processing is highly centralised with only a limited number of processing plants on the islands. SMINA Poultry Products Ltd, the industry partner of this project (MCST, 2024) ` (P. Spiteri, Personal Communication, 02/02/2023). To better understand the local poultry production industry, SMINA Poultry Products Ltd, as RECP project partner, willingly assisted the research by shedding light on the poultry production process.

This proved to be an important and essential step in describing the industrial byproduct in agricultural exploited for this research, that is the fibres. Understanding this process was necessary to define the product process and material flows analysis, the sourcing of the feathers and sampling procedures at the abattoir for eventual processing in the laboratory.

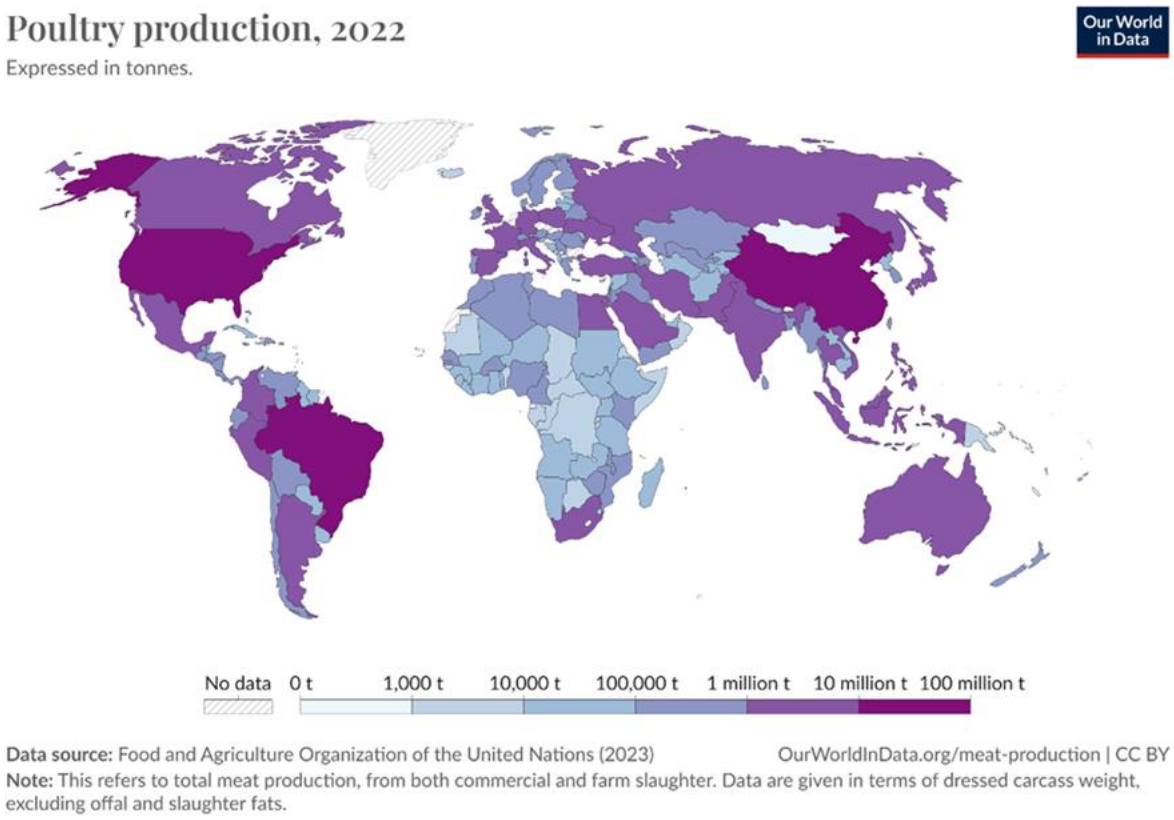

Figure 1.1 - Global Chicken Meat Production in 2022 (Food and Agriculture Organization of the United Nations, 2023).

1.1.2.1 Local Poultry Processing at the SMINA Poultry Processing Plant

SMINA Poultry Products Ltd is a local poultry processing plant in Fawwara (Siġġiewi), Malta, which slaughters around 7,000 chickens per night, 5 nights a week. The company employs around 60 people and is run by the Spiteri family, and there is always a veterinary doctor present on site during hours of production, monitoring quality of chickens and the production. This ensures constant high-quality assurance at the processing plant. The plant receives live chickens at around 6pm, begin their slaughter at 7pm and continue overnight until around 11am the next morning, where the plant is thoroughly cleaned and disinfected for the next slaughter. The process is mostly done using modern equipment and machinery, and is mostly automated. The complete poultry production process is summarised in Figure 1.2, and further explained in Appendix A. To the authors knowledge, to date, the poultry processing

at SMINA Poultry Products Ltd remained unchanged from the time of data collection during 2022 and 2023.

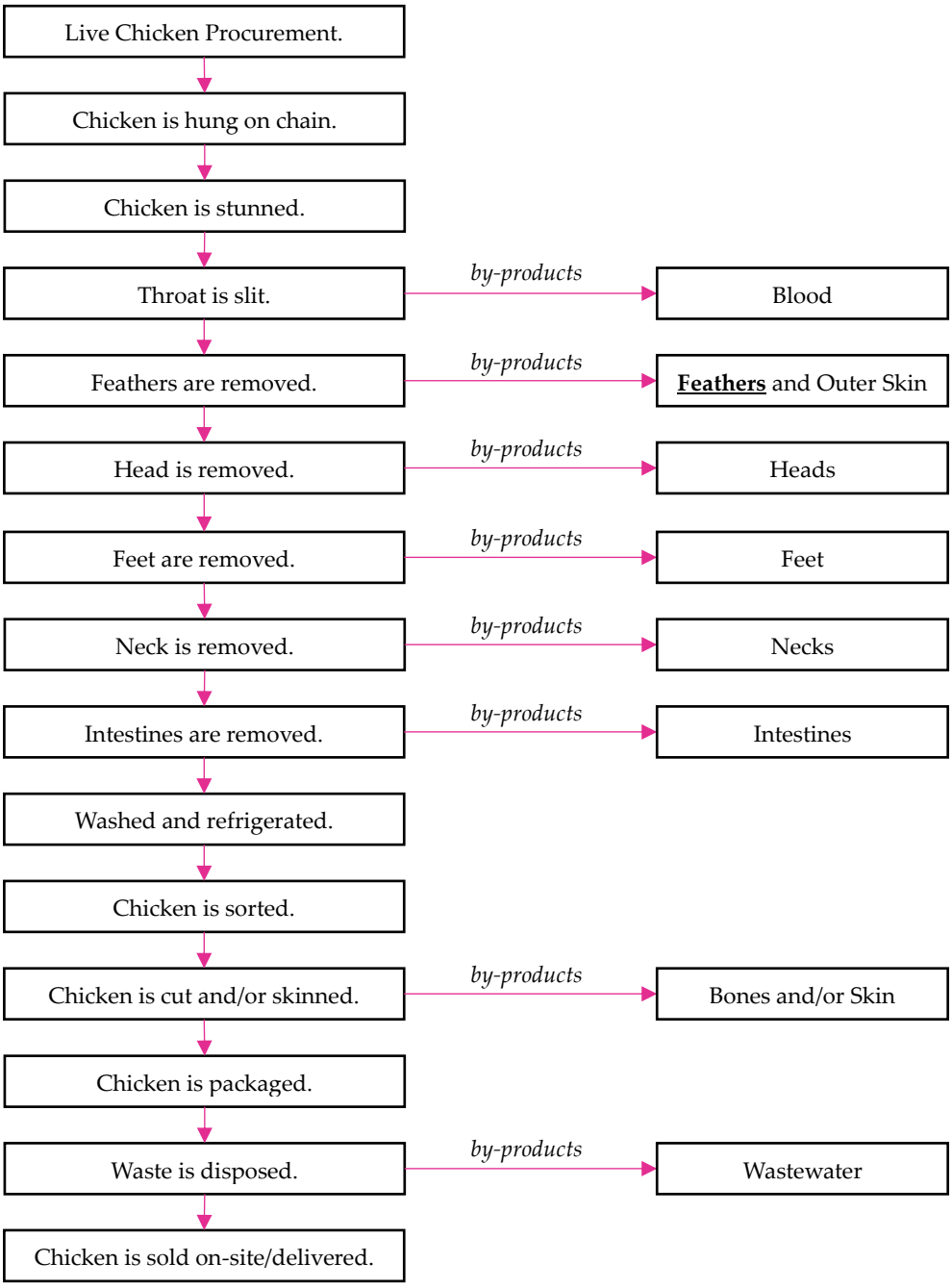

Figure 1.2 - The process of poultry production and its by-products produced in each stage.

The final product is sold fresh as whole chickens or cut chickens, most of which are delivered to various localities across the island, while some of which is kept to be sold on-site. While it is usually whole chickens or parts (breasts, legs, drumsticks, wings, and thighs) which are sold, the necks and livers are sometimes sold, particularly

during winter, or gifted to customers depending on the company's production and marketing plans.

For quality assurance purposes and for a deeper understanding on the proportions of chickens processed, the on-site engineer conducts sampling based on data collection in production. A sample test is presented in the table in Figure 1.3, and transcribed below in Table 1.1, listing the proportions of the chickens according to their live size. The measurements included are recorded as wet weights, as the process involves a substantial volume of water during production.

Table 1.1 - Chicken Processing: Transcription of the table in Figure 1.3

Part	*Weight*					
	g	*G*	*g*	*g*	*g*	*g*
Whole Chicken	**2030**	**2150**	**2297**	**2300**	**2340**	**2700**
Head of Chicken	42	44	54	48	58	52
Blood of Chicken	63	66	60	72	72	110
Chicken with Feathers	1740	2072	2176	2100	2143	2540
Chicken without Feathers	1713	1943	2021	2040	2065	2431
Feathers of Chicken	27	133	155	60	78	109
Feet of Chicken	60	83	74	58	65	85
Neck of Chicken	38	51	37	43	31	28
Chicken without Neck and Feet	1615	1855	1910	1931	1999	2300
Intestine of Chicken	179	209	250	233	235	230
Chicken without Intestine	1427	1655	1640	1700	1680	2040
Breast of Chicken (with Bone)	537	654	510	580	580	730
Breast of Chicken	394	500	426	500	455	560
Legs of Chicken	535	690	625	580	720	668
Wings of Chicken	124	148	140	125	150	134
All Bones of Chicken	247	226	258	220	230	280

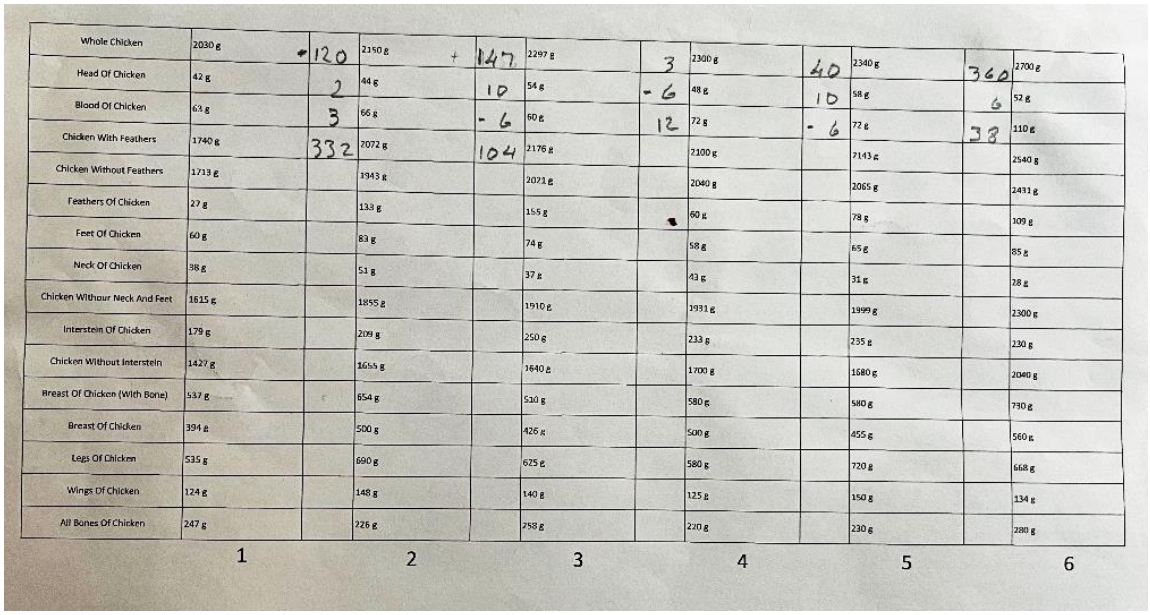

	1		2		3		4		5		6
Whole Chicken	2030 g	+ 120	2150 g	+ 147	2297 g	3	2300 g	40	2340 g	360	2700 g
Head Of Chicken	42 g	2	44 g	10	54 g	- 6	48 g	10	58 g	6	52 g
Blood Of Chicken	63 g	3	66 g	- 6	60 g	12	72 g	- 6	72 g	38	110 g
Chicken With Feathers	1740 g	332	2072 g	104	2176 g		2100 g		2143 g		2540 g
Chicken Without Feathers	1713 g		1943 g		2021 g		2040 g		2065 g		2431 g
Feathers Of Chicken	27 g		133 g		155 g		60 g		78 g		109 g
Feet Of Chicken	60 g		83 g		74 g		58 g		65 g		85 g
Neck Of Chicken	38 g		51 g		37 g		43 g		31 g		28 g
Chicken Withour Neck And Feet	1615 g		1855 g		1910 g		1931 g		1999 g		2300 g
Interstein Of Chicken	179 g		209 g		250 g		233 g		235 g		230 g
Chicken Without Interstein	1427 g		1654 g		1640 g		1700 g		1680 g		2040 g
Breast Of Chicken (With Bone)	537 g		654 g		510 g		580 g		580 g		730 g
Breast Of Chicken	394 g		500 g		426 g		500 g		455 g		560 g
Legs Of Chicken	535 g		690 g		625 g		580 g		720 g		668 g
Wings Of Chicken	124 g		148 g		140 g		125 g		150 g		134 g
All Bones Of Chicken	247 g		226 g		258 g		220 g		230 g		280 g

Figure 1.3 - Chicken Processing Record: Table prepared by the on-site engineer.

1.1.2.2 Waste Generation in the Poultry Production Process

The production itself is a wasteful process, both in materials and consumption of water and energy. Further to the aforementioned process, the head, blood, feathers, feet, intestines, and bones are always disposed of and burnt at the incineration facilities at WasteServ, the national company responsible for organising, managing and operating integrated systems for waste management, located in Marsa. For instance, in the month of December 2022, the waste which the plant produced accumulated to 71,510 kg for the whole month, which was taken to the incineration plant (based on the WastesServ receipt for the duration of December 2022, shown in Figure 1.4). Furthermore, from the data gathered in Figure 1.3, an overview of the waste proportion as compared to that actually sold for consumption is shown in Figure 1.5; 5% by weight of which is chicken feather. This figure is a substantial amount when considering the annual poultry produced on a global scale.

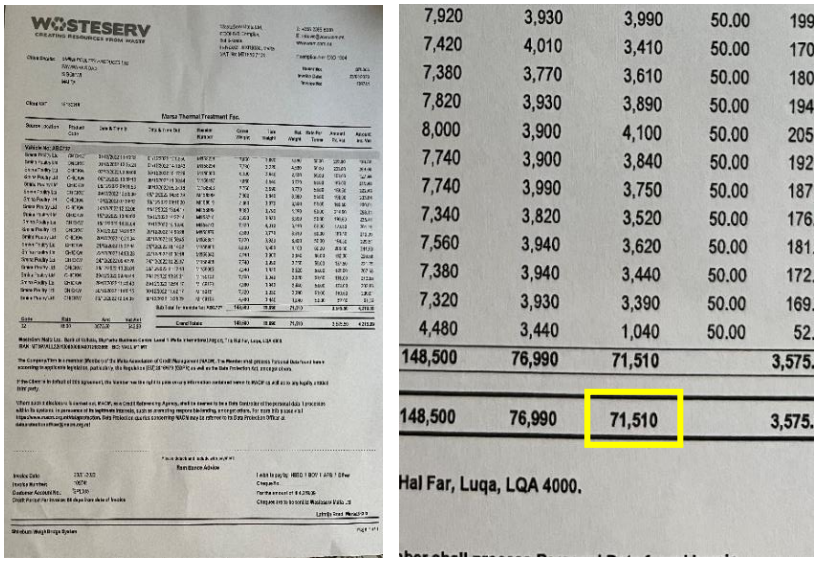

Figure 1.4 - Receipt from WasteServ for December 2022 showing mass of waste delivered in kilograms.

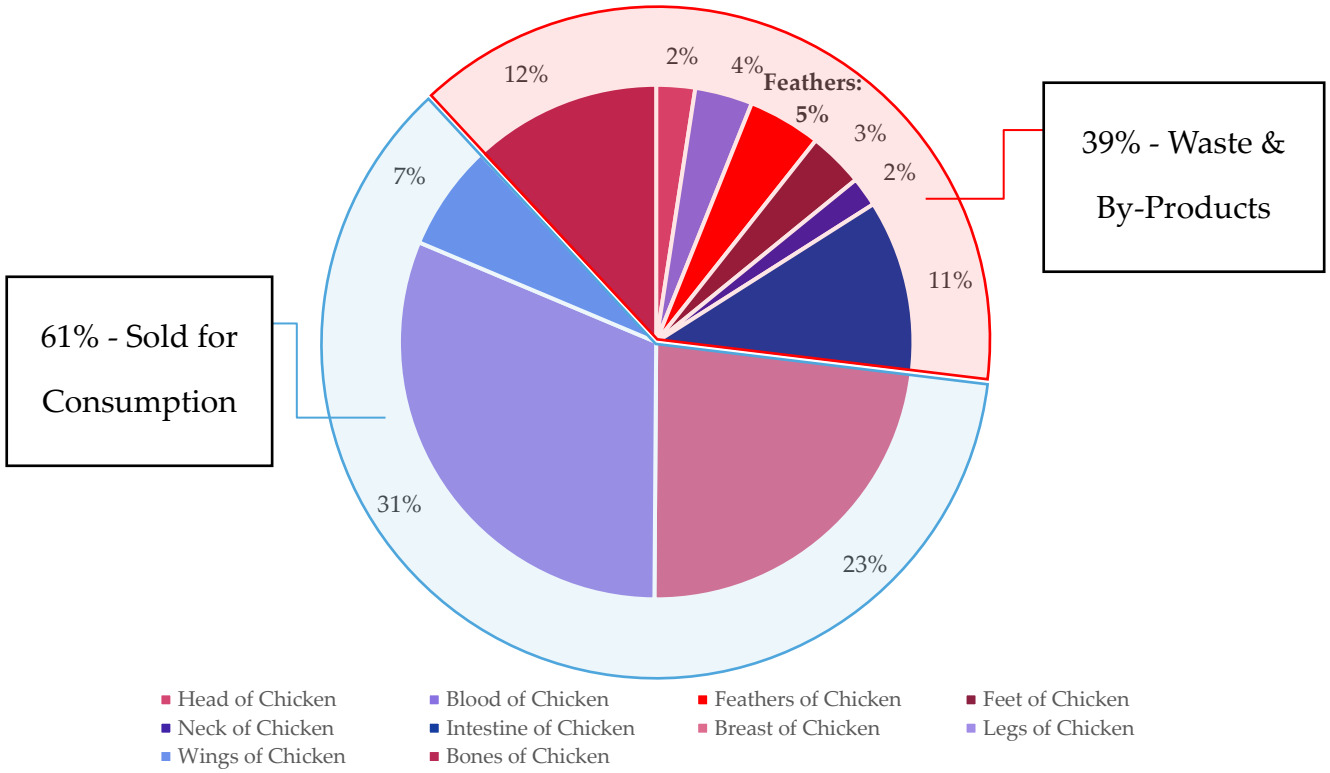

Figure 1.5 - Waste and Food Consumption Proportions by weight of Chicken.

The feathers are among the first by-products to be removed, allowing for easy separation from the rest of the waste, therefore facilitating the possibility to be taken to be reused in the construction industry. The processing, mostly done in an automated manner, is summarised in Figure 1.2, which specifically highlights the by-products which are generated at the various stages throughout the process. It was observed that

overall, since the by-products of the production process are generated at various stages throughout the plant, collection of such waste materials is relatively simple and can be organised at industrial scale should components be exploited. The waste at all stages is either collected in a bin if it is solid waste, or in a trough if it is liquid waste. This provides for practical separation and collection of waste materials before it is disposed of into the mechanical drum at the end of the production process, where all waste materials are mixed together and collected in bins.

In addition to the already wasteful process, there is also a considerable water and power consumption to be considered. The company have provided the following information on the usage of water and power during hours of production:

- Water Consumption: 8 cubic meters per hour.
- Power Consumption: 311 kVA per hour.

These high values are due to the lengthy process to produce poultry, as well as the cooling requirements. During one hour of production 1,000 chickens are slaughtered, and it takes approximately 2 hours for a single chicken to pass through the entire facility from being alive to packaging. The entire facility maintains a constant temperature of 12°C during hours of production, with overhead cooling shown in Figure 1.6. The cooling and heating equipment is turned on one hour prior to the commencement of poultry processing to be used throughout the duration of processing, and is not used during the remainder of the day as the plant is only being cleaned at daytime. The water and power consumption listed previously do not account for the water and power used during daytime cleaning but refers only to the intensive overnight production time. The entire facility is thoroughly washed with water throughout the cleaning time, but this has not been accounted for in the reading and is not dependant on the amount of production. The equipment is operational for approximately 6-7 hours each night, depending on the amount of production. Overall, the facility processes about 1.2 million chickens each year.

Figure 1.6 - Overhead cooling devices throughout the plant.

1.1.3 Sustainable Development Goals

In 2015, the 2030 Agenda for Sustainable Development was adopted by United Nations Member States, which includes Malta, to establish a collective blueprint for peace and prosperity for both the people and the planet, both now and in the future (United Nations, 2020).

There are 17 Sustainable Development Goals (SDGs), illustrated in Figure 1.7, that require immediate action from all nations to tackle poverty, health, education, inequalities, economic growth, climate change, and the conservation of oceans and land ecosystems (*Sustainable Development Goals*, 2015).

Figure 1.7 - Sustainable Development Goals (Source: https://www.un.org/sustainabledevelopment).

The four Sustainable Development Goals which are most relevant to this research are as follows:

- SDG 7: Affordable and Clean Energy
- SDG 11: Sustainable Cities and Communities
- SDG 12: Responsible Consumption and Production
- SDG 13: Climate Action

While the impact of utilising feather fibres will be discussed in the discussion chapter, the relevant core principles of the SDGs are discussed below.

1.1.3.1 Sustainable Development Goal 7: Affordable and Clean Energy

This goal is to ensure universal access to affordable, reliable, and modern energy services, by focusing on providing access to energy for all individuals, particularly in underserved and developing regions.

Secondly, this goal also aims to double the global rate of improvement in energy efficiency, by encouraging improvements in energy efficiency across various sectors,

including industrial, residential, and transportation, to reduce energy consumption and emissions.

1.1.3.2 Sustainable Development Goal 11: Sustainable Cities and Communities

Firstly, this goal focuses on access to adequate, safe, and affordable housing and basic services for all, by promoting inclusive urban planning and development to provide housing and services to all community members.

Furthermore, the goal aims to enhance inclusive and sustainable urbanisation and capacity for participatory, integrated, and sustainable human settlement planning, by encouraging participatory and integrated approaches to urban planning that consider social, economic, and environmental sustainability.

Lastly, the goal also aims to reduce the adverse per capita environmental impact of cities, by addressing pollution, waste management, and resource consumption to mitigate the environmental impact of urbanisation.

1.1.3.3 Sustainable Development Goal 12: Responsible Consumption and Production

This goal, possibly the most relevant, aims to implement the 10-year framework of programmes on sustainable consumption and production, by adopting sustainable practices in consumption and production to reduce environmental impact.

This goal also aims to achieve sustainable management and efficient use of natural resources by promoting the efficient use of resources to minimise waste and environmental degradation.

Other relevant principles of the goal include aiming to substantially reduce waste generation through prevention, reduction, recycling, and reuse, by encouraging waste management practices that prioritise waste prevention and material recovery, as well as to substantially reduce waste generation through prevention, reduction, recycling, and reuse, by encouraging waste management practices that prioritise waste prevention and material recovery.

Finally, this goal aims to halve per capita global food waste at the retail and consumer levels, by reducing food waste throughout the supply chain, from production to consumption. Given that the poultry production industry is a large producer of waste, aiming to minimise the waste in this industry would directly tackle this goal.

1.1.3.4 Sustainable Development Goal 13: Climate Action

This goal aims to promote mechanisms for raising capacity for effective climate change-related planning and management in least developed countries and small island developing states, by supporting vulnerable nations in developing and implementing climate strategies. Given that poultry production is an industry available on a world-wide scale, education on utilising the by-products of this industry would benefit not only developed countries but also smaller and less developed countries.

1.1.4 Addressing the Scope of this Work

This section has highlighted the highly wasteful nature of both the construction industry and the poultry processing industry. The world's growing population results in an increasing requirement for sustainable development, as highlighted by the SDGs mentioned previously. This population growth also demands increased productivity in both construction, with a large demand for housing, as well as food industries, with poultry being one of the most consumed meats. Hence, on an international level, there is a drive towards more sustainable industries with large efforts to create circular economies in various industries.

Consequently, to comply to this drive, a possible solution to investigate would be the utilisation of waste materials such as chicken feathers in construction as fibres, which would be able to offset some of the waste generated by the poultry production industry. This reduction of waste promotes not only a cleaner poultry production, but also a more sustainable construction material, one which does not depend on synthetic fibres but rather natural ones. The ease of extraction of such feathers allows for this material to be accessible worldwide, and hence reducing costs and carbon emissions

related to the transportation of materials, while also allowing for underdeveloped countries to have access to such resources.

1.2 Goals and Objectives of the Research

The aim of this dissertation is to bring forth the dual benefits of reducing waste being generated in the poultry production industry and exploiting by-products in fibre-reinforced concrete production, by utilising natural waste fibres as opposed to synthetic fibres to produce a mix which could potentially be used as a building material. The focus of this study is on utilising chicken feathers, typically considered waste, emphasising their potential to be processed and incorporated into concrete mixes, thereby reducing the volume of waste sent to landfills and lowering the environmental impact of poultry farming; and hence creating a circular economy in these two industries.

More specifically, this dissertation examines the behaviour of concrete with chicken feather fibre reinforcements, by means of an extensive experimental program. The research involved the development of mix designs for self-compacting mortar and concrete, trial mixes and the assessment of fibres with respect to a control. The mortar and concrete was assessed with respect to different properties in various phases, including the fresh and rheological properties, early-stage plastic and drying shrinkage cracking, mechanical properties and durability properties. These performance characteristics were determined through specific test methods outlined below. The focus of the experimental program was as follows:

1. Characterisation and classification of the chicken feather fibres;
2. Preparation of the chicken feathers to be used as fibres for reinforcement;
3. Development of the mix design for fibre-reinforced self-compacting concrete;
4. Fresh and rheological properties of the fibre-reinforced concrete;
5. Early-age shrinkage properties of the fibre-reinforced concrete and mortar;
6. Physical and mechanical properties of the fibre-reinforced concrete and mortar;
7. Durability properties of the fibre-reinforced concrete.

While some studies are being carried out globally on the compressive and tensile strength of such mixes, as discussed in the literature review chapter, there are few and limited studies concerning the cracking of concrete and performance assessment of fibre reinforced concrete based on natural fibres such as keratin fibres including feathers.

Studying the crack control of a cement-based construction material with varying amounts and aspect ratios of feather fibres is a higher level of research and as yet unexplored, with early-stage plastic cracking (occurring within the first 24 hours) and drying shrinkage cracking (occurring after 24 hours) being an area of concern. Hence, the main objectives of this research were to conduct a thorough analysis of the overall behaviour of these materials, by conducting a rigorous experimental program.

The overarching goal of this research was to develop new cement-based construction materials which would benefit from the addition of feather fibres as reinforcement, or at least not compromise their properties. The intention behind creating such materials was to create and support circular economy between two very wasteful industries, the construction industry and the poultry industry in the field of agriculture.

1.3 The Research Question and Hypothesis

This study was designed to assess whether incorporating feather fibres with varying amounts and aspect ratios into cement-based construction materials will improve crack control, specifically reducing early-stage plastic cracking and drying shrinkage cracking.

It was also aimed to establish whether the inclusion of feather fibres would affect or compromise the fresh, mechanical, and durability properties of the concrete.

1.4 Overview of the Research Methods

As previously mentioned, this research was carried out by following an exhaustive experimental program compromising of a series of tests based on European and

international standards and other adapted methodologies referenced in the methodology chapter, to assess the following properties of the mixes:

- **Feather Analysis and Preparation**: Tests include feather characterisation and classification (statistical analysis on length, thickness, and aspect ratio).
- **Rheological Properties and Workability**: Tests including empirical test methods (Concrete Flow test and T_{500} test, V-Funnel, and L-Box passing ability) and rheological parameters (two-point tests to determine yield and viscosity using an ICAR Plus Concrete Rheometer).
- **Early-Stage Cracking Behaviour**: Tests including plastic shrinkage through environmental chamber, restrained drying shrinkage through ring test, and restrained mortar shrinkage through Kraai test.
- **Mortar Physical and Mechanical Properties**: Tests on mortar including mortar density, compressive strength, flexural strength, and ultrasonic pulse velocity.
- **Concrete Physical and Mechanical Properties**: Tests on concrete including concrete density, compressive strength, indirect tensile strength, flexural strength, and pull-out test of feather fibres from cement paste.
- **Durability Properties**: Indirect durability indicator through vacuum saturation porosity and direct indicator through Rapid Chloride Penetration Test (RCPT).

This structured experimental program was intended to investigate whether feather fibres contribute to improvements in crack behaviour of concrete, whilst determining the concrete fresh and hardened properties and assessing whether feather fibres in concrete would compromise the fresh, mechanical, and durability properties of the concrete.

1.5 The Structure of the Dissertation

Chapter 1: An introduction to the dissertation, outlining the scope of this work and giving an overview of the two main industries involved in this research; the construction industry and the poultry production industry.

Chapter 2: An in-depth analysis of the available literature on self-compacting concrete, fibre-reinforced concrete, chicken feather fibres, feather fibre-reinforced cement-based materials, tests on the latter, and addressing the research gap to be explored.

Chapter 3: An overview of the methods carried out throughout the experimental program, starting from material collection and procurement, fibre analysis and preparation, development of the mix designs, the protocols for mixing and casting, examination of the fresh properties and rheology, the physical and mechanical properties, the shrinkage properties, and the durability properties.

Chapter 4: A detailed description of the results gathered throughout the experimental program, their analysis, and discussing their significance in the construction industry. This is followed by a discussion on the implications on circular economy and sustainability.

Chapter 5: A comprehensive conclusion to sum up the research carried out throughout this project, while highlighting the strengths and limitations of the outcomes. Possible future work is also outlined in this chapter, listing suggestions for further studies.

Chapter 2

Literature Review

2 Literature Review

This chapter outlines the relevant research and literature available on the subject of this project, reviews the key areas developed and reported, whilst highlighting the research gaps which need to be explored.

2.1 Self-Compacting Concrete

2.1.1 Historical Development of Self-Compacting Concrete

Self-compacting concrete (SCC), sometimes also referred to as self-consolidating concrete, is an innovative construction material that has revolutionised the method of placing and finishing concrete. The origins of this new concrete technology can be linked to the late 20th century, as a response to the issues related to traditional concrete placement techniques.

Researchers in Japan in the 1980s developed self-compacting concrete to eliminate the need for mechanical vibration during formwork filling (Zhang et al., 2020). This was driven by the aim to enhance the quality and longevity of concrete structures, while also tackling concerns about worker safety and the environmental effects of traditional concrete placement methods (Nagaraju, 2020; Ng et al., 2018).

The key progressions that made self-compacting concrete possible were the introduction of high-performance chemical admixtures, like new generation polycarboxylic-based superplasticisers (Sahmaran et al., 2005), and the refinement of the concrete mix formula. Superplasticisers aided in decreasing the amount of water needed for concrete, enabling an increased binder amount and better workability while maintaining strength. Optimisation of aggregate gradation, proportions, and use of supplementary cementitious materials enhanced flow and passing ability of self-compacting concrete (Georgiadis et al., 2010).

The introduction of SCC in Europe began with the Netherlands and Sweden being among the first countries to implement such technologies in the 1990s (Bennenk, 2005).

In recent years, self-compacting concrete has become widely used in the construction sector, especially in areas facing labour shortages, limited entry points, and a demand for superior finishes but also enhanced durability. The creation of standards and requirements for self-compacting concrete in different nations has made it easier to use widely, allowing engineers and builders to confidently and consistently incorporate this innovative concrete technology (Nagaraju, 2020; Ng et al., 2018).

Overall, the total construction expense can be lowered by substituting conventional concrete for SCC, due to the lower machinery requirements for compaction. However, it cannot be ignored that the cost of materials for SCC is typically higher compared to those used for traditional concrete (Wehbe & Stripling, 2009), such as the higher volume of cement as well as the use of specialised superplasticisers. This obstacle has hindered the utilisation of SCC in certain projects and diminished the potential benefits of SCC for those projects.

2.1.2 The Uses of Self-Compacting Concrete

As mentioned, SCC is especially valuable in projects with complicated formwork and intricate architectural designs. The smooth finish and high-quality surface of SCC are achieved by its ability to flow easily into complex moulds and around crowded reinforcement, preventing voids or defects. This is particularly advantageous in buildings with intricate architectural elements, where obtaining a top-notch finish is important. SCC is suitable for architectural concrete applications due to its capacity to create attractive and smooth surfaces (Felekoğlu et al., 2007). SCC also results in decreased labour expenses and construction time, due to the minimal vibration requirements. Enhanced durability is also achieved with the concrete structure's improved longevity due to the absence of voids and defects. However, some studies have shown that SCC typically requires more cement and admixtures, leading to higher material costs (Okamura & Ouchi, 2003).

The precast concrete sector also sees a substantial advantage from utilising SCC. The ability of SCC to flow and settle under its own weight guarantees that precast elements

are consistent and void of honeycombing and other imperfections. This characteristic is crucial for thin-walled and intricate precast elements, as conventional concrete may have difficulty fully filling the formwork. According to available literature, SCC improves the quality and accuracy of precast concrete components, making it a favoured option in the industry (Grünewald & Walraven, 2001). SCC ensures that precast elements have uniform density and strength, improving the overall quality of the product. The use of SCC can also streamline the production process, reducing the need for additional finishing work and hence speeding up production times. The elimination of mechanical vibration in the production process is also beneficial as it significantly reduces noise pollution in the factory environment.

The use of SCC in the construction of bridges is one of the largest growing trends, starting in Japan and also expanding to Europe in the 1990s. SCC has been used to construct a number of bridge components, such as girders, beams, piers, pylons, columns, towers, joints, anchorages, etc. (Okamura & Ouchi, 2003). One example of SCC being used in the construction of bridges is the Grand Wisata Cable-Stayed Bridge in Indonesia (Wang & Supartono, 2011). Cast in-situ SCC was used in three caissons located in one of the abutments. The caissons were strongly reinforced with steel rebars and stirrups. Both the fresh and hardened properties of the SCC were thoroughly examined, with the results showing satisfactory performance of the SCC for this specific use. The use was primarily due to the extensive reinforcement in the bridge pylon, particularly near the cable anchors. Therefore, a SCC mixture with a 650 mm slump flow and a compressive strength of 60 MPa was chosen for the construction of the pylon. Additionally, a non-shrink SCC mix with a compressive strength of 60 MPa was used to fill the joints between the precast girders. The coarse aggregates in the mixture were restricted to a maximum size of 10 mm, with a required slump flow of 750 mm due to the dense reinforcement in the joints.

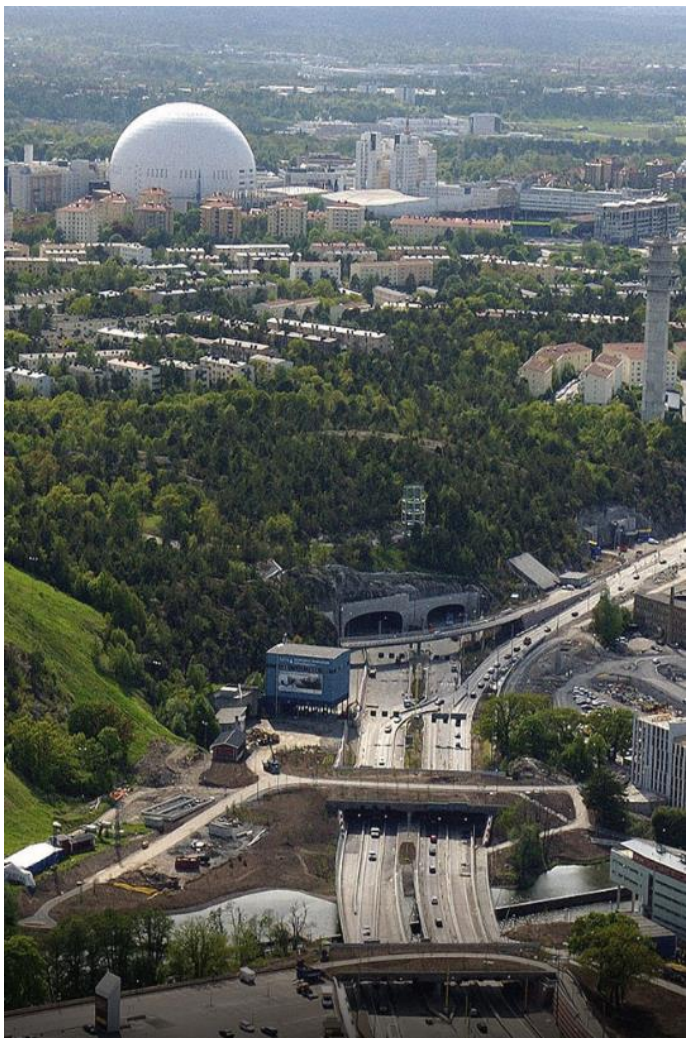

Figure 2.1 - The Sodra Lanken Project in Sweden (Saieh, 2009).

Apart from bridges, the use of SCC in infrastructural projects is also one of the primary uses of the material. The Sodra Lanken (SL) Project in Sweden, shown in Figure 2.1, is known as one of the biggest infrastructure projects in the country (Moravvej & Rashidi, 2020). The SL Project planned to establish a 6 km connection in the southern parts of Stockholm and included seven main links with tunnel entrances, bridges, concrete box tunnels, and earth retention walls. The total length of the rock tunnels, some of which are concrete lined, is 16.6 km. The project required around 225,000 m^3 of concrete (Okamura & Ouchi, 2003). Two tunnels running parallel for approximately 20 m were missing a complete rock covering and hence, they were blasted and dug out in deep frozen moraine. The most effective method to support the tunnels, which had thin rock in some areas and exposed in others, was by constructing concrete arches. The goal was to create a sturdy and durable structure, and due to the complicated design

featuring uneven rock surfaces and dense reinforcement, it was decided to utilise SCC in the two arches. This project was also awarded the Swedish Road Administration's prize for architecture in 2007 (Saieh, 2009).

SCC is also widely utilised in the restoration and improvement of current structures as well. Its capacity to easily enter narrow areas and fill cavities and larger cracks without requiring any vibration, makes it ideal for fixing broken concrete structures and filling voids. SCC can be pumped into position, guaranteeing complete consolidation and bonding to the current structure, hence improving the structural strength and prolonging the life of the repaired element. It was found that utilising SCC in repair situations results in enhanced gap filling and increased longevity of repaired structures (Khayat & Guizani, 1997). Repair works can also be completed with minimal disturbance due to lower vibration requirements and easy placement, making it ideal in sensitive structures.

2.1.3 Development of Mix Designs for Self-Compacting Concrete

The initial method for determining SCC mix proportions was created in 1988 using the regular materials used in conventional concrete (Ozawa et al., 1989). The model showed good performance in terms of both fresh and hardened properties such as shrinkage and density. However, the proportion of cement in the model was significantly higher than that in regular concrete, leading to a decrease in the amount of coarse aggregate present (Gaimster & Dixon, 2003).

Several researchers contributing to the study on SCC (Ozawa, 1989; Yurugi et al., 2000) acknowledged that there are three key factors influencing the characteristics of fresh concrete:

(i) the fresh properties of the mortar;
(ii) the amount of coarse aggregate in the mix;
(iii) application of a superplasticizer to improve workability.

The paste and mortar's fresh properties have clear effects on the concrete properties similar to traditional concrete. The workability of the mixture is significantly

influenced by the water/cement ratio, as well as the amount of fine aggregate in the mortar mix (Yurugi et al., 2000). The amount of coarse aggregate in the concrete mix will also impact both workability and segregation resistance (Gaimster & Dixon, 2003).

2.2 Fibre-Reinforced Concrete

Fibre reinforcement involves the incorporation of small, discrete fibres into concrete to improve its properties. They are generally classified as either natural fibres or synthetic fibres, as can be seen in Figure 2.2. Natural fibres are obtained from plants, animals, and minerals, providing different characteristics depending on their source. On the other hand, artificial fibres are categorised into regenerated man-made fibres, completely synthetic fibres, and inorganic fibres, with each group designed for specific performance needs.

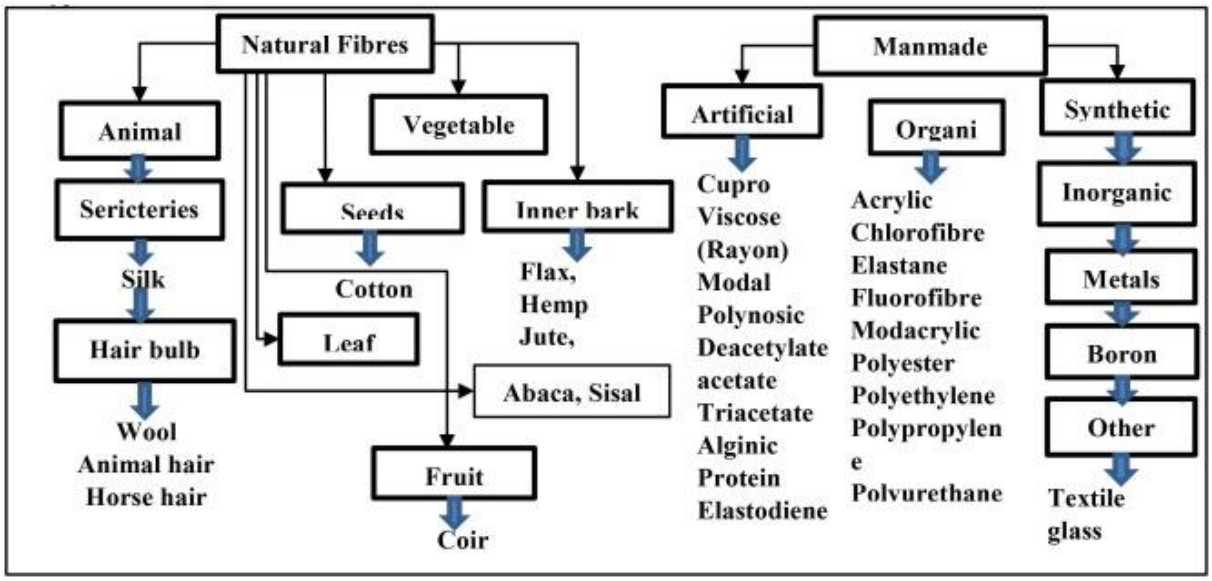

Figure 2.2 - Types of Fibres (Basu et al., 2023).

2.2.1 Historical Development of Fibre Reinforcement in Construction

The addition of fibres to brittle matrix materials has a lengthy and extensive tradition. Proof of this can be traced back to a minimum of 3,500 years ago, shown through the utilisation of straw-reinforced sun-dried bricks in building the 57-meter-tall Aqar Quf hill close to Baghdad (Hannant, 2003). The initial utilisation of natural fibres laid the

foundation for contemporary fibre reinforcement methods. Asbestos fibres had been used for strengthening cement products for about a hundred years in recent history. Furthermore, cellulose fibres have been utilised for a minimum of 70 years, with steel, polypropylene, and glass fibres also being used for the same purpose for the last 50 years (Hannant, 2003).

Current efforts in research being made to improve concrete properties with fibre additions are vast and varied. Firstly, fibres are employed to enhance the rheological characteristics and reduce plastic cracking in the material when it is still fresh, especially during the initial six hours following placement. In addition, fibres work to increase the tensile and flexural strength of concrete, which helps to address a weakness it naturally has. Furthermore, the inclusion of fibres greatly enhances the impact resistance and durability of the material, increasing its ability to withstand dynamic loads and sudden forces.

Additionally, it is crucial to control cracking and change the failure mode by increasing post-cracking ductility. Fibres assist in connecting cracks and dispersing stress more uniformly, thus averting disastrous breakdowns and prolonging the material's durability. Finally, improving the strength of concrete is an important goal, with fibre reinforcement being essential in enhancing resistance to environmental elements and chemical assaults. All of these goals work together to create stronger, more durable concrete buildings, demonstrating the advancement and complexity of fibre-reinforcement methods throughout history.

Throughout history, various materials such as steel, glass, and carbon fibres have been commonly used as strengthening components in construction projects (Anandamurthy et al., 2017). Although traditional reinforcing materials have successfully improved the performance of concrete and other building materials, they are commonly sourced from non-renewable and unsustainable origins.

Introducing these fibres into concrete offers better management of crack formation and spread, resulting in improved durability, structural longevity, achieving higher elastic modulus, and reduced brittleness (Selmi, 2014). According to Selmi, steel fibres are

commonly utilised in structures that experience loads exceeding serviceability limits, and in cases where impacts or dynamic forces are common, such as in seismic events or cyclic movements.

2.2.2 The Uses of Fibre-Reinforced Concrete

Fibre-reinforced concrete is utilised across various applications in the construction industry due to its enhanced mechanical properties, crack resistance, and overall durability. This section explores the uses of fibre-reinforced concrete, highlighting the advantages and disadvantages of using fibre-reinforced concrete compared to normal concrete.

2.2.2.1 Industrial Flooring

Fibre-reinforced concrete is commonly used for industrial flooring because of its capability to endure heavy loads and resist wear and tear (Adesina et al., 2020). Adding fibres enhances the tensile strength and ductility of the concrete, making it suitable for locations under significant mechanical stress like warehouses, factories, and distribution centres. The fibres help to distribute loads more evenly and prevent the development of cracks, leading to longer-lasting floors. Following this, enhanced durability and crack resistance result in lower maintenance and repair costs over time, as floors can better absorb impacts more effectively, reducing damage from dropped objects or heavy machinery. However, the greatest drawback is the high initial construction costs, as fibre reinforcement is costly and requires a specific finishing process.

There is a possibility that some fibres may protrude from the surface, and their occurrence is normal. It is suggested that the frequency of occurrence can be decreased through the application of a dry-shake topping (The Concrete Society, 2013).

Surface fibres can be sliced flush with the surface. Any noticeable imperfections that emerge can be addressed using an appropriate resin-based substance. Macro-synthetic fibres are typically created through the power finishing method, resulting in fan-shaped marks and untangled fibres.

2.2.2.2 Pavements

Fibre-reinforced concrete is used in the construction of pavements (Ragavendra et al., 2017), where it provides improved load-bearing capacity and resistance to cracking (Adesina et al., 2020). This makes it suitable for areas with heavy pedestrian traffic and adverse weather conditions, where the concrete requires extra ductility. Fibre-reinforced concrete pavements have a longer lifespan due to their enhanced resistance to cracking and fatigue. The fibres also help to distribute traffic loads more evenly, reducing the occurrence of surface deformations which could be a safety hazard for pedestrians.

2.2.2.3 Precast and Structural Building Elements

Fibre-reinforced concrete is used in the manufacture of precast concrete products (Rossi & Chanvillard, 2000), such as pipes, panels, and beams. The fibres improve the structural performance and durability of these elements, making them suitable for a wide range of applications. Fibre-reinforced concrete is also employed in structural elements such as beams, columns, and slabs in buildings (Ragavendra et al., 2017). The fibres enhance the load-bearing capacity and resistance to cracking, making these elements more robust and durable.

2.2.3 Synthetic Fibres as Reinforcement

2.2.3.1 Steel Fibre Reinforcement

Steel fibres themselves exhibit a range of characteristics that make them particularly suitable for reinforcement in concrete. Typically, these fibres are produced from high-carbon or stainless steel, which provides excellent tensile strength and resistance to corrosion. They are available in various shapes, such as straight, hooked, crimped, or deformed, each designed to optimise their bonding and anchorage within the concrete matrix (Zheng & Feldman, 1995). Hooked and crimped fibres, for instance, are particularly effective at providing mechanical interlock, enhancing the load transfer capabilities between the fibres and the concrete, and thus improving the composite material's overall performance (Bentur & Mindess, 2006).

The dimensions of steel fibres are also critical to their reinforcing effectiveness. Generally, they range from 0.25 to 1.00 mm in diameter and from 12 to 60 mm in length, leading to an aspect ratio (length-to-diameter ratio) that is typically between 40 and 100 (Banthia & Gupta, 2006). Higher aspect ratios contribute to better crack-bridging capabilities and increased toughness. The surface of steel fibres can be smooth or textured to further improve bonding with the cementitious matrix (Johnston, 2014). Textured surfaces increase the mechanical interlocking between the fibre and the matrix, thus enhancing the composite's ability to resist crack propagation and providing higher post-cracking strength (Naaman, 2003). These physical and mechanical properties of steel fibres play a crucial role in determining the overall performance of fibre-reinforced concrete.

2.2.3.2 Polypropylene Fibre Reinforcement

Polypropylene fibre is utilised in concrete for numerous applications in overall construction and especially in ground-floor slabs. Certain applications have involved the utilisation in sprayed concrete (shotcrete), precast elements, and in scenarios where fire retardancy is crucial (EFNARC, 1999). This is done by the fibres melting and creating channels in the concrete that allow steam to escape, thus enhancing the resistance to spalling (Khoury, 2008). Additionally, almost 10% of ready-mixed concrete in the United States is reported to include polypropylene fibres, indicating its increasing usage in overall construction (Hannant, 2003). Certain structures utilise a blend of polypropylene and steel fibres in which the advantages of each type of fibre can be mutually beneficial.

Polypropylene has a high resistance to alkalis found in concrete, and the concrete itself acts as a barrier against ultraviolet light, preventing chain scission and degradation of the fibres. There has been minimal alteration in fibre strength over 18 years in various exposure conditions, with accelerated tests forecasting a lifespan well over 30 years (Hannant, 2003). For early age properties, fibre durability is not crucial; only the hardened properties are affected by any degradation of fibres in the longer term.

2.2.3.3 Glass Fibre Reinforcement

There are limited applications for incorporating glass fibre reinforcement in large amounts of concrete due to the high cost of adding a sufficient quantity of random glass fibre, which is rarely economically viable. Additionally, mixing challenges would be significant (Majumdar & Nurse, 1974) for typical concrete mixes when the fibre content exceeds 1%.

However, even a small amount of 0.03 percent in volume (equivalent to 0.8 kg/m^3) of 12 mm long fibres can enhance the ability of normal concrete to resist plastic shrinkage cracking, similar to polypropylene fibres. These combinations will prevent bleeding and plastic shrinkage cracking by containing 2 to 200 million fibres per cubic meter of concrete, depending on whether the filaments disperse from the strands.

2.2.4 Natural Fibres used as Reinforcement

2.2.4.1 Hemp Fibre

Hemp fibres come from the hemp plant, which belongs to the Cannabis family, and are renowned for being one of the most durable natural fibres (Amaducci & Gusovius, 2010). These fibres are greatly appreciated for their ability to resist tensile force and last a long time. Hemp fibres are composed of cellulose, hemicellulose, lignin, and extractives, along with a larger quantity of hydrophobic waxy cuticle layers and inorganic silica, which sets them apart from wood. Their durability and environmentally friendly characteristics make them popular for making textiles, ropes, and bio-composites (Roulac, 1997). Furthermore, hemp fibres have excellent resistance against UV light and mould, making them ideal for use outdoors (Mohanty et al., 2005).

2.2.4.2 Elephant Grass Fibre

Elephant grass, also known as Napier grass or *Pennisetum purpureum*, originates from Africa and is characterised by its rapid growth and high biomass yield compared to other tall grasses. The plant can grow up to 7 meters tall and is primarily used as animal feed, but its fibrous composition has also been studied for making bioenergy

and bio-composite materials. (Suttie & Food and Agriculture Organization of the United Nations, 2000). The presence of cellulose, hemicellulose, and lignin in elephant grass fibrous material enhances its potential for sustainable material uses (Johannes et al., 2024).

2.2.4.3 Coconut Fibre (Coir)

Coconut fibres, also called coir, are often found in tropical regions and are obtained from the outer husk of coconuts. Coir fibres have great durability, can resist saltwater, and possess outstanding insulation properties (Jayasekara & Amarasinghe, 2010). They have a large amount of lignin, which gives them stiffness and strength, and are often utilised in items like mats, brushes, and mattresses (Hill et al., 2009). Coir's capacity to hold water and deter microbial decay makes it well-suited for erosion control and horticultural purposes (Sapuan et al., 2018).

2.2.4.4 Flax Fibre

Flax fibres are derived from the outer layer of the flax plant's stem and are recognised for their durability and pliability. Arranged in slender bundles and grouped closely around the central wooden cylinder, these fibres form thin filaments. Flax fibres contain a large amount of cellulose, which enhances their mechanical characteristics and makes them appropriate for textile, paper, and composite material applications (Akin, 2010). They are biodegradable and have minimal environmental impact, offering a sustainable option over synthetic fibres (Baley, 2002).

2.2.4.5 Sisal Fibre

The source of sisal fibres is the Agave Sisalana plant, which thrives in hot, dry regions, especially in Mexico. These fibres are recognised for their robustness, longevity, and ability to resist decay in salty conditions (Anandjiwala & John, 2010). Sisal fibres comprise cellulose, hemicellulose, and lignin, essential for mechanical strength in products like ropes, twines, and agricultural matting. Sisal fibres are considered an environmentally friendly choice for strengthening composite materials due to their ability to biodegrade and renew (Abir et al., 2015).

2.2.4.6 Jute Fibre

Jute fibres are obtained from the plants Corchorus olitorius and Corchorus capsularis, which are indigenous to the Indian subcontinent. Jute fibres, harvested all year, are derived from the inner sections of the plant stem and are commonly utilised because of their cost-effectiveness, ability to naturally decompose, and adaptability. Jute fibres, with their high cellulose content, provide strength and rigidity and are frequently utilised in making sacks, ropes, and geotextiles (Rahman, 2010). Their capacity to absorb sound and provide thermal insulation also render them appropriate for use in construction materials (Farzana et al., 2022).

2.2.5 Comparison of Natural Fibres

A study by Lau and Cheung was conducted to compare the properties of natural fibres for their value as reinforcements in composites. The data in Table 2.1 shows a comparison of a few commonly used fibres, comparing their ultimate tensile strength, their elongation at failure, and their elastic modulus; three properties which are crucial to ensure effective reinforcement. The results indicate that natural fibres exhibit a wide range of mechanical properties, with some exhibiting high tensile strengths, such as flax and hemp fibres, and others demonstrating higher elongation at failure, such as coir, wool, and spider silk (Lau & Cheung, 2017).

Table 2.1 - Mechanical properties of different types of potential natural fibres for composite applications (Lau & Cheung, 2017).

Natural Fibres	*Ultimate Tensile Strength*	*Elongation at Break*	*Elastic Modulus*
	MPa	*%*	*GPa*
Flax	300 - 1500	1.3 - 10	24 - 80
Jute	200 - 800	1.16 - 8	10 - 55
Sisal	80 - 840	2 - 25	9 - 38
Pineapple	170 - 1672	2.4	60 - 82
Banana	529 - 914	3	27 - 32
Coir	106 - 175	14.21 - 49	4 - 6
Hemp	310 - 900	1.6 - 6	30 - 70
Wool	120 - 174	25 - 35	2.3 - 3.4
Spider Silk	875 - 972	17 - 18	11 - 13
Cotton	264 - 800	3 - 8	5 - 12.6

2.3 Chicken Feather Fibres as By-Products

2.3.1 The Wastefulness of the Poultry Production Industry

The poultry production industry generates a significant amount of waste on a global scale. Management of the poultry waste is an uneconomical task as it involves transporting the waste to an incineration plant for the proper disposal procedure. Research by Williams suggests various possibilities for the safe repurposing of waste in developing countries, such as "land application of crop nutrients", "animal refeeding", and "bioenergy production" (Williams, 2013).

Amongst this waste are the chicken feather fibres, which when compared to other keratinous wastes, accounts for the largest proportion of waste, at 40%, shown in Figure 2.3. (Chukwunonso Ossai et al., 2022). This research studies the possibility of valorising keratinous waste, by producing value-added keratin-based materials, as opposed to their typical disposal methods, which include "burying, open dumping, burning, landfilling, composting, mechanical grinding, and incineration" (Chukwunonso Ossai et al., 2022).

It is also noted that, in "rural developing communities, people usually get rid of keratinous wastes simply by dumping the wastes in dumpsites or burning the wastes" (Chukwunonso Ossai et al., 2022), which coincidentally is also the case for Malta.

An issue with disposal in dumpsites is that the wastes contribute to a bad odour, while also making a breeding ground for pests. Another issue with dumping this waste is that it also promotes dermatophytes saprophytic development (Perța-Crișan et al., 2021), a fungi which requires keratin to develop, which is obviously in abundance in keratin waste such as feathers.

2.3.2 Typical Disposal of Chicken Feathers

Incineration is the most common method for disposing of feathers (Kodak et al., 2019), but it prevents the reuse of waste for additional benefits and results in the emission of greenhouse gases, contributing to global warming. Therefore, it is crucial to find

alternative methods in the future, and those which align with the Sustainable Development Goals (United Nations, 2020).

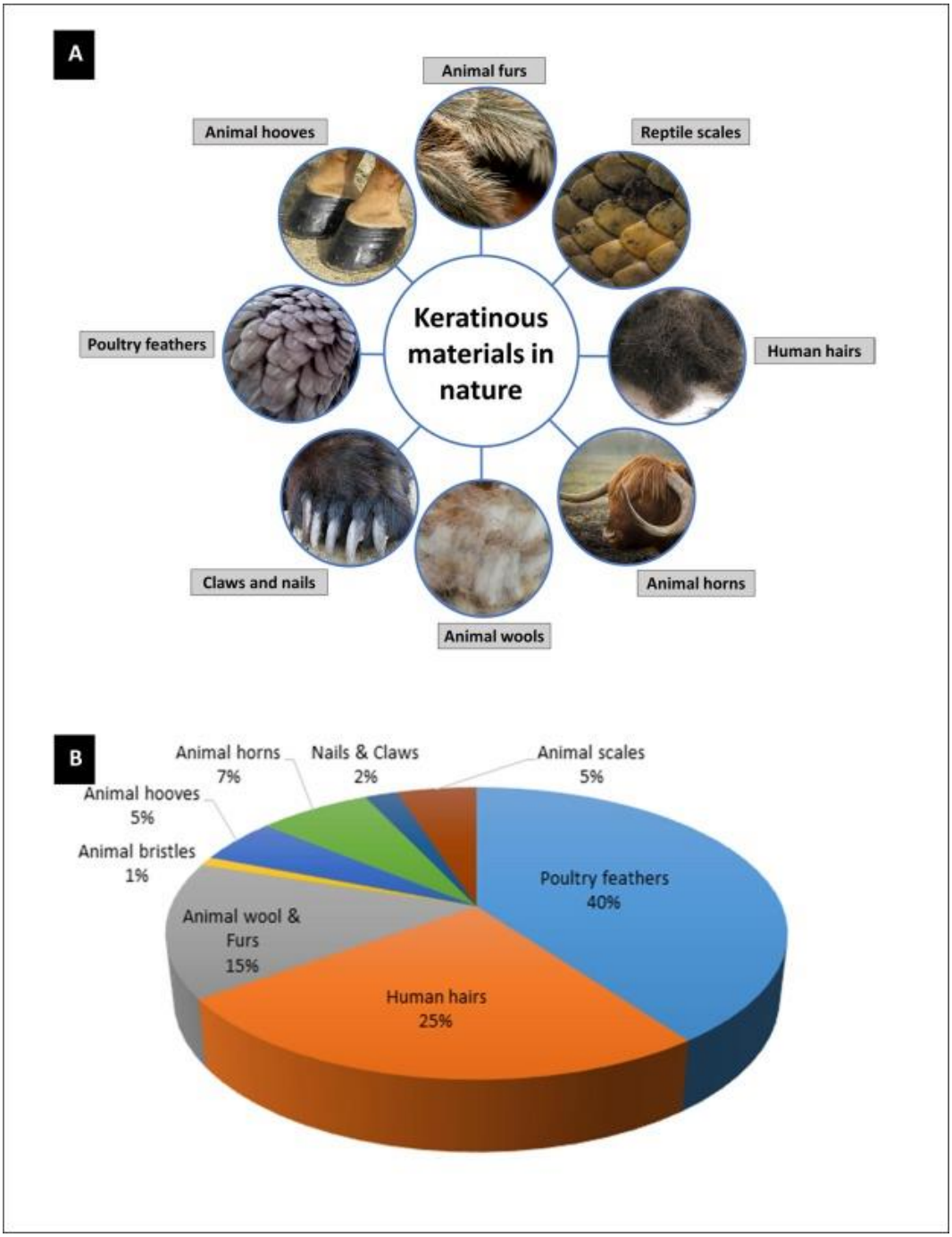

Figure 2.3 - (a) Keratinous materials in nature. (b) Keratinous wastes biomass distributions (Vineis et al., 2019).

Table 2.2 - Feather waste disposal methods (Ben Hamad Bouhamed & Kechaou, 2017; Cornejo et al., 2018; Ghaffar et al., 2018; Glanville et al., 2009; Marculescu & Stan, 2011; Ramos et al., 2019; Sakudo, 2020; Stingone & Wing, 2011; Tamreihao et al., 2019; Tesfaye et al., 2017).

Method of Treatment	*Advantages*	*Disadvantages*
Incineration	• Ash produced is safe and decontaminated • Ash may be used as a fertilizer • Allows the disposal of large volumes of waste	• Air pollution • Causes bad smell, fumes, and smog • Special equipment required
Burial	• Avoids unpleasant odours • A relatively economical option	• Groundwater contamination risk • Soil and water pollution risk • Landfill area required • Burial is difficult when the ground is wet or frozen
Chemical hydrolysis	• Results in the production of low molecular weight components	• Requires dangerous, harsh chemicals • Requires disposal or recycling of residues and undesirable salts needed • Large amounts of wastewater produced
Biodegradation	• Allows the obtainment of hydrolysate containing single compounds such as oligopeptides and amino acids • A relatively energy-efficient process • No emissions and environmental pollution • Safe for people and animals	• Potentially difficult to scale up

Incineration, on the other hand, is not ideal as the "combustion releases ammonia (NH_3), hydrogen sulphide (H_2S), sulphur oxide (SO_2), thiols, thiazole, thiophene, phenols, carbonyl sulphide, nitrile, pyrroles, and pyridines" (A. Gupta, 2014; Shestakova et al., 2021). An overview of common disposal methods and their implications is outlined in Table 2.2.

New management strategies that support a circular bioeconomy can help prevent the accumulation of keratinous waste in the environment. Utilising keratinous waste can effectively address this issue. The vast amount of biomass produced in nature provides

industries with resources, feedstock, and raw materials for creating keratin-based by-products with enhanced uses. Valorising this waste can reduce keratinous waste in the waste stream, support a healthier environment, and enhance the sustainability of commercial processes and the circular economy, as shown in Figure 2.4.

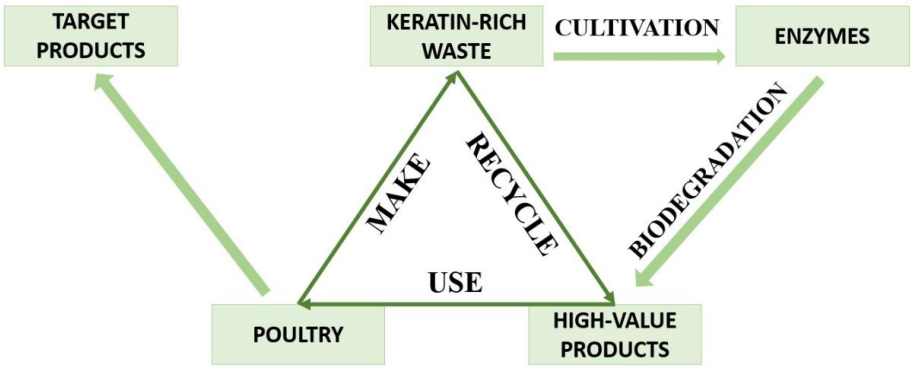

Figure 2.4 - Biodegradation of keratin-containing waste in the poultry production cycle (Shestakova et al., 2021).

This valorisation also considers the impacts on air quality and as well as the possible contamination of water and soil. This contamination could result in possible further environmental damage. Other reutilisation options for feathers include the production of yarn and nonwoven fabrics (Evazynajad et al., 2002), chicken meal (Papadopoulos, 1985), as well as the potential utilisation of keratinolytic fungi as a biodegrading agent for chicken feathers (Sutoyo et al., 2019).

2.3.3 Physical Properties of the Chicken Feather Fibre

The distinct composition of chicken feather fibres, notably including detailed barbules and barbs, has been extensively studied in the area of bio-inspired design (Clark et al., 2016). Chicken feather fibres, as shown in Figure 2.5, contain two main components, the stiffer central shaft and the softer barbs emerging from the shaft. The shaft, also referred to as the rachis, is a hollow tube which runs the length of the fibre and has a honeycomb core, shown in Figure 2.6, known as the medulla, which contributes to its lightweight nature and low density. The barbs are formed by connected barbules which is composed of hooks which provide bulk to the feather (Wang et al., 2016). The hollow structure of the feather contributes to the hygroscopic, hydrophilic, and hydrophobic nature of the fibre (Fraser & Parry, 2008).

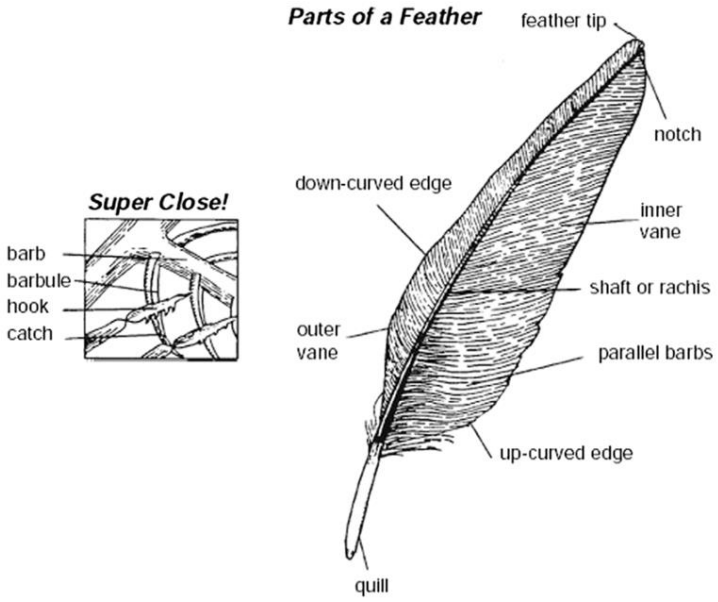

Figure 2.5 - Parts of a Feather (Hwang et al., 1999).

Being a biomaterial, chicken feather fibres vary in shape and size as would be expected. Literature has shown that the range of thicknesses of the barbs lies within the range of 5 – 50 μm (Lau & Cheung, 2017). The shape of the fibre, as shown in Figure 2.5, narrows out towards the tip, with the barbs becoming less downy as the feather closes together.

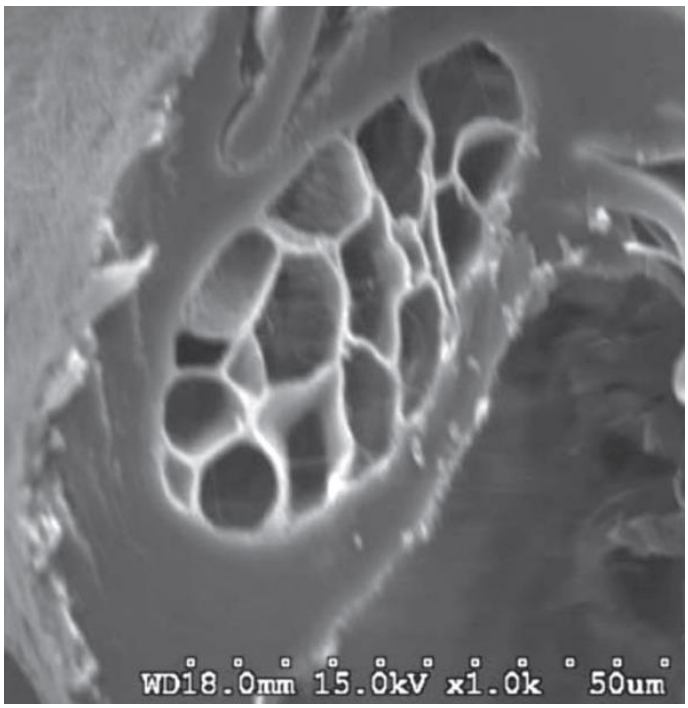

Figure 2.6 - SEM picture of internal Honeycomb Structure (Reddy & Yang, 2007).

Analyses using advanced microscopic techniques, such as optical, transmission, and scanning electron microscopy, have revealed a complex hierarchical organisation

within the individual fibres. At the nanoscale, the feather fibres display a fibrillar morphology, with aligned protein strands grouped together to form the larger filamentous structures (Martínez-Hernández et al., 2005). The complex structure of chicken feathers gives them both strong tensile strength whilst being light weight, making them suitable for various uses such as textiles and composites (Kumar et al., 2020; Oladele, 2016).

Beyond the nanoscale, the feather fibres present a coarse and uneven surface texture (Martínez-Hernández et al., 2005), showcasing clear barbs and barbules seen through increased magnification, shown in Figure 2.7. This intricate outer structure probably enhances the special light-interacting characteristics of chicken feathers, like their bright colours and glossy appearance.

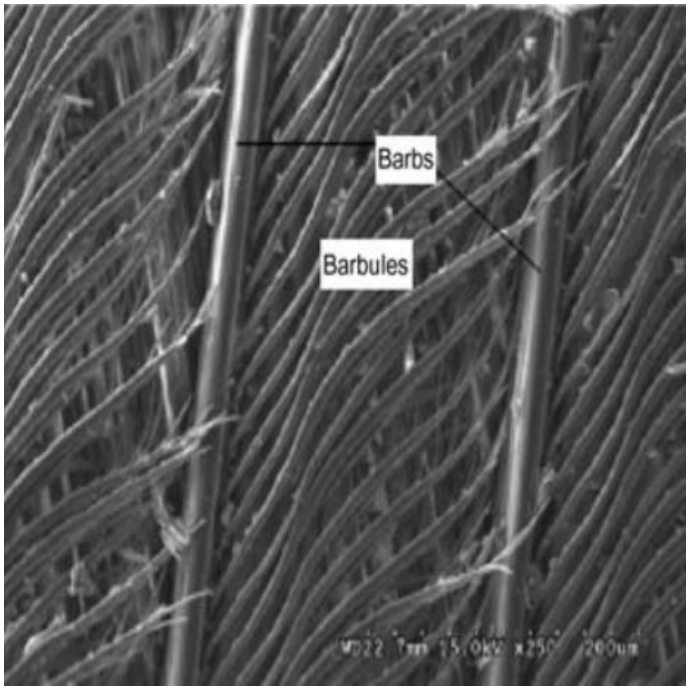

Figure 2.7 - SEM picture of Barbs and Barbules (Hwang et al., 1999).

The inner structure of chicken feather fibres is also noteworthy. Microscopic examinations have shown that the fibres do not have a consistent solid composition, but rather include a central medullary canal that runs the length of the fibres (Martínez-Hernández et al., 2005).

2.3.4 Chemical Composition of the Chicken Feather Fibre

Research by Lau and Hoi Yan Cheung has shown that the chemical composition of the fibre consists of "approximately 91% protein (keratin), 1% lipids, and 8% water" (Lau & Cheung, 2017).

As various studies have shown, a large proportion of the fibre is keratin protein. One study explores the secondary structure of feather keratin, emphasising its predominantly alpha-helical configuration interspersed with beta-sheet regions (Fraser & Parry, 2008). This structural arrangement is essential for the protein's functionality, allowing it to withstand the repetitive bending and stretching experienced during feather movement.

2.3.5 Mechanical Properties of the Chicken Feather Fibre

The tensile modulus of the fibres is around 3.59 ± 1.09 GPa where the average tensile strength is shown to be around 203 ± 74 MPa (Zhan & Wool, 2011). The flexural stiffness is largely attributed to the morphology of the cross-section, rather than the properties of the protein (Bonser & Purslow, 1995).

Since the feather fibre itself is a natural biomaterial, one limitation could be to note that the dimensions are not regular, and there can be variations in the aspect ratio of the fibres. This variation can also be linked to a variation in the mechanical properties of the fibres. It is also noted that even fibres obtained in a similar manner can present deviation due to the growth irregularities which is typical of natural fibres (Ullah et al., 2011).

It has also been noted by Morton and Hearle (2008) that the tensile strength of the rachis, as compared to the barb, is greater. The barb, however, presents similar tensile properties to wool, and greater than that of cotton (Morton & Hearle, 2008). Cotton also presented a lower elongation at failure than feather fibres did, while wool presented a higher elongation at failure when compared to feather fibres (Alonso et al., 2013).

In the latter research by Alonso, it has also been noted that when the behaviour of the feather fibre was assessed with changes in temperature, by subjecting the fibres to thermal treatment and calculating the percentage of retraction compared to the original dimensions, the fibres were not affected. There was no shrinkage present in any of the samples which did not break during the testing procedure. The author noted that this would be beneficial to ensure that the dimensional stability of the biomaterial would not be compromised with temperature changes during possible storage and transportation of the biomaterial (Alonso et al., 2013). Given the oft remoteness of poultry production plants, this would be a beneficial trait for the biomaterial, given the requirements to store and transport the fibres before their incorporation in composite materials.

2.3.6 Elongation of the Chicken Feather Fibre

The elongation behaviour of feather fibres is a crucially important property that has been thoroughly researched due to its potential impact on high-performance composite material development. Researchers have examined how chicken feather fibres stretch under different processing conditions (Oladele, 2016). Experiments revealed that the length of the fibres affects the flexural strength and modulus of the resulting composites. Fibres measuring 10 to 15 mm display better mechanical properties than shorter ones (Kumar et al., 2020).

Along with fibre length, the methodology in which feathers are processed can also impact the stretching properties of the fibres produced. Researchers have investigated methods like thermo-mechanical treatment to enhance the properties of feather fibres, potentially resulting in improved elongation characteristics (Oladele, 2016). These thermo-mechanical processes involved cleansing the feathers to eliminate impurities, dividing the quills from the barbs, and exposing the fibres to different thermal and mechanical procedures. The quills have demonstrated enhanced harmony with polymer matrices, resulting in improved dispersion and stronger mechanical characteristics of the produced composites (Amieva et al., 2015).

Additionally, there have been investigations into altering the chemical composition of feather fibres to enhance their stretch capabilities and ability to work well with polymer matrices. Research has also explored the tensile strength and tensile modulus of composites reinforced with chicken feather fibres, indicating that these fibres can enhance the overall mechanical properties of the materials (Oladele, 2016).

Research indicates that chicken feather fibres can demonstrate elongation characteristics between 8-15% when subjected to tensile forces. Studying these stretch properties is crucial for research, as they can be pivotal in creating new composite materials with improved mechanical performance (Choudary & Nehanth, 2019).

2.3.7 Thermal Properties of the Chicken Feather Fibre

Thermogravimetric analysis (TGA) shows that adding chicken feather fibres greatly improves the thermal stability of composite materials (Martínez-Hernández et al., 2007). This research showed that enhancing the amount of biofibres in the composite poly(methyl methacrylate) matrix resulted in a significant enhancement in thermal stability. This is most likely due to the keratin in chicken feathers having thermal properties that cause it to break down at higher temperatures than other organic materials. When the amount of biofibre increased, the composite shows increased ability to withstand thermal degradation, showing that feather fibres helped maintain structural integrity in high temperatures.

Additionally, the TGA graphs showed a change in the beginning of decomposition at higher temperatures with an increase in the amount of chicken feather fibres. This showed that the fibres not only improved the thermal stability, but also prolonged the thermal degradation process. Enhancements like these are essential for applications that prioritise thermal resistance, like building materials used in environments with varying temperatures or high levels of heat. Hence, the integration of chicken feather fibres in composites not only utilises their mechanical advantages but also greatly enhances thermal stability, broadening the possibilities for their application in different high-performance scenarios.

2.3.8 Water Absorption of the Chicken Feather Fibre

Considerable research has also been carried out on the water absorption qualities of these fibres, which are considered essential for their effectiveness and application.

Feather fibres exhibit both hydrophobic and hydrophilic characteristics (Martínez-Hernández et al., 2005). While the keratin composition of the fibres makes them naturally hydrophilic, the presence of a waxy cuticle layer on the surface of the fibres can contribute to their hydrophobic properties. The ability to tailor the water absorption properties of chicken feather fibres through various treatments and modifications is an important consideration in their successful integration into a wide range of applications.

The chemical composition and physical structure of chicken feather fibres primarily affect their water absorption properties (Jaya et al., 2018). The chicken feather fibres are widely recognised for the hydrophilic quality of the protein keratin (Martínez-Hernández et al., 2005). This indicates that the fibres naturally absorb water, potentially impacting the mechanical and physical characteristics of the materials they are incorporated into.

Numerous research studies have examined the water absorption characteristics of chicken feather fibres. According to research, chicken feather fibres can absorb between 50% and 200% of water, with the absorption rate varying based on processing and treatment methods (Oladele et al., 2018). Another study discovered that modifying the fibres chemically, such as with the use of silane coupling agents, can decrease water absorption and enhance hydrophobic characteristics (Vinodh Kumar et al., 2021).

Water absorption in composites can create problems by compromising the connection between fibres and the polymer matrix, leading to reduced mechanical properties of the material.

Researchers have investigated various techniques such as chemical treatments, surface modifications, and hybrid composites to improve the hydrophobic nature of chicken

feather fibres. Advancements have been made to enhance the performance of these composite materials (Amieva et al., 2015).

2.3.9 Electrical Conductivity Properties of the Chicken Feather Fibre

It is also known that feather fibres have high resistivity when considering electric properties, with a dielectric constant of 1.7. The magnitude of the dielectric constant was most likely to be substantial due to the voids in the inner structure of the fibre. The barbs and rachis also have an electrical resistance of 6.74×10^{11} ohms and 8.13×10^{11} ohms respectively (Tesfaye et al., 2018). This could suggest the possible use of such fibres in electrical insulation materials, as well as in electronic components.

2.3.10 Degradation of the Chicken Feather Fibre

The keratin in chicken feathers is cross-linked by disulfide bonds, and this keratin structure exhibits remarkable resistance to degradation due to their robust structural properties. The keratin protein forms a tight, helical structure with extensive cross-linking via the aforementioned disulfide bonds, providing resilience against physical and chemical attacks. Despite their inherent durability, chicken feathers can undergo degradation through several mechanisms. Microbial degradation is a significant pathway, particularly involving keratinolytic microorganisms such as certain bacteria and fungi that produce keratinase enzymes (R. Gupta & Ramnani, 2006). This research outlines how the microbial keratinases enzymes degrade keratin in chicken feathers. These enzymes break down the disulfide bonds and peptide linkages in keratin, leading to the gradual decomposition of the feathers. In natural environments, where these microorganisms thrive, chicken feathers can be decomposed over months or years, depending on conditions such as moisture, temperature, and microbial activity.

Environmental factors also contribute to the degradation of chicken feathers. Exposure to ultraviolet (UV) radiation from sunlight can induce photodegradation, breaking down the keratin proteins' molecular structure. UV radiation causes the breakdown of amino acids and the disruption of disulfide bonds, leading to a loss of mechanical integrity and eventual fragmentation of the feathers (Cui et al., 2023). In the context of

the study's findings on improving biodegradation through microbial action, as mentioned in the previous paragraph, UV exposure may accelerate the initial breakdown of chicken feathers, making them more accessible to microbial enzymes for accelerated degradation. However, prolonged UV exposure can also lead to the degradation of the same microbial populations. Therefore, while UV radiation can facilitate initial degradation processes, its long-term impact on the overall degradation of chicken feathers in environmental contexts would depend on factors such as exposure duration, intensity, and subsequent microbial activity.

2.4 Chicken Feather Fibres in Cement-Based Mixes

A selection of research is available on the assessment of the behaviour of cement-based materials reinforced with chicken feathers. In one research project, the rachises were added at both 1% and 2% by mass of cement, and mechanical properties, namely compressive strength and tensile strength were observed to be greatest with 1% (Wahab & Osmi, 2012). In this study, however, there was no further testing done other than compressive strength test and tensile splitting test on cubes and cylinders after 7 and 28 days of curing. In other projects, the amount of fibres incorporated into the mix varies depending on the length of the fibres, with a combination of short fibres at 3 mm length, and long fibres at 20 mm length (Khan et al., 2022).

When considering ground feathers, it was observed that boards with ground feather, at 5%-10% by mass of cement, performed favourably in comparison with industrially available fibre cement board (Acda, 2009). In this literature, these boards were most notably tested for their durability when exposed to termites and decay fungi for 12 weeks, and then compared to wood and wood-based composites.

2.4.1 Processing of Feather Fibre to be used as Reinforcement

At present, there are various studies on how chicken feather fibres can be processed to be utilised in cement-based construction materials. In most cases, feathers are thoroughly cleaned, in order to remove any debris from the slaughterhouse including blood, oil, and other contaminants, using water and detergent over several wash

cycles, and then left to thoroughly dry in the sun for three days. In the project undertaken at the University of the Philippines Los Baños, the use of sodium chlorite was also used in the wash cycle (Mendoza et al., 2021). In a similar project at the Graphic Era University, Dehradun, India, running water and partial C_2H_5OH was used in order to remove the fatty layer on the feathers, before being left to dry for 24 hours (Bansal et al., 2017).

In order to extract the required aspect ratios of feathers required, various preparation methods have been done at different scales. In some projects, a combination of both long fibres and ground fibres have been used in the mix, such as in the case of the feather-board made at the University of the Philippines Los Baños with a combination of whole feather, ground feather, and an amalgamation of both (Acda, 2009).

In various projects, it is only the rachis that was used, where the barbs of the feather would be cut off using a pair of scissors, such as the case of the project undertaken by the Universiti Malaysia Pahang. The feather rachises were trimmed to 20 mm-40 mm lengths, to be added to the mix to create cube and cylinder samples of grade 30 concrete (Wahab & Osmi, 2012).

2.4.2 Chemical Treatments to Modify the Chicken Feather Fibre

Researchers have also studied the utilisation of coatings, chemical modifications, or surface treatments to enhance the bonding between chicken feather fibres and concrete (Huda et al., 2013). Coatings that enhance the connection between the fibre and matrix can improve stress transfer, increasing the composite's mechanical strength.

A demonstration of surface treatments was conducted by chemically modifying chicken feathers and integrating them into a high-density polyethylene matrix (Oladele et al., 2018). The procedure included alkali treatment and silane coupling, enhancing fibre-matrix adhesion and improving mechanical properties of the composites compared to unmodified fibres.

Another particular study involved treating feather fibres with sodium hydroxide, 10% maleinised polybutadiene rubber, and a silane-coupling agent (Huda et al., 2013). The

improvement in fibre properties, coupled with better adhesion between fibre and matrix, resulted in better mechanical properties of the composite materials. Surface-treated fibre-reinforced materials were discovered to have better mechanical properties than untreated fibre-reinforced composite materials (Huda et al., 2013).

Another chemical treatment example was conducted in which two distinct methods were studied - one method involved directly applying a water-repellent substance, while the other method involved treating the feathers with a blocking agent before applying a water-repellent coating. Both methods were shown to enhance the compressive, tensile, and flexural strengths of the concrete compared to untreated samples reinforced with feathers (Hamoush & El-Hawary, 1994).

2.5 Testing on Fibre Reinforced Cement-Based Mixes

Most literature compares the standard mechanical properties of the cement-based materials, including the compressive strength, tensile strength, and durability. Some projects involved assessing the impact on setting and hydration when working with feather fibre reinforced cement-based mixes. It has been observed that while the mix adds favourable characteristics in terms of strength (both tensile and compressive), it seemed to have an increased setting time when compared to control samples. It was also noted that the fibres had possibly blocked the effect of hydration sites or retarded the curing of cement by preventing the crystallisation of cement (Mendoza et al., 2021).

Studies dating back just over two decades at the University of Kuwait also show that feather fibre-reinforced concrete was tested to assess their compressive and tensile strength, using uniaxial compression tests and split tension tests. These were tested after 14, 28, and 56 days to be able to record the curing progress of the fibre reinforced concrete. During this testing however, it was noted that there was some decay in the feathers, once they were observed at the failure surfaces (Hamoush & El-Hawary, 1994).

2.5.1 Feather Fibres as Reinforcement for other Composites

It is also relevant to note that the use of feather fibres is not solely restricted as additives of cement-based materials. The incorporation of feather fibres in other materials, such as Ethylene Propylene Diene Rubber was also done at the Institute of Building Materials Research, Germany. This research involved a large variety of tests on samples of the elastomer with feather fibres as an additive in 2 mm and 5 mm thin sheets. The tests on this material included hardness and rebound resilience testing, uniaxial tensile testing, compression testing, small amplitude oscillatory shear testing, attenuated total reflection–Fourier transform infrared spectroscopy (ATR-FTIR) measurements, thermogravimetric analysis (TGA), Soxhlet extraction of vulcanised EPDM without sulphur, and scanning electron microscopy (SEM). So far, there has not been any notable research which goes into such depth for cement-based materials, however, the conclusions varied for each test depending on the length of the fibres used (Brenner & Weichold, 2021).

In another particular study, the behaviour of hot mix asphalt concrete with the incorporation of both processed (shredded) and unprocessed (not shredded) fibres was tested (Dalhat et al., 2020). When determining the mechanical properties for the mixes with shredded fibres, they produced lower strengths as compared to their unprocessed counterparts. The rationalisation for this is that the processed fibres relied mostly on the individual barbs, while the unprocessed fibres had more integrity when still connected to the rachis, which allowed for better load transfers between the fibres and the mix. The Marshall Stability was also noted to increase with the increase of fibre incorporation up to a percentage of 0.3%, and a reduction in stability was noted thereafter. A reduction in density and increase in air void was also noted with the incorporation of chicken feather fibres.

Another study examines the capillary, mechanical, impact and abrasion performance of earthen materials reinforced with chicken feather fibres (Gonzalez-Calderon et al., 2020). This study established that the capillarity improved with the increase of fibres in the mix, due to the hollow inner structure of the fibres. Mechanically, there was not

much variation from the control mix, which was expected due to the smaller dosages being tested. This, however, did not apply for flexural toughness, as an improvement in the post-cracking performance was noted. Similarly, it also proved significant positive effects on the impact strength, and the resistance to dry abrasion.

While in most studies the fibres are processed, either by grinding and/or shredding, there is also an effort in reducing the processing time by utilising the feather fibre as a whole. Research carried out in Nebraska in the United States of America, observed the impact of using whole chicken feathers as reinforcement for light-weight polypropylene composites (Reddy & Yang, 2010). The scope of this study was to exploit the already existing features of the feather fibres, namely the hollow core structure and the hierarchical arrangement of the quill, barbs, and barbules. These properties are difficult to replicate in synthetic fibres, which makes them preferable for light-weight composites. The results obtained from this study proved that the voids in the fibres allowed for better sound absorption and lower density, but had reduced mechanical performance.

2.6 Life Cycle Analysis on Chicken Feather Fibre Reinforced Composites

Very limited research exists on the life cycle analysis (LCA) of chicken feather fibre reinforced composites, and to the author's knowledge, there are none on feather fibre reinforced concrete.

A related study exists on chicken feathers with polylactide, a biodegradable plastic (Molins et al., 2012). The research focused on the LCA to determine the environmental impact of chicken feather/polylactide composites compared to conventional composites. The LCA framework used in this study follows the European Union's guidelines for sustainable development. The goal was to assess the environmental impacts of chicken feathers/polylactide composites, with varying chicken feathers content (0% to 35%), from the extraction of raw materials to the gate of the manufacturing facility.

The feathers underwent a cleaning and sanitising process with either a surfactant or sterilisation with steam. Then, the cleaned and crushed chicken feathers were mixed with polylactide and processed into composite plates using a Brabender mixer and a hot plate press. The study focused on six impact categories: abiotic depletion, acidification, eutrophication, global warming potential, ozone layer depletion, and photochemical oxidation. The data for the life cycle inventory were gathered from laboratory experiments and international databases.

The autoclave (steam sterilisation) process had less environmental impact than the surfactant cleaning process, mainly due to the reduced wastewater effluents in the autoclave process. Increasing the chicken feathers content in the composite plates resulted in a proportional increase in environmental impact. This was mainly due to the high energy consumption in the drying processes.

Therefore, it was concluded that the chicken feathers pre-treatment process significantly affects the environmental impact of the final composite material. The drying stage, in particular, is crucial for minimising environmental impacts. However, the study did not consider the environmental benefits of diverting chicken feathers from traditional waste management (incineration, composting), which might reduce the apparent environmental burden of chicken feathers polylactide composites.

Future studies should include the environmental impacts of post-use material disposal and the avoided burdens of traditional chicken feather waste management. Continued research is needed to optimise pre-treatment processes and to quantify the full life cycle impacts of polylactide or other composites such as concrete, reinforced with chicken feathers.

2.7 Lacunae in Research

The study of synthetic fibres as reinforcements in concrete has garnered significant attention due to their established mechanical properties and widespread availability. Similarly, there has been a growing interest in utilising feather fibres, a waste material from the poultry industry, as a sustainable alternative reinforcement in concrete. These

trends can indicate that there has been a steady rise in interest in synthetic fibre reinforced concrete, particularly in studying cracking behaviour and crack control of the material.

The strong emphasis on both synthetic and feather fibre reinforced concrete reflects a shift towards more sustainable and environmentally conscious construction methods. By repurposing waste materials like feathers into valuable resources for construction, researchers are contributing to the circular economy and diminishing dependence on synthetic resources.

The examination of synthetic fibres as reinforcements in concrete has attracted considerable attention owing to their well-established mechanical properties and wide availability. Likewise, there has been an increasing interest in employing feather fibres, a by-product of the poultry industry, as an eco-friendly alternative reinforcement in concrete. These trends suggest a consistent rise in the interest surrounding synthetic fibre reinforced concrete, particularly concerning the study of cracking behaviour and crack control in the material. On the other hand, while searching for literature on concrete cracking concerning natural fibres, specifically feathers, no relevant research was found, indicating an important gap in this area.

In conclusion, there is a lacuna in research when it comes to the crack control of such fibre reinforced cement-based materials. It has been observed in literature, that adding fibre "can improve the characteristic of concrete such as increase flexural strength and toughness, increase impact resistance, reduce shrinkage and cracking and also improve the durability by stabilization of microcracks" (Wahab & Osmi, 2012). However, the research does not extend to any experimental tests carried out to assess the possibility to control such cracks with feather fibre reinforcement. The use of fibres in cement-based materials could improve the existing cracking situation of concrete and other cement-based materials, where the brittle nature of concrete can be transformed into ductility with the addition of the feather fibres.

Therefore, the key contribution to knowledge of this research is the assessment of performance of early-stage cracking of cement-based materials using keratin feathers

fibres. An effective incorporation of feather fibres would envisage to create a circular economy by linking the waste from the poultry industry as reinforcement in the construction industry, while also proving that chicken feathers can be an accessible reinforcement material on a global scale.

Chapter 3

Methodology

3 Methodology

This chapter discusses the methodology which was utilised throughout the research, with particular focus on the preparation of the fibres, application in cement-based materials and performance assessment through an experimental investigation. This methodology was designed to systematically explore the development and performance of cement-based feather fibre reinforced materials. This research formed part of a larger project (MCST, 2024) which was funded by the MCST (now *Xjenza* Malta) Research Excellence Awards, which specified certain deliverables from the procurement of feathers and the development of the mix design to the preparation of cement-based fibre-reinforced materials. The research was structured into a series of stages, each employing specific methods and experimental setup and apparatus intended to achieve the research objectives. These stages ensured a logical and coherent progression from material characterisation to the final production of the fibre-reinforced cement-based construction material specimens according to European and international standards together with adapted methodologies.

3.1 Material Procurement and Collection

This section describes the materials which were utilised in the research and the methods of collection which were carried out. Unless otherwise stated, all the materials utilised in this research were procured from local sources and are already being used by the construction industry on a regular basis.

3.1.1 Cement

The cement used in this research was Ordinary Portland cement, specifically CEM II/A-LL 42.5 R packed locally by Central Cement Ltd, as shown in Figure 3.1. This cement is in accordance with the EN 197-1 standard. Overall, the selection of CEM II/A-LL 42.5 R cement in this research was based on its proven performance characteristics and its widespread use in local construction practices. This type of cement is particularly prevalent in local construction practices due to its optimal

balance of performance and availability. This composition and properties were essential in meeting the specific requirements of the high-strength and SCC formulations investigated in this study.

Figure 3.1 - Cement used in all Concrete and Mortar Mixes.

CEM cements consist of a number of constituent materials and are statistically homogeneous in composition resulting from quality in both the production and material handling processes (EN 197-1:2011, 2011). The composition of CEM II/A-LL 42.5 R includes a clinker content ranging from 80 to 94%, complemented by 6 to 20% limestone powder. This specific formulation enhances the properties of the cement, making it suitable for a variety of high-performance applications, as well as it being readily available on the market.

The clinker component, constituting the majority of the cement, imparts the necessary hydraulic properties, allowing the cement to set and harden through hydration. This is crucial for achieving the desired strength and durability in concrete structures. The inclusion of limestone powder not only contributes to the fineness and workability of

the cement but also aids in reducing the overall environmental impact by partially substituting clinker, which is energy-intensive to produce.

CEM II/A-LL 42.5 R is highly regarded for its versatility and is commonly employed in the production of high-strength concrete, which demands superior mechanical properties and durability. It is a medium strength cement (42.5) with rapid strength development, denoted by the 'R' classification, making it an excellent choice for applications where early strength gain is essential. This characteristic is particularly beneficial in construction projects with tight schedules or where structural elements need to be rapidly brought into service.

Furthermore, this type of cement is also well-suited for SCC, which requires excellent flowability and the ability to fill complex formwork without the need for mechanical vibration. The rheological properties imparted by CEM II/A-LL 42.5 R contribute to the production of SCC with consistent quality, enhancing both the ease of placement and the finished product's aesthetic and structural integrity.

The cement was delivered to the laboratory in 25 kg bags, keeping them sealed and stored in a cool, dry place until needed, to prevent the cement from hydrating while in storage. Prior to using the cement in the SCC mixture, the material was visually inspected to ensure that there was no cement hydration already taking place in the sack.

3.1.2 Aggregate

Dolomite aggregate was utilised in this research for both coarse and fine aggregate applications. Figure 3.2 shows a sample of the coarse aggregate stored in Jumbo Bags before being dried for use. The choice of dolomite, specifically sourced from Italy, was based on its favourable physical properties, which make it an ideal material for concrete production, particularly in self-compacting mixes.

The selection of dolomite aggregate was influenced by the fact that, while local aggregates are more readily available, the uniformity and consistency of reliability of

Italian dolomite in SCC mixes made it a superior choice. This reliability is paramount in ensuring the consistency and quality of the SCC, justifying the slightly higher emissions due to transportation. Despite the higher emissions associated with transporting foreign aggregate, the decision was justified by the uniformity and superior reliability of dolomite in achieving the desired performance in SCC when compared to lower quality, locally sourced coralline limestone aggregate.

Fortunately, dolomite aggregate from Italy is already readily available on the island as it is consistently used on various projects, eliminating the need for any additional deliveries specifically for this research. This availability further supported the decision to use this high-quality aggregate without compromising the environmental considerations excessively.

Figure 3.2 - The Dolomitic Aggregate used in the Research.

The coarse aggregate particles ranged from 10mm to 4mm in size. The reported oven dry particle density was 2.83 g/cm³ and a saturated surface-dried density was also 2.83 g/cm³ (Appendix D), with a very low water absorption of 0.2%. These densities indicate a high quality aggregate, essential for providing the necessary strength and durability in concrete structures.

For the fine aggregate, particles ranged from 4mm to 0mm. The fine aggregate had an oven dry particle density of 2.75 g/cm³ and a saturated surface-dried density of 2.76

g/cm³. These properties are critical for achieving the desired workability and cohesiveness in the concrete mix, ensuring a uniform distribution of the fine particles throughout the mixture.

The water absorption rates of the aggregates were also taken into account to ensure the accuracy of the mix design. The coarse aggregates had a water absorption rate of 0.2%, while the fine aggregate had a slightly higher absorption rate of 0.3%. These values were derived from the data sheets provided and are consistent with the standards required for high-quality concrete production.

In accordance with BS 812-109 (1990), the aggregates were oven dried for 24 hours at a temperature of 105°C before being used in the mixing process (BS 812-109:1990, 1990). This step was crucial to remove any moisture content in the aggregates, thereby ensuring control and accuracy of the water-to-cement ratio in the concrete mix and preventing any adverse effects on the concrete's strength and durability. Allowance was determined and made for the water absorption of aggregate in the mix.

This research was significantly supported by the sponsorship of CEM II/A-LL 42.5 R cement and dolomite aggregate provided by Central Cement Ltd.

3.1.3 Chemical Admixture

To achieve a self-compacting concrete mix, the liquid superplasticizer MasterGlenium SKY 698 shown in Figure 3.3 was utilised. This superplasticizer was sourced from Philip A. Tabone Ltd. and produced by BASF Construction Chemicals. MasterGlenium SKY 698 is specifically formulated to impart concrete with the fluidity and self-compaction capabilities required for SCC applications.

Figure 3.3 - Chemical Admixture used in the Research.

The use of this superplasticizer allowed for a significant reduction in the water-to-cement ratio without compromising the concrete's ability to resist segregation. This is crucial for maintaining high workability and ensuring the consistency of the SCC mix (BS EN 934-2:2001, 2003). The high-performance characteristics of MasterGlenium SKY 698 are particularly beneficial in achieving the desired properties of self-compacting concrete, which requires excellent flowability and stability.

The selection of MasterGlenium SKY 698 was based on its proven efficacy in reducing the water content while maintaining the required workability and stability of the SCC mix. This capability is essential for ensuring that the concrete can flow easily into formwork and around reinforcements without the need for mechanical vibration, which is a key requirement for SCC applications.

The recommended dosage for MasterGlenium SKY 698 is between 1.2 and 1.6 litres per 100 kg of binder. This dosage range is critical to achieving the optimal balance between fluidity and stability. Additionally, the superplasticizer has a relative density of 1.059

to 1.099 g/cm³ at 20°C. It contributes as an essential effective ingredient in SCC in enhancing the concrete mix's rheological performance.

By using MasterGlenium SKY 698, the research ensured that the SCC mix maintained its integrity and performance, meeting the stringent demands of self-compacting concrete. This choice was integral to the success of the project, providing the necessary properties to produce high-quality, durable concrete structures.

The research benefited greatly from the sponsorship of the MasterGlenium SKY 698 superplasticizer by Philip A. Tabone Ltd.

3.1.4 Fibres

The waste feather fibres which were used in this research were obtained from SMINA Poultry Products Ltd, supplied as shown in Figure 3.4. These fibres would have been separated from the remaining parts of the chicken to be sold or disposed of, as described in subsection 3.1.4.1. They were washed and stored in large bags for collection the next morning to be transported to the laboratory, where they would be stored in refrigerators until preparation for use. This preparation involved the decontamination and cleaning of the fibres, discussed in subsection 3.1.4.2, and a statistical analysis, outlined in subsection 3.1.4.3, in order to better understand the nature of the fibre before casting. The density of the fibres, as described in subsection 3.1.4.4, was also determined in order to be able to define the volume fraction to be incorporated into the mix. It was also decided that fibres would also be shredded to examine the behaviour of the materials with short and long fibres being incorporated. The shredding and separation of fibres is outlined in subsection 3.1.4.5.

Figure 3.4 - Collection of Fibres from SMINA Poultry Products Ltd.

3.1.4.1 Relevant Poultry Processing Stages at SMINA Poultry Products Ltd

During the sample collection period, SMINA Poultry Products Ltd obtained chickens from external sources, arriving at the farm for slaughter between 4.5 and 6 weeks of age. These chickens were supplied by around thirty approved farms, with orders placed well in advance. The process from ordering to hatching chicks took about 21 days. Once the chickens reached the appropriate age, they were transported to the plant based on size requirements; larger chickens were used for cuts, while smaller ones were sold whole. They arrived in crates designed to hold ten chickens, although larger chickens sometimes required crates holding only eight.

Upon arrival at the production plant, the chickens were manually hung upside-down on a motorised chain that spanned the entire facility, powered by two 1HP electric motors. This chain carried the chickens through the processing stages.

The first stage involved passing the chickens through a machine that administered a small electric shock to stun them. This shock was just strong enough to temporarily disorient the chickens, allowing them to regain consciousness and walk within 30 seconds, in compliance with Halal meat production standards. This disorientation made the subsequent neck-slitting process more humane. The blood was collected in a trough beneath the chain until the chickens were fully drained, and thus preventing contamination of any further parts.

Feather removal was carried out in two stages, as shown in Figure 3.5, to avoid damaging the skin or extremities. First, the chickens were exposed to hot water jets at temperatures between 50°C and 60°C, scalding them to facilitate feather removal. Next, rotating machine heads with rubber fingers gently removed the feathers as the chickens passed through. The removed feathers were then placed in bins and transferred into large bags for collection the following morning.

Figure 3.5 – (right) Scalder to Facilitate Feather Removal and (left) Tunnel Picker to Remove the Feathers.

On the back end, the waste accumulated from the process is collected outside and then pumped into a large drum. The pump is the largest engine on the facility, rating at 15HP and shown on the left in Figure 3.6. The drum, shown on the right in Figure 3.6, is used to separate the solids from the wastewater and is powered by an engine with a rating of approximately 1.1-1.2HP. The wastewater is treated and disposed, while the

mixed waste solids are dumped into large reusable plastic bins, which are transported to the WasteServ Thermal Treatment Facility (TTF) in Marsa. The TTF is 8.6km away, and each truck can carry up to six bins. Approximating from the receipt given by WasteServ, shown in the introductory chapter, each delivery contains between 3,500-4,500 kg of waste.

Figure 3.6 - (right) Collected waste is pumped up to the drum and (left) Drum which empties solids into the large plastic bin.

3.1.4.2 Cleaning and Degreasing Fibres

The preparation stage began with a thorough cleaning and degreasing process at the Built Environment Laboratory at the University of Malta. The fibres as samples, were initially coated with a fatty layer which needed to be removed, as can be seen in Figure 3.7 to ensure their suitability for use as fibre reinforcement.

Figure 3.7 – Feather Fibres before (left) and after (right) Cleaning Process.

This cleaning process involved repeatedly washing and rinsing the fibres with a degreasing detergent at least three times by hand. The cleaning agents used in the detergent were sodium laureth sulfate (20 to 30%) and lauramine oxide (5 to 10%), which are both surfactants ideal for breaking down oils and suspending dirt to be easily rinsed away. Detergents with sodium laureth sulfate and lauramine oxide are all readily available and are also simple and inexpensive to buy or make. This manual procedure was essential for effectively removing not only the fatty layer but also any blood, dirt, soil, and remaining pieces of skin that may have remained attached to the fibres. Ensuring the fibres were completely clean was crucial from a health and safety aspect, and for achieving the desired properties in the final concrete mix.

Figure 3.8 – Mechanical Drum used to Facilitate Cleaning Process.

After the washing and rinsing, the fibres were allowed to dry on trays in a ventilated oven, shown in Figure 3.9, set at 50°C for 24 hours. This drying period was carefully monitored until the mass of the fibres remained constant, indicating that they were thoroughly dried. Achieving a consistent mass was vital to ensure that the fibres would not introduce any additional moisture into the concrete mix, which could affect its properties, therefore ensuring control on the mix water content.

Figure 3.9 - Oven used for Drying Fibres at 50ºC for 24 hours.

Following the drying process, the feathers were visually inspected once again. Any remaining fragments or unwanted substances were carefully removed to ensure the purity and quality of the fibres. This final inspection step was critical to guarantee that only the cleanest and most suitable fibres were used in the subsequent stages of the research.

3.1.4.3 Statistical Analysis of Fibres

The aspect ratio of fibres is an essential parameter in fibre-reinforced concrete as it influences how effectively fibres can enhance concrete properties. Generally, fibres with a high aspect ratio, meaning they are longer and thinner, provide superior reinforcement to improve concrete properties. Multiple measurements were taken to determine the average diameter of waste chicken feather fibres, as they naturally vary in diameter.

The aspect ratio was calculated using an average of 400 measured samples, and by taking an average on the diameters measured at three points along the length of the fibre using a pair of calibrated digital vernier callipers for all measurements, shown in Figure 3.10. The following equation was used to calculate the aspect ratio:

$$\text{aspect ratio} = \frac{\text{length}}{\text{average diameter}}$$

In addition to the aspect ratio analysis, other important statistical tests using IBM SPSS Statistics (Version 29) were conducted, including assessing the distribution of fibre lengths, fibre thicknesses, and their correlations through descriptive statistical analysis, as well as normality tests (Kolmogorov-Smirnov and Shapiro-Wilk). These all would provide an insight on the characteristics of the fibres as they are received, to assess repeatability and scalability.

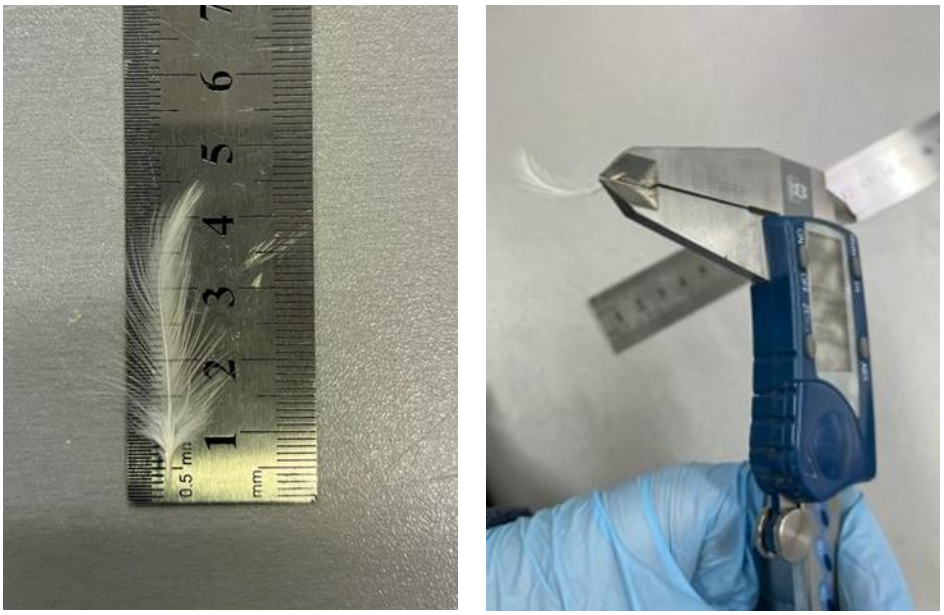

Figure 3.10 – Geometric Analysis of the Feather Fibres.

The sample size consisted of 400 feathers that were hand-measured for this classification and grouping process. Feathers were sorted into different groups based on their dimensions such as length and diameter. This classification was crucial to understand the distribution of feather sizes within the sample set, as well as their variability and uniformity. This information was essential for determining how

different size categories of feathers might influence the performance and characteristics of the fibre-reinforced concrete materials being studied.

Characterisation of the waste is an essential step, for classification and enabling the use of feathers as fibres, that is a product, in concrete. Furthermore, this statistical analysis provided a foundation for making informed decisions about the selection and utilisation of feathers in various stages of the research and development process. It helped optimise the manufacturing processes and ensure consistency in the fibres used for the final cement-based materials.

3.1.4.4 Density of Fibres

The density of the fibres was also assessed in order to appropriately account for them in the concrete mix design. Further to review of literature, it was decided to refer to method used for the determination of particle densities (BS EN 196-6:1989, 1992) in order to determine the density of feathers. The method entails a pycnometer being weighed empty, with fibres, and with fibres and deaerated water (BS EN 1097-6:2000, 2000), as shown in Figure 3.11. The following equation was used to calculate the density, based on the BS EN 196-6:1989 Standard:

$$P = \frac{W_4 \times P_L}{W_3 + W_4 - W_5}$$

where:

P is the density of fibres (in g/cm^3);

P_L is the density (in g/cm^3) of displacement liquid at the selected operating temperature;

W_3 is the mass (in g) of pycnometer, stopper and displacement liquid to fill the pycnometer at the selected operating temperature;

W_4 is the mass (in g) of sample of fibres;

W_5 is the mass (in g) of pycnometer, stopper, fibres sample and displacement liquid to fill the pycnometer at the selected operating temperature.

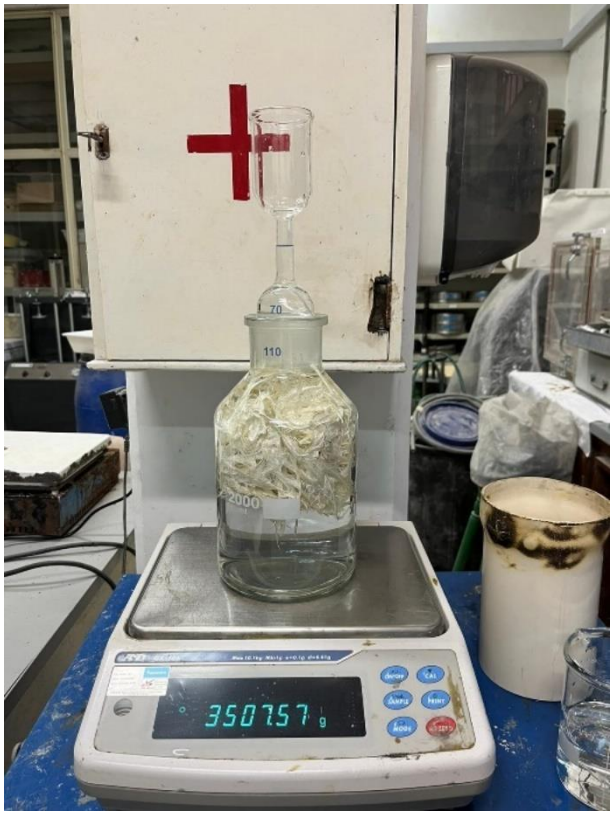

Figure 3.11 - Pycnometer and Digital Balance used to Measure Density.

3.1.4.5 Separation and Shredding of Fibres

The next steps involved shredding and cutting the fibres to specific lengths to obtain different aspect ratios for the mix designs cast. The long, stiff fibres, shown in Figure 3.12, were carefully separated by hand and set aside for possible use in casting large panel boards. A modified paper shredder was employed to facilitate this process, resulting in a range of short, shredded fibres and a collection of longer, unshredded fibres.

Various challenges arose when shredding the fibres, particularly due to their lightweight nature. In order to prevent fibres from escaping the blades, an aluminium tray was moulded to take the shape of a wider mouth to the shredder, to prevent the feathers from falling out of the narrow mouth. An adjusted steel handle was also used

to push the fibres into the blades, as there was a substantial amount of blockage when the fibres could not be pushed in further than a fingertip's length. While the narrowness of the paper shredder mouth is designed as a safety feature, it was preventing clumps of feathers from entering the blades without clogging up, so the use of the steel handle was a way to bypass this feature without risking injury or damage to the blades. Shredding was also done at short intervals, as the paper shredder would often heat up and activate the automatic shut-off safety feature, so care was taken to prevent any damage to the motor of the shredder. The air ventilation system was regularly cleaned out as this would get clogged with small loose feather fibres.

Figure 3.12 - The long, stiff feathers (b) were removed. The separation was done manually in order to leave only short, flexible fibres (a) for shredding.

This preparation of the fibres allowed for the development of various mix designs, enabling a comprehensive investigation into the performance of concrete reinforced with different fibre lengths and aspect ratios. The versatility in fibre preparation was crucial for tailoring the concrete mixes to specific performance criteria and applications.

3.2 Development of Mix Design

Initially, mix designs for a self-compacting mortar (SCM) were developed and assessed.

3.2.1 Self-Compacting Mortar Mix Design

On the basis of the control mix design, trial mixes for SCM were prepared in smaller batches in order to minimise waste of materials. The iterative approach was taken in order to optimise the mix design and relate the relative mix proportions to the fresh mortar properties as key performance criteria in the first stage. The mix design which was used for the SCM samples is shown in Table 3.1.

Table 3.1 - Self-Compacting Mortar Mix Design per Unit Volume.

Mix Proportions		*Control*	*0.125%*	*0.25%*	*0.5%*
Cement	kg	495	495	495	495
Water	kg	247.50	247.50	247.50	247.50
Fine Aggregate	kg	1728	1728	1725	1723
Superplasticiser	kg	5.94	5.94	5.94	5.94
Water Absorption	kg	5.18	5.18	5.18	5.17
W/C Ratio		0.50	0.50	0.50	0.50
Fibres Volume Fraction	%	0.00	0.125	0.25	0.50
Fibre Mass	kg	0.00	2.00	2.00	4.00

3.2.2 Self-Compacting Concrete Mix Design

Subsequently, the focus shifted towards evaluating and incorporating coarse aggregate to formulate a suitable SCC mix. This process involved meticulous adjustments and refinements to ensure that the SCC mix met the specified self-compacting properties and workability criteria outlined by EFNARC (European Federation for Specialist Construction Chemicals and Concrete Systems).

The control mix, which served as the baseline for comparison, was formulated without the inclusion of any fibres. In contrast, additional mixes were developed with varying dosages of fibres. This variation necessitated a volumetric adjustment through reduction in the amount of coarse aggregate used in each fibre reinforced mix. This adjustment was essential to accommodate the additional weight introduced by the fibres while maintaining the overall integrity and performance of the concrete.

Furthermore, trial mixes were prepared and extensively evaluated to validate the self-compacting properties and workability of each formulation. These trials were crucial in determining the optimal fibre dosages and their effects on the concrete's mechanical and durability properties. This iterative process ensured that the final mix formulations not only met the project objectives but also to observe any deviations from the industry standards for SCC.

By carefully managing the balance between fibres and coarse aggregate, the research aimed to enhance the structural integrity and performance characteristics of the concrete. This approach not only addressed the technical challenges associated with fibre reinforcement but also contributed to advancing sustainable construction practices by utilising waste materials effectively in concrete production. The mix design proportions are as shown in Table 3.2.

Following the development of the mix design, a standard naming convention was used in order to distinguish between samples shown in Table 3.3, and this varied according to fibre volume fraction % incorporation as well as the length range of the fibres, short (S) and long (L). The C annotation was used to specify that the mixes being cast were concrete mixes with both fine and coarse aggregates.

Table 3.2 - Self-Compacting Concrete Mix Design per Unit Volume.

Mix Proportions		*Control*	*0.125%*	*0.25%*	*0.50%*
Cement	kg	495	495	495	495
Water	kg	222.75	222.75	222.75	222.75
Fine Aggregate	kg	1080	1080	1080	1080
Coarse Aggregate	kg	648.0	645.5	643.0	638.0
Superplasticiser	kg	5.94	5.94	5.94	5.94
Water Absorption	kg	5.18	5.18	5.17	5.15
W/C Ratio		0.45	0.45	0.45	0.45
Fibres Volume Fraction	%	0.00	0.125	0.25	0.50
Fibre Mass	kg	0.00	1.00	2.00	4.00

Table 3.3 - Naming Convention for Self-Compacting Concrete Mixes.

Mix Code	*Fibre %*	*Fibre Length*
C0	-	-
C0.125S	0.125%	5 - 42mm
C0.125L	0.125%	30 - 75mm
C0.25S	0.25%	5 - 42mm
C0.25L	0.25%	30 - 75mm
C0.5S	0.50%	5 - 42mm
C0.5L	0.50%	30 - 75mm

SCM mixes used in the Kraai Test followed a similar naming convention, as shown in Table 3.4. It is to be noted that it would not have been possible to hand trim the quantity of fibres needed for the SCM panels used in the Kraai Test; which is why the same shredded fibres were used in the SCM as in the SCC.

Given that the SCM mixes were done on a smaller scale, it was possible to hand cut the fibres using a pair of scissors to exact lengths as follows, 15 mm, 25 mm, 35 mm, and 50 mm, at varying percentages as shown in Table 3.5. This selection of lengths was based on the nature of the mortar prism moulds, as since the shortest side would be 40 mm, it would not have been ideal to have fibres exceeding this length by a considerable amount. This refinement was intended to better understand the effect of feather fibre aspect ratio on the performance of mortar properties, given it is typically easier to handle and manage smaller volumes of material at mortar scale enabling assessment based on a wider fibre range.

Table 3.4 - Naming Convention for Self-Compacting Mortar Mixes used for Kraai Test Panels.

Mix Code	*Fibre %*	*Fibre Length*
M0	-	-
M0.125S	0.125%	5 - 42mm
M0.25S	0.25%	5 - 42mm
M0.5S	0.50%	5 - 42mm

Table 3.5 - Naming Convention for Self-Compacting Mortar Mixes.

Mix Code	*Fibre %*	*Fibre Length*
M0	-	-
M15-0.25	0.25%	15 mm
M25-0.25	0.25%	25 mm
M35-0.25	0.25%	35 mm
M50-0.25	0.25%	50 mm
M15-0.50	0.5%	15 mm
M25-0.50	0.5%	25 mm
M35-0.50	0.5%	35 mm
M50-0.50	0.5%	50 mm
M15-0.75	0.75%	15 mm
M25-0.75	0.75%	25 mm
M35-0.75	0.75%	35 mm
M50-0.75	0.75%	50 mm
M15-1	1%	15 mm
M25-1	1%	25 mm
M35-1	1%	35 mm
M50-1	1%	50 mm

3.3 Concrete Mixing and Casting

Following the establishment of the mix design, the mixing stage commenced according to the mix protocol based on sequence of added material and mixing time; followed through by the determination of the fresh properties of the mixes and then the casting of samples for the determination of early-stage properties and hardened concrete properties.

3.3.1 Concrete Mixing Protocol

Self-Compacting Concrete is a highly fluid mixture that has the capability to flow and fill all voids in a mould without the need for external compaction. The following procedure, based on previous work carried out at the University of Malta (Vella, 2018), outlines the steps undertaken to achieve a consistent and homogeneous SCC mix:

a. Buttering of the Mixer: The process commenced with the buttering of the mixer, where a small amount of cement and water were mixed for 1 minute. This step ensured that the inner surfaces of the mixer were coated, preventing initial material loss.
b. Loading Aggregates: The mixer was then loaded with both coarse and fine aggregates. These components were mixed for a duration of 3 minutes to ensure thorough blending.
c. Initial Water Addition: At 2 minutes into the mixing process, around 60% of the total water was incrementally added to the aggregates. This step was followed by an additional minute of mixing to facilitate initial hydration and distribution of water among the aggregates.
d. Rest Period for Water Absorption: The mixer was switched off for 2 minutes to allow the aggregates to fully absorb the added water. This rest period was crucial for achieving the desired moisture content within the aggregates, enhancing the overall mix quality.
e. Superplasticizer Addition: The remaining water, along with the superplasticizer, was then added to the mixture.

f. Resuming Mixing: The mixing process was resumed, combining the cement and aggregates for an additional 2 minutes.
g. Incorporating Fibres: After 1 minute of mixing, the feather fibres were introduced into the mixture. These fibres were gently dusted and scattered over the top of the mixture and constantly visually inspected to ensure that the fibres were not clumping, particularly at the blades of the mixer.
h. Final Mixing: The mixture was then left to mix for an additional 2 minutes. This final mixing period ensured that the fibres were uniformly distributed throughout the SCC, resulting in a homogeneous and consistent final product.

A digital timer and a well-functioning and lubricated pan mixer shown in Figure 3.13 were used in order to ensure consistency between mixes. This detailed procedure ensured the production of high-quality SCC, characterised by its excellent flowability, self-compaction ability, and enhanced mechanical properties. The careful monitoring and control of each step in the mixing process was crucial for achieving the desired performance characteristics of the final concrete product.

Figure 3.13 - Pan Mixer used for Casting all SCC Mixes.

3.3.2 Self-Compacting Concrete Sample Casting

The preparation and use of moulds for casting concrete specimens followed a standard procedure to ensure the integrity and quality of the specimens. All moulds were prepared and thoroughly greased with a de-moulding agent prior to mixing. This step was crucial for ensuring the easy removal of the concrete specimens from the moulds without causing any damage. This step is carried out well in advance and before the mixing stage in order to minimise time losses which would affect the quality of the sample.

After the concrete mix was prepared and its fresh properties were tested, it was cast into the moulds according to the specific requirements of each test, as shown in Figure 3.14. All samples were individually labelled with the mix code and date of casting for identification. The following moulds were utilised for casting the specimens:

- Cubes measuring 100 x 100 x 100 mm; these cubes were used to determine the compressive strength of the concrete.
- Beams measuring 150 x 150 x 550 mm; these beams were used for flexural strength tests.
- Cylinders with dimensions of 150 mm in diameter and 300 mm in height; these cylinders were employed for indirect tensile strength tests.
- Cylinders with dimensions of 100 mm in diameter and 200 mm in height; these cylinders were then sliced and used to test the durability of concrete with respect to chloride ion penetration.
- Environmental Chamber Slab specimens measuring 560 x 355 x 100 mm; these specimens were used to study the effects of the intense environmental conditions on the concrete.
- Ring specimens with an outer diameter of 405 mm and inner hollow diameter of 330 mm, and a height of 150 mm; these were used to test the restrained drying shrinkage over 28 days.

Figure 3.14 - Samples cast in the various Moulds to be Demoulded.

Following the casting process, all moulds were left covered in plastic sheeting and undisturbed to allow the concrete to harden. After a period of 24 hours from casting, the moulds were carefully removed by dismantling them and the specimens were extracted.

3.3.3 Curing of Samples

The demoulded specimens were then placed in a controlled water tank for further curing, as shown in Figure 3.15. This curing process continued until the specimens were ready for testing, ensuring optimal hydration and strength development. The water tank was constantly inspected for leaks and the temperature was monitored on a daily basis, to ensure that the samples were being cured at 21°C in a controlled environment as specified in BS EN 12390-2 Standard. Before placing the samples in the tank, the paper label was replaced with a paint marker label, to ensure that the specimens would all be distinguishable even after 28 days of water curing. The labelled sides of the specimen were placed facing upwards in the tank, which would prevent any disturbances to the other specimens when extracting the ones to be tested.

Figure 3.15 - Specimens curing in Controlled Water Tank (BS EN 12390-2:2009, 2009).

3.4 Experimental Program on Fibre-Reinforced Self-Compacting Cement-Based Materials

3.4.1 Fresh Properties of Concrete

The initial evaluation of the concrete mix focused on its fresh properties. Given that this mix was designed as SCC, it was crucial to thoroughly examine these properties to ensure that the mix, even with the inclusion of fibres, met the established SCC standards. Assessing the fresh properties of SCC involves examining parameters such as flowability, viscosity, passing ability, and resistance to segregation (EFNARC, 2005). These properties were evaluated through a series of empirical tests: namely the Slump Flow, T_{500}, V-Funnel, and L-Box tests.

To maintain consistency in the assessment, the testing methodology followed was comparable to that used previously at the University of Malta (Abdilla, 2021; Vella, 2018). The sequence of testing began with the Slump Flow test, followed by the V-Funnel and L-Box tests, all conducted within two minutes of each other. These evaluations were performed at three different intervals: immediately after mixing (t_0), 15 minutes after mixing (t_{15}), and 30 minutes after mixing (t_{30}). The SCC was at rest and mixed again at each time interval. This approach provided insight into how the fresh properties of SCC mixtures responded to varying amounts and lengths of feather fibres, over time, when the concrete was in its fresh state. For a more in-depth analysis of the fresh properties of the mix, the rheology was assessed using an ICAR Plus Concrete Rheometer.

3.4.1.1 Workability and Flowability Test

The Slump Flow test began with positioning a slump cone in the centre of a 900 mm by 900 mm glass sheet. The cone, as shown in Figure 3.16, was filled with a pour of concrete without any mechanical compaction. Any excess concrete that spilled onto the glass sheet was carefully removed. The cone was then lifted vertically, and the time required for the concrete to spread to a diameter of 500 mm (t_{500}) was recorded. This time was recorded with a digital stopwatch to the nearest 0.5 s. Once the concrete flow

stabilised, the average diameter of the slump flow was calculated by measuring two perpendicular diameters. This test adhered to the BS EN 12350-8 Standard.

Figure 3.16 - Slump Flow Test Setup (BS EN 12350-7:2009, 2019).

The equation used to determine the slump flow is as follows:

$$SF = \frac{\left(d_1 + d_2\right)}{2}$$

where:

SF is the slump flow, (in mm);

d_1 is the largest diameter of the flow spread, (in mm);

d_2 is the flow spread at 90° to d_1, (in mm).

The classification for the slump flow was then determined based on Table 3.6, whilst the T_{500} classification was determined as stated in Table 3.7

Table 3.6 - Slump Flow Classification (EFNARC, 2005).

Class	*Slump Flow in mm*
SF1	550 to 650
SF2	660 to 750
SF3	760 to 850

Table 3.7 - T_{500} Classification (EFNARC, 2005).

Class	*T_{500} time in s*
VS1	≤ 2
VS2	> 2

3.4.1.1.1 Slump Test

In the highest percentage of fibre incorporation, the Slump Flow Test designed for SCC was not possible, so the Slump Test (BS EN 12350-2:2000, 2000) designed for conventional concrete was carried out in its place. The slump cone was placed on a glass sheet and held down steadily while the concrete was poured in three stages. Between each stage, the concrete was tamped 25 times with a rod. Following the third and final filling and tamping stage, the excess concrete was levelled off the top and the glass sheet was cleaned from any spillage. The cone was then lifted swiftly and vertically to present a slump, and the height of the slump was measured from the ground. The shape of the slump was also visually inspected to ensure that a true slump was achieved, as opposed to a collapse or shearing. This test conformed to the BS EN 12350-2 Standard.

3.4.1.2 Viscosity and Flowability Test

For the V-Funnel test, the SCC was poured into the funnel shown in Figure 3.17, positioned on a flat surface, without any mechanical compaction, ensuring the hinged gate was closed. After levelling the top surface of the concrete, it was allowed to settle for 10 ± 2 seconds before opening the gate. The time (t_v) taken for the concrete to flow out of the funnel was recorded. This test followed the BS EN 12350-9 Standard. The classification of viscosity was then determined based on

Table 3.8.

Figure 3.17 - V-Funnel Test Setup (BS EN 12350-9:2010, 2010).

Table 3.8 - Viscosity Classification for V-funnel Test.

Class	*V-Funnel time in s*
VF1	≤ 8
VF2	9 to 25

3.4.1.3 Passing Ability Test

The L-Box test involved pouring the concrete vertically into the back container of the L-shaped apparatus shown in Figure 3.18, with the sliding gate closed, and allowing it to settle for approximately 60 ± 10 seconds. A rectangular shaped funnel was used to facilitate the filling process. The gate was then opened to permit the concrete to flow. Measurements of the heights H_1 and H_2 were taken at three different points, and their averages were calculated to determine the PL ratio for each mix. This test was conducted in accordance with BS EN 12350-10 Standard.

Figure 3.18 - L-Box Test Setup (BS EN 12350-10:2010, 2010).

The PL ratio is calculated as follows:

$$PL = \frac{H_2}{H_1}$$

where:

PL is the passing ability ratio measured by the L box test;

H_1 is the mean depth of concrete in the vertical section of the box (in mm);

H_2 is the mean depth of concrete at the end of the horizontal section of the box (in mm).

The classification of passing ability was then determined based on Table 3.9 below.

Table 3.9 - Passing Ability Classification for L-Box Test

Class	*V-Funnel time in s*
PA1	≥ 0.80 with 2 rebars
PA2	≥ 0.80 with 3 rebars

3.4.1.4 ICAR Plus Concrete Rheometer: Rheology of Concrete

The rheological properties of the concrete were assessed using an ICAR Plus Concrete Rheometer, shown in Figure 3.19, a device commonly used to evaluate the flow characteristics and workability of SCC (German Instruments A/S, 2010). A fresh concrete sample was poured into a steel container with a diameter of 205 mm and a height of 312 mm. The rheometer measured the torque and rotation as a four-bladed vane was inserted into the container. Two tests were conducted: the stress growth test and the flow curve test.

Figure 3.19 - ICAR Plus Concrete Rheometer.

The stress growth test aimed to compute the static yield stress by establishing the maximum torque and static yield. This test used an input speed of 0.025 rps. The stress growth test gently induced spinning from the vane to shear the concrete at a steady rotational speed while measuring the torque. The static yield stress, which is the stress that must be exceeded to initiate flow from a rest state, was equivalent to the maximum torque observed. The shear history of the sample significantly impacted the results of the stress growth test.

The flow curve test was conducted to determine the dynamic yield stress and plastic viscosity, using a rotation speed of 0.5 rps. The relative Bingham parameters were determined by taking torque measurements at seven different speeds, ranging from 0.5 rps to 0.05 rps. The setup of these parameters is shown in Figure 3.20. This test calculated the Bingham parameters of yield stress and plastic viscosity, as well as the correlation between shear stress and shear rate. In this test, the stress resulting from a decrease in the rate of deformation from high to low values was referred to as the dynamic yield stress. Therefore, the stress required to maintain flow correlated with the SCC slump-flow values. The rotating speed in the flow curve test was typically increased from zero to a relatively high value and then sustained long enough to break down any thixotropic structure.

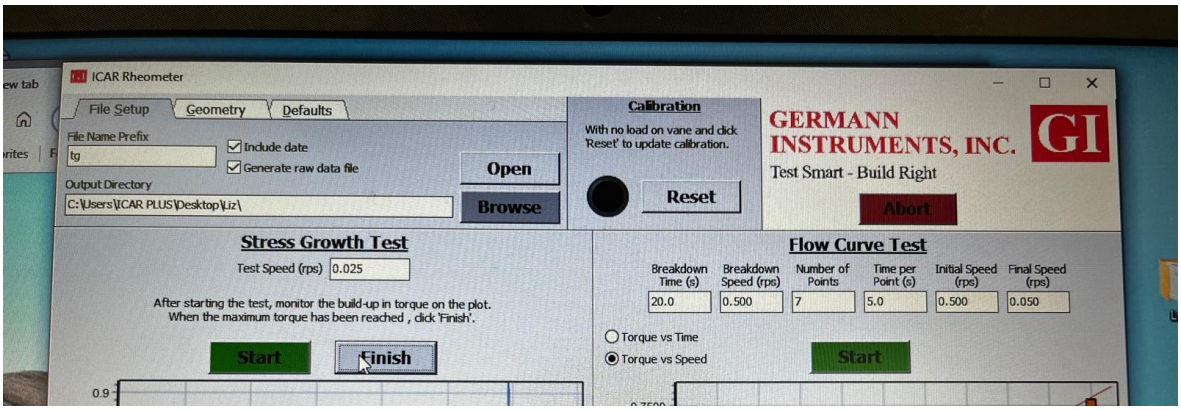

Figure 3.20 - Setup of Parameters on ICAR Rheometer Software.

The equation then used to describe the Bingham Model was as follows:

$$\tau = \tau_0 + \mu_{pl}\dot{\gamma}$$

where:

τ is the shear stress (in Pa);

τ_o is the yield stress (in Pa);

μ_{pl} is the plastic viscosity in (Pa·s);

$\dot{\gamma}$ is the shear rate (in s^{-1}).

Since all the empirical tests were repeated thrice, the surfaces were all cleaned with a damp cloth in between each of the tests to prevent hindrance with the results. The ICAR Plus Concrete Rheometer was only used at the t_0 time interval, as the duration of these tests was significantly longer than the empirical tests, and it would not have been possible to adhere to the same time frame.

This comprehensive evaluation of the fresh properties of the SCC mixes provided valuable insights into how the inclusion of feather fibres affected the mix's performance over time.

3.4.2 Physical and Mechanical Properties of Self-Compacting Mortars

3.4.2.1 Self-Compacting Mortar Density Test

The hardened mortar density test was conducted to evaluate the SCM's strength and durability. Initially, the 40 x 40 x 160 mm SCM prisms were removed from the curing tank and any residual water was carefully wiped off with a damp cloth. Each prism was then measured for its dimensions using a pair of calibrated digital vernier callipers, and its mass was accurately recorded using a calibrated digital balance. Following this, the specimen was placed on a stirrup as shown in Figure 3.21, and the scale was tared to zero to ensure precise measurements. The prism was then fully submerged in the tank with clean water, and its submerged mass was recorded again. This test was performed on the 3rd, 7th and 28th day after casting, and was performed in strict accordance with the BS EN12390-7 standard to ensure consistency and reliability in the results.

Figure 3.21 - Mortar Prism on the Stirrup before Submersion (BS EN 12390-7:2009, 2009).

3.4.2.2 Ultrasonic Pulse Velocity Test

The ultrasonic pulse velocity test aimed to determine the time it takes for an ultrasonic pulse to travel through the SCM sample, providing insight into the material's uniformity and integrity (BS EN 12504-4:2004, 2004). Prior to each test, the equipment was meticulously calibrated to ensure accuracy. Petroleum jelly was applied to the flat surfaces of the 40 x 40 x 160 mm SCM prisms to act as a coupling medium, facilitating efficient transmission of the ultrasonic pulse. Two transducers were placed on opposite faces of the specimen as shown in Figure 3.22 to enable direct transmission. The time taken for the pulse to travel through the SCM prism was then recorded. This test was performed on the 3rd, 7th and 28th day after casting, adhering to the guidelines outlined in BS EN 12504-4 (2004), to ensure standardised and comparable results.

Figure 3.22 - Ultrasonic Pulse Velocity Test Setup (BS EN 12504-4:2004, 2004).

The equation to calculate the velocity of the pulses was as follows:

$$V = \frac{L}{T}$$

where:

V is the pulse velocity (in km/s);

L is the path length (in mm);

T is the time taken by the pulse to transverse (in μs).

3.4.2.3 Flexural Strength Test

Similarly to the concrete compression test, smaller 40 x 40 x 160 mm SCM prisms were tested for their flexural strength. These tests were carried out on the 3rd, 7th, and 28th days from casting. This test was carried out with a three-point bending rig shown in Figure 3.23, similar to the one used for the SCC mentioned above. This smaller setup, however, applied a load rate of 50 N/s onto the prisms. The distance between the rollers was kept constant at 100 mm and the top roller was placed at the mid-point of the prism. This test was carried out in accordance with BS EN 1015-11 (1999).

Figure 3.23 - Mortar Flexural Test Setup (BS EN 1015-11:1999, 1999).

The equation used to calculate the flexural strength of the SCM was:

$$f = 1.5\frac{Fl}{bd^2}$$

where:

f is the flexural strength (in N/mm^2);

F is the maximum load (in N);

l is the distance between the two rollers (in mm);

b is the width of specimen (in mm);

d is the depth of the specimen in (in mm).

3.4.2.4 Compressive Strength Test

Once the specimen was split into two halves, each of the halves would then proceed to be tested for its compressive strength. The specimens were then placed in a compression testing machine in a manner such that the rough, cracked surface does

not interfere with the loading plates, as in Figure 3.24, and a constant loading rate of 2400 N/s was applied until failure occurred. Prior to loading, it was crucial to dust off any fragments remaining from the flexural tests, as these would have acted as a point load on the surface of the specimen. Post-failure, the cubes were visually examined to ensure they failed in a satisfactory manner, with any loose concrete removed using a steel hammer. These tests were carried out in accordance with BS EN 1015-11 (1999) and were carried out on the 3rd, 7th, and 28th days from casting.

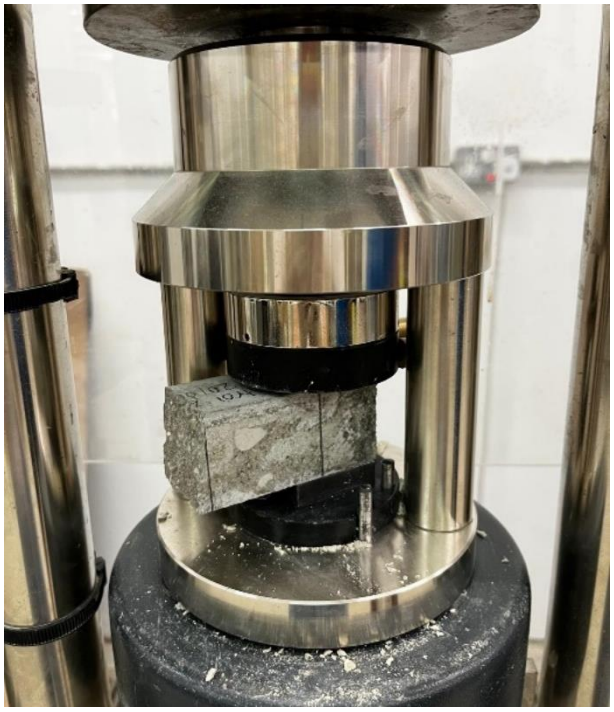

Figure 3.24 - Compression Test Setup (BS EN 1015-11:1999, 1999).

The results of the compressive strength test were calculated using the following equation:

$$f_c = \frac{F}{A_c}$$

where:

f_c is the compressive strength (in MPa or N/mm^2);

F is the maximum load (in N);

A_c is the cross-sectional area of specimen (in mm^2).

3.4.3 Physical and Mechanical Properties of Self-Compacting Concrete

3.4.3.1 Density Test

The hardened concrete density test was carried out to determine and compare the SCC's density among the fibre-reinforced mixes. Initially, the 100 x 100 x 100 mm SCC cubes were removed from the curing tank and any residual water was carefully wiped off with a damp cloth. Each cube was then measured for its dimensions using a pair of calibrated digital vernier callipers, and its mass was accurately recorded using a calibrated digital balance. Following this, the specimen was placed on a stirrup and the scale was tared to zero. The prism was then fully submerged in the clean water tank, and its submerged mass was recorded again. This test was performed in accordance with the BS EN12390-7 standard.

3.4.3.2 Compressive Strength Test

Compressive strength tests were conducted on cube specimens measuring 100 x 100 x 100 mm on both the 7th and 28th days from casting of each mix design. After removing the cubes from the curing tank, they were wiped clean, measured for dimensions, and weighed to obtain accurate data. The cubes were then placed in a compression testing machine as shown in Figure 3.25 where a constant loading rate of 0.6 MPa/s was applied until failure occurred.

Figure 3.25 - Concrete Cube Compression Test Setup (BS EN 12390-3:2009, 2009).

Post-failure, the cubes were visually examined to ensure they failed in a satisfactory manner, with any loose concrete fragments removed using a steel hammer. This thorough procedure followed the guidelines specified in BS EN 12390-3 (2009), ensuring the integrity and reliability of the test results.

The results of the compressive strength test were calculated using the following equation:

$$f_c = \frac{F}{A_c}$$

where:

f_c is the compressive strength (in MPa or N/mm^2);

F is the maximum load (in N);

A_c is the cross-sectional area of specimen (in mm^2).

3.4.3.3 Splitting Tensile Strength Test

Tensile splitting strength tests were performed on cylinder specimens, each measuring 150 mm in diameter and 300 mm in height, on the 7th and 28th days after casting for each mix design. The cylinders were carefully cleaned, measured, and centred in the tensile testing machine as shown in Figure 3.26. A load of 0.05 MPa/s was applied to the specimens until they reached failure. Post-failure, the specimens were visually inspected to observe the ductility of the samples. This test followed the detailed guidelines outlined in BS EN 12390-6 (2009), ensuring that the tensile properties of the concrete were accurately assessed.

Figure 3.26 - Splitting Tensile Stress Test Setup (BS EN 12390-6:2009, 2009).

The equation used to calculate the tensile splitting strength was:

$$F_{ct} = \frac{2 \times F}{\pi \times D \times L}$$

where:

F_{ct} is the tensile splitting strength (in MPa or N/mm^2);

F is the maximum load (in N);

L is the length of specimen (in mm);

D is the diameter (in mm).

3.4.3.4 Flexural Strength Test

Flexural strength tests were conducted on two concrete beams for each mix design, each measuring 150 x 150 x 550 mm, on the 7th and 28th days after casting. Before testing, the beam samples were wiped to remove excess water and carefully measured. A 5 mm ridge was made at the centre, shown in Figure 3.27, across the bottom width of each beam to induce the crack and to insert a crack mouth opening displacement (CMOD) transducer to measure the crack opening.

Figure 3.27 – Table Saw and 5mm Ridge cut in Flexural Test Specimens (BS EN 14651:2007, 2007).

A three-point bending rig consisting of two roller supports and a central top roller that applied a point load, shown in Figure 3.28, was used to determine the flexural strength of each beam. Additionally, two linear variable differential transformers (LVDTs) connected to a data logger were positioned on either side of the top roller to record the deflection accurately, and a load rate of 0.2 mm/min was applied. This comprehensive test was conducted following the (BS EN 14651:2007, 2007) standard to ensure precise and reliable results. These results would then proceed to be used to determine the flexural toughness factor (JSCE-SF4, 2005), a characteristic which is assessed according to the JSCE-SF4 Standard.

Figure 3.28 – Flexural Strength Test Setup (BS EN 14651:2007, 2007).

The equation used to calculate the flexural strength of the concrete (BS EN 14651:2007, 2007) was:

$$F_{R,j} = \frac{3 \times F_j \times l}{2 \times b \times h_{sp}^{\ 2}}$$

where:

$F_{R,j}$ is the residual flexural tensile strength (in MPa or N/mm²);

F_j is the maximum load (in N);

l is the distance between the two rollers (in mm);

b is the width of the specimen (in mm);

h_{sp} is the height of the specimen (in mm).

The equation used to calculate the flexural toughness factor (JSCE-SF4, 2005) was:

$$\sigma_b = \frac{T_b}{\delta_{tb}} \times \frac{l}{bh^2}$$

where:

σ_b is the flexural toughness factor (in MPa or N/mm²);

T_b is the flexural toughness – area under load-deflection graph (in N·mm);

δ_{tb} is the deflection of L/150 of span (in mm);

l is the span between rollers (in mm);

b is the breadth of sample (in mm);

h is the height of sample (in mm).

3.4.3.5 Pull-Out Test

A series of pull-out tests were conducted to assess the bonding between the fibre and the concrete matrix, similar to those conducted for PET plastic (Borg et al., 2016). The purpose of these tests was to examine the fibre's adhesion to the cement paste by applying a vertical tensile load. For test preparation, various 50 x 50 x 50 mm cement paste cubes were cast, with a single fibre embedded at a depth of 10 mm from the surface. This depth provided sufficient adhesion to the matrix and allowed for controlled vertical application to prevent torsion during the pull-out testing.

After curing for 7 days, the samples were carefully set up in a Testometric tensile testing machine, shown in Figure 3.29, with a load cell of 500 N was applied, with a resolution of 0.001 N and an accuracy of ± 0.1%. Before securing to the bottom clamp, the sample was rotated to ensure proper alignment with the upper clamp, to prevent any torsion between the fibre and the clamp. Once secure, the fibre was securely gripped with a rubber-lined clamp, and the positioning was sensitively adjusted to eliminate any initial stresses in the fibre. Once the initial stresses were zeroed, a loading rate of 0.5 mm/min was applied to carefully examine the relationship between the fibre and the cement paste without tearing the fibre. Additionally, dedicated lighting and a mounted camera were used to capture steady images of the fibre pull-out at 30-second intervals.

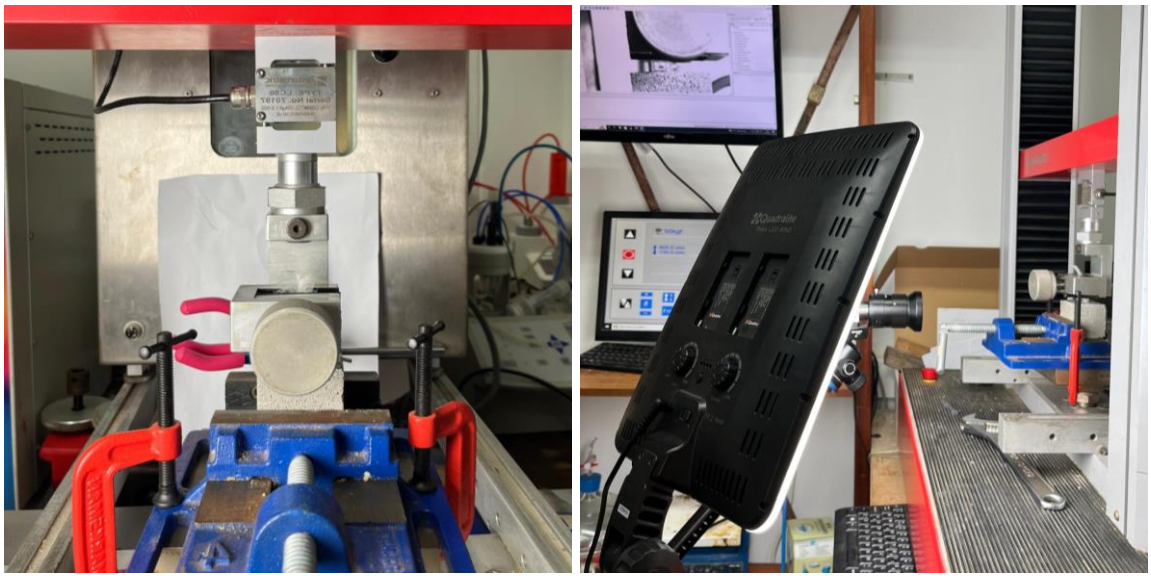

Figure 3.29 - Sample set up in Tensile Loading Machine with 500 N load cell (left) and Camera (right).

3.4.4 Shrinkage Properties of Concrete

3.4.4.1 Restrained Shrinkage Cracking Test

This test aimed to determine the age at which concrete developed shrinkage cracks due to tensile stresses under constrained shrinkage conditions (ASTM C1581-04, 2004). The testing apparatus consisted of an outer PVC ring and an inner steel ring, secured by four eccentric washers during casting. Dimensions of the mould are presented in the annotated diagram in Figure 3.30. To measure the strain on the inner ring, two strain gauges (FLA-30-11-5L) were attached at mid-height on opposite sides of the inner steel ring, shown in Figure 3.31.

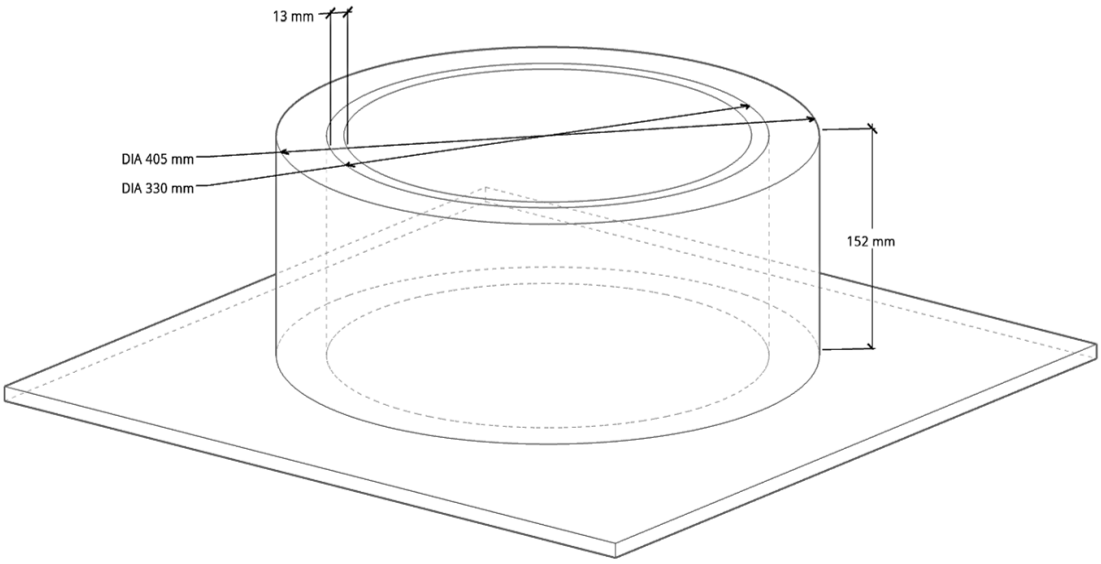

Figure 3.30 - Ring Test Specimen Size adapted diagram (ASTM C1581-04, 2004).

Figure 3.31 - Strain Gauge attached to the inner wall of the Ring.

Before casting, an epoxy coating was applied to the mould to reduce frictional restraints. The ring was kept in a controlled environment at a temperature of 23 ± 2°C. Following the casting process, the eccentric washers were loosened as shown in Figure 3.32, and a data logger began recording the strain every 10 minutes. After 24 hours, the

outer PVC ring was carefully removed, and paraffin wax was applied to seal the top surface of the specimen. The sample was visually inspected daily for any cracks which may have appeared on the surface. A sudden drop in strain values on the steel ring usually indicated that the concrete had cracked. The sample was left undisturbed until the 28th day from casting, where on the 29th day, the concrete ring was destroyed, and the apparatus was reused for other mix designs. This procedure was conducted according to ASTM C1581-04 (2004).

Figure 3.32 - Top View of Ring Specimen during the 28-day testing duration.

3.4.4.2 Plastic Shrinkage Cracking Test

This test subjected various fibre-reinforced concrete samples to controlled environmental conditions to study the plastic shrinkage of SCC. The environmental chamber used for this test was constructed following the guidelines of ASTM C1579-06 (2006), which standardises the evaluation of plastic shrinkage cracking in fibre-reinforced concrete (ASTM C1579-06, 2006).

The setup of the controlled environmental chamber, shown in Figure 3.33, similar to that used at the University of Malta in previous studies (Abdilla, 2021; Borg et al., 2016; Vella, 2018), included a half-inch thick particleboard chamber with dimensions of 1460 mm in length, 560 mm in height, and 840 mm in width. The roof of the chamber had 5

mm thick poly(methyl methacrylate) acrylic panels for visual inspection while maintaining a sealed environment and not disturbing any of the apparatus. The concrete specimen, along with a water-filled container on a calibrated digital balance, was placed on a raised steel frame table. A sheet metal deflector directed airflow from a high-speed industrial fan to provide constant air movement.

Figure 3.33 - Environmental Chamber Setup adapted chamber (ASTM C1579-06, 2006).

Three halogen heaters maintained a consistent temperature within the chamber: two inside the chamber, shown in Figure 3.34, and one outside, behind the industrial fan. The concrete specimen was cast in a rectangular mould with internal dimensions of 560 mm in length, 355 mm in width, and 100 mm in depth, made from 6 mm welded metal sheets. The mould featured three internal stress risers to control crack development and 17 mm bolts at the ends to restrain the concrete sample. The dimensions of the mould are shown in the diagram in Figure 3.35.

Figure 3.34 - Halogen Heaters inside the Environmental Chamber.

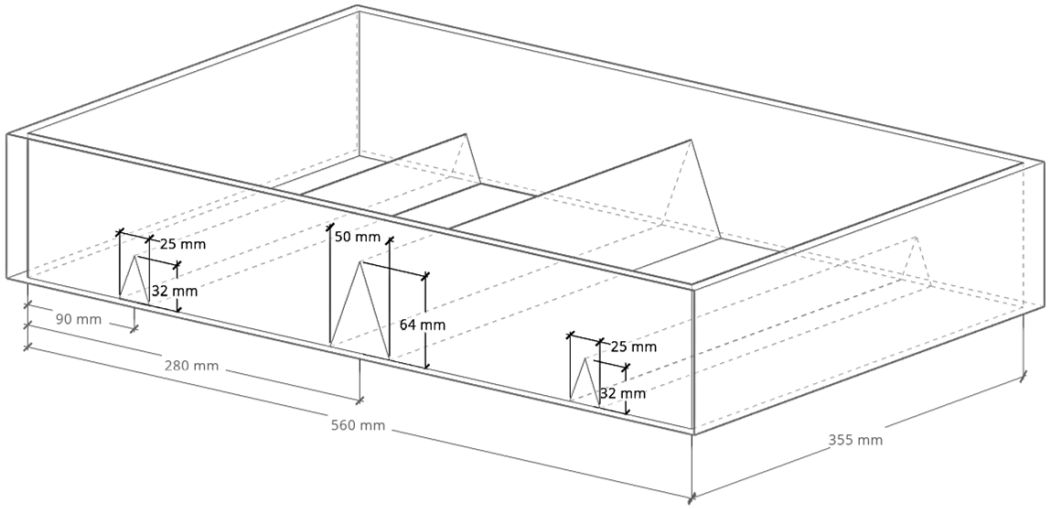

Figure 3.35 - Dimensions of the Mould used in the Environmental Chamber adapted diagram (ASTM C1579-06, 2006).

Before each test, the industrial fan and halogen heaters were turned on for 30 minutes to achieve the required environmental conditions: relative humidity of 30 ± 10%, constant temperature of 36 ± 3˚C, and wind velocity over 4.7 m/s. These conditions were monitored using a data logger and a handheld anemometer, aiming for an evaporation rate of about 1.0 kg/m² per hour. The weight loss of the water container shown in Figure 3.36 (plan area of 0.1 m²) was recorded every 30 minutes for the first

three hours, then every hour for the next three hours. These measurements were converted to the evaporation rate per square metre per hour.

Figure 3.36 - Water Container in the Environmental Chamber.

The temperature of the concrete was monitored with a thermocouple inserted into the specimen, with readings taken every 30 minutes. The concrete panel was visually inspected for cracks every 15 minutes, and the time of the first crack appearance was recorded. After six hours, the specimen was removed from the environmental chamber, covered, and stored in controlled ambient conditions.

Twenty-four hours after casting, the crack width was measured at ten different points along the crack length using a calibrated USB microscope shown in Figure 3.37. Measurements within 25 mm of the mould edges were not taken to avoid any restraints from the mould itself.

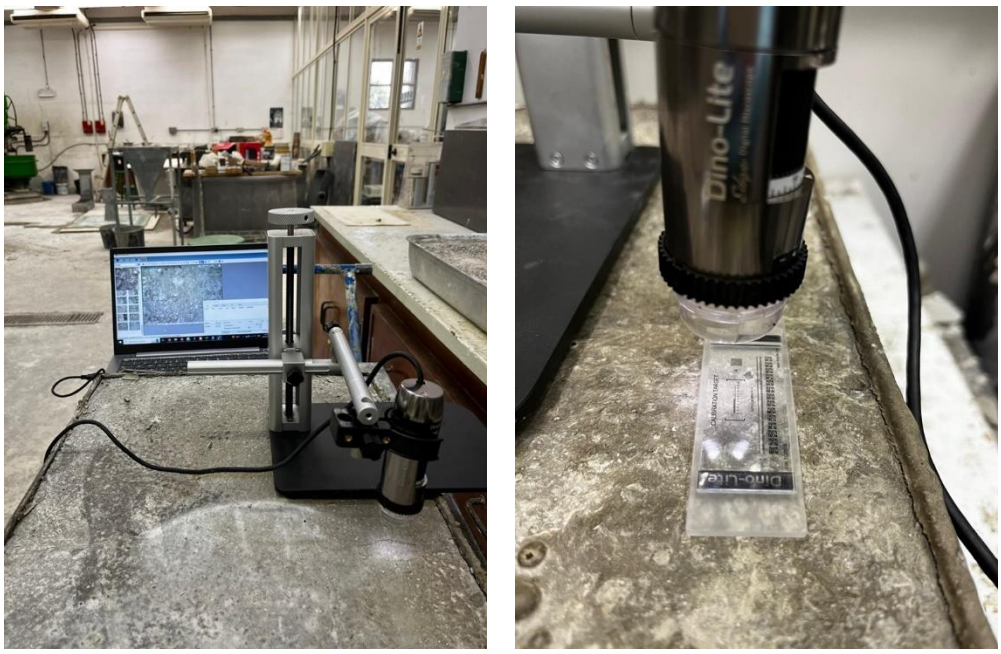

Figure 3.37 – USB Microscope used to Measure Cracks after 24 hours.

3.4.5 Shrinkage Properties of Self-Compacting Mortar Panels

3.4.5.1 Kraai Test

This test was conducted to assess the potential of fibre-reinforced SCMs to develop cracks in thin slabs. The moulds used had dimensions of 610 x 914 mm and a depth of 19 mm, constructed from plywood sheets that were glued and nailed together resembling a frame, shown in Figure 3.38. To prevent water absorption by the plywood and to avoid restraining the SCM during the testing duration, the inner surfaces were lined with a single polyethylene sheet, stretched and pinned down to the base to prevent any rises in the base of the mould which would inevitably induce cracking. Restraints along the entire inner perimeter were added by using chicken-wire steel mesh, positioned at regular intervals. The mesh was bent at right angles using a hammer and clamp to protrude into the SCM and was secured to the base with pins over the polyethylene sheet. This setup adhered to the guidelines provided by Kraai in the test to determine the cracking potential due to drying shrinkage of concrete (Kraai, 1985).

Figure 3.38 - Kraai Test Setup (Kraai, 1985).

Once the SCM was mixed following the same standard procedure as the concrete, the SCM was poured into the flat mould and levelled with a trowel to achieve a smooth finish. The panels were then placed in a controlled environment with a temperature of 22 ± 2°C and relative humidity of 50 ± 2%. For the first five hours, the SCM was exposed to a wind speed of 6 m/s, generated by a floor-standing industrial fan, to encourage crack formation. The wind speed was regularly checked using a handheld anemometer.

The surface of the SCM mix was evaluated 24 hours after casting. For each specimen, the average crack length and width were measured using a pair of calibrated digital vernier callipers. The crack widths were categorised into four different groups, each assigned a specific weighted value, which was then inputted into the following equation:

$$\text{average weighted value} = \text{weighted value} \times \text{crack length}$$

The sum of each of the average weighted values, coined the 'total weighted average value', provided a comparative measure of the each of the specimen's crack potential.

The weighted value for each of the cracks was based on the following rubric in Table 3.10 below.

Table 3.10 - Rubric for Crack Weighting (Kraai, 1985).

Crack Width	*Weighted Value in mm^2*
Large (about 3 mm)	3
Medium (about 2 mm)	2
Small (about 1 mm)	1
Hairline (about 0.5 mm)	0.5

3.4.6 Durability Properties of Concrete

3.4.6.1 Rapid Chloride Penetration Test

Prior to commencing this test, cylinders with 100 mm diameter and 200 mm height were removed from the curing tank on the 28th day from casting. These samples were sliced into 50 mm thick slices in order to be the appropriate size for this test procedure. This Rapid Chloride Penetration Test (RCPT) was carried out in accordance to the ASTM C1202-12 Standard.

Prior to starting the test, the sample required vigorous conditioning to extract accurate results from the chloride penetration test. Approximately 10 g of rapid setting epoxy resin coating was prepared and brushed onto the side surface of the specimen for sealing. The sample was placed on a suitable support during coating to ensure complete coverage of the sides, as shown in Figure 3.39. The coating was allowed to cure until it was no longer sticky to the touch. Any visible holes in the coating were filled, and additional curing time was allowed as needed. This was done to prevent any ions from deviating from the ideal uniaxial direction of travel. When working with epoxy resin coatings, proper ventilation and the use of personal protective equipment, including gloves and masks were essential to prevent inhalation of fumes and skin

contact. Additionally, spills were immediately cleaned, and all safety data sheets were reviewed to ensure safe handling and disposal of materials.

Once fully cured, the specimen was then conditioned prior to testing as shown in Figure 3.40. The specimen was placed directly in the vacuum desiccator with both end faces exposed. The desiccator was sealed, and the vacuum pump or aspirator was started. The pressure was reduced to less than 6650 Pa within a few minutes and maintained at this level for 3 hours. A separatory funnel or similar container was filled with deaerated water earlier. With the vacuum pump still running, the water stopcock was opened, and enough water was drained into the beaker or container to cover the specimen, ensuring no air entered the desiccator through the stopcock. The water stopcock was closed, and the vacuum pump was allowed to run for an additional hour. The vacuum line stopcock was then closed, and the pump was turned off. The vacuum line stopcock was then adjusted to allow air to re-enter the desiccator. The specimen was soaked under water in the beaker for 18 ± 2 hours.

Figure 3.39 - Specimens while outer Epoxy Resin Coating is Curing (ASTM C1202-12, 2012).

Figure 3.40 - Conditioning Setup for Chloride Penetration Samples (ASTM C1202-12, 2012).

Once the specimen has been conditioned, it was placed inside the test cell apparatus and the ends of the sample were sealed with silicone sealant, to prevent any leaks from the gaps between the concrete and rubber stoppers. The actual testing involved monitoring the electrical current passing through the cylinders every 30 minutes over a 6-hour period by means of a digital datalogger. A 60 V DC potential difference was maintained across the ends of the specimen, with one end immersed in with 3.0% Sodium Chloride solution (catholyte) connected to the negative terminal, and the other in a 0.3 N Sodium Hydroxide solution (anolyte) connected to the positive terminal. Thermocouples were also placed on either side to measure the temperature difference at both ends of the specimen. The total charge passed, measured in coulombs, was used to assess the specimen's resistance to chloride ion penetration, shown in Table 3.11. The equation used to measure this relationship was:

$$Q = 900(I_0 + 2I_{30} + 2I_{60} + ... + 2I_{300} + 2I_{330} + I_{360})$$

where:

Q is the charge passed (in coulombs);

I_0 is the current (in amperes) immediately after voltage is applied;

I_t is the current (in amperes) at t min after voltage is applied.

The charge passed through the samples is then compared to Table 3.11, which indicates the chloride ion penetrability of the mix.

Table 3.11 – Chloride Ion Penetrability Based on Charge Passed (ASTM C1202-12, 2012).

Charge Passed in Coulombs	*Chloride Ion Penetrability*
> 4,000	High
2,000 – 4,000	Moderate
1,000 – 2,000	Low
100 – 1,000	Very Low
< 100	Negligible

This relationship provided a measure of the material's durability and its ability to withstand chloride ion penetration. This test was done in accordance with the ASTM C1202-12 (2012) Standard.

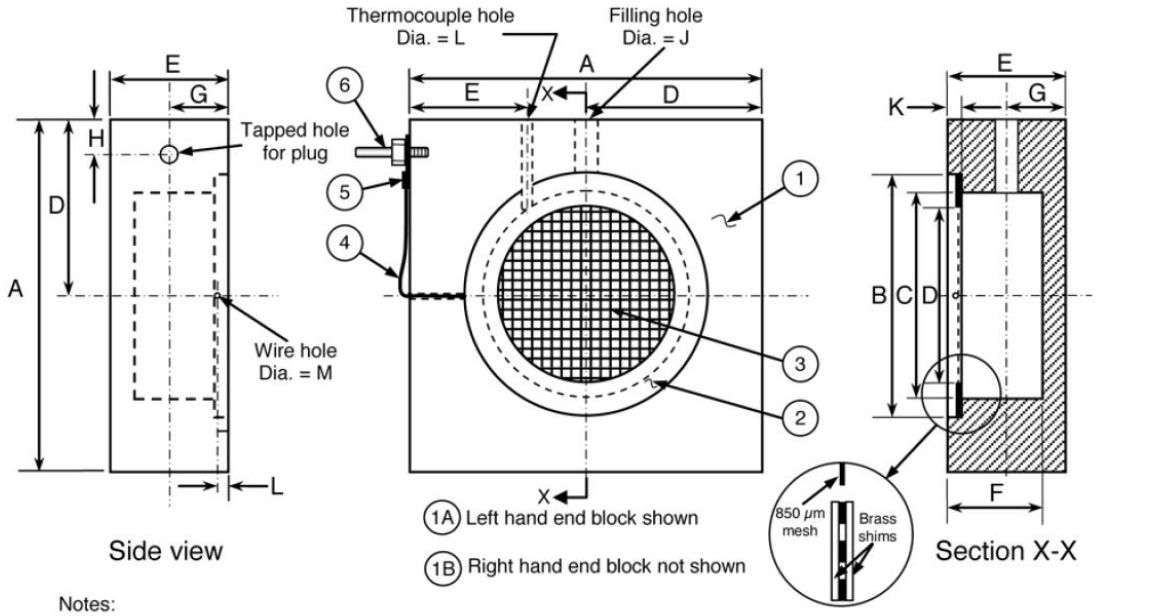

Dimensions, mm

A	B	C	D	E	F	G	H	J	K	L	M
150	105	89	75	50	41	25	15	10	6	5	2.5

Figure 3.41 - Chloride Penetration Machine (ASTM C1202-12, 2012).

3.4.6.2 Vacuum Saturation Porosity Test

Four days before testing, the cylinder samples were sliced to 50 mm thick slices, washed, and then placed back in the curing tanks. On the test date, 28 days from casting, the specimens were placed in a vacuum desiccator with both trimmed end faces of the cylinder exposed. The desiccator was then sealed with a lid and vacuum pump grease. Another desiccator was filled with deaerated water. The desiccators were connected to a vacuum pump through a water trap with a vacuum line connector, to which a pressure gauge was also attached.

The vacuum pump was activated for a period of three hours at a pressure of -90 kPa, ensuring the removal of air bubbles from both the concrete specimens and the water in the second desiccator. At the end of this three-hour period, the stopcock of the water-filled desiccator was closed, and the vacuum was released. Immediately after closing the vacuum line of the desiccator holding the test specimens, the water line was opened, allowing deaerated water to flow from the second desiccator to completely

cover the test samples in the first desiccator. This process created a pressure difference between the two desiccators, causing water to be drawn into the first desiccator containing the specimens. Subsequently, the water line was closed, and the vacuum line was reopened.

The specimens which were submerged in water, were then subjected to vacuum for an additional hour. After the four-hour period, the vacuum line stopcock for the specimen desiccator was closed, the vacuum pump was turned off, and air was slowly allowed to enter the desiccator. The specimens were then left in the desiccator, under water, for another 20 hours.

At the end of this period, the saturated surface dry mass and the buoyant mass of the specimens were determined. The samples were then placed in an oven for a period of at least 48 hours at a temperature of 105±5 °C, ensuring that the oven dry weight did not vary by more than 0.1% between successive readings taken 24 hours apart. When handling hot samples, proper protective equipment, including heat-resistant gloves and lab coats were always worn.

The vacuum saturation permeable porosity was then calculated using the following equation:

$$\text{Permeable Porosity} = \left(\frac{W_s - W_d}{W_s - W_b} \right) \times 100\%$$

where:

W_b is the buoyant mass of the saturated specimen in water (in g);

W_d is the oven-dry mass of the specimen in air (in g);

W_s is the saturated surface-dry mass of the specimen in air (in g).

Chapter 4

Results and Discussion

4 Results and Discussion

This chapter presents and discusses the results of the statistical analysis on the fibres and the experimental program on the behaviour of the cement-based mixes with feather fibre reinforcement. The statistical analysis provides a better understanding of the nature of the biomaterial as collected, which allowed for a more comprehensive reporting on the mixes.

As a result of this analysis, the decision to separate the very long rigid fibres identified as outliers, as well as the decision to shred the fibres was taken, and was proved effective, as will be discussed in this chapter.

Furthermore, the results of the experimental program then outline the prominent improvements in early-stage shrinkage cracking as well as in the overall compressive strength and ductility, while however compromising some of the fresh characteristics of these mixes.

4.1 Analysis of Feather Fibres

A sample of 400 feathers was taken from different fibre collections, and their geometry, with measurements taken as in Figure 4.1, was assessed to characterise the fibres used in this research. Note that the thickness and hence aspect ratio for each fibre was calculated by measuring three points along the feather, as shown in Figure 4.1: at the base (the thickest point), the midpoint, and the furthest point from the base (the thinnest point). These three measurements were taken using a pair of calibrated, digital vernier callipers, to get an accurate average diameter along the length of the fibre, with a representative sample shown in Table 4.1. The data gathered was analysed using IBM SPSS Statistics Version 29.

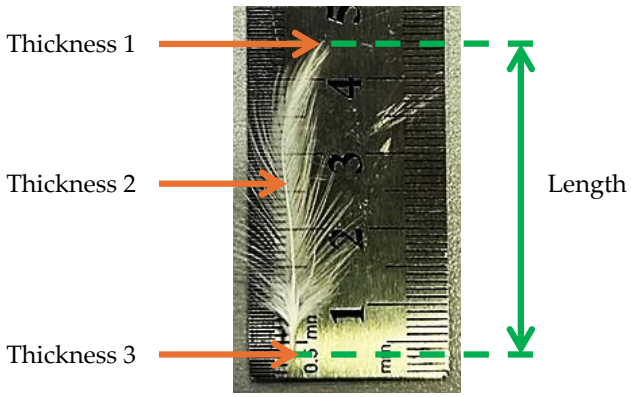

Figure 4.1 - Measurement Points on Feather Fibre.

Table 4.1 - Sample Measurements for Aspect Ratio Calculations.

Sample	*Length*	*Ø 1*	*Ø 2*	*Ø 3*	*Average Ø*
#	**mm**	**mm**	**mm**	**mm**	**mm**
1	152.00	2.42	1.20	0.23	1.28
20	99.00	1.19	0.75	0.06	0.67
40	78.00	0.88	0.43	0.05	0.45
60	70.00	0.64	0.17	0.03	0.28
80	66.00	0.66	0.22	0.06	0.31
100	63.00	0.42	0.11	0.07	0.20
120	60.00	0.24	0.11	0.11	0.15
140	56.00	0.55	0.18	0.03	0.25
160	55.00	0.60	0.17	0.06	0.28
180	54.00	0.33	0.10	0.06	0.16
200	50.00	0.92	0.11	0.06	0.36
220	45.00	0.51	0.19	0.03	0.24
240	43.00	0.36	0.13	0.05	0.18
260	39.00	0.24	0.17	0.10	0.17
280	35.00	0.63	0.16	0.06	0.28
300	34.00	0.02	0.01	0.01	0.01
320	31.00	0.25	0.11	0.02	0.13
340	30.00	0.28	0.10	0.04	0.14
360	28.00	0.43	0.09	0.02	0.18
380	23.00	0.46	0.25	0.06	0.26
400	12.00	0.14	0.06	0.05	0.08

4.1.1 Statistical Analysis of the Length of Fibres

The data collected as well as the analysis is visually represented in Figure 4.2 and Figure 4.3, while the descriptive analysis is shown in Table 4.2.

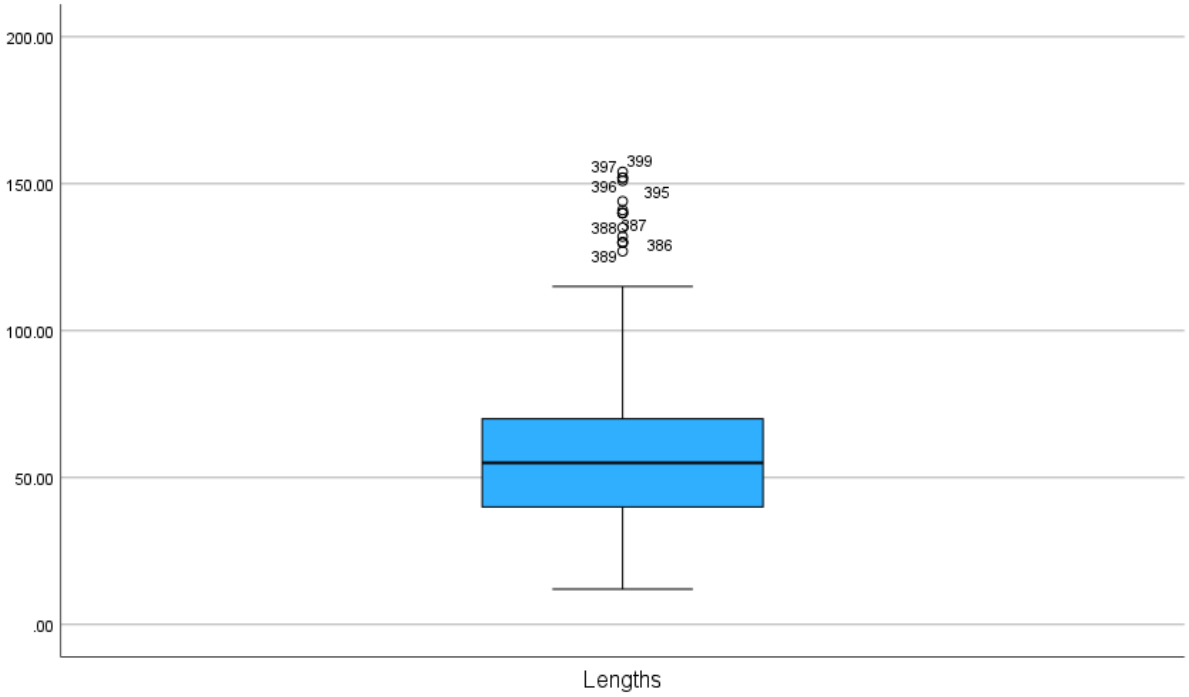

Figure 4.2 - Box Plot of Lengths of 400 Feathers from IBM SPSS Statistics v. 29.

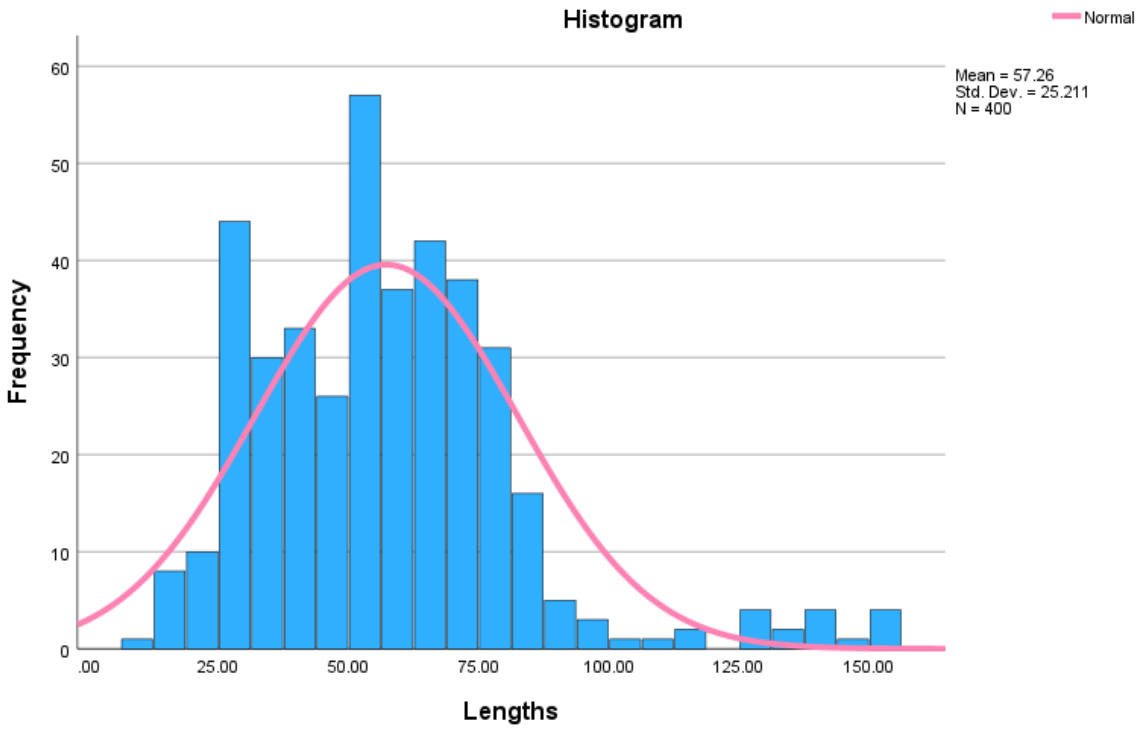

Figure 4.3 – Frequency and Normal Distribution of 400 Feather Fibre Lengths from IBM SPSS Statistics v. 29.

Table 4.2 - Descriptive Statistics for 400 Feather Fibre Lengths from IBM SPSS Statistics v. 29.

Descriptives

		Statistic	Std. Error
Mean		57.2557	1.26053
95% Confidence Interval for Mean	Lower Bound	54.7776	
	Upper Bound	59.7338	
5% Trimmed Mean		55.2369	
Median		55.0000	
Variance		635.577	
Std. Deviation		25.21065	
Minimum		12.00	
Maximum		154.00	
Range		142.00	
Interquartile Range		30.00	
Skewness		1.211	.122
Kurtosis		2.613	.243

Table 4.3 - Results from Normality Tests from IBM SPSS Statistics v. 29.

Tests of Normality

	Kolmogorov-Smirnov[a]			Shapiro-Wilk		
	Statistic	Df	Sig.	Statistic	df	Sig.
Lengths	.092	400	<.001	.916	400	<.001

a. Lilliefors Significance Correction

The data revealed considerable variation in feather fibre lengths. This variability could lead to potential variations and uncertainties in concrete mixes. Feather fibres, like other natural materials, differ in geometric characteristics such as length and diameter. Understanding this variability through statistical analysis was crucial for ensuring consistency in the fibres used, which in turn was essential for achieving repeatable mechanical properties in concrete. The statistical analysis also provided information on how fibre properties are distributed and their average values.

The statistical analysis especially showed that the fibres varied greatly in length, with certain fibres being particularly longer than the rest, identified as outliers, as shown in Figure 4.2. At closer inspection, it was found to be that these outliers are the long, rigid feathers, known as the flight feathers. This variation has the potential to cause an uneven spread in the concrete mixture, impacting both the fresh and hardened properties.

Using IBM SPSS Statistics Version 29, it was possible to graphically represent the samples measured to better understand the distribution, as shown in Figure 4.3. It was noted that the distribution was asymmetrical, with a right positive skewness of 1.2114. The shape of such distribution is known as leptokurtic, with long heavy tails, which is influenced by the longer flight feathers.

A detailed descriptive analysis of the feather lengths is provided in Table 4.2, showing a mean length of 57.2557 mm, a range of 142 mm, and once again identifying longer flight feather fibres as outliers. The normality tests carried out, including the Kolmogorov-Smirnov and Shapiro-Wilk tests, indicated a significance level of <0.001, as shown in Table 4.3, suggesting that the data does not follow a normal distribution.

4.1.2 Statistical Analysis of the Thickness of Fibres and Aspect Ratio

Following this statistical analysis, using the measurements taken from the 400 fibres, it was possible to determine and analyse the thickness and aspect ratio of the fibres, as shown in Figure 4.4, Figure 4.5, Figure 4.6, and Figure 4.7.

Further statistical analysis showed that the distribution of the fibre thicknesses is also noteworthy. All three distributions show a long tail, influenced by the thicker flight feathers, which skew the distribution charts. The thickest point of the fibres has the largest distribution and standard deviation as the base of the thick fibres was significantly thicker than the average distribution of the range of feathers which were eventually used in the research. The second and third thickness readings had increasingly smaller distributions and standard deviations, given that the typical

structure of feathers is to narrow out at the ends. It is also noted that from the 400 measured feathers, there were only 14 which had bases which were thicker than 2 mm.

Further analysis of the feather fibre diameters shows that the lengths, the three thicknesses, and their average are correlated amongst each other. This was calculated using IBM SPSS Statistics to check for bivariate correlation, shown in Table 4.4, which showed that the Pearson correlation coefficients indicated strong positive correlations, with significance values smaller than 0.001, suggesting a highly significant relationship between the datasets. The least significant relationship was observed in the third thickness measurement, as it was highly dependent on the orientation of the feather fibre barbs when measuring the upper tip thickness.

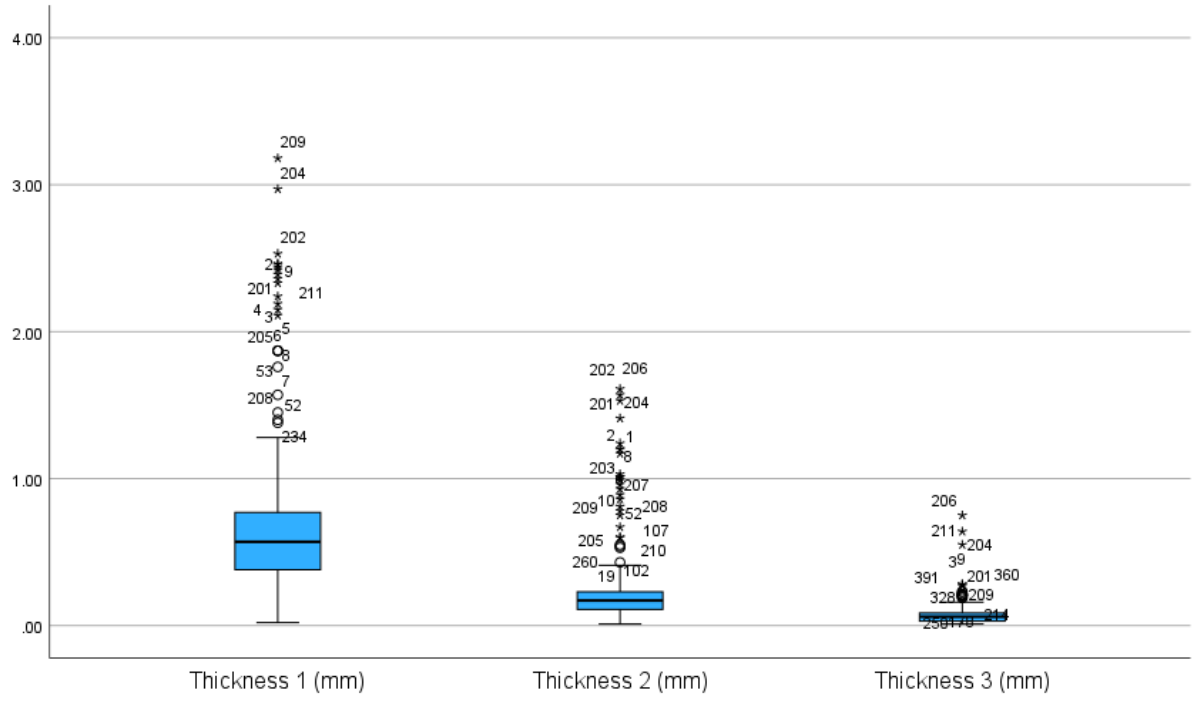

Figure 4.4 - Box Plot Thicknesses of 400 Feathers from IBM SPSS Statistics v. 29.

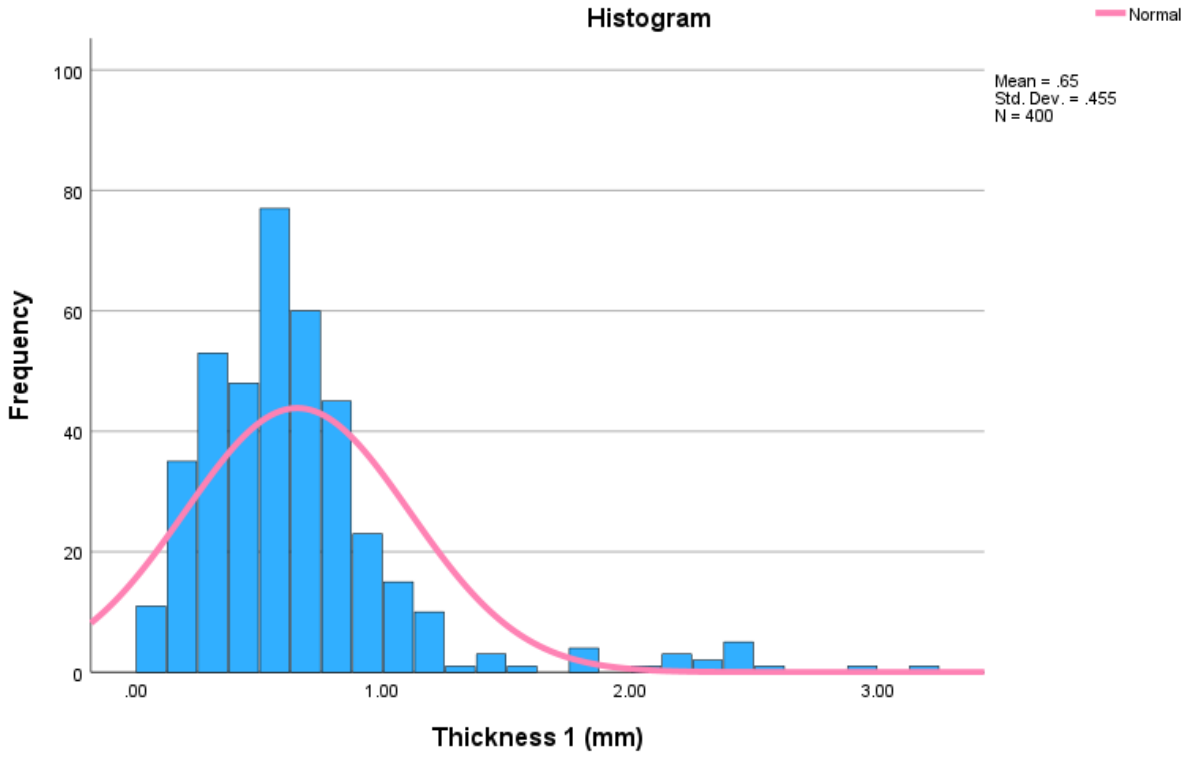

Figure 4.5 - Frequency and Normal Distribution of 400 Feather Fibre Thicknesses at the base from IBM SPSS Statistics v. 29.

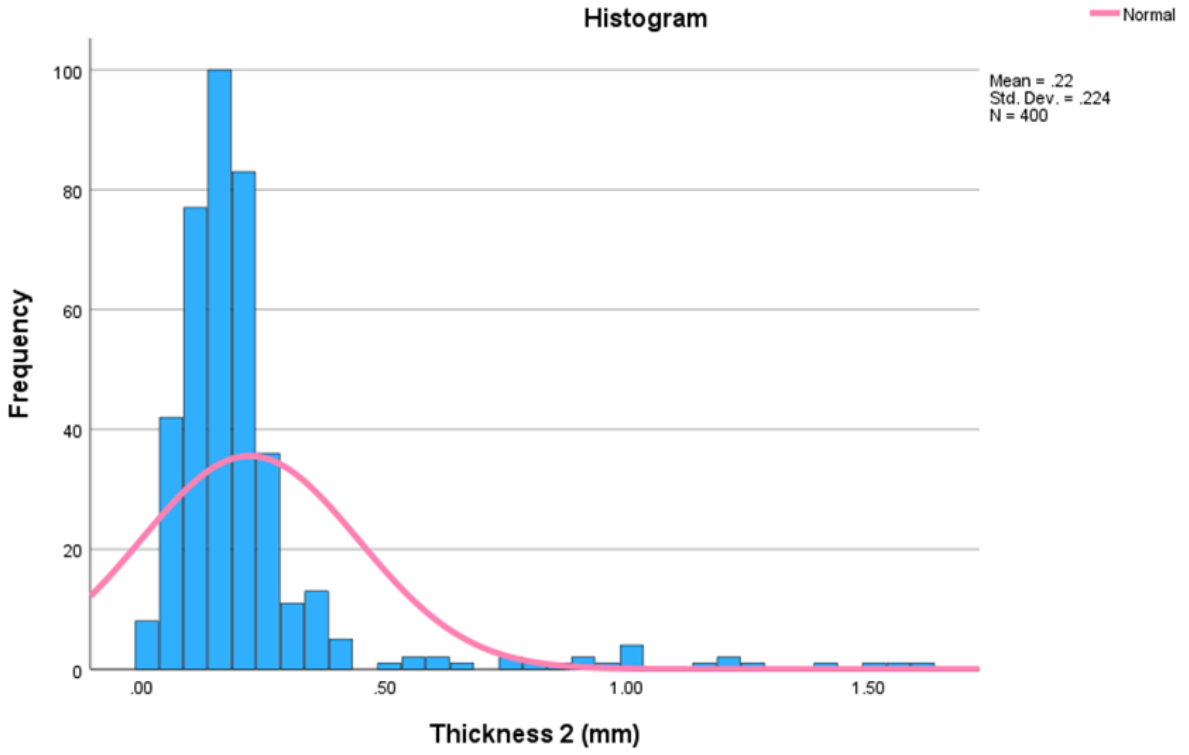

Figure 4.6 - Frequency and Normal Distribution of 400 Feather Fibre Thicknesses at midpoint from IBM SPSS Statistics v. 29.

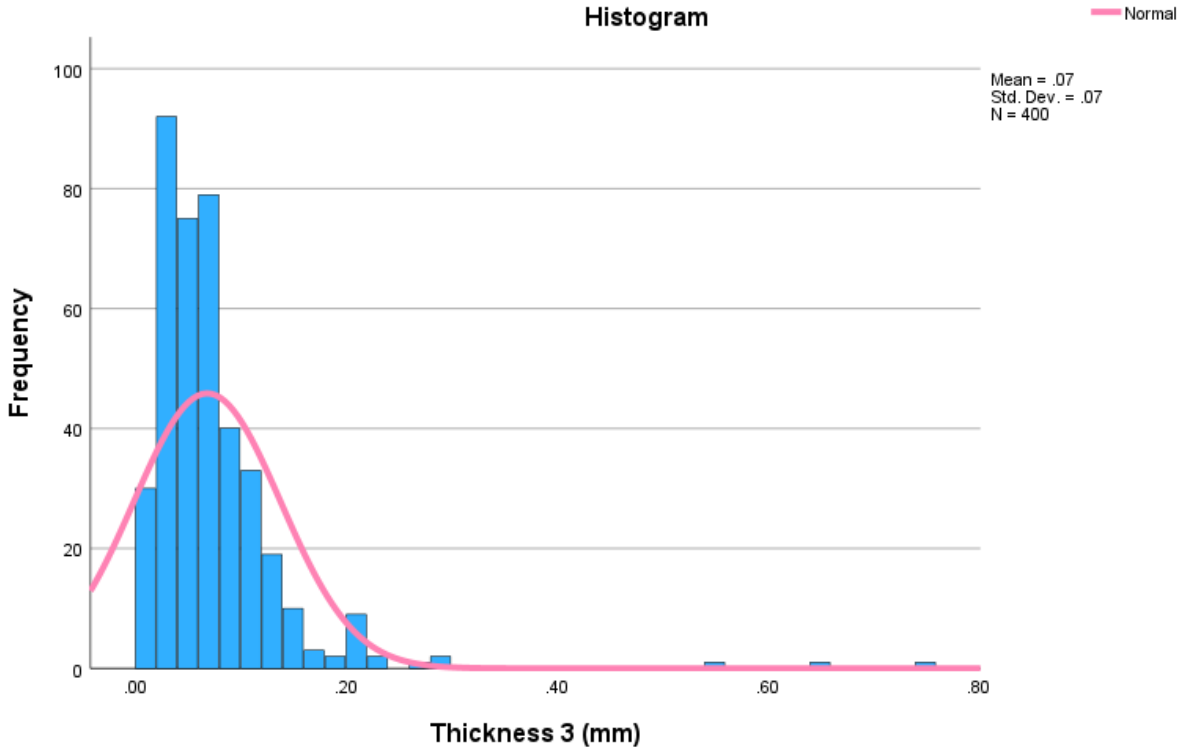

Figure 4.7 - Frequency and Normal Distribution of 400 Feather Fibre Thicknesses at the thinnest point from IBM SPSS Statistics v. 29.

Table 4.4 - Bivariate Correlation from IBM SPSS Statistics v. 29.

Correlations

			Thickness			
		Length	1	2	3	AVG
Length	Pearson Correlation	1	.803**	.772**	.527**	.813**
	Sig. (2-tailed)		<.001	<.001	<.001	<.001
	N	400	400	400	400	400
Thickness 1	Pearson Correlation	.803**	1	.867**	.636**	.980**
	Sig. (2-tailed)	<.001		<.001	<.001	<.001
	N	400	400	400	400	400
Thickness 2	Pearson Correlation	.772**	.867**	1	.703**	.943**
	Sig. (2-tailed)	<.001	<.001		<.001	<.001
	N	400	400	400	400	400
Thickness 3	Pearson Correlation	.527**	.636**	.703**	1	.730**
	Sig. (2-tailed)	<.001	<.001	<.001		<.001
	N	400	400	400	400	400
Average Thickness	Pearson Correlation	.813**	.980**	.943**	.730**	1
	Sig. (2-tailed)	<.001	<.001	<.001	<.001	
	N	400	400	400	400	400

**. Correlation is significant at the 0.01 level (2-tailed).

The fibres were noted to be separable into two distinct groups, the long, stiff, flight feather fibres, which were eventually excluded from the main project, and the average fibres. The average fibres were then grouped together and the aspect ratio of the longer and shorter end of this dataset was calculated.

The results of the aspect ratio calculations based on a selection of the data were as follows, for the very large flight feathers: 124.60; for the longer average fibres: 264.43; and for the shorter average fibres: 246.17.

Notably, there is a large discrepancy in aspect ratios between the very long flight fibres and that of the regular fibres. The aspect ratio of the average fibres on the longer end and the shorter end have comparable aspect ratios, at 264.43 and 246.17, respectively. However, the aspect ratio of the flight fibres was significantly smaller, at 124.60. This

implies that the flight fibres are extremely distinct in their morphology from the much more abundant regular fibres. This difference in structure is to be expected, given that these very long flight fibres are few and serve a different purpose to the other fibres, as the flight fibres are found along the wing, whilst the other fibres are there to provide protection and insulation.

The large discrepancy between the large fibres and the other fibres further supports the decision to separate these fibres, as their aspect ratio is not comparable to the majority of the fibres collected, and easily separatable. As mentioned previously, the large fibres were not used for the casting of SCC and SCM as the aspect ratios and rigidity of the structure were not appropriate for the purpose of this study. Following the separation of the long flight feathers, the range of length of the remaining fibres was still relatively large, and shredding of fibres was considered to reduce this range.

4.1.3 Shredding of Fibres

The goal of shredding the regular fibres was to trim the fibre lengths to two, more distinct, length ranges, henceforth referred to as the shredded and unshredded fibres in this section, which would both be examined in the concrete mixes. This produced two sets of fibres, with the shredded one shorter than the other. Without this adjustment, the fibres varied too widely in length, which could lead to inconsistent results in the small volume fractions used. This modification was anticipated to enhance the overall effectiveness of the concrete, guaranteeing that the advantages of fibre reinforcement could be uniformly achieved in various batches and uses.

A modified paper shredder shown in Figure 4.8 was used to achieve a consistent length range of short, shredded fibres which was repeatable for all the mixes required in the experimental program.

Figure 4.8 - Modified Paper Shredder used to Trim Feather Fibres to a Shorter Length Range.

Once the fibres were shredded, another statistical analysis was carried out on the shredded and unshredded fibres, shown in Table 4.5. This statistical analysis was done to differentiate the length ranges which would in turn be the "short" and "long" fibre lengths, as these would be the constituent fibres for all the SCC mixes, and the significance between the two different length ranges is shown in Table 4.6, with a p-value less than 0.05, at <0.001, hence justifying the "short" (S) and "long" (L) annotations used henceforth.

Table 4.5 - Statistical Analysis on Shredded and Unshredded Fibre Lengths.

#	***Shredded***	***Unshredded***
	mm	*mm*
1	7	30
2	9	30
3	10	34
4	15	35
5	25	35
6	25	40
7	25	40
8	25	41
9	30	43
10	30	43
11	35	45
12	35	45
13	35	49
14	35	50
15	35	50
16	35	50
17	35	60
18	40	62
19	40	68
20	40	68
21	43	70
22	45	70
23	45	75
24	55	75
25	56	75

Furthermore, since the SCM prisms were cast on a much smaller scale, it was possible to hand trim to fibres to an exact length, namely 15 mm, 25 mm, 35 mm, and 50 mm, however, those fibres lengths would only be used for the small prism specimens. These fibres are not included in the statistical analysis presented hereunder.

The short (shredded) and long (unshredded) fibres were used in the majority of concrete tests, and the length ranges are outlined as follows in Table 4.5 and Figure 4.9. These values show that the shredding of fibres has effectively shortened the overall length range of the fibres, resulting in two distinct groups of fibre lengths.

Table 4.6 - Test for Significance between Shredded and Unshredded Fibres.

Independent Samples Test

		t-test for Equality of Means					
				Significance			
		t	Df	One-Sided p	Two-Sided p	Mean Difference	Std. Error Difference
Length	Equal variances assumed	-4.779	48	<.001	<.001	-18.92000	3.95926
	Equal variances not assumed	-4.779	46.789	<.001	<.001	-18.92000	3.95926

Table 4.7 - Feather Fibre Length Range Classification.

	Fibre Length Range
Short	5 - 42 mm
Long	30 - 75 mm

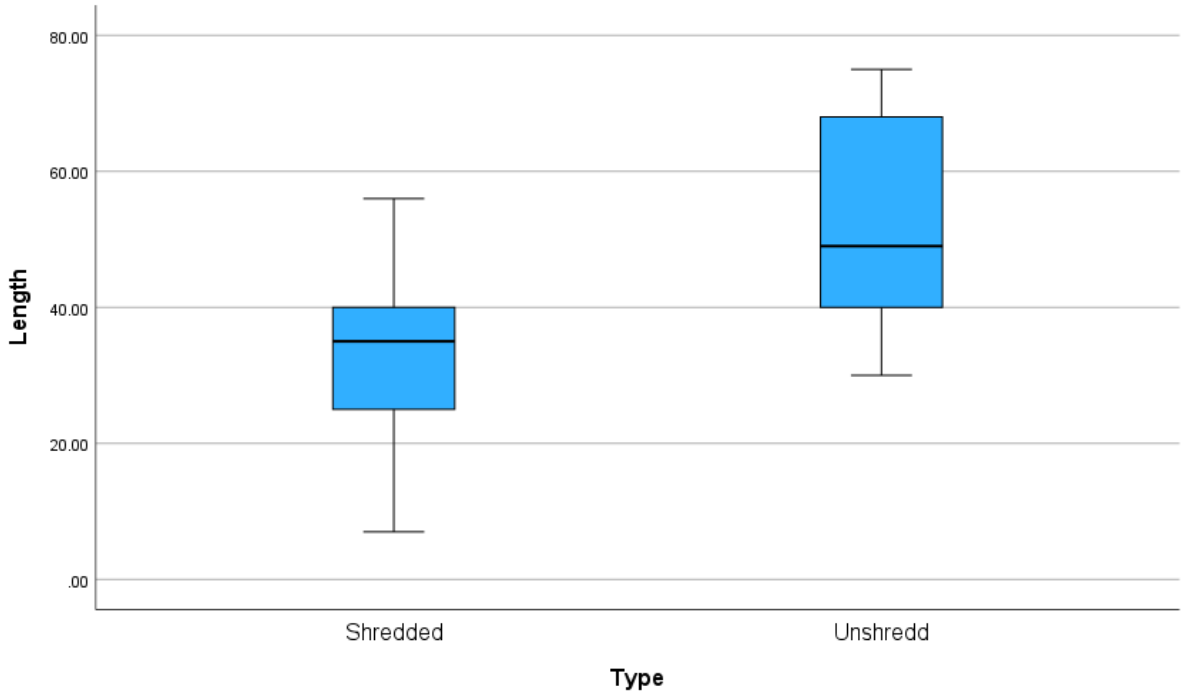

Figure 4.9 - Feather Fibre Length Range Classification Distribution.

Once the fibres were sorted and/or shredded, they were stored in sealed plastic bags where they would be kept in a cool, dry room until they were needed for the incorporation into the mixes, as shown in Figure 4.10.

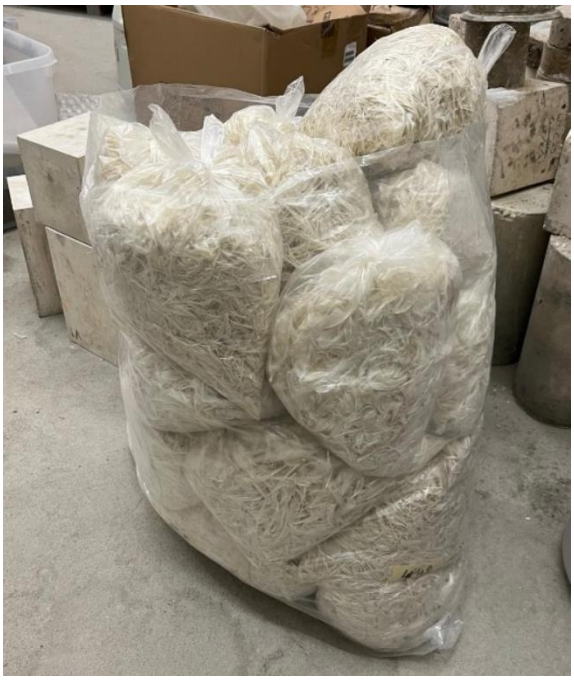

Figure 4.10 - Storage of Clean and Processed Feather Fibres.

4.1.4 Density of Fibres

Calculating the density of the fibres was another crucial step in the analysis of the fibres. This calculation was necessary to compute the volume fraction needed in each of the mix designs, based on the density of the fibres. The calculation of density was not easy to achieve given that the density of the fibres is less than 1 g/cm^3, which means that the fibres float in the water, which was the displacement medium. To bypass this problem, the fibres were left to saturate for 48 hours before taking the new mass readings, to ensure that there were no air bubbles when measuring the final mass of the water, which would interfere with the calculation of density. The results of this test concluded that the fibres had an average density of 0.83 g/cm^3. This density was then used to calculate the adjusted amount of fibre to incorporate in each of the SCC and SCM mixes without needed to resort to the laborious task of measuring the volume. It is to be noted that this value related to and is in the same range as values reported in literature for feather density (Gonzalez-Calderon et al., 2020).

4.2 Experimental Program on Fibre-Reinforced Self-Compacting Cement-Based Materials: Results and Interpretation

4.2.1 Fresh Properties of Self-Compacting Concrete

The empirical tests to evaluate the fresh properties of SCC involved assessing properties such as flowability, viscosity, passing ability, and resistance to segregation (EFNARC, 2005). These properties were evaluated through a series of empirical tests: namely the Slump Flow, V-Funnel, and L-Box tests. For a more in-depth analysis of the fresh properties of the mix, the rheology was assessed using an ICAR Plus Concrete Rheometer.

4.2.1.1 Workability and Flowability Tests

Workability and flowability was assessed using slump flow and T_{500} tests across all fibre volume fractions in SCC mixes. As the proportion of fibres increased, there was a noticeable decrease in flowability properties over most time intervals. Specifically, mixes with the highest fibre volume fractions exhibited a low performance with respect to slump flow, indicating notable impairment in their ability to spread and flow freely, as can be seen in Figure 4.11. The diameter was measured as shown in Figure 4.12. This reduction could be attributed to the possible absorption of water by fibres in the mix, and increased resistance and impediment to flow caused by the fibres, which disrupted the natural movement and settlement of concrete during pouring, typical for fibre reinforced concrete due to increase in internal friction due to fibres. The mixes with the smallest volume fraction, namely C0.125S, provided results which were comparable to the control mix, indicating that the incorporation of such small proportion of fibres did not alter the flowability of the mix, which can be seen in Figure 4.13. Corresponding to the EFNARC characterisation system, all mixes bar the C0.125S mix, achieved a SF1 classification, while the latter achieved a SF2 classification. This highlights the challenge of maintaining optimal flow characteristics in SCC mixes with

high fibre content, crucial for ensuring that the concrete can self-compact effectively and fill intricate formwork without segregation.

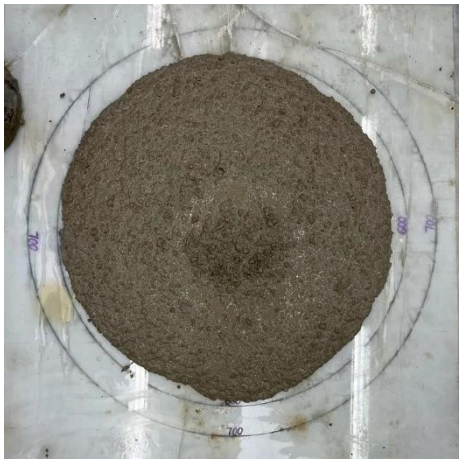

C0 (Control) Mix

C0.125S Mix

C0.125L Mix

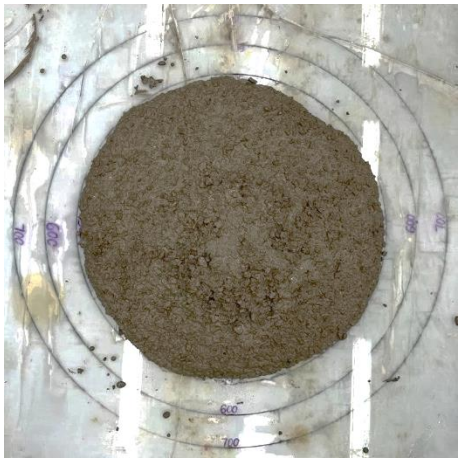

C0.25S Mix

C0.25L Mix

Figure 4.11 - Slump Flow Test Results exhibiting decreasing Workability (Note that the external diameter mark refers to 700 mm).

Figure 4.12 - Slump flow diameter being measured.

As for the T_{500} test results, shown in Figure 4.14, indicated similar trends in performance to the slump flow test, as mixes with the highest fibre volume fractions (0.5%) did not flow to the required 500 mm radius mark, and readings for these two mixes could not be recorded. Both the control mixes and the mixes with fibre ratios 0.125% and 0.25% otherwise passed this test, and the time was recorded. The longest time taken for the mix to flow to the 500 mm mark was the C0.25S mix, which took 9 seconds at the t_{15} time point. This same mix did not achieve the required diameter when testing at the t_{30} time point. This signifies that as the time elapsed, there was a reduction in workability and flowability of the mix. This trend was also noted in all other mixes; however, it was most significant in the C0.25 mixes.

The mixes with the smallest volume fraction, namely C0.125S and C0.125L, provided results which had a flow greater than that of the control mix, indicating that the incorporation of such small proportion of fibres did not alter the flowability of the mix, but rather slightly improved it. According to the EFNARC characterisation, all mixes except the C0.125S mix achieved a VS2 classification, while the latter mix achieved a VS1 classification. It is also observed that for 0.125% fibre content, whilst the small fibres resulted in higher flow which was maintained over time, the larger fibres resulted in lower flow at t_0 and reduction in flow properties with time. On the other hand, for the higher fibre fraction of 0.25%, the shorter fibres resulted in lower

workability whilst both short and long fibre mixes indicated reduction of flow with time. It was also observed that none of the mixes demonstrated segregation noted by the absence of bleed water in these tests.

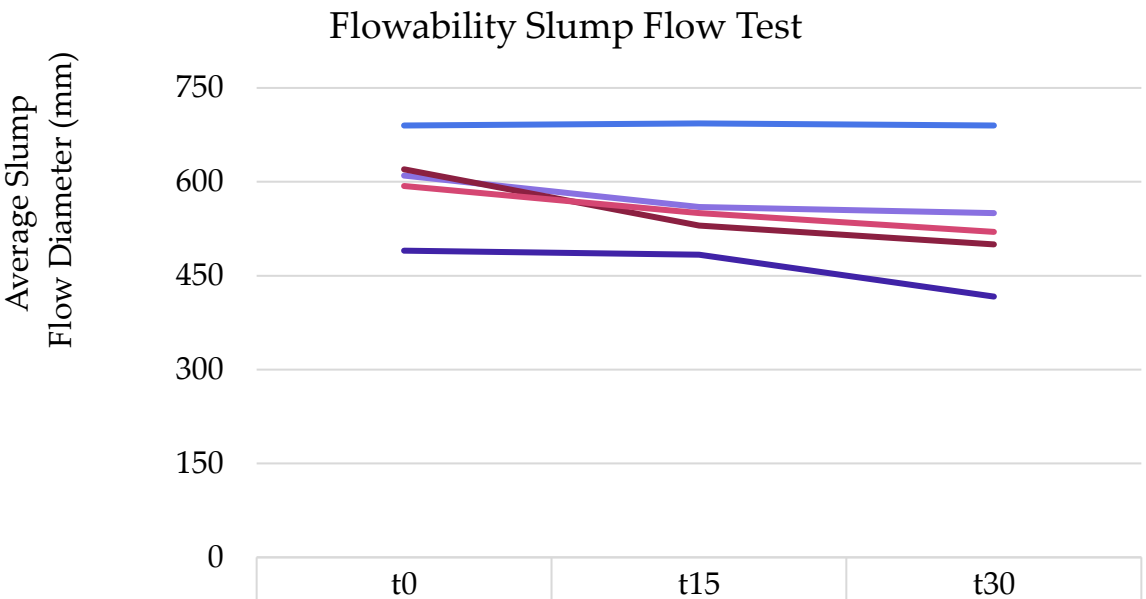

	t0	t15	t30
Mix C0	610	560	550
Mix C0.125S	690	693	690
Mix C0.125L	620	530	500
Mix C0.25S	490	483	417
Mix C0.25L	593	550	520

Figure 4.13 - Flowability - Slump Flow.

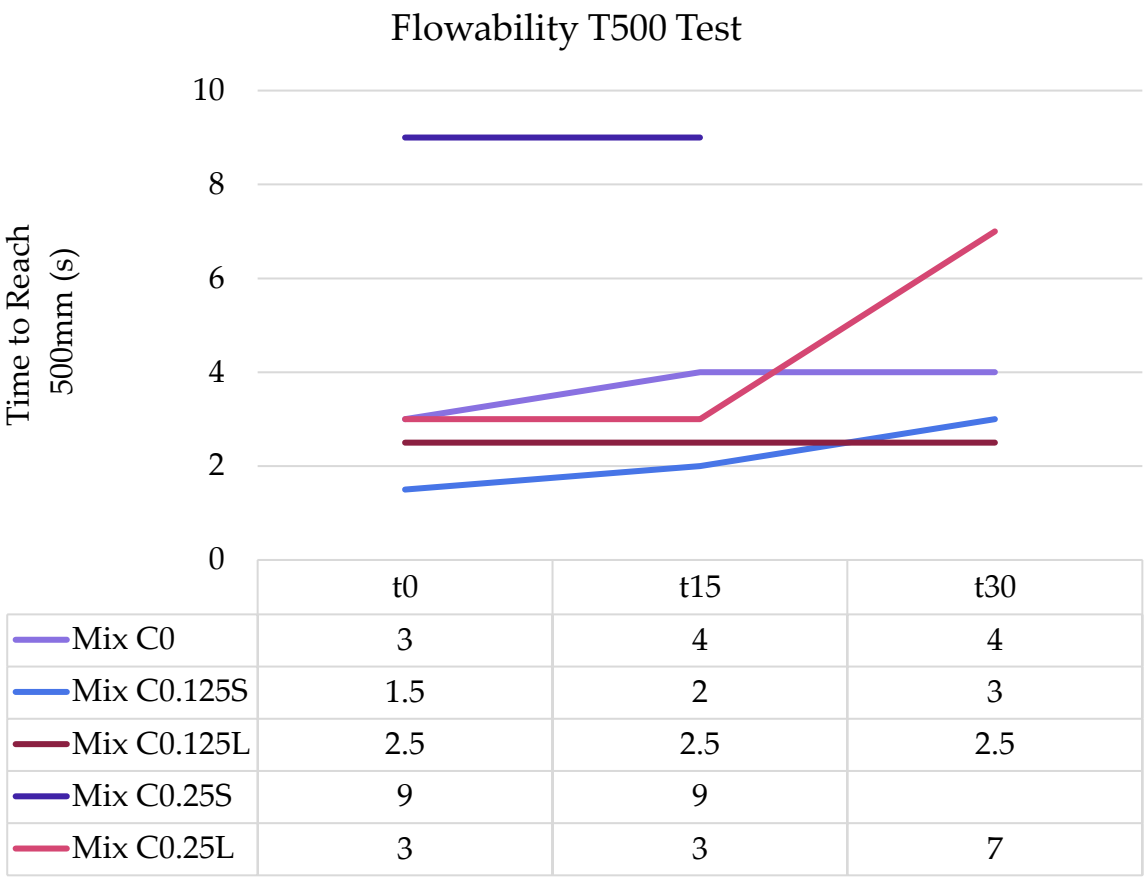

	t0	t15	t30
Mix C0	3	4	4
Mix C0.125S	1.5	2	3
Mix C0.125L	2.5	2.5	2.5
Mix C0.25S	9	9	
Mix C0.25L	3	3	7

Figure 4.14 - Flowability - T_{500}.

4.2.1.1.1 Slump Test

As mentioned in the previous subsection, in the highest percentage of fibre incorporation, the Slump Flow Test was not possible, so the Slump Test as shown in Figure 4.15 was carried out in its place. This test was carried out exclusively for the mixes containing the highest volume fractions of fibres (C0.5S and C0.5L), and both mixes recorded true slumps of 190 mm and 210 mm for short and long fibres respectively, highlighting the substantial reduction in flowability. This reduction could be attributed to the increased fibre water absorption and the resistance and impediment to flow caused by the fibres, which disrupted the natural movement and settlement of concrete during pouring and compaction, the latter typical in fibre reinforced concrete where fibres increase SCC viscosity and internal material friction. This, however, implies that the concrete had notably deviated from its original self-

compacting characteristics, and it is important to note that slump tests were used for conventional concrete as opposed to the slump flow test for self-compacting concrete.

Figure 4.15 - Slump Cone being tamped for 25 times.

C0.5S Mix C0.5L Mix

Figure 4.16 - Workability - Slump Cone Test Results.

4.2.1.2 Viscosity and Flowability Test

Viscosity, as assessed through the V-funnel test shown in Figure 4.17, was critical for understanding how the varying self-compacting concrete mixes could flow and fill formwork without excessive resistance. The test revealed that while the smallest fibre volume fraction did not notably alter viscosity, there was a proportional decrease in

viscosity with increasing fibre content, as can be seen in Figure 4.18. Mixes with the highest fibre volume fractions exhibited considerable viscosity, leading to difficulties in flow and significant clogging issues during the V-funnel test.

Figure 4.17 - Viscosity - V-Funnel test apparatus after use.

Overall, the results ranged from readings at 7 seconds up to 41 seconds. In a similar manner to the former two tests discussed, the two mixes with the highest volume fraction, C0.5S and C0.5L both did not pass this test, indicating poor flowability and high viscosity, which is the opposite of the desired behaviour of self-compacting concrete. Consequently, their results were not recorded and hence not tabulated in Figure 4.18.

High viscosity in SCC can hinder effective self-compaction, diminishing its flowability and potentially compromising concrete quality and workability during pours. Therefore, it is essential to carefully manage fibre content to maintain optimal viscosity levels in SCC. This is critical for achieving the desired flow characteristics necessary for easy placement in construction applications. According to EFNARC standards, the control mix (C0.125S and C0.125L) achieved both VF1 and VF2 classifications, indicating good flowability. In contrast, mixes with higher fibre volumes (C0.25S and C0.25L) achieved only a VF2 classification. This classification trend suggests that as fibre volume increase, the mix tends towards a higher VF2 classification, highlighting the influence of fibre characteristics on SCC flow properties. It was also noted that

longer fibres for each specific volume fraction (0.125% and 0.25%), resulted in a lower V funnel time as an indicator of SCC viscosity and filling ability.

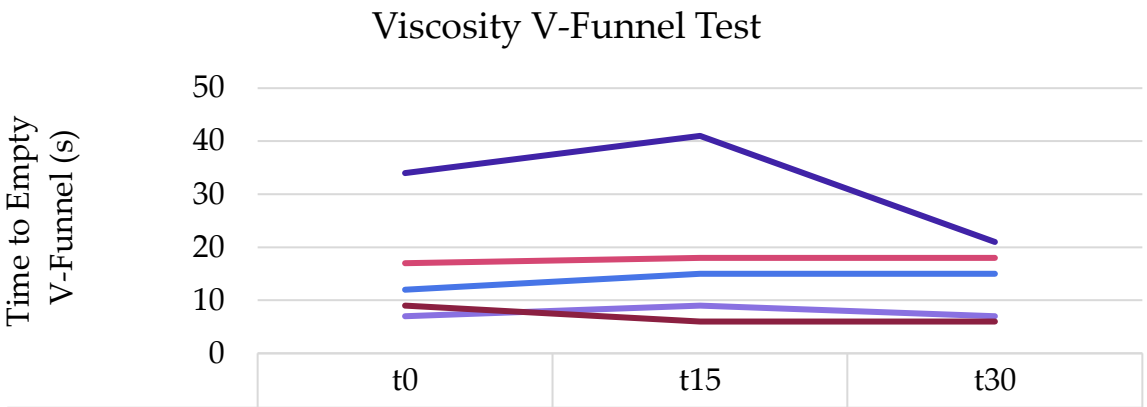

	t0	t15	t30
Mix C0	7	9	7
Mix C0.125S	12	15	15
Mix C0.125L	9	6	6
Mix C0.25S	34	41	21
Mix C0.25L	17	18	18

Figure 4.18 - Viscosity - V-Funnel.

4.2.1.3 Passing Ability Test

The L-box test provided insights into the passing ability of SCC mixes, particularly how well the concrete could flow through narrow spaces without segregation or blockage. The results indicated that while the smallest volume fraction of fibres did not significantly affect passing ability as shown in Figure 4.19, higher fractions, especially with long fibres, led to substantial clogging at the base of the L-box apparatus, as in Figure 4.20. This finding highlights the critical role of fibre type and length in maintaining uniform flow and distribution of SCC mixes. It is also noteworthy that the results at the t_0, t_{15}, and t_{30} marks, namely in the C0.125S and C0.125L mixes, exhibit notable changes as shown in Figure 4.21. This implies that the fibre water absorption over time could contribute to the passing ability of the concrete. It is noted that the dolomite aggregate used for the production of SCC has very low water absorption and had a very low contribution to water absorption. Both the C0.5S

and C0.5L mixes did not pass this test, indicating poor passing ability as the L-box clogged at the base and no concrete was able to pass through the rods. This scenario is not ideal as it would result in very poor pours.

C0 Passing Ability

C0.125S Passing Ability

C0.25S Passing Ability

C0.5S Passing Ability

Figure 4.19 - L-Box Test Results showing decreasing Passing Ability.

Figure 4.20 - Passing Ability - Fibres Clogging in L-Box Test showing reduced Passing Ability.

Results like these highlight the need for careful selection and optimisation of fibres to ensure that SCC can pass through tight gaps and complex formwork efficiently, enhancing its application in construction where consistent flow is essential.

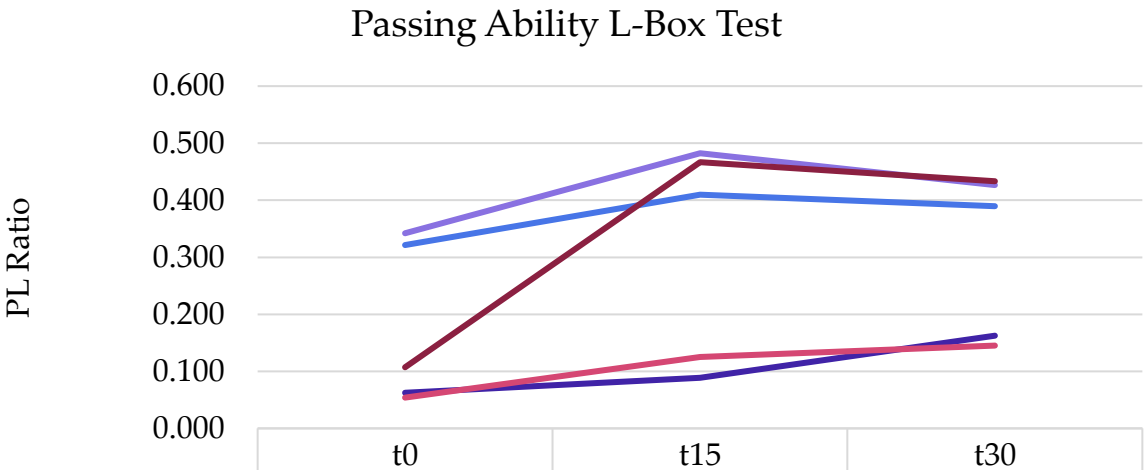

	t0	t15	t30
Mix C0	0.342	0.482	0.426
Mix C0.125S	0.321	0.410	0.390
Mix C0.125L	0.107	0.467	0.433
Mix C0.25S	0.063	0.089	0.163
Mix C0.25L	0.054	0.125	0.145

Figure 4.21 - Passing Ability - L-Box.

4.2.1.4 ICAR Plus Concrete Rheometer Test

The rheological properties of the concrete were assessed using an ICAR Plus Concrete Rheometer as shown in Figure 4.22. The rheological properties, analysed through stress-strain graphs and torque measurements, provided insights into the internal flow behaviour and resistance within SCC mixes. The study observed a steeper gradient in the stress-strain graph with higher fibre percentages as shown in Figure 4.23 and higher torque in Figure 4.24, indicating increased viscosity and reduced flowability. Once again, the rheological properties of mixes with the highest fibre volumes (C0.5S and C0.5L) were not evaluated due to their poor workability, and in order to minimise risk of damaging the sensitive equipment. This aligns with established research suggesting that higher fibre contents led to greater resistance to flow due to increased internal friction and viscosity.

Figure 4.22 - ICAR Plus Concrete Rheometer in use.

Moreover, when examining mixes containing identical fibre volume fraction but larger fibre length, the static yield stress also rose. This suggests that increased shear stress is required to initiate the flow of concrete from a stationary state when fibre volume or

length is increased. The torque measurements further confirmed these observations, highlighting the challenges posed by excessive fibre content in SCC mixes, which could hinder the ability of concrete to self-compact efficiently. These findings highlight the need for careful consideration of fibre volume and type in SCC formulations to optimise rheological properties and ensure consistent flow behaviour during construction, especially in higher volume fraction incorporation.

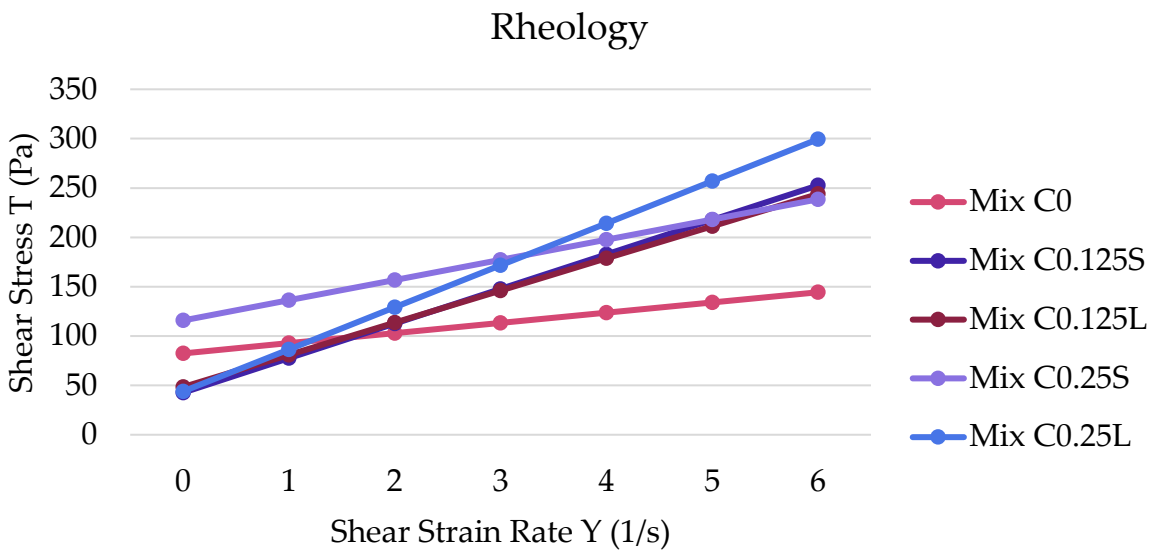

Figure 4.23 - Rheology - ICAR Plus Concrete Rheometer.

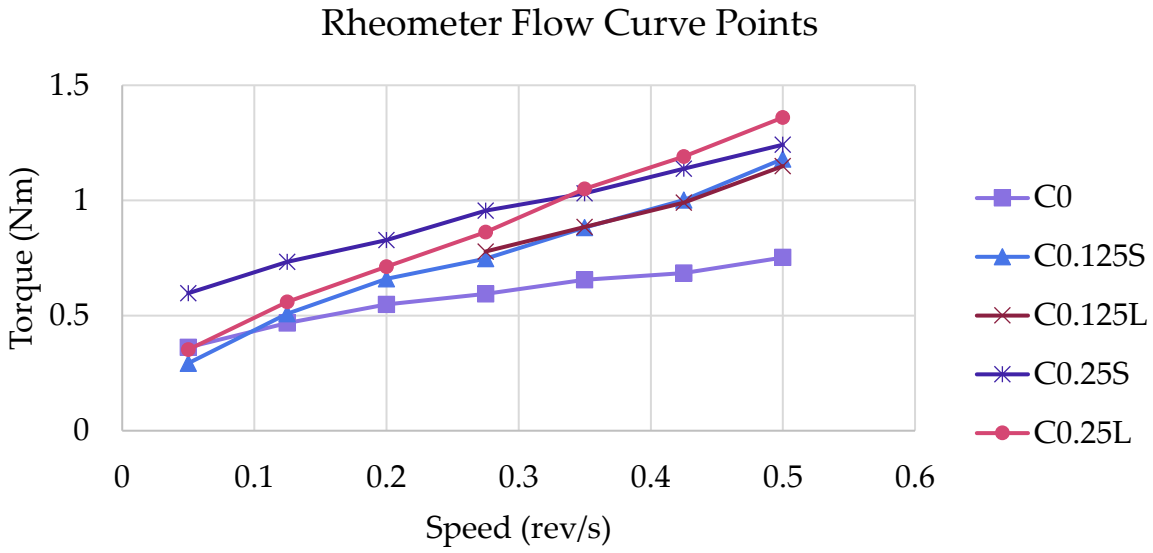

Figure 4.24 - Flow Curve Points - ICAR Plus Concrete Rheometer.

4.2.2 Comparison to Existing Literature on Fresh Properties

As previously outlined in the literature review chapter, there is very limited literature available on the fresh properties of feather fibre reinforced concrete, thus it is not easy to compare directly the results obtained from this experimental program with those in literature.

The fresh and early-stage performance of cement-based material is quite complex, also in view of the hydration processes of cement which depends on the type of materials and additions in the mix. A particular study has shown that the addition of keratin fibres to Portland cement can significantly impact the hydration and setting characteristics of the cement (Mendoza et al., 2021). Specifically, the authors found that the inclusion of keratin fibres delayed both the initial and final setting times of the cement paste, suggesting a retarding effect on the hydration process. The literature study referenced however is based on a paste and utilised small barbs rather than whole fibres in concrete with fine and coarse aggregate. The barbs have different morphological properties to the whole feathers, as used in this study.

Additionally, Mendoza noted that the keratin fibres were observed to modify the heat of hydration, with a lower peak and a longer time to reach the maximum heat of hydration (Mendoza et al., 2021). This was attributed to the potential influence of the keratin fibres on the cement hydration kinetics. Furthermore, the researchers reported that the keratin fibres enhanced the degree of hydration of the cement paste, likely due to their ability to provide additional nucleation sites for cement hydration. These findings have important implications for the potential use of keratin fibres as a sustainable and environmentally friendly additive in the development of advanced cement-based composites. However, the limited amount of literature on the effects of keratin fibres in cement-based materials highlights the need for further research to fully understand the underlying mechanisms and optimise the use of feather fibres.

Furthermore, there has been a much more extensive discussion on the use of synthetic fibres, such as polypropylene and polyester (Bolat et al., 2014; Ghanem et al., 2021; Shafei et al., 2021).

In this study, four concrete mixtures were prepared: a reference sample made of plain concrete, and three fibre-reinforced concrete mixtures incorporating steel, polyester, and polypropylene fibres, respectively. The ratio of fibres was set at 4.25% of the concrete volume (Bolat et al., 2014). The fresh properties of these concrete mixtures, including slump flow, workability, and viscosity, were then evaluated and compared.

The results indicate that the incorporation of synthetic fibres, particularly polypropylene, can significantly impact the fresh properties of concrete (Leung & Balendran, 2003). The presence of polypropylene fibres was observed to reduce the concrete workability. This is attributed to the effect of the fibres which can hinder the flow of the concrete mixture. The reduced workability noted in the aforementioned study are in agreement with the results gathered in the experimental program in this research, as there has been an overall reduction in workability, notably in the larger volume fractions.

4.2.3 Physical and Mechanical Properties of Self-Compacting Mortars

4.2.3.1 Density Test

Various 40 x 40 x 160 mm mortar prisms were measured for their dimensions using a pair of calibrated digital vernier callipers, and their mass was accurately recorded using a calibrated digital balance.

It is known that incorporation of certain types of fibres in concrete could potentially increase the density of the composite material, as will be discussed, even though feathers themselves have a very low density. This phenomenon can be explained by several factors related to the microstructure and interaction between the fibres and the cement matrix.

Firstly, feather fibres, despite being lightweight, contributed to a denser packing of particles within the concrete or mortar matrix, which can be seen in the results below in Figure 4.25. When fibres were added to the mix, they most likely filled voids and reduced the amount of air entrapped in the concrete. This reduction in air content could have led to the higher overall density of the composite material. Such reduction of air voids is known to be a crucial factor in increasing the density and strength of concrete (Neville, 1973).

When most of the fibres were added, the concrete mixes exhibited increased density, reflecting the fibres' ability to fill voids and enhance the compaction of the concrete. These fibres effectively reduced the amount of trapped air and created a denser material. On the other hand, the mixes containing the largest amount of fibres demonstrated an overall lower density compared to those with shorter and less fibres. This reduction in density was attributed to the longer fibres creating air holes within the concrete matrix. Due to their greater length and overall volume incorporation in the mix, these fibres were more likely to overlap, entangle, and create pockets of trapped air, leading to increased porosity and thus a lower overall density.

Therefore, while fibre reinforcement generally improved the density of concrete, the volume fraction of the fibres played a critical role. Less fibres contributed to a denser mix by reducing air voids and enhancing compaction, whereas larger volumes tended to create air pockets, which decreased the density. The mortar with lower fibre content had higher flow characteristics similar or on par to those of regular SCC, whereas those with larger fibre content had reduced flow properties also resulting lower packing density.

The mechanical interlocking between the feather fibres and the cementitious matrix could also enhance the observed compaction of the concrete. The fibres can act as bridges across voids and cracks, effectively knitting the material together more tightly. This enhanced compaction can lead to a denser and more uniform concrete structure. The presence of fibres improves the packing density by filling gaps between the larger

aggregate particles and the cement paste, thus reducing the porosity and increasing the density of the material (Hoseini et al., 2009).

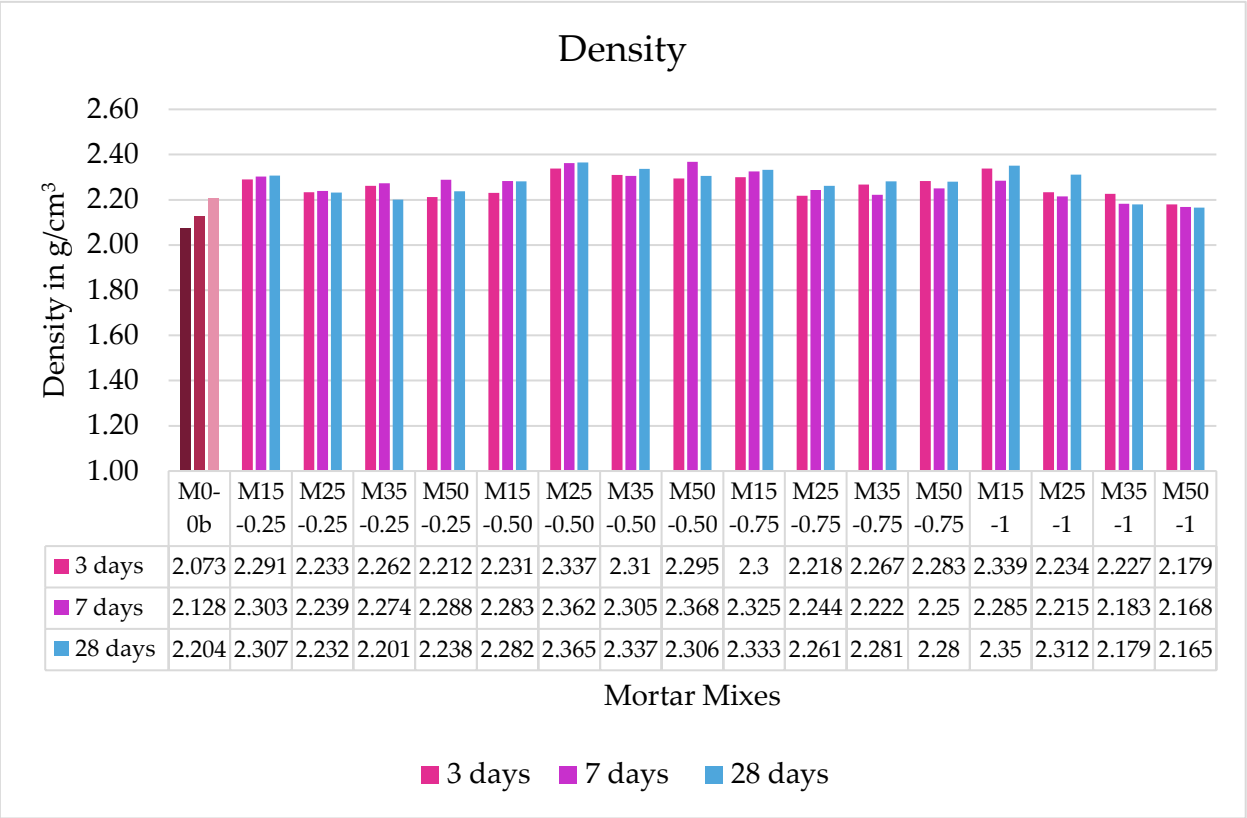

	M0-0b	M15-0.25	M25-0.25	M35-0.25	M50-0.25	M15-0.50	M25-0.50	M35-0.50	M50-0.50	M15-0.75	M25-0.75	M35-0.75	M50-0.75	M15-1	M25-1	M35-1	M50-1
3 days	2.073	2.291	2.233	2.262	2.212	2.231	2.337	2.31	2.295	2.3	2.218	2.267	2.283	2.339	2.234	2.227	2.179
7 days	2.128	2.303	2.239	2.274	2.288	2.283	2.362	2.305	2.368	2.325	2.244	2.222	2.25	2.285	2.215	2.183	2.168
28 days	2.204	2.307	2.232	2.201	2.238	2.282	2.365	2.337	2.306	2.333	2.261	2.281	2.28	2.35	2.312	2.179	2.165

Figure 4.25 - Density of Mortar Mixes.

There was an increase in density for most of the mortar mixes, however, the most substantial increase was present in those mixes with a shorter fibre length, namely those with 15 mm and 25 mm. As the fibre volume fraction and the length of the fibres increased proportionally, the density began to reduce once again to values comparable to the control mix, shown in Figure 4.25 for contrast, which could likely be because of the clumping that could have formed in the mix, creating the air voids which the shorter fibres served to fill. Thus, the lower volume resulted in a higher density.

Furthermore, the chemical interaction between the feather fibres and the cement matrix is likely to play a role in increasing the density. Since feather fibres are primarily composed of keratin, this can interact with the alkaline environment of the cement paste and hence can lead to the formation of additional binding phases within the concrete, contributing to the overall density. In an alkaline environment, keratin may

undergo partial hydrolysis, breaking down into smaller peptides or amino acids. This process exposes additional reactive groups that can chemically bond with the cement matrix. The chemical bonding between the fibres and the cement paste improves the integrity and compaction of the mix, leading to a denser final product (Mendoza et al., 2021).

In summary, while feather fibres themselves are low-density materials, their incorporation into mortar led to a trend with an overall increase in density due to improved particle packing, enhanced mechanical interlocking, and chemical interactions within the cement matrix. These factors work together to reduce voids and increase the solid content of the mortar or concrete, resulting in a denser composite material.

4.2.3.2 Ultrasonic Pulse Velocity Test

The same prisms which were used to evaluate the density were then used to measure the ultrasonic pulse velocity through the mortar, as shown in Figure 4.26. There was very little variation in the results gathered from the Ultrasonic Pulse Velocity (UPV) test, as shown in Figure 4.27.

When feather fibres were incorporated into the mortar, the results of the UPV test remained largely unchanged. All results were within the 2 and 2.5 km/s range, which does not indicate that the feather fibres had any significant effect on the time it takes for ultrasonic pulses to travel through the different mixes. This suggests that the presence of fibres did not extensively affect the material's internal structure in a way that could be detected by the UPV test. The fibres did not create substantial voids or defects that would slow down the pulse velocity, indicating that the overall homogeneity and density of the mortar were maintained.

Figure 4.26 - Ultrasonic Pulse Velocity of a prism being measured.

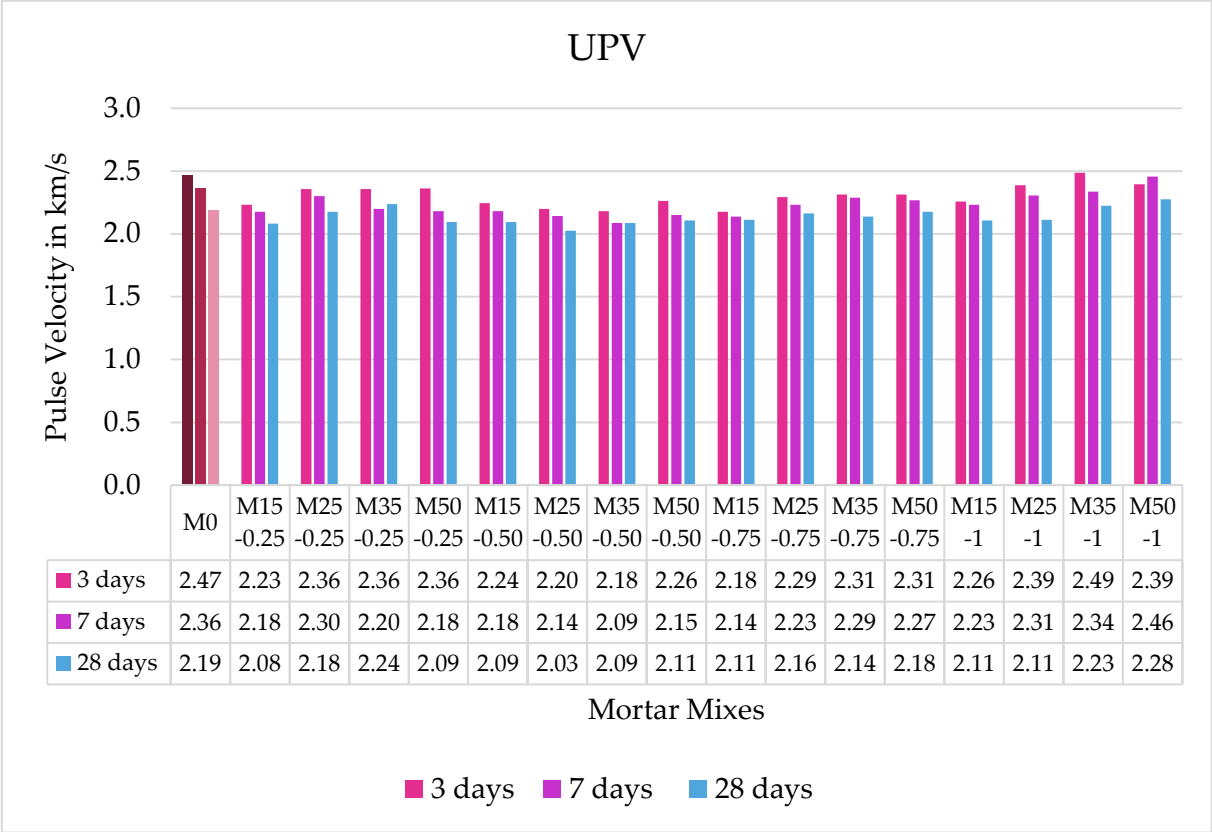

	M0	M15 -0.25	M25 -0.25	M35 -0.25	M50 -0.25	M15 -0.50	M25 -0.50	M35 -0.50	M50 -0.50	M15 -0.75	M25 -0.75	M35 -0.75	M50 -0.75	M15 -1	M25 -1	M35 -1	M50 -1
3 days	2.47	2.23	2.36	2.36	2.36	2.24	2.20	2.18	2.26	2.18	2.29	2.31	2.31	2.26	2.39	2.49	2.39
7 days	2.36	2.18	2.30	2.20	2.18	2.18	2.14	2.09	2.15	2.14	2.23	2.29	2.27	2.23	2.31	2.34	2.46
28 days	2.19	2.08	2.18	2.24	2.09	2.09	2.03	2.09	2.11	2.11	2.16	2.14	2.18	2.11	2.11	2.23	2.28

Figure 4.27 - Ultrasonic Pulse Velocities.

4.2.3.3 *Flexural Strength Test*

After measuring the density and ultrasonic pulse velocity, the prisms were tested for their mechanical strengths, namely flexural and then compressive. The flexural strength test utilised a three-point bending rig, as shown in Figure 4.28, to calculate the flexural strength in MPa or N/mm². The dimensions obtained from the density measurements were applied, and the distance between the rollers kept fixed to ensure uniform support for each prism. Notable improvements in flexural strength were observed in mortar mixes containing shorter fibres, particularly with 15 mm fibres enhancing the 0.5% and 0.75% volume fraction mixes, as depicted in Figure 4.29. The most substantial increase in flexural strength was found in the mortar mixes M15-0.50 and M25-0.50, representing the 0.5% volume fraction with 15 mm and 25 mm fibres, respectively, showing an increase of over 10%. However, it was also observed that for all fibre lengths, mixes with the largest volume fraction (1%) and those with longer fibres (35 mm and 50 mm) exhibited a notable decrease in flexural strength. This reduction indicates that while shorter fibres can enhance flexural strength at lower volume fractions, longer fibres and higher fibre content may introduce weaknesses, leading to diminished performance.

Figure 4.28 – Mortar Prism before and after Failure in the Three-Point Bending Test.

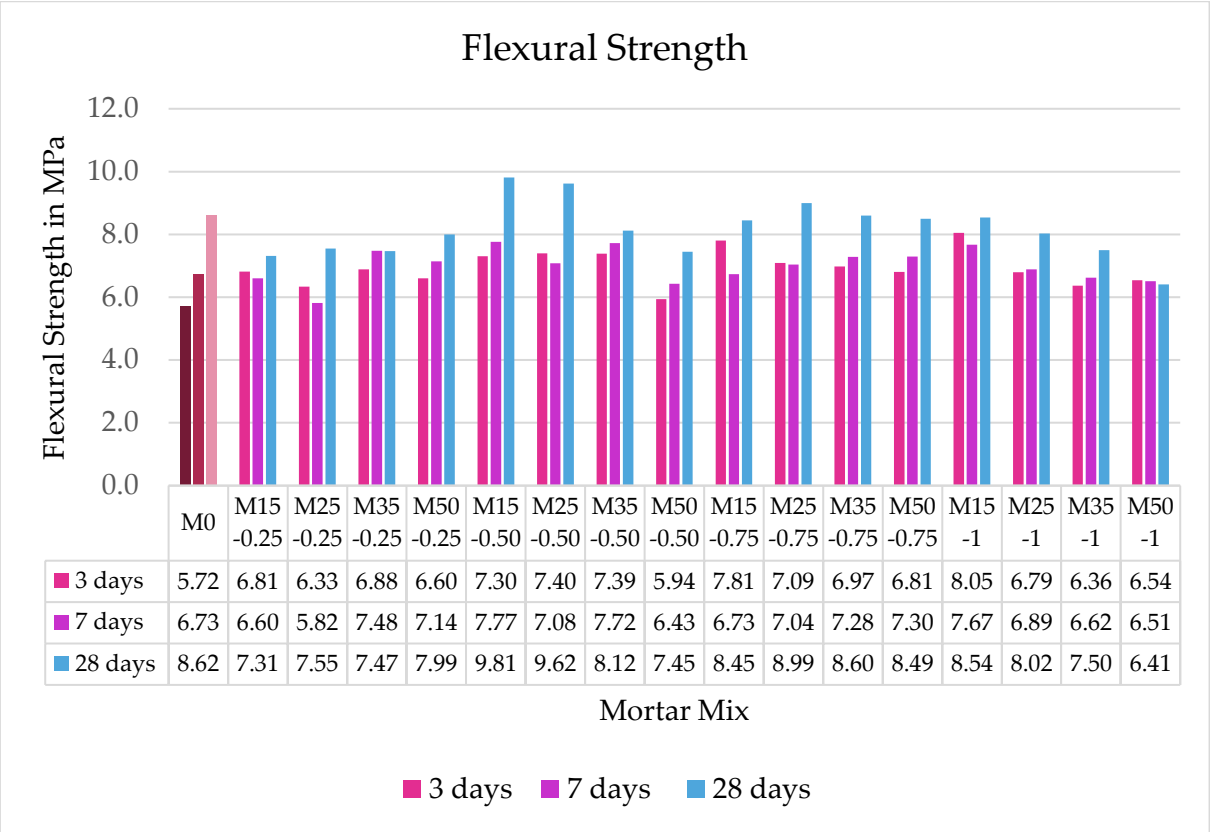

	M0	M15 -0.25	M25 -0.25	M35 -0.25	M50 -0.25	M15 -0.50	M25 -0.50	M35 -0.50	M50 -0.50	M15 -0.75	M25 -0.75	M35 -0.75	M50 -0.75	M15 -1	M25 -1	M35 -1	M50 -1
3 days	5.72	6.81	6.33	6.88	6.60	7.30	7.40	7.39	5.94	7.81	7.09	6.97	6.81	8.05	6.79	6.36	6.54
7 days	6.73	6.60	5.82	7.48	7.14	7.77	7.08	7.72	6.43	6.73	7.04	7.28	7.30	7.67	6.89	6.62	6.51
28 days	8.62	7.31	7.55	7.47	7.99	9.81	9.62	8.12	7.45	8.45	8.99	8.60	8.49	8.54	8.02	7.50	6.41

Figure 4.29 - Flexural Strength of Mortar Prisms.

The observed improvements in flexural strength for mortar mixes containing shorter fibres, especially with 15 mm fibres at 0.5% and 0.75% volume fractions, were not unexpected. Shorter fibres are more likely to distribute evenly throughout the mortar matrix, effectively bridging microcracks and enhancing the overall structural integrity. This distribution enables the fibres to contribute significantly to the flexural strength by improving the crack resistance and load-bearing capacity of the mortar. The most notable increase in flexural strength was found in the mixes M15-0.50 and M25-0.50, showing an increase of over 10%, which aligns with the expected behaviour of well-distributed shorter fibres at optimal volume fractions.

Furthermore, the observed decrease in flexural strength for mixes with the largest volume fraction (1%) and those containing longer fibres (35 mm and 50 mm) was also somewhat expected but highlights the complexity of fibre reinforcement. At higher volume fractions, the increased amount of fibres can lead to clumping and poor distribution within the matrix, creating stress concentrations and potential weak points. Longer fibres, due to their greater length, are more prone to overlapping and

entangling, which can result in air pockets and inconsistencies in the mortar. These factors introduce weaknesses that can compromise the overall structural integrity, leading to diminished flexural performance.

In summary, while shorter fibres at lower volume fractions enhance flexural strength by evenly distributing and effectively bridging microcracks, longer fibres and higher fibre content can introduce weaknesses due to poor distribution and increased likelihood of air pockets. Therefore, the observed results were aligned with the expected outcomes based on the behaviour of fibres in the mortar matrix.

4.2.3.4 Compressive Strength Test

The second mechanical property to be tested was the compressive strength. The two halves of the fractured prism were then taken to the compression machine shown in Figure 4.31, and a constant loading rate of 2400 N/s was applied until failure occurred.

Improvements in compressive strength were observed in mixes incorporating shorter fibres, specifically 15mm fibres, which enhanced the strength of the 0.5%, 0.75%, and 1% volume fraction mixes, i.e. the M15-0.5, M15-0.75, and M15-1, mixes respectively, shown in Figure 4.30. These shorter fibres were most likely able to integrate more effectively into the mortar matrix, reinforcing the structure and providing additional resistance to compressive forces. However, mixes with longer fibres exhibited a different trend, showing lower compressive strength compared to those with shorter fibres. This discrepancy became particularly pronounced at higher volume fractions. The largest volume fraction of longer fibres resulted in a notable drop in compressive strength. This reduction in performance could be attributed to the challenges associated with uniformly distributing longer fibres within the concrete mix, leading to potential weak spots and compromising the structural integrity of the concrete. Consequently, while the shorter fibres improved compressive strength across various volume fractions, the longer fibres proved less effective, particularly at higher concentrations, highlighting the importance of fibre length in optimising the mechanical properties of fibre-reinforced mortar.

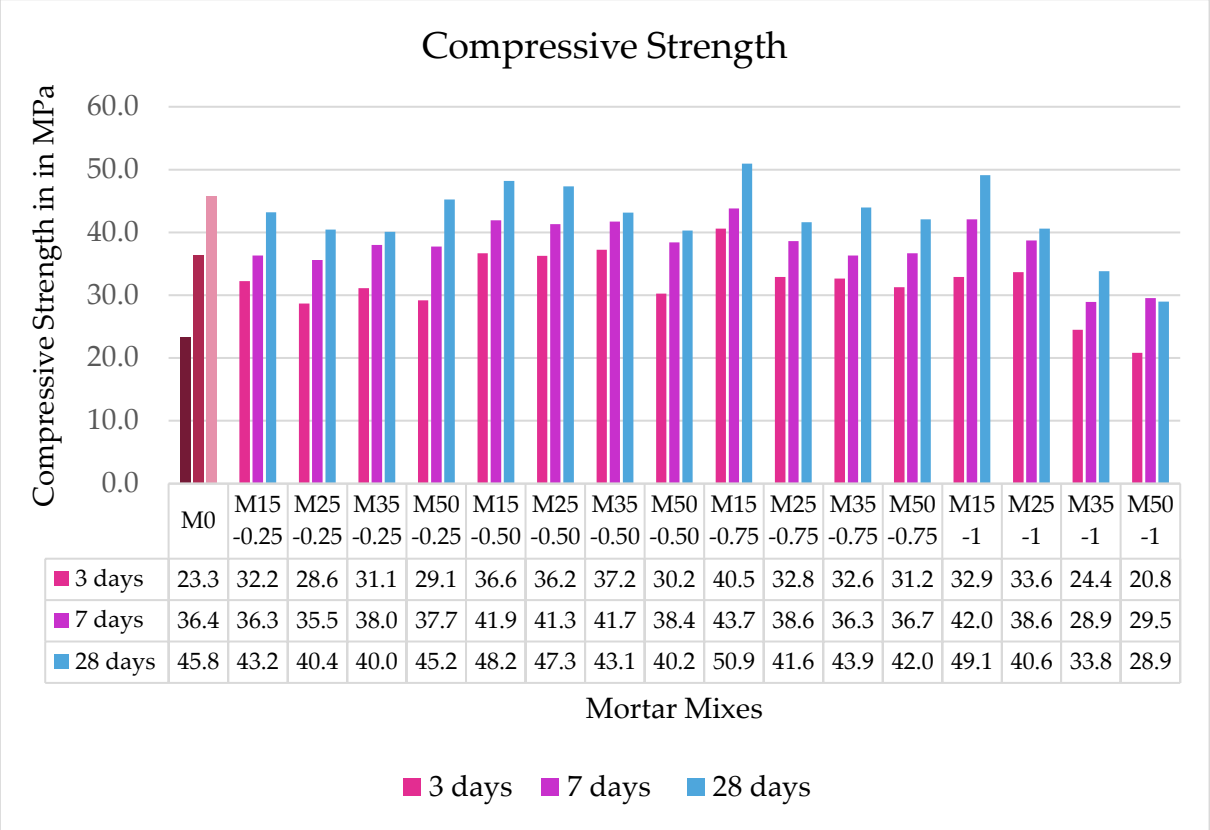

	M0	M15 -0.25	M25 -0.25	M35 -0.25	M50 -0.25	M15 -0.50	M25 -0.50	M35 -0.50	M50 -0.50	M15 -0.75	M25 -0.75	M35 -0.75	M50 -0.75	M15 -1	M25 -1	M35 -1	M50 -1
3 days	23.3	32.2	28.6	31.1	29.1	36.6	36.2	37.2	30.2	40.5	32.8	32.6	31.2	32.9	33.6	24.4	20.8
7 days	36.4	36.3	35.5	38.0	37.7	41.9	41.3	41.7	38.4	43.7	38.6	36.3	36.7	42.0	38.6	28.9	29.5
28 days	45.8	43.2	40.4	40.0	45.2	48.2	47.3	43.1	40.2	50.9	41.6	43.9	42.0	49.1	40.6	33.8	28.9

Figure 4.30 - Compressive Strength of Mortar Prisms.

Figure 4.31 – Mortar Prism after Failure in the Compression Test.

Overall, the observed trends in compressive strength for fibre-reinforced mortar mixes, with improvements noted for shorter fibres and reductions for longer fibres, were largely expected based on known principles of fibre reinforcement in concrete.

The substantial improvements in compressive strength for mixes incorporating shorter fibres (e.g., 15 mm fibres) were expected. Shorter fibres can be more evenly distributed throughout the mortar matrix, ensuring a more homogeneous mix. This uniform distribution helps in bridging microcracks effectively and contributes to a denser and more cohesive matrix, which enhances compressive strength.

Shorter fibres are also less likely to entangle and overlap, which means they can bond better with the surrounding mortar. This improved bonding increases the load transfer efficiency between the fibres and the matrix, contributing to higher compressive strength. Shorter fibres are more effective at bridging microcracks, preventing them from propagating and thus maintaining the structural integrity of the concrete under compressive loads.

The data showing that mixes like M15-0.5, M15-0.75, and M15-1 had higher compressive strengths confirms these expected benefits. For instance, the M15-0.75 mix achieved a compressive strength of 50.9625 MPa at 28 days, substantially higher than the control mix M0 at 45.8150 MPa.

The observed reductions in compressive strength for mixes with longer fibres (e.g., 35 mm and 50 mm) were also anticipated, as longer fibres are more difficult to distribute uniformly within the mortar matrix. This can lead to fibre clumping and the formation of air pockets, both of which create weak spots in the concrete.

The longer fibres can introduce more air into the mix, which reduces the overall density and compressive strength. This is evident from the notable drop in compressive strength for the M50-1 mix, which had only 28.9594 MPa at 28 days, compared to the control mix and shorter fibre mixes. Longer fibres are also prone to entanglement and overlapping, which can interfere with the effective bonding between the fibres and the matrix. This reduces the load-bearing capacity and the efficiency of load transfer within the concrete. The presence of longer fibres can also finally lead to stress concentrations around the fibres, which can induce cracking and reduce the overall compressive strength of the concrete.

Given these factors, the reductions in compressive strength for mixes with longer fibres and higher volume fractions were mostly expected. The challenges associated with incorporating longer fibres uniformly into the mix compromise the structural integrity, leading to lower performance under compressive loads.

Overall, the observed results align well with theoretical expectations and prior research on fibre-reinforced concrete. The improvements in compressive strength with shorter fibres and the reductions with longer fibres highlight the importance of fibre length and volume fraction in optimising the mechanical properties of fibre-reinforced mortar.

4.2.4 Physical and Mechanical Properties of Self-Compacting Concrete

4.2.4.1 Density Test

The SCC density tests established similar trends to those observed in the SCM results. An increased density, as shown in Figure 4.32, was noted for most fibre-reinforced SCC mixes, when compared to the control mix.

The overall increase in density can be attributed to the SCC properties of the matrix enhancing the compaction of the material, resulting in a more compact matrix. It could also be due to the fibres effecting filling the air voids, and hence resulting in a more compact mix overall.

The increased density of the mixes will later be acknowledged in the increased strength properties of the SCC, as a reduction in density would have ultimately led to a reduction in strength, which was not the case for most mixes.

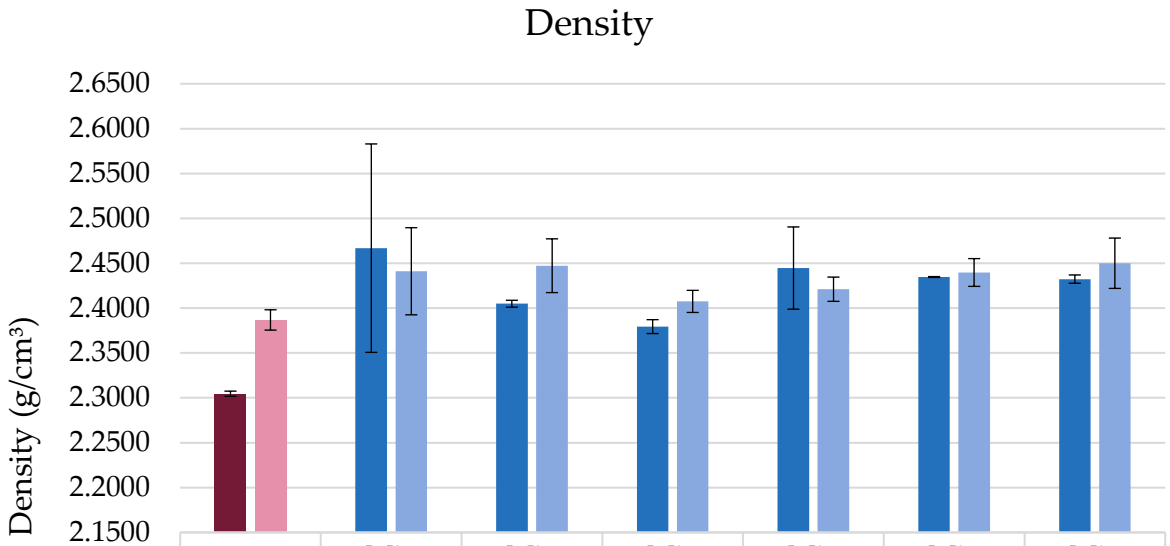

	Mix C0	Mix C0.125S	Mix C0.125L	Mix C0.25S	Mix C0.25L	Mix C0.5S	Mix C0.5L
7 days	2.3046	2.4668	2.4049	2.3794	2.4446	2.4346	2.4323
28 days	2.3868	2.4410	2.4472	2.4075	2.4211	2.4397	2.4500

Figure 4.32 - Self-Compacting Concrete Density

4.2.4.2 Compressive Strength Test

Compressive strength tests were conducted on 100 x 100 x 100 mm cube specimens on both the 7th and 28th days from casting for each mix design. All cubes failed in a satisfactory manner, as shown in Figure 4.33. Results for the SCC showed notable improvement, particularly in the mixes with the largest volume fractions of fibres, namely C0.5S (short fibres) and C0.5L (long fibres). These improvements in compressive strength can be attributed to the stronger bonds formed within the concrete matrix. Although these high-fibre mixes lost some of their self-compacting properties, they gained substantial resistance to compressive loading as the fibre volume fraction increased to this volume fraction. The overall higher density of the fibre-reinforced mixes could have possibly replaced the compacting properties of SCC by the mechanical linking of the fibres within the matrix, and hence leading to a better distribution of stresses amongst the samples.

Figure 4.33 – Compressive Test Cubes after Failure – Fibres visible in some faces.

At the 7-day mark, the control mix C0 exhibited a compressive strength of 38.37 MPa. Notably, Mix C0.125S achieved a compressive strength of 46.28 MPa, performing 20.6% better than the control. Mix C0.5L also showed an increase, with a compressive strength of 43.19 MPa, which was 12.6% higher than the control. In contrast, Mix C0.25S demonstrated a compressive strength of 42.45 MPa, which was 10.6% better than the control, but it underperformed relative to other fibre mixes. However, it is noteworthy that all mixes, regardless of fibre volume fraction, exhibited improved compressive strength when testing at the 7th day from casting. This improvement could be to the effect of confinement and reduced brittle performance of the material due to the fibres bridging micro-cracks formed, redistributing stresses within the material. Further, it may also be linked to the effect of fibres absorbing mix water affecting workability and also leading to a lower water/cement ratio which is related to higher strength.

By the 28-day mark, the control mix C0 showed a compressive strength of 51.12 MPa. Mix C0.5L exhibited the highest compressive strength of 59.76 MPa, outperforming the control by 16.9%. Mix C0.5S also demonstrated a substantial improvement, with a compressive strength of 58.19 MPa, 13.8% higher than the control. Mix C0.125S slightly outperformed the control with a compressive strength of 51.83 MPa, an increase of 1.4%. This suggests that incorporating a small volume of fibres has a negligible effect on the 28-day strength of these mixes. However, Mix C0.25S showed a notable drop,

with a compressive strength of 37.54 MPa, which was 26.6% lower than the control, indicating potential issues with this mix over time.

The analysis of these results highlights several key trends. Mixes C0.5S and C0.5L consistently showed the most substantial improvement in compressive strength at both 7 and 28 days. Mix C0.5L, in particular, stood out with the highest compressive strength at 28 days, indicating its superior long-term performance. Conversely, Mix C0.25S showed a notable decline in strength at 28 days.

When visually inspecting the type of failure of the cubes tested, it was noted that all cubes failed in a satisfactory manner, as indicated on the standard MSA EN 12390-3 (2009), listed in the previous methodology chapter.

Since improvements were noted in compressive strength for all volume fractions, it is significant to consider the early strength gain of the fibre-reinforced mixes. The 7-day tests confirmed that for all mixes, there was an improvement in compressive strength. It was also noted that shorter fibres performed slightly better than longer fibres for most volume fractions.

Furthermore, the drastic improvement in the largest volume fraction, for both the short and the long fibres (C0.5S and C0.5L), shows strong potential for this mix to be used as a construction material. Being able to withstand large compressive loads is one of the main uses of concrete in the construction industry, and enhanced compressive strength would certainly serve as a selling point for this concrete.

Taking a step back to the discussion on the fresh properties of the mixes, it is also important to note that these two particular mixes, C0.5S and C0.5L, did not conform to the EFNARC standards for self-compacting concrete and were not examined for

most of the self-compacting concrete fresh property empirical tests compared to the other volume fraction counterparts.

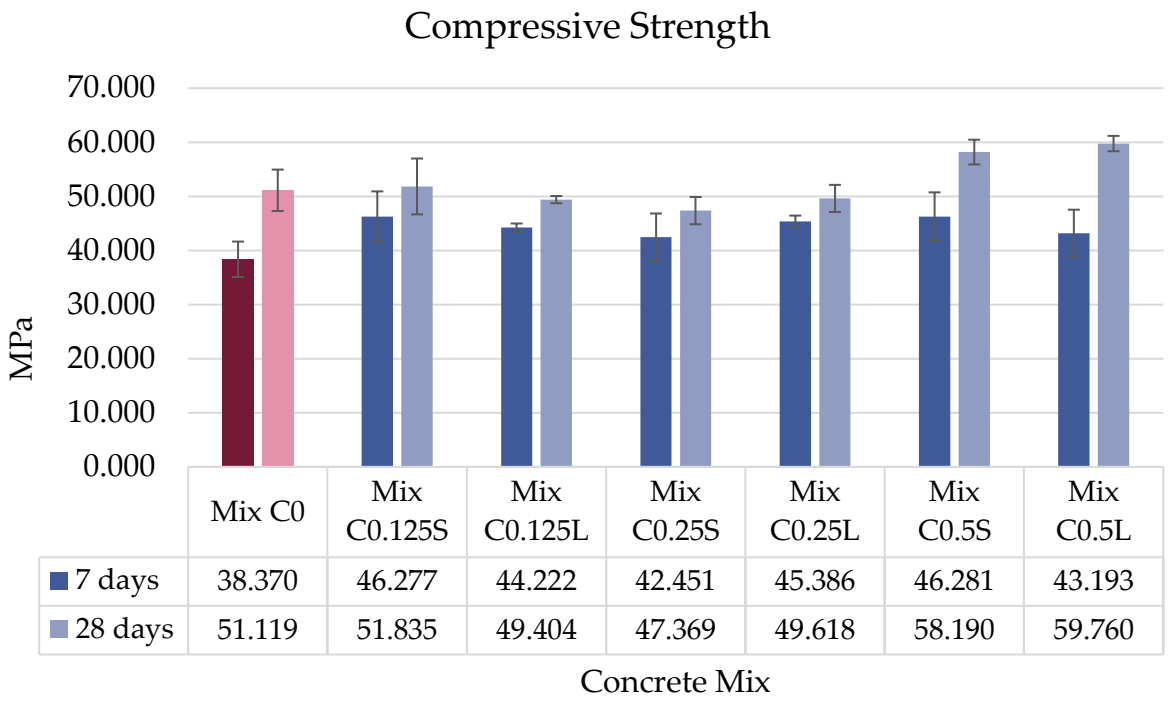

	Mix C0	Mix C0.125S	Mix C0.125L	Mix C0.25S	Mix C0.25L	Mix C0.5S	Mix C0.5L
7 days	38.370	46.277	44.222	42.451	45.386	46.281	43.193
28 days	51.119	51.835	49.404	47.369	49.618	58.190	59.760

Figure 4.34 – Mean Compressive Strength of Self-Compacting Concrete.

The overall improvement in compressive strength observed in fibre-reinforced concrete was not unexpected. Fibre reinforcement in concrete materials enhances strength primarily by arresting the formation and propagation of microcracks within the concrete matrix. When microcracks begin to form, the fibres bridge these cracks, preventing them from growing into larger, more notable fractures. This crack-bridging mechanism is crucial as it effectively increases the compressive strength of the concrete.

Moreover, fibres play a vital role in distributing loads more evenly throughout the concrete matrix. This uniform distribution of stress helps to minimise stress concentrations that can lead to premature failure. By mitigating these stress concentrations, fibres contribute to a stronger concrete structure. The experimental results clearly showed that all samples reached a satisfactory peak load before failure, indicating that the inclusion of fibres effectively prevented premature failures and enhanced the overall compressive strength of the concrete.

Another noteworthy factor contributing to the improvement in compressive strength is the enhanced bonding between the cement paste and the aggregates, facilitated by the presence of fibres. The fibres improve the toughness of the concrete mix, and help in improving the Poisson's effect. This enhanced bonding is critical because it ensures that the various components of the concrete work together more effectively, thereby increasing the material's overall strength.

Overall, the consistent performance across all samples, reaching satisfactory peak loads without premature failures, highlights the value of fibre reinforcement in enhancing the compressive strength of concrete materials. This improvement highlights the potential of fibre-reinforced concrete in various structural applications where enhanced strength and durability are paramount.

4.2.4.3 Splitting Tensile Strength Test

Tensile splitting strength tests were performed on cylinder specimens, each measuring 150 mm in diameter and 300 mm in height, on the 7^{th} and 28^{th} days after casting for each mix design.

The results of the tensile strength tests at 7 days and 28 days for various fibre volume fractions and fibre lengths are shown in Figure 4.35.

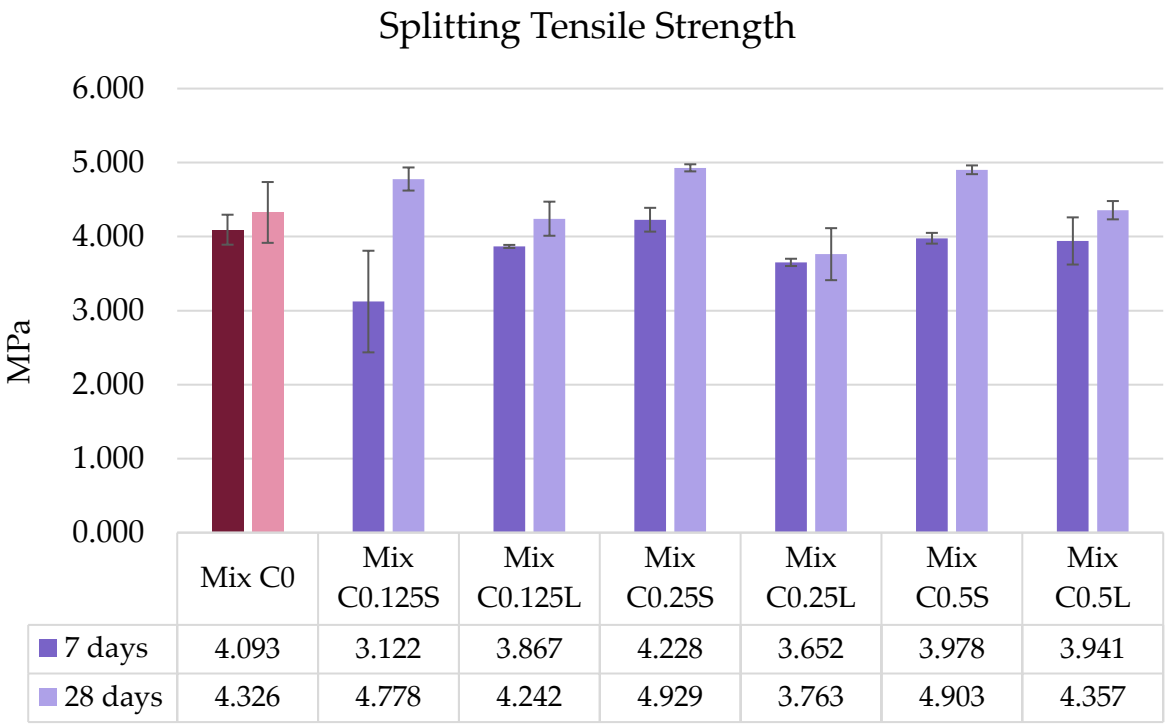

	Mix C0	Mix C0.125S	Mix C0.125L	Mix C0.25S	Mix C0.25L	Mix C0.5S	Mix C0.5L
7 days	4.093	3.122	3.867	4.228	3.652	3.978	3.941
28 days	4.326	4.778	4.242	4.929	3.763	4.903	4.357

Figure 4.35 – Mean Tensile Strength of Self-Compacting Concrete.

At the 7-day mark, the control mix C0 exhibited a tensile strength of 4.093 MPa. Notably, Mix C0.25S achieved a tensile strength of 4.228 MPa, performing 3.3% better than the control. Conversely, Mix C0.125S had a particularly lower tensile strength of 3.122 MPa, which was 23.7% less than the control. However, while a decrease in tensile strength was noted for fibre-reinforced mixes at the 7-day test mark, visual inspections revealed a trend with an increase in the ductility of the mixes, as can be seen in Figure 4.36, where fibre-bridging of cracks was observed.

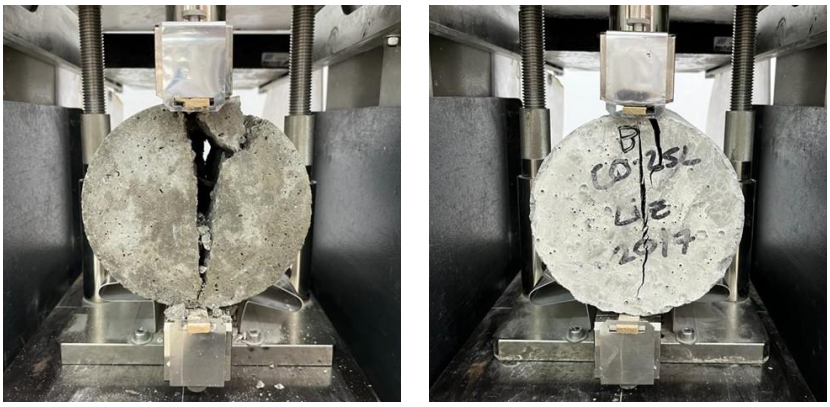

C0 (Control) Mix C0.25L Mix

Figure 4.36 – Splitting Tensile Test after Failure – Fibres showing improved Ductility.

By the 28-day mark, the control mix C0 showed a tensile strength of 4.326 MPa. Mix C0.25S continued to perform well, exhibiting the highest tensile strength of 4.929 MPa, which was 13.9% better than the control. Mix C0.125S also showed substantial improvement, with a tensile strength of 4.778 MPa, 10.4% higher than the control. In contrast, Mix C0.25L had a tensile strength of 3.763 MPa, which was 13% lower than the control.

The analysis of these results reveals interesting patterns. Mix C0.25S consistently showed the best improvement at both 7 days (+3.3%) and 28 days (+13.9%), indicating notable strength gain over time. Mix C0.125S demonstrated substantial improvement at 28 days, with an increase of 10.4%. These results suggest that short fibres contribute positively to long-term strength, probably due to higher distribution of fibres in the matrix, for the specific fibre fraction. In contrast, Mix C0.25L consistently performed worse than the control mix at both 7 days (-10.8%) and 28 days (-13%).

The improvement in the ductile behaviour of fibre-reinforced concrete mixes is also expected. Fibres can bridge microcracks that begin to form during curing or testing, contributing substantially to the mix's ductility. The previous results have consistently shown an improvement with the incorporation of shorter fibres into the mix. These shorter fibres likely spread more thoroughly throughout the matrix, bridging a higher number of microcracks compared to their longer counterparts.

The incorporation of feather fibres also enhances the energy absorption capacity of concrete. These fibres can deform and pull out under stress, absorbing energy and thereby enhancing the overall toughness and ductility of the concrete mix. The pulling out of the fibres absorbs additional energy by resisting stress, thereby delaying crack propagation and the ultimate failure of the concrete. This capacity for energy absorption and deformation under stress prevents sudden failure and allows the concrete to sustain larger deformations before breaking.

When analysing these results, it is evident that they conform to the current knowledge that fibre-reinforced concrete exhibits significantly improved ductility compared to conventional concrete. This improvement is primarily due to the inclusion of fibres, which enhance the concrete's ability to deform under stress without experiencing sudden failure. The incorporation of fibres in the concrete matrix provides better control over crack initiation, growth, and propagation, thereby enhancing structural durability, increasing the elastic modulus, and reducing brittleness, which is also likely to be the case for the samples in this experimental program.

For example, existing research on fibre reinforced concrete highlighted that the inclusion of steel fibres can increase the fatigue resistance of concrete by up to 70% (Bhat & Khan, 2018). It is also noted that fibres improve the crack-bridging capacity, energy absorption, and overall toughness of concrete (Selmi, 2014). These enhancements contribute to a more ductile and resilient concrete that performs better under various loading conditions.

In conclusion, the ductile behaviour of fibre-reinforced concrete is significantly enhanced due to the crack-bridging ability of the fibres, their contribution to uniform stress distribution, and their role in energy absorption. Shorter fibres, in particular, spread more effectively throughout the matrix, bridging more microcracks and further enhancing ductility. The incorporation of fibres not only improves ductility but also enhances the overall toughness, fatigue resistance, and durability of concrete, making it a superior choice for a wide range of structural applications where ductility is a priority, such as in seismic regions where structures are subject to dynamic loads and require materials that can deform without sudden failure.

4.2.4.4 Flexural Strength Test

Flexural strength tests were conducted on two concrete beams for each mix design, each measuring 150 x 150 x 550 mm, shown in Figure 4.37, on the 7th and 28th days after casting. Using the data-loggers attached to the testing apparatus, the flexural strength

was analysed for various aspects, including the peak load before failure, the flexural strength, and the flexural toughness factor.

However, due to limitations in the laboratory, a hand-operated mechanical pump was used for flexural testing instead of an automatic displacement loading machine introduced variability in the loading rate. Furthermore, the absence of a functioning CMOD transducer limited the ability to measure and analyse crack opening widths accurately.

Figure 4.37 – Flexural Strength Test before and after Failure.

4.2.4.4.1 Peak Load before Failure

The comparison of peak load before failure among various fibre-reinforced concrete mixes revealed notable differences relative to the control mix C0, as can be seen in Figure 4.38. It is noted that the general trend is for the peak load of fibre mixes, to not increase with respect to the control, with values in the same range. At the initial 7-day testing stage, the control mix C0 demonstrated an average peak load of 20.42 kN. Mix C0.125S outperformed significantly, with an average peak load of 28.10 kN, indicating an improvement of approximately 37.5%. Mix C0.125L also showed a higher peak load

of 23.66 kN, a 15.9% increase over the control. However, Mix C0.25S showed a marginal increase with a peak load of 20.74 kN, only 1.5% better than the control.

On the 28-day mark, the control mix C0 exhibited an average peak load of 29.34 kN. Mix C0.125L performed the best with an average peak load of 30.28 kN, representing a 3.2% improvement. Mixes C0.125S and C0.5S showed slight reductions compared to their initial values but remained competitive, with average peak loads of 27.79 kN and 27.89 kN respectively, closely matching the control. On the other hand, Mix C0.25S showed a notable decline to 22.22 kN, 24.3% lower than the control.

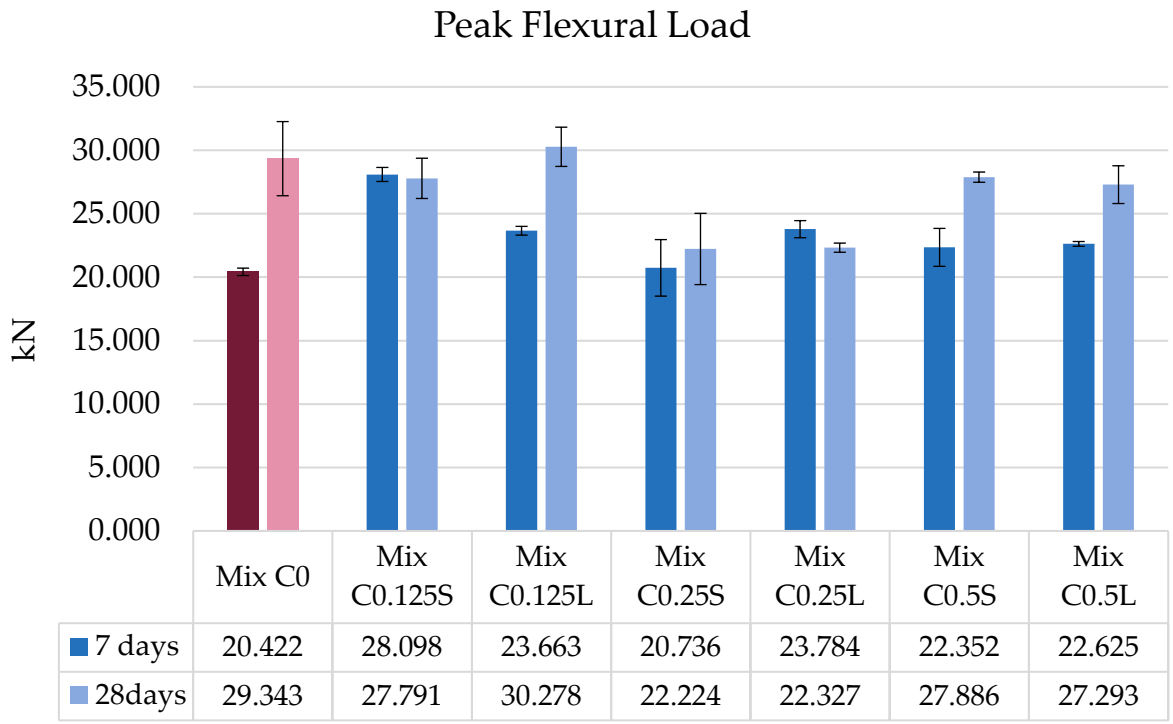

	Mix C0	Mix C0.125S	Mix C0.125L	Mix C0.25S	Mix C0.25L	Mix C0.5S	Mix C0.5L
7 days	20.422	28.098	23.663	20.736	23.784	22.352	22.625
28days	29.343	27.791	30.278	22.224	22.327	27.886	27.293

Figure 4.38 - Mean Peak Flexural Load before Failure of Self-Compacting Concrete Beams.

In conclusion, Mix C0.125L consistently demonstrated the highest peak loads before failure at both initial (7 day) and final (28 day) testing stages, making it a promising option for applications requiring high load-bearing capacity. Mix C0.25S, however, showed a notable decrease in performance.

4.2.4.4.2 Average Flexural Strength

From the values obtained for the peak load, the analysis of average flexural strength among the various mixes, shown in Figure 4.39, provided insights into their performance in bending stress conditions. In general, the fibres did not contribute to the flexural strength of the concrete.

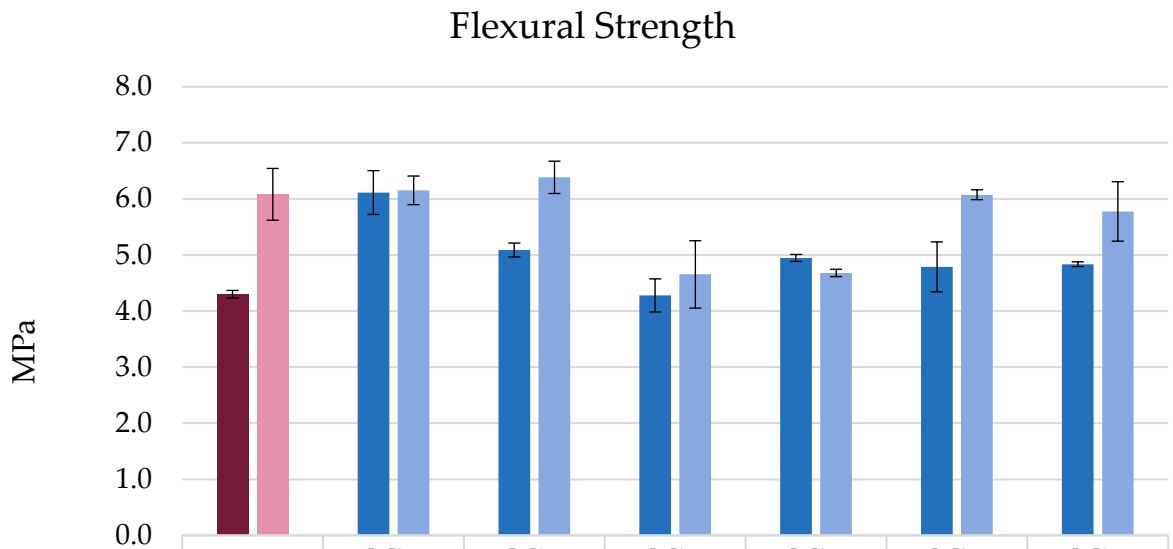

	Mix C0	Mix C0.125S	Mix C0.125L	Mix C0.25S	Mix C0.25L	Mix C0.5S	Mix C0.5L
7 days	4.301	6.113	5.089	4.279	4.947	4.787	4.835
28 days	6.082	6.153	6.384	4.654	4.680	6.075	5.776

Figure 4.39 - Mean Flexural Strength of Self-Compacting Concrete Beams.

At 7 days, the control mix C0 had an average flexural strength of 4.30 MPa. Mix C0.125S demonstrated superior performance with an average flexural strength of 6.11 MPa, a substantial increase of 42.1%. Mix C0.125L also performed well, achieving 5.09 MPa, an 18.2% improvement over the control. Mix C0.25S, however, showed a slight decrease, with an average flexural strength of 4.28 MPa, nearly matching the control.

At 28 days, the control mix C0 exhibited an average flexural strength of 6.08 MPa. Mix C0.125L outperformed all, with an average flexural strength of 6.38 MPa, representing a 5% improvement. Mix C0.125S maintained a strong performance with an average of 6.15 MPa, slightly better than the control. Mix C0.5S also performed well, achieving

6.08 MPa, closely matching the control. Conversely, Mix C0.25S showed a notable reduction, with an average flexural strength of 4.65 MPa, 23.6% lower than the control.

Overall, Mix C0.125L showed the most consistent and highest performance in terms of flexural strength at both testing stages, making it ideal for applications requiring strong bending resistance. Mix C0.25S, however, showed decreased performance.

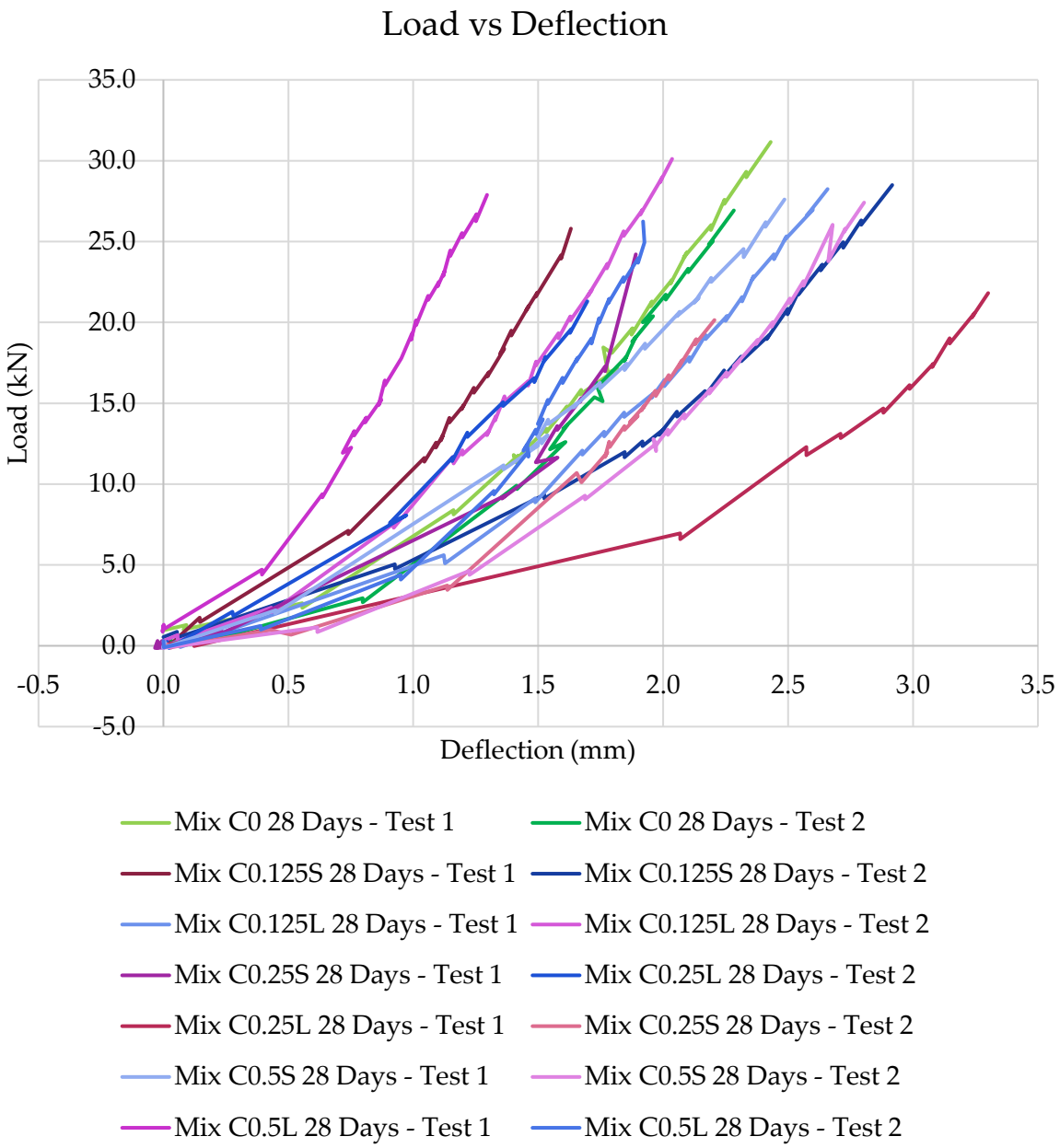

Figure 4.40 - Flexural Load vs Deflection Graph at 28 Days.

The load vs deflection graphs did not show any post-peak behaviour, and it can be noted that all mixes exhibited brittle failure implied by examining the graphs shown

in Figure 4.40. As can be observed, all of the test specimens exhibited sudden failure, in both the first and second specimens.

4.2.4.4.3 Flexural Toughness Factor

The evaluation of flexural toughness factor among the mixes, shown in Figure 4.41, provided insights into their ability to absorb energy and resist fracture under bending stress.

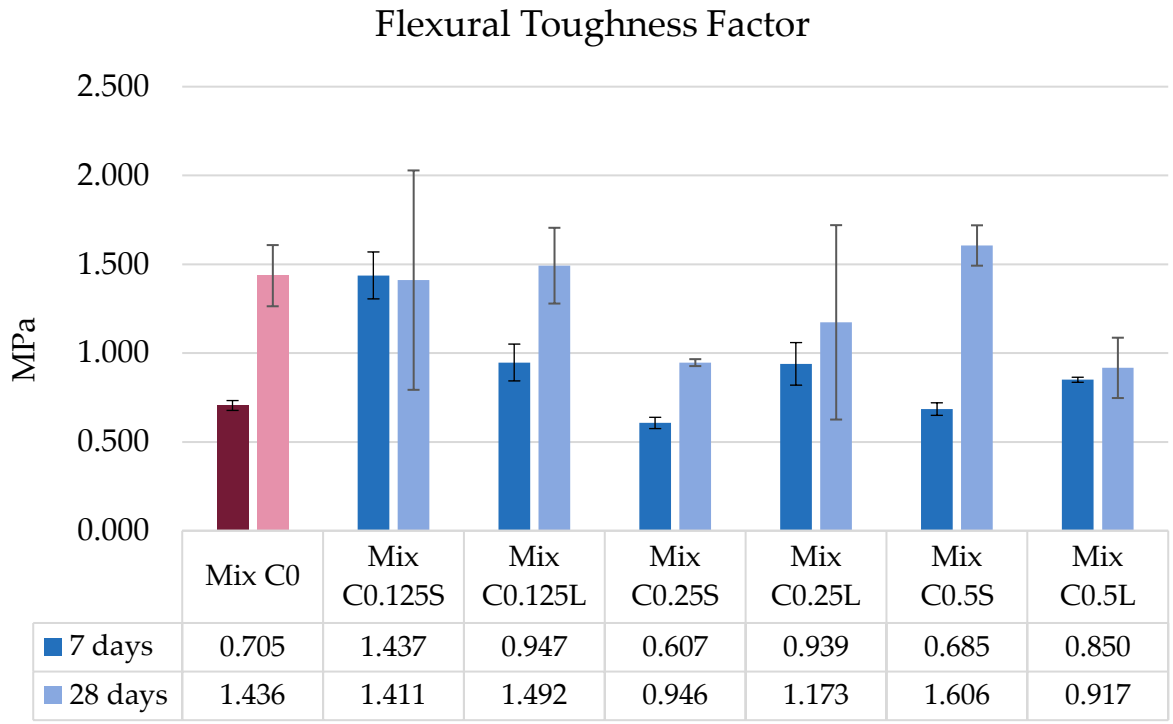

	Mix C0	Mix C0.125S	Mix C0.125L	Mix C0.25S	Mix C0.25L	Mix C0.5S	Mix C0.5L
7 days	0.705	1.437	0.947	0.607	0.939	0.685	0.850
28 days	1.436	1.411	1.492	0.946	1.173	1.606	0.917

Figure 4.41 - Mean Flexural Toughness Factor of Self-Compacting Concrete Beams.

At 7 days, the control mix C0 demonstrated an average toughness factor of 0.71 MPa. Mix C0.125S significantly outperformed the control with an average toughness factor of 1.44 MPa, a 104% increase. Mix C0.5S also showed an improvement, achieving 0.68 MPa, which was a 3.5% decrease from the control but still performed well compared to other mixes. Mix C0.25S, however, showed a reduction with an average toughness factor of 0.61 MPa, indicating a 14% decrease compared to the control.

At 28 days, the control mix C0 had an average toughness factor of 1.44 MPa. Mix C0.5S demonstrated the highest toughness factor of 1.61 MPa, an increase of 11.5% over the

control. Mix C0.125L also performed well, achieving 1.49 MPa, a 3.8% improvement. Mix C0.5L showed a reduction with an average toughness factor of 0.92 MPa, 36.3% lower than the control, indicating potential weaknesses in this mix over time.

Overall, Mix C0.125S consistently demonstrated the highest flexural toughness factor at both testing stages, making it a candidate for applications requiring high energy absorption and fracture resistance. Mix C0.5L, however, showed a notable decrease in performance over time, suggesting it may not be suitable for long-term durability in structural applications.

In general, the ineffectiveness of feather fibres in enhancing flexural strength and toughness is partly due to their inefficient bonding with the cement matrix. This bonding would have helped to transfer loads efficiently and improve the composite action of the concrete, which could explain the lack of improvement in flexural strength.

4.2.4.5 Pull-Out Test

Following the observations made during the flexural strength testing, gaining a better understanding of the adhesion between the fibres and the matrix was essential. To achieve this, pull-out tests were conducted on specifically cast cement paste cubes, tested following the 7th day after casting. The data logger and the dedicated photography apparatus provided further insights on the behaviour of the fibre adhesion to the matrix.

During these tests, it was consistently observed that the fibres slipped from the cubes, as shown in Figure 4.42, indicating poor adhesion with the matrix. This was confirmed by the limited resistance measured by the data logger on the tensile testing apparatus, shown in Figure 4.43, as well as the fibre rachis slipping from the cubes with minimal damage. In some instances, it was noted that the barbs of the fibres were stripped from the rachis, suggesting that the barbs had greater adhesion to the matrix. The graphs also indicated some post-peak behaviour, indicating that there was some resistance

present, likely due to the barbs being still attached to the matrix. This could be a contributing factor to the previously noted improvements in strength.

The noticeable fibre slippage from the cubes likely caused the reduction in flexural strength, as the barbs themselves were likely too small to contribute significantly to the matrix reinforcement. Consequently, the overall flexural strength was likely more reliant on the rachis, which did not adhere properly and thus was insufficient in providing additional flexural support. Understanding this behaviour helps identify the limitations in the fibre-matrix interaction and highlights the need for improving fibre adhesion to enhance the overall performance of fibre-reinforced SCC and SCM.

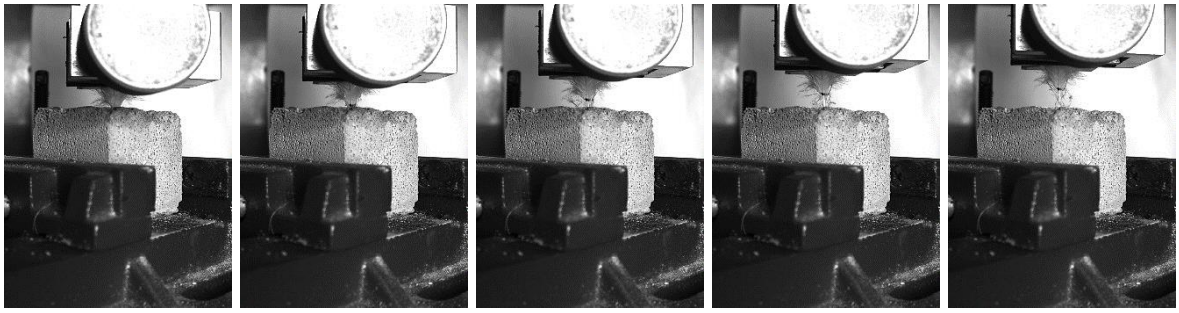

Figure 4.42 - Slipping of Fibre during Pull-Out Test.

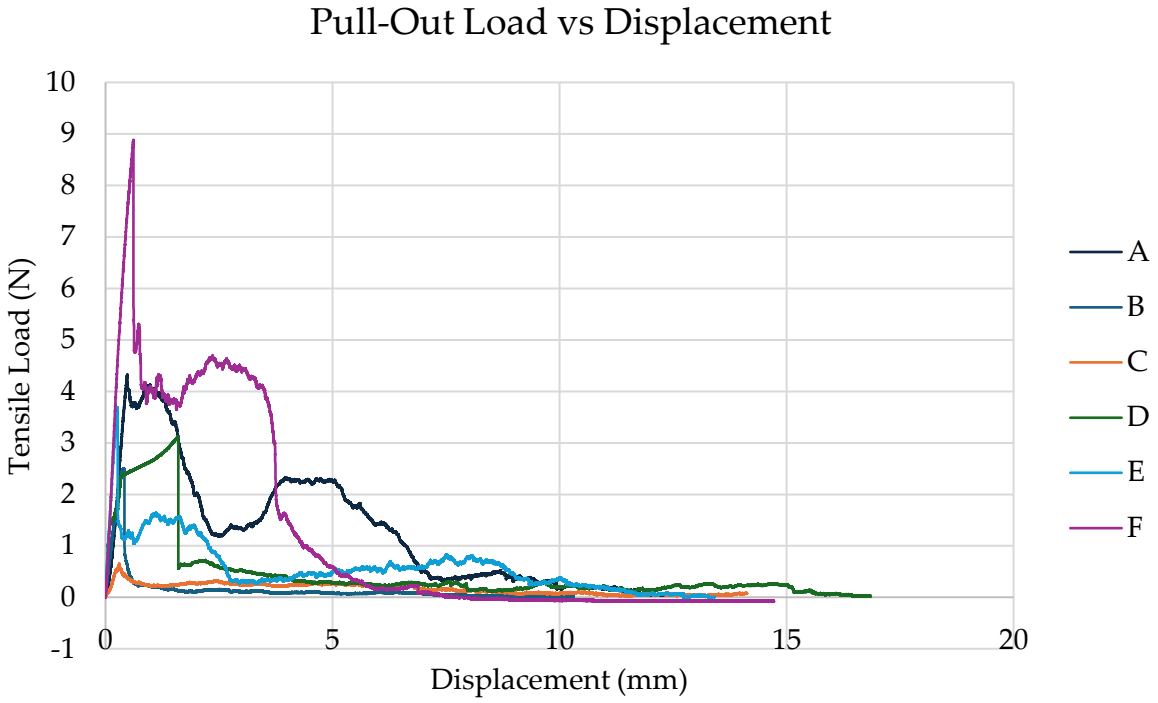

Figure 4.43 - Load vs Displacement of Six Pull-Out Tests, revealing limited resistance to Tensile Load.

4.2.5 Comparison to Existing Literature on Hardened Concrete Properties

In a 1994 study by Hamoush and El-Hawary, the compressive strength of conventional concrete specimens was found to decrease as the volume fraction of chicken feather fibres increased. The reduction in compressive strength ranged from 12% to 18% for the various fibre contents tested (Hamoush & El-Hawary, 1994). The reduction in compressive strength was attributed to the lower stiffness and strength of the chicken feather fibres compared to the concrete matrix, which results in less efficient load transfer within the material (Araya-Letelier et al., 2020).

Other more recent studies, however, have observed an increase in the compressive strength, similar to the findings in this study. The inclusion of 1% chicken feather waste resulted in an increase in compressive strength compared to conventional concrete, whereas the 2% addition led to a decrease in both compressive and flexural strengths. Thus, the optimal condition for compressive strength was achieved with a 1% addition of chicken feathers. However, a 2% addition reduced both compressive and flexural strengths (Sutarno et al., 2021). Similarly, older studies also showed that flexural strength was highest in the concrete with 1% feather fibres, and the flexural strength was highest in the concrete with 2% feathers at age 56 days, but lower at 28 days (Hamoush & El-Hawary, 1994). These findings relate to the experimental program.

The reduced flexural strength with higher feather content is likely due to the feathers' poor binding characteristics with concrete and their tendency to absorb water, which prolongs the drying time during curing (Sutarno et al., 2021).

Similar to these findings, a reduction in splitting tensile strength was also observed for all ratios that were tested (Hamoush & El-Hawary, 1994). This reduction was observed at all ages of the concrete that was tested. The decrease in split tensile strength could be attributed to the deterioration of the feathers and a decline in feather strength. Feather decay was identified through examination of the failure surfaces of the tested samples. In cases where small feathers (less than 13 mm) were entirely dissolved in the

concrete, those feathers that remained protruding from the failure surfaces showed no resistance to being pulled out.

The studied literature indicated notable differences in concrete properties with the addition of chicken feather waste between 1% and 2%, making it crucial to find the optimum balance in mix design. Adding more than 1% resulted in decreased performance, highlighting that higher proportions were counterproductive. This emphasises the importance of precise mix design, as exceeding the optimal 1% led to worsening results. Additionally, there were no prior studies investigating very small fibre incorporations (0.125% and 0.25%), making it interesting to explore these lower proportions and their potential effects on concrete behaviour.

4.2.6 Shrinkage Properties of Concrete

4.2.6.1 Restrained Shrinkage Cracking Ring Test

The objective of this test was to evaluate the impact of different mixes containing various feather fibre dosages on their shrinkage characteristics. For this test, the control mix was compared to the mixes with short fibres, due to the narrow nature of the mould and the generally better performance of shorter fibres reported. The mixes with the smallest and largest volume fractions were tested, specifically C0.125S and C0.5S. The strain caused by the concrete shrinkage on the inner steel ring was measured using two strain gauges connected to a data logger. The results, illustrated in Figure 4.44, show the strain over a period of 28 days for the two strain gauges of the three different mixes.

The control mix exhibited cracking during the second week, specifically on the 10th day after casting, as indicated by the sudden drop in strain gauge readings in Figure 4.44. On the other hand, none of the fibre-reinforced mixes showed any abrupt decrease in strain during the first 28 days post-casting. This was confirmed by regular visual inspections, with an absence of visible cracks in any of the three ring samples.

All three mixes recorded positive influxes of strain during the testing period, due to temperature fluctuations in the room. These fluctuations were influenced by other tests being conducted nearby. Due to space limitations in the laboratory, it was not possible to maintain a perfectly controlled environment for the ring test apparatus. Consequently, the observed minor changes in strain are most likely caused by the variations in room temperature created by other tests being carried out in the vicinity.

These slight drops in strain were observed in the control mix as well as in the fibre-reinforced mixes. However, the latter mixes consistently recovered back to their regular strain values shortly after. This recovery indicates the beneficial role of the fibres in the concrete matrix. The fibres acted as a reinforcement network, effectively absorbing and redistributing the internal stresses that caused these temporary drops. This behaviour contrasted sharply with the control mix, which did not recover once a significant drop occurred, leading to permanent cracking confirmed by constant low strain values.

Overall, the ability of the fibre-reinforced mixes to return to regular strain values demonstrates the fibres' effectiveness in preventing crack formation and propagation. By providing additional tensile strength and flexibility, the fibres mitigated the effects of shrinkage stresses, maintaining the structural integrity of the concrete.

The observed results of the shrinkage test for concrete mixes containing feather fibres were also largely expected based on the known behaviour of fibre-reinforced concrete. The fibre-reinforced mixes C0.125S and C0.5S did not exhibit sudden decreases in strain, indicating no cracking within the first 28 days post-casting. This was anticipated because fibres are known to bridge microcracks in the concrete matrix, preventing their propagation and thus reducing the likelihood of visible cracking. The fibres act as a reinforcement network, absorbing and redistributing internal stresses caused by shrinkage. Regular visual inspections confirmed the absence of visible cracks, supporting the effectiveness of fibres in maintaining structural integrity.

The fibre-reinforced mixes also showed recovery from slight drops in strain, returning to their regular strain values shortly after each fluctuation. This behaviour was expected because fibres provide additional ductility to the concrete, allowing it to adapt to and recover from temporary internal stresses. The consistent recovery observed in fibre-reinforced mixes contrasts sharply with the control mix, which did not recover after significant drops, leading to permanent cracking. This positive outcome highlights the fibres' role in preventing crack formation and propagation, effectively enhancing the durability and longevity of the concrete.

The control mix exhibited cracking during the second week, specifically on the 10th day after casting. While some cracking in the control mix was anticipated due to the lack of fibre reinforcement, the exact timing and severity of the cracking might have varied, in other studies, it occurred on the 9th day (Calleja, 2023), on the 10th day (Baldacchino, 2014) or on the 12th day (Abdilla, 2021), however, the cracks were all similarly noted on the second week from casting. The sudden decrease in strain gauge readings clearly showed the beginning of cracking, which was also confirmed by visual inspections that revealed permanent cracks. The notable decrease in strain values in the control mix demonstrates the efficiency of fibres in the reinforced mixes. The fibres helped reduce the impact of shrinkage stresses on the concrete, preserving its structural integrity by increasing its ductility.

Overall, the results of the shrinkage test correspond favourably with the anticipated results from the recognised characteristics of fibre-reinforced concrete. The fibres showed clearly how they prevent cracks from forming and eventually propagating, showing their positive influence on improving concrete performance against shrinkage stresses.

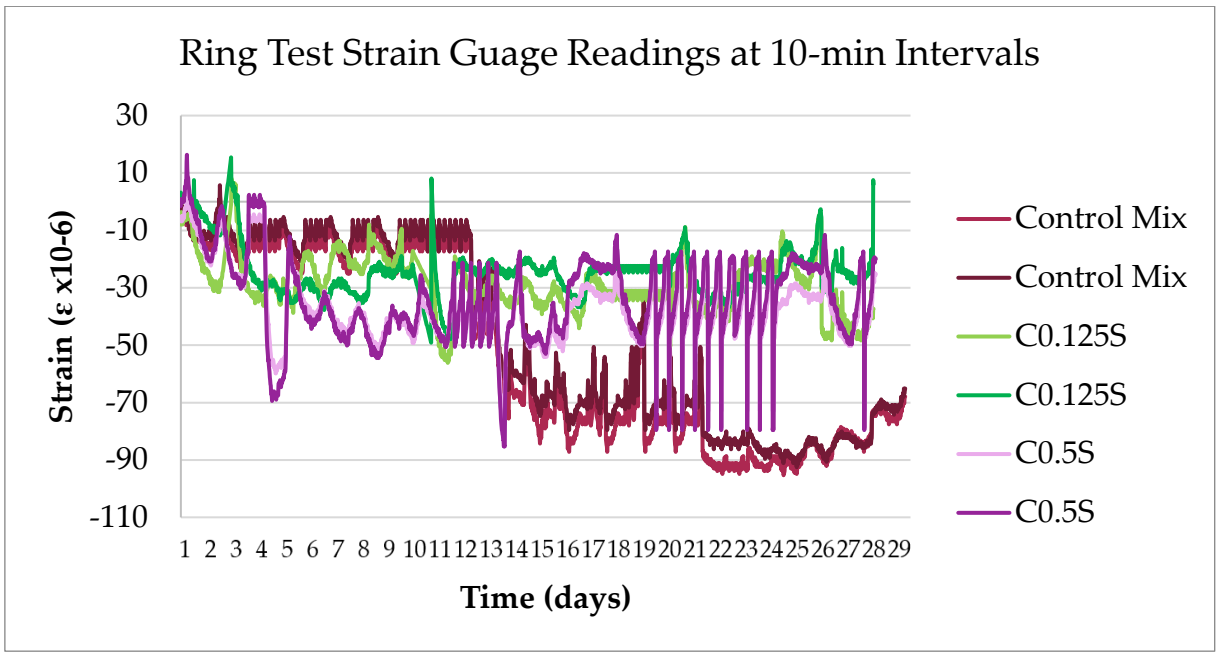

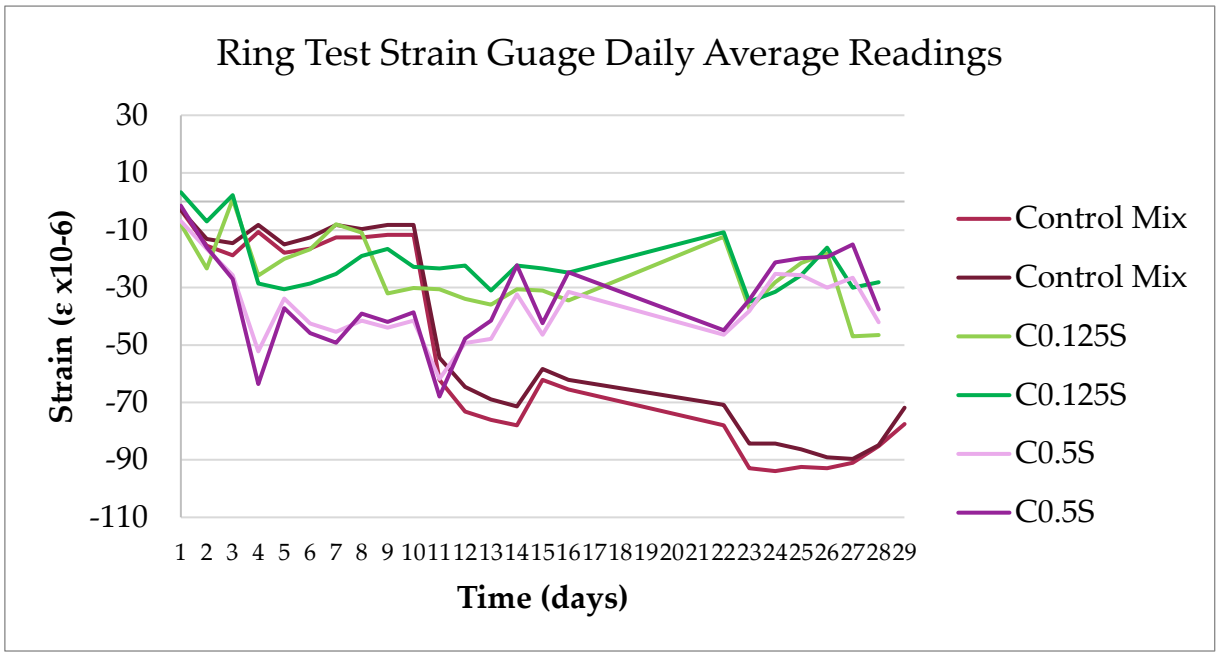

Figure 4.44 - Strain Gauge Readings showing Control Mix Strain Drop at 10th Day.

4.2.6.2 *Plastic Shrinkage Cracking Test*

Before casting the concrete specimen for this test, the industrial fan and halogen heaters were turned on for 30 minutes to achieve the required environmental conditions, described in the methodology chapter. The stress riser in the centre of the mould induced cracking in the central part of the mould, ideal for visual inspection, and crucial to obtain accurate measurements as most cracks were formed along this riser, as shown in Figure 4.45.

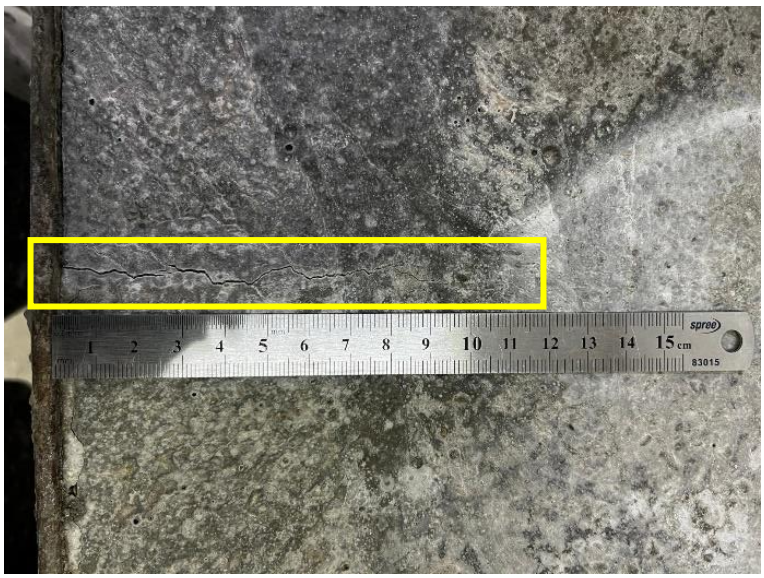

Figure 4.45 - Crack Formation above the Central Stress Riser in the Mould.

The temperature of the concrete and the ambient temperature of the chamber were both monitored with thermocouples, shown in Figure 4.46 as A and B respectively, with readings taken every 30 minutes.

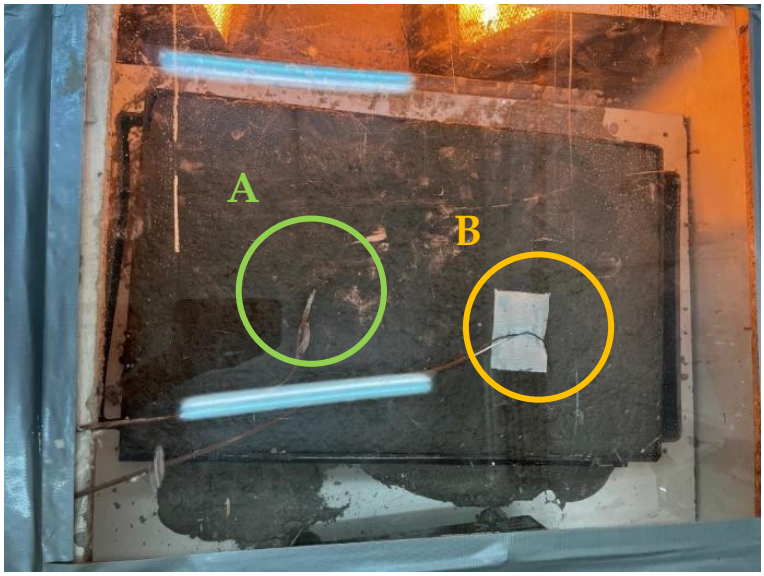

Figure 4.46 - Placement of Thermocouples for Concrete (A) and Ambient (B) Temperature Readings.

The results of these analyses are shown in Figure 4.47 and Figure 4.48, highlighting similar trends in all the mixes.

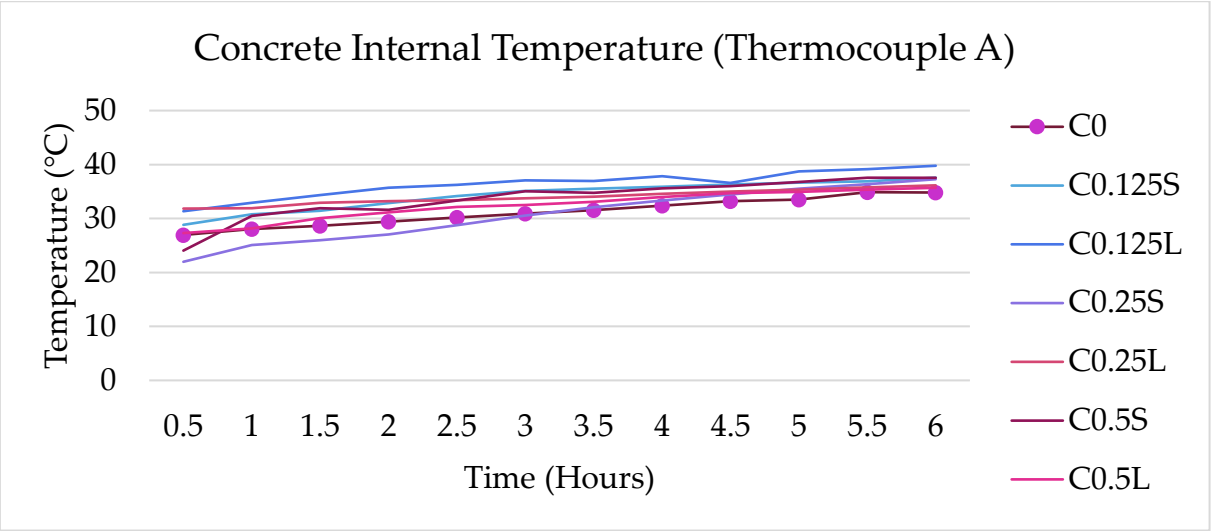

Figure 4.47 – Concrete Internal Temperature readings inside Environmental Chamber.

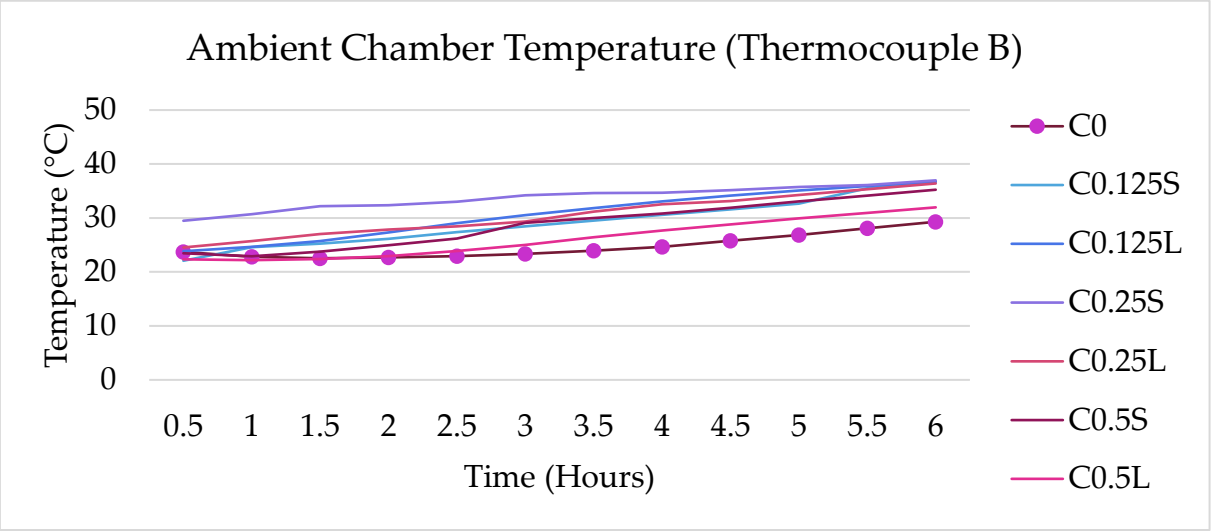

Figure 4.48 - Ambient Temperature readings of Environmental Chamber.

All feather fibre reinforced mixes in the study demonstrated delays in the time of first crack formation when compared to the control specimen. This trend highlights the beneficial effect of feather fibres in enhancing the crack resistance of concrete. The increased delay in crack formation with higher fibre percentages suggests that a greater volume of fibres effectively reinforces the concrete matrix, distributing stress more evenly and resisting the initiation of cracks. Similarly, longer fibres contribute to this effect by providing additional reinforcement and bridging capability across potential crack sites. The feather fibres created an internal network of bonds that effectively resisted the formation and propagation of early-stage cracks.

Comparisons of the time of first crack formation between the control mix and the six feather fibre-reinforced mixes revealed substantial differences in performance. The control mix cracked before all other mixes, demonstrating that feather fibre reinforcement effectively delayed crack formation within the first six hours. This is shown in Figure 4.49, and demonstrates how these delays increased proportionally with higher percentages of feather fibre incorporation. Additionally, mixes with longer fibre lengths showed further delays in the onset of the first crack.

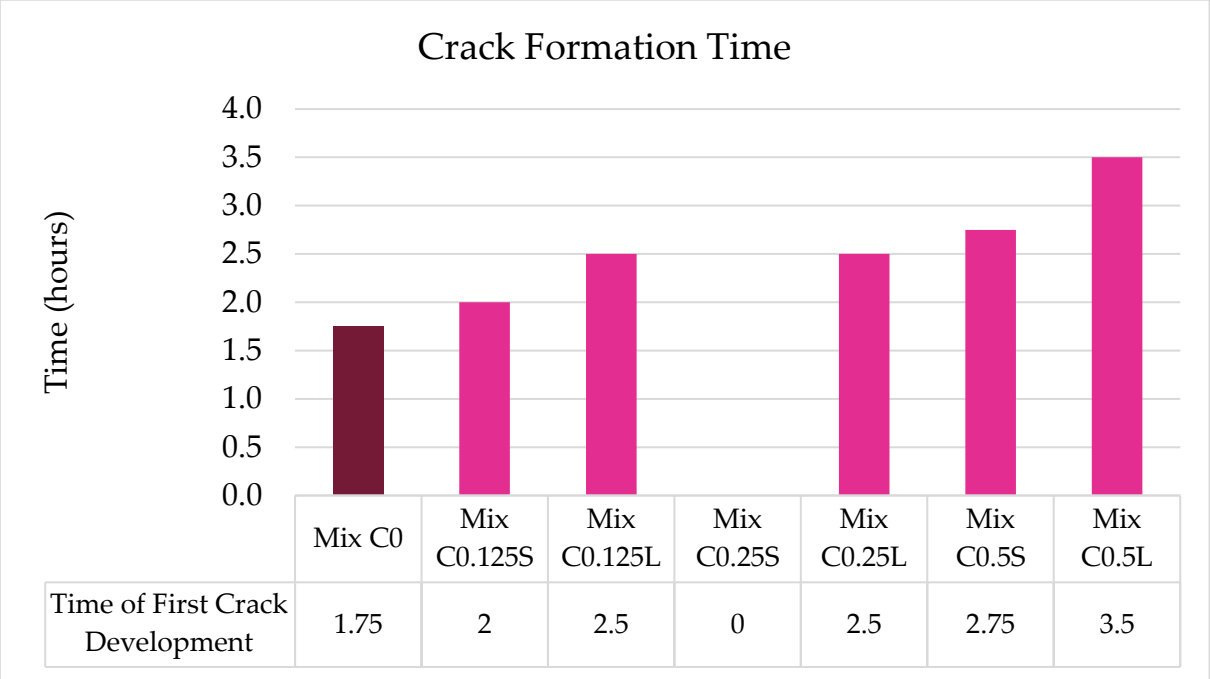

	Mix C0	Mix C0.125S	Mix C0.125L	Mix C0.25S	Mix C0.25L	Mix C0.5S	Mix C0.5L
Time of First Crack Development	1.75	2	2.5	0	2.5	2.75	3.5

Figure 4.49 - Time of All First Crack Developments.

This delay in crack formation indicates that the presence of feather fibres significantly enhances the concrete's resistance to early-stage cracking. The comparison of the first crack formation time and the average crack with has been shown on Table 4.8. Notably, mix C0.25S did not exhibit any cracks within the initial six-hour test period, and no further cracks developed during the 24-hour inspection.

Table 4.8 - Time of First Crack Formation and Average Width of Crack.

	Time of First Crack Development	*Average Crack Width*
Mix Code	***Hours***	***mm***
Mix C0	1.75	0.454
Mix C0.125S	2	0.325
Mix C0.125L	2.5	0.035
Mix C0.25S	0	0.000
Mix C0.25L	2.5	0.704
Mix C0.5S	2.75	0.278
Mix C0.5L	3.5	0.094

When comparing the control mix with mixes C0.125S and C0.125L, which had the least fibre content incorporation, the cracks in the fibre-reinforced mixes were particularly narrower, particularly in the mix with longer fibres (C0.125L), as can be seen in Figure 4.50. This suggests that even a small amount of feather fibre content can contribute to a noticeable improvement in crack resistance, with longer fibres offering additional benefits by bridging cracks more effectively and distributing stress more evenly throughout the concrete.

Similarly, the control mix was compared with mixes C0.5S and C0.5L, which had the largest fibre content incorporation. The cracks in the fibre-reinforced mixes were also considerably narrower, the C0.5L and C0.5S mixes having the second and third narrowest fibres overall, respectively, following the aforementioned C0.125L. This further confirms the positive impact of feather fibre reinforcement on concrete's durability, with higher fibre content and longer fibres providing greater resistance to cracking by creating stronger bonds within the concrete matrix.

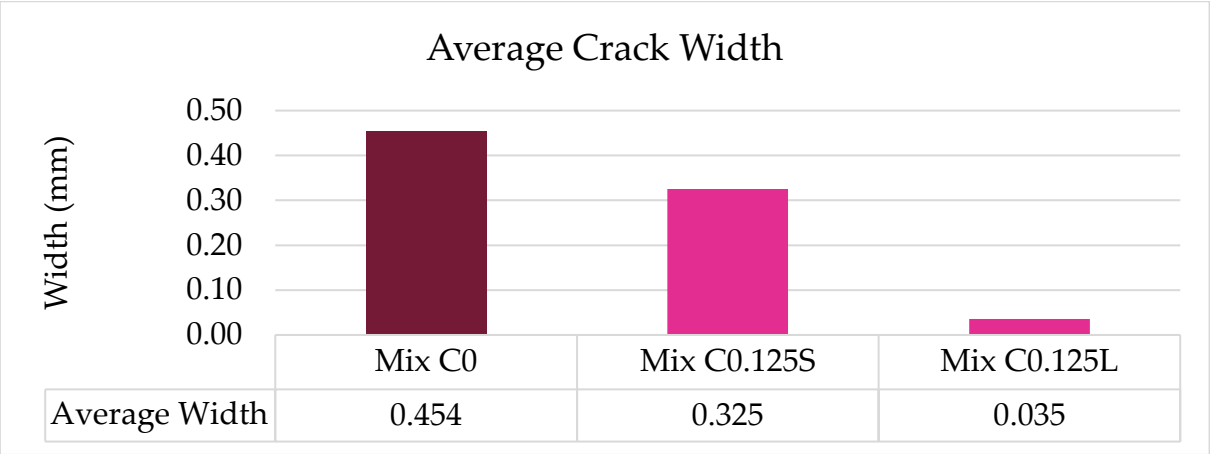

Figure 4.50 - Comparison of Control Mix and C0.125 Mixes Crack Widths.

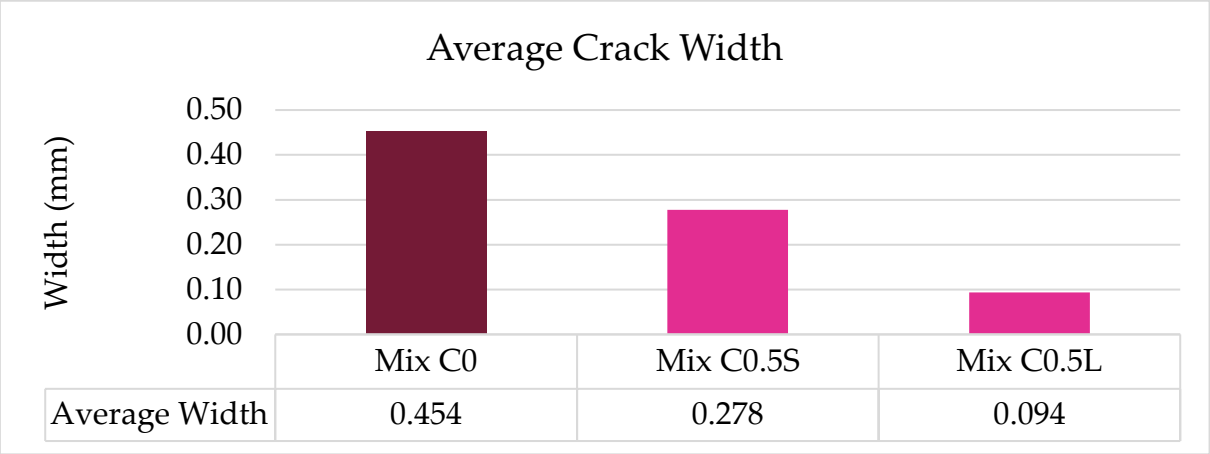

Figure 4.51 - Comparison of Control Mix and C0.5 Mixes Crack Widths.

Mixes C0.5L and C0.125L exhibited average crack widths of 0.094 mm and 0.035 mm, respectively, both measuring less than a tenth of a millimetre, and a fraction of the average width of the cracks on the control specimen. These measurements were obtained using a calibrated USB microscope, photographs shown in Figure 4.52, and were recorded at the 24-hour mark from casting, allowing ample time for any additional cracking to manifest. Importantly, no further cracking was observed in any of the mixes during this observation period. This indicates the effectiveness of feather fibre reinforcement in mitigating crack propagation and maintaining the integrity of the concrete structures over time. The minimal crack widths recorded highlight the ability of feather fibres to enhance the durability and resistance to cracking in concrete, underscoring their potential application in improving the longevity of construction materials.

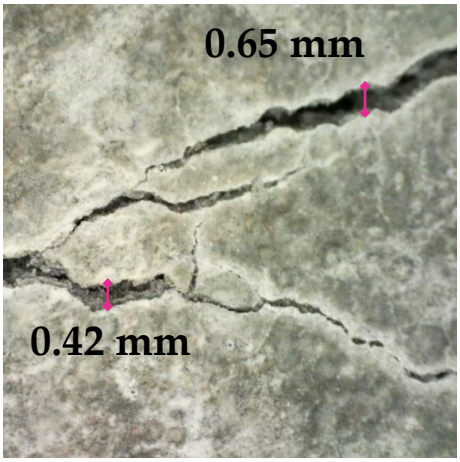

C0 (Control) Mix

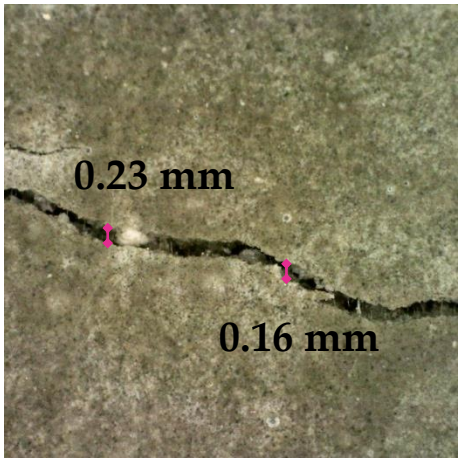

C0.125S Mix

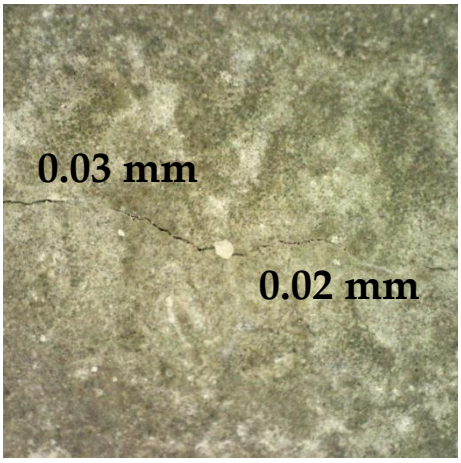

C0.125L Mix

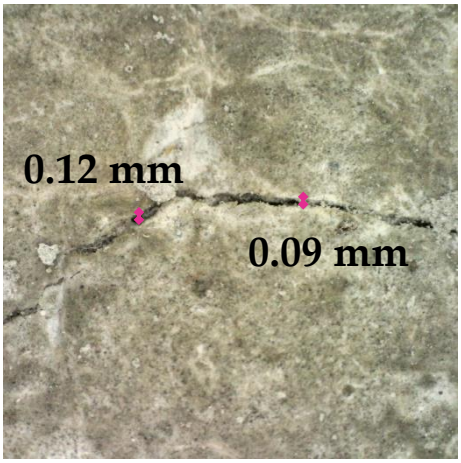

C0.5S Mix

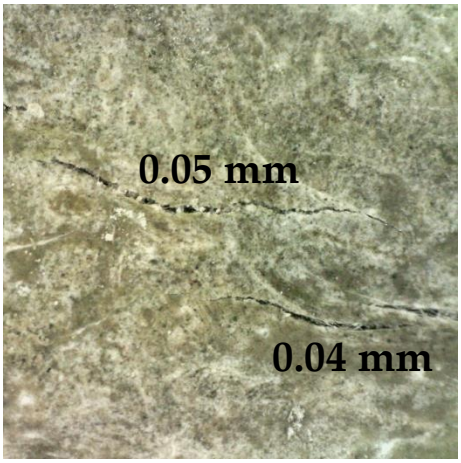

C0.5L Mix

Figure 4.52 – Narrowing Crack Width Measurements 24-hours from Casting.

The results of the plastic shrinkage cracking test were both anticipated and beneficial. The delay in crack formation and the reduced crack widths observed in the fibre-reinforced mixes compared to the control mix also align with the known benefits of

fibre reinforcement in concrete. Feather fibres, like other types of fibres, are expected to enhance the crack resistance of concrete by providing additional ductility and bridging capabilities that prevent the propagation of microcracks.

The conclusion that higher fibre percentages and longer fibres led to even greater delays in crack formation and narrower crack widths was anticipated, based on the mechanics of fibre reinforcement. A greater volume of fibres in the mix would naturally lead to a more robust internal network, effectively distributing stress more evenly and resisting crack initiation. Similarly, longer fibres have a greater capacity to bridge across potential crack sites, further enhancing the concrete's ability to withstand early-stage cracking.

The absence of cracks in mix C0.25S within the initial six-hour period in the subsequent 24-hour inspection, highlights the positive impact of feather fibre reinforcement. This outcome was due to the fibres' role in absorbing and redistributing internal stresses, thereby maintaining the structural integrity of the concrete. The narrower cracks in mixes with the least fibre content (C0.125S and C0.125L) and the largest fibre content (C0.5S and C0.5L) further confirm the beneficial effects of fibre reinforcement, demonstrating its effectiveness even at different dosages and fibre lengths.

The formation of the first crack was consistently delayed in all fibre-reinforced mixes compared to the control mix. This delay can be attributed to the feather fibres' ability to bridge microcracks and distribute internal stresses more evenly throughout the concrete matrix. The fibres effectively hinder the early formation of cracks by reducing stress concentration at potential crack sites. This improved stress distribution not only postpones the development of the initial crack but also enhances the overall durability of the concrete.

Overall, the benefits of delaying the first crack formation in concrete are remarkable. Delaying crack formation reduces the likelihood of crack propagation and expansion, which can compromise the structural integrity of concrete over time. The fibre-reinforced mixes' ability to withstand stress for longer periods without cracking ensures a more durable and long-lasting material. This is especially beneficial in

situations where concrete is subjected to different levels of pressure and weather conditions, as the improved strength given by the fibres can result in decreased upkeep expenses and an extended lifespan for concrete buildings. Moreover, the enhanced ability to resist cracks aids in preserving the aesthetic look of concrete surfaces, stopping the formation of unattractive cracks that could diminish the overall visual attraction of a building.

4.2.7 Shrinkage Properties of Mortar Panels

4.2.7.1 Kraai Test

The Kraai Test was used to establish the crack potential of thin mortar panels, and the control mix was compared to all fibre volume fractions using short fibres. Short fibres were selected to prevent interference with the shallow mould, as longer fibres would have protruded from the mould and induced stresses on the surface. This decision ensured the integrity of the test and allowed for an accurate assessment of crack resistance in the fibre-reinforced mortar panels.

In the Kraai Test shown in Figure 4.53, the performance of fibre-reinforced mortar panels was substantially better compared to the control mix. This test was conducted to assess the potential of fibre-reinforced mortars to develop cracks in thin slabs, shown in Figure 4.54.

Figure 4.53 - Kraai Test after 6-hour Wind Loading Period.

The control mix exhibited cracking at the 5-hour mark, indicating its susceptibility to shrinkage under the test conditions. This is consistent with regular cracking behaviour of concrete or mortar mixes without fibre reinforcement. Conversely, the fibre-reinforced mortar panels (M0.125S, M0.25S, and M0.5S) demonstrated superior resistance to cracking, as none of these panels developed any cracks within the 6-hour testing period.

Given that the panels were all expected to crack within this period, the result was encouraging as it demonstrated strong resistance to crack formation in the fibre-reinforced mortar panels. This outcome was particularly noteworthy considering the intense environmental conditions during the testing period, where industrial fans generated substantial wind loads to induce cracking in the panels. The enhanced performance of the fibre-reinforced panels highlights the effectiveness of fibre additives in mitigating shrinkage and improving durability under stress.

M0 - Control Mix – Visible Cracking

M0.125S Mix – No Cracks

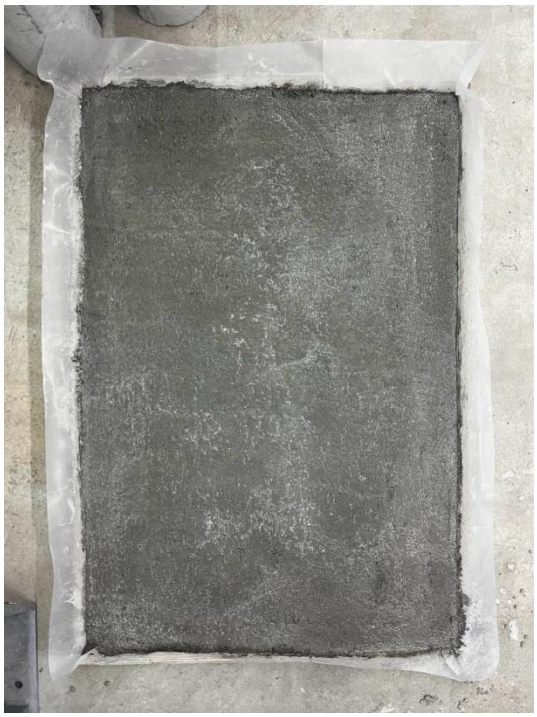

M0.25S Mix– No Cracks

M0.5S Mix– No Cracks

Figure 4.54 – Kraai Panel Test Results following the 6-Hour Test Duration.

The surface of the mortar mix was thoroughly evaluated 24 hours after casting to ensure a comprehensive assessment. It is important to note that none of the specimens developed any further cracking following the 6-hour testing period, confirming the initial observations. This stability over time indicates the long-term benefits of feather fibre reinforcement in preventing crack propagation.

For the control specimen, which was the only sample to exhibit cracking, detailed measurements of the average crack length and width were taken using calibrated digital vernier callipers. These precise measurements provided a clear quantification of the cracking extent, which was essential for comparing the performance of different mixes. Given that the control mix was the sole sample with visible cracks, the results of the average weighted crack value were recorded, as shown in Table 4.9 below.

Table 4.9 – Average Crack Weighting.

	Average Weighted Value
Mix Code	***mm²***
M0 - Control Mix	18.5
M0.125S	0
M0.25S	0
M0.5S	0

The Kraai Test yielded extremely positive results, surpassing what was anticipated. The inclusion of fibres in fibre-reinforced panels (M0.125S, M0.25S, and M0.5S) substantially enhances crack resistance, as demonstrated by the comparison. The lack of cracks in these panels, even when subjected to harsh testing conditions, shows the promise of fibre-reinforced mortars for applications needing strong durability and resistance to environmental pressures. The performance exceeded expectations, demonstrating how the fibre additives improved the durability and structural integrity of the mortar. The promising potential of feather fibre-reinforced concrete to

enhance the durability and strength of construction materials is highlighted by the lack of cracks in the panels during rigorous testing.

4.2.8 Durability Properties of Concrete

4.2.8.1 Rapid Chloride Penetration Test

While the time constraints of experimental program did not allow for long term testing, testing such as the RCPT as seen in Figure 4.55, helped to give an indication on the durability of the concrete. The chloride penetration results for the different SCC mixes, shown in Table 4.10, provide insights into their potential durability and suitability for various applications.

Table 4.10 – Comparison of Chloride Ion Penetrability.

	Charge Passed	*Chloride Ion Penetrability*
Mix Code	***Coulombs***	
Mix C0	4632.075	Very High
Mix C0.125S	4497.138	Very High
Mix C0.125L	4573.751	Very High
Mix C0.25S	3803.760	High
Mix C0.25L	3439.710	High
Mix C0.5S	3628.512	High
Mix C0.5L	3310.610	High

Mix C0 had a chloride penetration value of 4632.08 C, categorised as "very high". This indicates a notable susceptibility to chloride ingress, suggesting a lower resistance to corrosion in environments exposed to chlorides. Similarly, Mix C0.125S and Mix C0.125L also fell into the "very high" category, with values of 4497.14 C and 4573.75 C

respectively. Although these values are slightly lower than Mix C0, the high penetration indicates that these mixes too have a considerable risk of chloride-induced corrosion, signifying that the incorporation of the smallest amount of fibres had a negligible effect on the chloride penetrability.

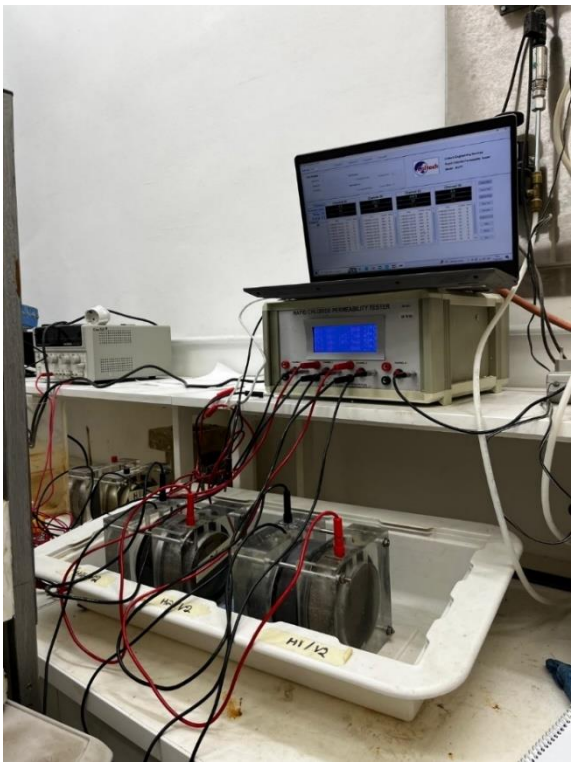

Figure 4.55 – Rapid Chloride Penetration Test in use.

On the other hand, Mix C0.25S and Mix C0.25L showed a marked improvement, falling into the "high" category with values of 3803.76 C and 3439.71 C respectively. This indicates a reduced susceptibility to chloride ingress compared to the control mix and the 0.125 fibre volume mixes. Mix C0.25L, in particular, showed a notable decrease, suggesting better performance in terms of resistance to chloride penetration.

Mix C0.5S and Mix C0.5L also demonstrated improved performance with chloride penetration values of 3628.51 C and 3310.61 C respectively, placing them in the "high" category. Mix C0.5L showed the lowest chloride penetration value among all the mixes tested, indicating the best resistance to chloride ingress.

These results were somewhat expected, as the experimental design aimed to assess the impact of varying fibre content on concrete's durability, specifically its resistance to chloride penetration. The findings showed a clear trend: as the amount of fibres increased in the mixes tested, there was a corresponding decrease in chloride ion penetrability. This aligns with established knowledge in concrete research, which suggests that fibre reinforcement can enhance the material's ability to resist chloride ingress, thereby improving its durability in chloride-rich environments.

This outcome is beneficial for concrete applications where exposure to chlorides is a concern, such as marine structures or environments where de-icing salts are used. By reducing the risk of chloride-induced corrosion, concrete mixes with higher fibre content offer a practical solution to extend the lifespan and maintain the structural integrity of constructions subjected to harsh environmental conditions.

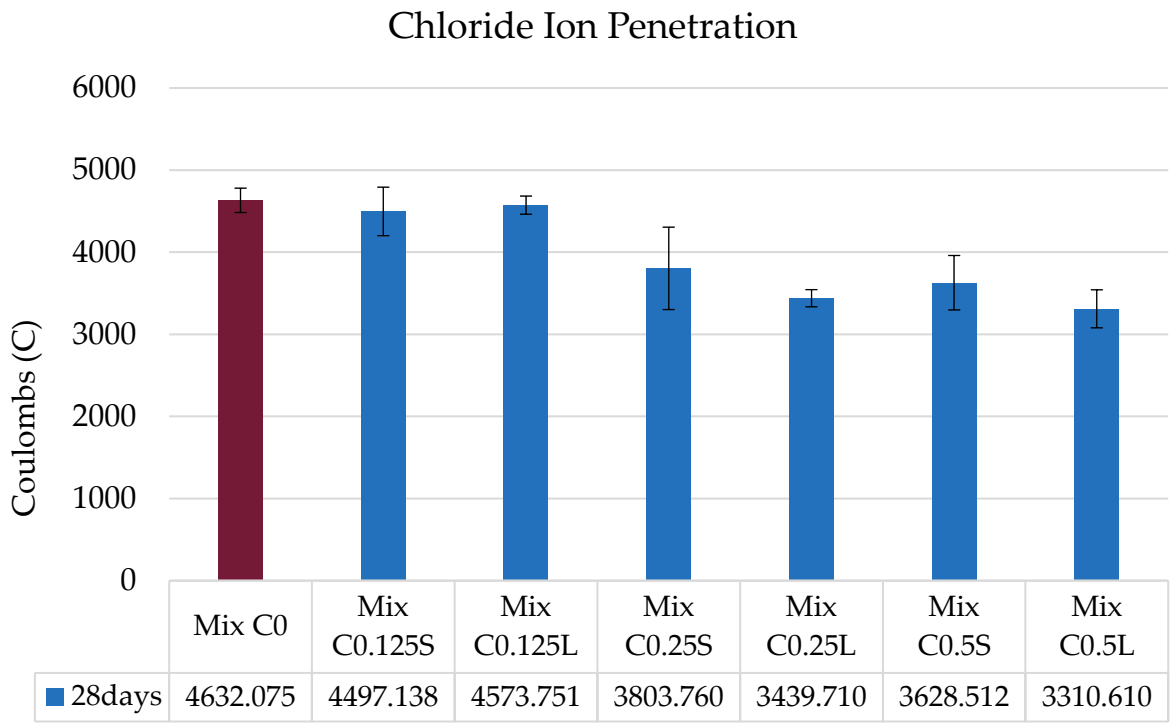

Figure 4.56 – Chloride Ion Penetration.

4.2.8.2 Vacuum Saturation Porosity

The second durability test carried out was an indirect durability test, intended to examine the porosity of the concrete matrix. Permeable porosity in concrete is a critical factor influencing its durability, strength, and resistance to various environmental conditions. Lower porosity typically indicates higher resistance to water and chemical ingress, enhancing the concrete's longevity and performance. The results of this test are shown in Figure 4.57.

Mix C0, the control mix, had a permeable porosity of 11.41%, serving as the baseline for comparison. When short fibres were added at a volume fraction of 0.125 (Mix C0.125S), the permeable porosity slightly decreased to 10.83%. This marginal improvement suggests that the addition of short fibres enhances the concrete's density and reduces its permeability to some extent. In contrast, Mix C0.125L, which used longer fibres at the same volume fraction, exhibited a notably higher permeable porosity of 16.48%. This substantial increase indicates that longer fibres might not integrate as well within the mix, possibly creating more voids and channels for water and chemicals to penetrate.

Increasing the volume fraction of short fibres to 0.25 (Mix C0.25S) resulted in a permeable porosity of 12.92%, higher than both the control mix and the short fibre mix at 0.125%. This suggests that a higher concentration of short fibres did not effectively reduce porosity and might have slightly worsened it. Similarly, Mix C0.25L, with longer fibres at the same volume fraction, showed a permeable porosity of 13.58%. This higher porosity indicates that the long fibres, particularly at increased volume fractions, may not blend optimally, leading to increased porosity.

A more notable reduction in permeable porosity was observed with Mix C0.5S, which had a value of 11.00%, lower than the control mix. This suggests that a higher volume fraction of short fibres can notably improve the concrete's density and reduce its permeability, thereby enhancing its overall durability. However, Mix C0.5L, which used long fibres at the same volume fraction, exhibited a permeable porosity of 13.69%, higher than both the control mix and the C0.5S fibre mix.

This trend indicates that long fibres tend to increase permeable porosity, particularly at higher volume fractions, possibly due to the creation of more voids or inadequate integration within the concrete matrix. This was not beneficial as lower porosity generally correlates with improved resistance to water and chemical ingress, offering longer service life and reduced maintenance costs for infrastructure exposed to challenging environmental conditions.

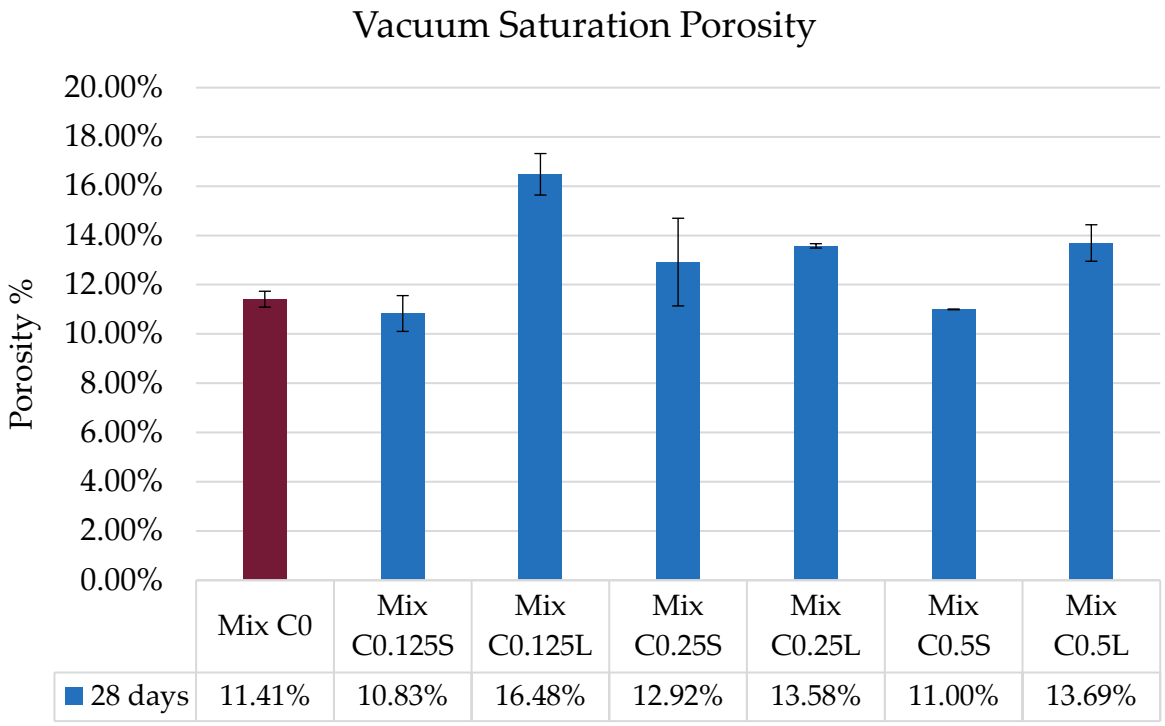

Figure 4.57 - Vacuum Saturation Porosity.

4.2.9 Conclusive Discussion on Experimental Program

The use of feather fibres as reinforcement in concrete offers several notable improvements alongside some limitations. Characterisation of the fibres revealed a considerable length range and high aspect ratio, which are ideal for reinforcement. Statistical analysis indicated that fibre length is sufficient to differentiate between fibre morphologies, eliminating the need to measure thicknesses. The development of a simple and scalable shredding process effectively reduced the fibre length range, making the preparation process more efficient.

The primary benefit of incorporating feather fibres is the improved crack behaviour in concrete and mortar. Significant improvements were observed in early-stage and plastic shrinkage cracking, with some mixes showing no cracking within the testing durations. This enhanced crack resistance is crucial for the durability and longevity of concrete structures. Additionally, the use of short fibres contributed to increased compressive strength and ductility, particularly in lower volume fractions. The fibre-reinforced mixes exhibited improved density and enhanced compaction, which is beneficial for the structural integrity of the concrete.

Based on the observations from the pull-out tests, it became clear that the barbs were in fact the most well-bonded to the matrix and is most likely the reason for the reduction in the shrinkage related stresses. The barbs had a greater adhesion to the matrix than the rachis, which eventually slipped from the sample when a tensile load was applied. This led to an overall reduction in the crack formation and in the width of the cracks.

However, some limitations were noted. As the fibre volume fraction increased, workability and flowability of the concrete mixes decreased, particularly with longer fibres. The largest volume fractions failed to pass flowability and viscosity tests, indicating challenges in handling and mixing. The decreased workability and increased viscosity highlight the need for careful consideration of fibre volume fractions in practical applications. Furthermore, longer fibres created air voids, leading to lower density and reduced compressive strength in some mortar mixes.

Despite these limitations, the overall improvements in concrete performance due to feather fibre reinforcement are enough to be considered. The reduction in crack formation and in some cases, improvements in compressive strength and ductility, particularly with shorter fibres, demonstrate the potential of feather fibres as a viable reinforcement material. This innovative approach not only addresses environmental and economic challenges by repurposing waste materials but also enhances the sustainability and resilience of concrete structures. The integration of feather fibres

into concrete mixes can serve as a model for similar initiatives, promoting the transition towards a circular economy and more sustainable construction practices.

4.3 Further Discussion

4.3.1 Creating a Circular Economy

The positive results reported in the previous section, with respect to the inclusion of chicken feather fibres in SCC and SCM, particularly those related to cracking, should not be solely considered in the perspective of material science. One of the targets of this research involving wasteful industries is to create a circular economy which can reuse materials which were otherwise at their end-of-life (European Commission, 2016). This research aligns perfectly with the principles of a circular economy, providing multiple environmental, economic, and social benefits by creating high-value products as shown in the diagram in Figure 4.58 - Biodegradation of keratin-containing waste in the poultry production cycle (Shestakova et al., 2021). The aforementioned benefits are outlined in the sections below.

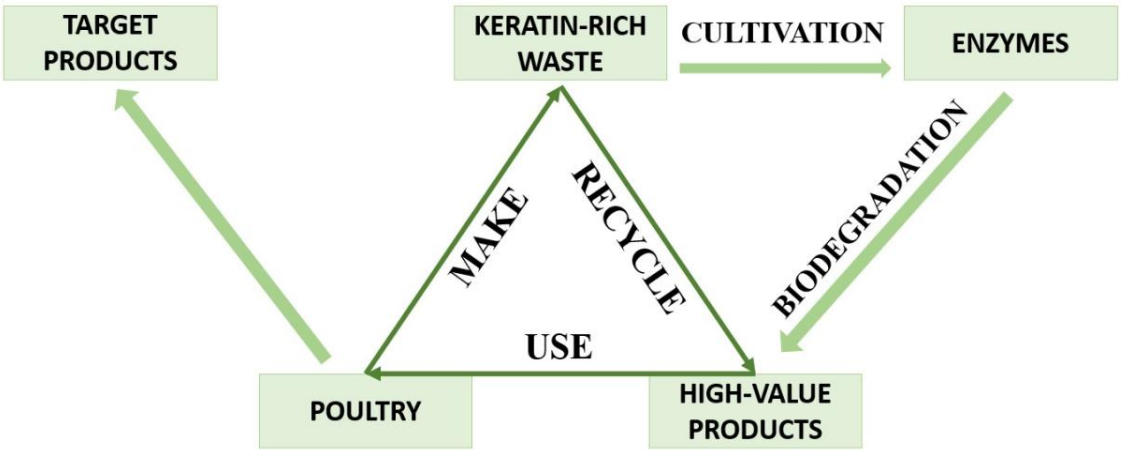

Figure 4.58 - Biodegradation of keratin-containing waste in the poultry production cycle (Shestakova et al., 2021).

4.3.1.1 Valorisation of Waste

One of the core principles of a circular economy is the valorisation of waste, transforming it into valuable resources. Chicken feathers, a by-product of the poultry

industry, are typically considered waste and are often incinerated or sent to landfills, as outlined in the Literature Review chapter. This project reimagines these feathers as a valuable reinforcement material for concrete. By doing so, it prevents waste from ending up in landfills and reduces the environmental impact associated with waste disposal processes such as incineration, which releases greenhouse gases and other pollutants.

4.3.1.2 Resource Efficiency

Incorporating chicken feathers into concrete enhances resource efficiency in several ways. First, it reduces the demand for traditional synthetic fibres used in fibre-reinforced concrete production. These materials often require significant energy for processing, contributing to environmental degradation and resource depletion. By substituting synthetic fibres with feather fibres, the construction industry can lower its ecological footprint.

4.3.1.3 Energy Savings

The production and processing of natural feather fibres consume less energy compared to synthetic fibres or steel reinforcement. The production and processing of natural feather fibres consume less energy because they are an inevitable by-product of the poultry industry and require only basic cleaning and separation, unlike synthetic fibres or steel, which involve energy-intensive processes like polymerisation or smelting at high temperatures. For instance, steel production requires mining iron ore and energy-intensive processes like smelting in blast furnaces, which operate at very high temperatures, up to 2,000 °C, while the drying oven used in this experimental program was set to a maximum of 50 °C. Feathers to be used as fibres only require minimal processing, including cleaning, drying, and mechanical separation of fibres, which are low-energy processes.

Additionally, specific feather fibre-reinforced concrete products can offer better thermal insulation properties, leading to energy savings in buildings by reducing the need for heating and cooling. This contributes to the reduction of overall energy

consumption in the built environment, aligning with the goals of improving energy efficiency and reducing greenhouse gas emissions. Feather fibre-reinforced concrete will likely be a good insulator due to the properties of the feathers themselves. Feathers have excellent thermal insulation properties due to their unique structure. Feathers are composed of keratin, which has low thermal conductivity, reducing heat transfer. Furthermore, feathers are also hollow, with a honey-comb structure in the rachis which creates air pockets which will further improve the insulation properties by trapping air.

4.3.1.4 Enhanced Material Lifecycle

The incorporation of feather fibres extends the lifecycle of concrete structures. Feather fibre-reinforced concrete has shown potential in improving the durability and crack resistance of concrete, which means structures made with this material may require less maintenance and have longer service lives. This durability reduces the need for frequent repairs and replacements, further conserving resources and reducing waste generation over the lifecycle of a building or infrastructure project.

4.3.1.5 Economic Benefits

Utilising locally available chicken feathers reduces the costs associated with importing traditional construction materials. This cost-effectiveness can make sustainable construction practices more accessible, particularly in developing regions where budget constraints often limit the adoption of green building technologies. Furthermore, creating a market for feather fibres can provide additional income streams for poultry farmers and waste processing facilities, stimulating local economies and supporting sustainable agricultural practices.

4.3.1.6 Social and Environmental Impact

Implementing this project promotes social and environmental benefits by reducing the environmental impact of poultry farming and concrete production. By integrating feather fibres into concrete, the construction industry can reduce its reliance on non-renewable resources, lower greenhouse gas emissions, and promote sustainable waste

management practices. Additionally, the reduced need for synthetic fibres and traditional raw materials supports biodiversity conservation by decreasing the environmental degradation associated with their extraction and production.

4.3.1.7 Innovation and Scalability

The project also encourages innovation in material science and construction practices by exploring the use of sustainable and unconventional materials like feather fibres in concrete. This encourages the development of eco-friendly alternatives to traditional construction materials, reduces reliance on high-energy inputs like steel or other synthetic fibres. Developing new methodologies for processing and integrating feather fibres into concrete can lead to broader applications of agricultural waste in other industrial processes. The scalability of this approach is significant; with the global poultry industry producing vast quantities of feathers, the potential for widespread adoption is substantial. This scalability means that the benefits of this project can be realised globally, contributing to a more sustainable and circular economy on a large scale.

4.3.2 Contribution to the Sustainable Development Goals

By integrating chicken feather fibres into concrete, the construction industry can make significant strides towards achieving these SDGs, promoting sustainability, reducing waste, and enhancing the resilience and affordability of infrastructure globally.

4.3.2.1 Sustainable Development Goal 7: Affordable and Clean Energy

As previously discussed in the introductory chapter, this SDG aims to ensure universal access to affordable, reliable, and modern energy services, by focusing on providing access to energy for all individuals, particularly in underserved and developing regions. The creation of feather fibre-reinforced concrete utilises an abundant and globally available waste material, chicken feathers. By incorporating these feathers into concrete, the construction industry can produce materials that are not only cost-effective but also accessible worldwide, including in underserved and developing

regions. The use of local resources reduces the need for importing costly materials, making modern construction more affordable and sustainable.

Furthermore, this SDG also aims to double the global rate of improvement in energy efficiency, by encouraging improvements in energy efficiency across various sectors, including industrial, residential, and transportation, to reduce energy consumption and emissions. Feather fibre-reinforced concrete has the potential to improve the thermal insulation properties of buildings. Better insulation reduces the need for heating and cooling, which in turn lowers energy consumption and emissions associated with residential and industrial buildings. This aligns with the goal of improving energy efficiency across various sectors.

4.3.2.2 Sustainable Development Goal 11: Sustainable Cities and Communities

As also previously discussed, this SDG focuses on access to adequate, safe, and affordable housing and basic services for all, by promoting inclusive urban planning and development to provide housing and services to all community members. The use of feather fibre-reinforced concrete can lower construction costs due to the inexpensive nature of the raw materials (feathers). This cost-saving can be passed on to consumers, making housing more affordable. Moreover, the enhanced properties of the concrete can lead to safer and more durable structures, ensuring access to adequate and safe housing.

Furthermore, the SDG aims to enhance inclusive and sustainable urbanisation and capacity for participatory, integrated, and sustainable human settlement planning, by encouraging participatory and integrated approaches to urban planning that consider social, economic, and environmental sustainability. The SDG also aims to reduce the adverse per capita environmental impact of cities, by addressing pollution, waste management, and resource consumption to mitigate the environmental impact of urbanisation. Utilising local waste materials like chicken feathers promotes inclusive and sustainable urbanisation. It encourages the integration of environmental sustainability into urban planning and development processes. By supporting the local

economy and reducing dependency on imported construction materials, communities can develop more resilient and self-sufficient urban areas.

The incorporation of feather fibres also helps to address the issue of waste management in urban areas. By diverting feathers from landfills and incineration, which contribute to pollution and greenhouse gas emissions, this practice reduces the per capita environmental impact of cities. It supports sustainable waste management practices and resource consumption.

4.3.2.3 Sustainable Development Goal 12: Responsible Consumption and Production

Additionally, the 12th SDG focuses on sustainable consumption and production, by adopting sustainable practices in consumption and production to reduce environmental impact. This SDG also aims to achieve sustainable management and efficient use of natural resources by promoting the efficient use of resources to minimise waste and environmental degradation. Feather fibre-reinforced concrete exemplifies sustainable consumption and production by adopting the 10-year framework of programmes. It promotes the efficient use of natural resources by recycling agricultural waste into valuable construction materials. This reduces the environmental impact associated with traditional concrete production.

Other relevant principles of the SDG discussed was the aim to substantially reduce waste generation through prevention, reduction, recycling, and reuse, by encouraging waste management practices that prioritise waste prevention and material recovery, as well as to substantially reduce waste generation through prevention, reduction, recycling, and reuse, by encouraging waste management practices that prioritise waste prevention and material recovery. This innovative use of chicken feathers significantly reduces waste generation. By integrating feather fibres into concrete, waste that would otherwise be incinerated or sent to landfills is repurposed, thus supporting waste prevention, reduction, recycling, and reuse. This aligns perfectly with the SDG of substantially reducing waste generation.

Finally, this SDG aims to halve per capita global food waste at the retail and consumer levels, by reducing food waste throughout the supply chain, from production to consumption. Given that the poultry production industry is a large producer of waste, aiming to minimise the waste in this industry would directly tackle this SDG. The poultry industry is a significant producer of waste, and utilising chicken feathers in concrete directly addresses the goal of halving per capita global food waste. By finding valuable uses for by-products like feathers, the industry can become more efficient and less wasteful, contributing to responsible consumption and production.

4.3.2.4 Sustainable Development Goal 13: Climate Action

Lastly, as mentioned, this SDG aims to promote mechanisms for raising capacity for effective climate change-related planning and management in least developed countries and small island developing states, by supporting vulnerable nations in developing and implementing climate strategies. Given that poultry production is an industry available on a world-wide scale, education on utilising the by-products of this industry would benefit not only developed countries but also smaller and less developed countries. Feather fibre-reinforced concrete supports climate action by promoting sustainable practices that can be adopted globally. The use of this material helps reduce greenhouse gas emissions associated with concrete production and waste disposal. It also enhances the resilience of buildings to climate-related impacts by improving their durability and insulation properties. The global availability of poultry production means that the technology and knowledge of using feather fibres in concrete can be shared with both developed and developing countries. This promotes the development and implementation of effective climate strategies worldwide, particularly benefiting least developed countries and small island developing states that are vulnerable to climate change.

Fibre concrete results in improved performance due to crack control and associated longer term durability performance. Therefore, this results in more durable structures which require lower maintenance and therefore less resources and reduced repair. These structures also relate to better performance throughout their life cycle, with

longer term durability liked to lower replacement requirements of buildings, therefore lower waste generation at building end-of-life and conservation of resources required for replacement of buildings.

Chapter 5

Conclusion

5 Conclusion

This chapter encapsulates the outcomes of this research, by highlighting the main findings of the experimental program, and commenting on the overall achievement of the research questions. It also highlights the strengths and limitations of this work, while also highlighting possible leads for future research.

5.1 Overview

The primary goals of this research were to attempt to reduce waste being generated in the poultry production industry and in fibre-reinforced concrete production, by utilising natural waste feather fibres as reinforcement. By reducing the volume of waste sent to landfills and hence lowering the environmental impact of poultry farming; a circular economy in these two industries would be created and make contributions to achievement of the Sustainable Development Goals.

Furthermore, the goals of this research were extended to completing an exhaustive experimental program, assessing whether incorporating readily available feather fibres with varying amounts and aspect ratios into cement-based construction materials would improve crack control, specifically reducing early-stage plastic cracking and drying shrinkage cracking. It was also aimed to establish whether improvements in crack behaviour would compromise the standard fresh, mechanical, and durability properties of the concrete.

Both of these goals were achieved as the concrete mixes developed and tested incorporating otherwise waste feather fibres, proved to be effective at reducing cracking and repeatable, and hence creating an accessible, low-cost fibre-reinforced cement-based material. The mixes also did not significantly compromise most of the mechanical strengths, namely compressive strength and ductility.

5.2 Conclusions based on Research Findings

In summary, the research carried out and results analysed from the rigorous laboratory experimental program on feather fibre-reinforced SCC and SCM are as follows:

i. **Fibre Characterisation:** The fibres were analysed and found to have a considerable length range, as well as a high aspect ratio, ideal for reinforcements. The statistical analysis proved correlation between the thicknesses and length, and effectively eliminated the need to measure thicknesses in future work. Hence, length ranges were sufficient to differentiate between fibre morphologies.

ii. **Fibre Preparation:** A repeatable process was developed to shorten the fibre length range by means of a modified paper shredder. This process is simpler, faster, and more scalable than hand trimming, which is very time intensive.

iii. **Mix Design Development:** The volume fractions of 0.125%, 0.25%, and 0.5% were chosen and hence overall mix designs developed for SCC and SCM, as lower volume fractions proved to be more effective in comparison to existing literature.

iv. **Flowability and Workability:** The lowest volume fraction did not result in any reduced workability or flowability SCC flowability classifications. However, both the slump flow test and T_{500} test indicated a decrease in workability properties at most time intervals as the fibre volume fraction increased further. The mix with the largest volume fraction failed the slump flow tests, and regular slump cone tests were conducted, revealing true slumps of 190 mm and 210 mm for short and long fibres, respectively.

v. **Passing Ability:** The L-box test demonstrated that the smallest volume fraction did not significantly affect passing ability, thus retaining SCC passing ability classification. However, a decrease in passing ability was observed with long fibres, as clogging began to occur at the base.

vi. **Viscosity:** The V-funnel test indicated that the smallest volume fraction did not affect viscosity, and also retained SCC viscosity classification, however, a proportional decrease was noted with the increase in fibre volume fraction. The

mix with the largest volume fraction did not pass the V-funnel test and caused significant clogging.

vii. **Rheology:** A steeper gradient was obtained in the stress-strain graph, with increasing fibre percentage, indicating that the mixes became less workable as the fibre incorporation increased. As previous studies have shown, an increase in fibres leads to higher viscosity and decreased flowability. This corresponds to the data collected, which showed an increase in torque with the increase in fibre volume fraction. It is relevant to note that the mixes with the largest volume fraction (C0.5S and C0.5L) were not assessed for their rheological properties due to the low workability of the mix.

viii. **Mortar Density:** In most fibre-reinforced mixes, the mortars exhibited a trend of increased density, suggesting an enhanced compact structure of the mortar, thus increasing the density. On the other hand, the mixes containing the largest amount of fibres demonstrated an overall lower density compared to those with shorter and less fibres. This reduction in density was attributed to the longer fibres creating air voids within the concrete matrix.

ix. **Mortar Ultrasonic Pulse Velocity:** The UPV test results mostly stayed the same when feather fibres were added to the mortar. The results consistently fell between 2 and 2.5 km/s, suggesting that feather fibres did not impact the speed of ultrasonic pulses passing through various mixtures. This indicates that the internal structure of the material was not significantly impacted by the presence of fibres in a manner observable through the UPV test.

x. **Mortar Compressive Strength:** The study revealed improvements in compressive strength for mixes featuring shorter fibres. Specifically, 15mm fibres led to enhancements in the 0.5%, 0.75%, and 1% volume fraction mixes. However, mixes containing longer fibres exhibited reduced strength, and the mix with the largest volume fraction of longer fibres experienced a considerable decline in compressive strength.

xi. **Mortar Flexural Strength:** Similar findings were observed in flexural strength. Shorter fibres, particularly 15mm fibres, contributed to improvements in the 0.5%

and 0.75% volume fraction mixes. Regardless of fibre length, all samples with the largest volume fraction of longer fibres demonstrated a notable decrease in flexural strength.

xii. **Concrete Density:** Increased density was noted for all fibre-reinforced SCC mixes.

xiii. **Concrete Compressive Strength:** Improvements were observed in compressive strength for all volume fractions, with shorter fibres generally outperforming their longer counterparts across most volume fractions.

xiv. **Concrete Indirect Tensile Strength:** An increase in tensile strength was noted in the fibre-reinforced mixes with short fibres, while a decrease was noted in those with the longer fibres.

xv. **Concrete Flexural Strength:** Similar results in flexural toughness were noted when compared to the control mix, for the smallest and the largest volume fraction. Overall, a decrease was noted for the peak load and the flexural toughness factor of the fibre-reinforced mixes.

xvi. **Plastic Shrinkage Cracking:** Significant improvements were observed in crack formation time for all volume fractions and fibre lengths, with note of the C0.25S mix, which did not exhibit any cracking during the entire test duration. There was also a notable reduction in crack width with increasing volume fractions of fibres.

xvii. **Restrained Drying Shrinkage Cracking:** Ring specimens containing fibres did not develop any cracks within the 28-day testing period, as opposed to the control which cracked on the 10^{th} day. The fibre-reinforced mixes also recovered from slight drops in strain readings, showing recovery from possible crack formations.

xviii. **Restrained Mortar Shrinkage Cracking:** All panels of fibre-reinforced mortar did not develop any cracks within the required 6-hour testing period despite the induced wind from the industrial fans, as opposed to the control mix panel. During the subsequent examination at the 24-hour mark, no further cracks were observed on any of the mortar panels.

xix. **Concrete Chloride Penetration:** As the amount of fibres increased in the mixes tested, there was a corresponding decrease in chloride ion penetrability,

suggesting that fibre reinforcement enhanced the material's ability to resist chloride ingress, thereby improving its durability in chloride-rich environments.

xx. **Vacuum Saturation Porosity:** Mixes with low volume fraction and short fibres showed slight reductions in permeability, suggesting that the addition of short fibres enhanced the concrete's compaction and hence reduced its permeability. On the other hand, longer fibres tended to increase permeable porosity, particularly at higher volume fractions, possibly due to the creation of more voids or inadequate integration within the concrete matrix.

5.3 Contribution to Knowledge

The data gathered throughout the project shows consistent results and proved that the incorporation of such fibres would in turn reduce the waste from the poultry production industry and create a circular economy between the construction and poultry production industries. Furthermore, the application of this on a global scale would also be possible due to the readily available materials in all the countries where poultry is consumed.

The overall conclusion and main contribution to knowledge based on the experimental program was that the most ideal volume fraction, when considering all properties, would be that with the smallest volume fraction, with either the shorter or longer fibres. These mixes proved to improve the mechanical properties of the SCC while they did not compromise on the fresh properties, and still remained within the self-compacting guidelines and requirements. If, on the other hand, a self-compacting mix is not essential and mechanical vibration can still take place, the greatest improvements of strength were noted in mixes with the largest volume fraction of 0.5%. Hence, depending on the specific vibration requirements for the use of this material in construction projects, it would be possible to use either the smallest or the largest volume fractions. This is an important contribution to knowledge, particularly when considering that these volume fractions are small enough to potentially be accessible on a widespread and industrial scale.

5.4 Contribution to Sustainability

By analysing the results of the experimental program, it is very clear that the incorporation of fibres has resulted in considerable improvements in the properties of the SCC and SCM mixes.

The scope of this research lies beyond the experimental program itself but aims to assess the overall practicality of creating such fibre-reinforced concrete. The exploration of incorporating chicken feather fibres into SCC and SCM represents a substantial step towards sustainable construction practices and the promotion of a circular economy.

The main contribution of this project was to assess potential benefits and challenges associated with using natural fibres, particularly keratin-rich chicken feathers, as reinforcement in concrete, addressing both environmental and practical aspects. This study has proven the possibility of using such reinforcement materials to create a stronger and accessible fibre reinforced SCC, with intrinsic benefits in multiple aspects.

5.4.1 Accessibility and Inclusivity

One of the primary motivations behind this project was to develop a sustainable construction material that is accessible to all, including communities in developing countries. Chemical treatments for fibres, while potentially enhancing certain properties, can significantly increase the cost and complexity of the material preparation process. By opting for untreated chicken feather fibres, one of the goals was to create a solution that is feasible and practical for use in diverse settings, especially where access to advanced chemical treatment facilities may be limited or non-existent. Chemical treatments involve additional expenses related to the purchase of chemicals, specialised equipment, and the need for skilled labour to perform the treatments. These costs can be prohibitive, particularly in developing regions where financial resources are often constrained. By avoiding chemical treatments, the overall costs of the development were kept low, making it more economically viable for

widespread adoption. This approach ensures that the benefits of feather fibre-reinforced concrete can be realised without placing undue financial burden on users.

Maintaining simplicity in the material preparation process was a key consideration. In many developing countries, the construction sector relies on straightforward, easily replicable methods that do not require extensive technical expertise. By using untreated fibres, it was ensured that the process remained straightforward and can be replicated with minimal training. The mechanical processing involved in trimming the fibres was also relatively simple and repeatable. This simplicity facilitates the dissemination and adoption of the technology in various regions, contributing to its potential for global impact.

5.4.2 Environmental Benefits

One of the primary motivations for this research was the environmental impact of poultry industry waste. Each year, the poultry industry generates substantial amounts of feather waste, which is typically disposed of through incineration, contributing to greenhouse gas emissions and environmental degradation. By repurposing these feathers as reinforcement in concrete, this project has highlighted a practical approach to waste reduction and resource efficiency. The use of chicken feather fibres helps in managing waste generated by the poultry industry, contributing to a circular economy, thus reducing the environmental burden of feather disposal. By repurposing waste materials, the project promotes the efficient use of natural resources, aligning with the principles of sustainable development and reducing the demand for synthetic materials in construction. The use of waste materials also aligns with global efforts to achieve the SDGs, particularly those related to responsible consumption and production (SDG 12) and climate action (SDG 13).

Furthermore, the use of chemical treatments often involves the use of substances that can have adverse environmental effects. The production, application, and disposal of these chemicals can contribute to pollution and pose health risks to workers and local communities. By forgoing chemical treatments, the environmental footprint of the

project was minimised, aligning with the principles of sustainable development. This approach also reduces the potential for chemical residues to contaminate natural ecosystems, promoting a healthier environment.

5.4.3 Circular Economy

Creating a circular economy through the use of feather fibre-reinforced concrete embodies the principles of waste valorisation, resource efficiency, and sustainable development. By transforming a common waste product into a valuable resource for construction, this project not only addresses environmental and economic challenges but also promotes a sustainable and resilient built environment. The successful integration of chicken feathers into concrete mixes could serve as a model for similar initiatives across various industries, driving the global transition towards a circular economy.

5.4.4 Socioeconomic Impact and Accessibility

A notable strength of this project is its emphasis on accessibility and socioeconomic impact. By avoiding complex and costly chemical treatments, the research aimed to develop a method that could be easily adopted in developing countries where technological and financial resources are limited. In many developing regions, obtaining the necessary chemicals for fibre treatment can be challenging due to supply chain limitations. Local markets may not stock the required chemicals, or they may be prohibitively expensive due to import costs, so by using untreated feathers, dependency on external resources was eliminated, allowing the project to be implemented using locally available materials. This autonomy supports the resilience and sustainability of the construction practices in these regions. The widespread availability of chicken feathers globally enhances the feasibility of this approach, making it a viable solution for communities seeking sustainable construction alternatives. This can lead to widespread adoption without relying on imported materials. This accessibility also supports the broader goals of sustainable development by promoting inclusive and affordable innovations in construction.

Furthermore, utilising chicken feathers directly from local poultry farms supports the local economy. Farmers and small businesses involved in poultry production can benefit from an additional revenue stream by supplying feathers for concrete reinforcement. This creates economic opportunities and promotes the circular economy within local communities. By keeping the process free from chemical treatments, it was ensured that the barrier to entry remains low, encouraging more participants to engage in this sustainable practice.

Another benefit to the socioeconomic aspect of this project is giving locals an opportunity for further education. Implementing a process that is repeatable and accessible, and does not rely on inaccessible chemical treatments, provides valuable educational opportunities. Local builders, engineers, and students can be given the opportunity to learn about sustainable construction practices and the innovative use of waste materials without needing access to advanced chemical knowledge or facilities. This hands-on experience can foster a greater appreciation for sustainable development and encourage further innovation within the community.

5.5 Strengths and Limitations of this Research

5.5.1 Strengths of this Research

The overall benefits of creating such materials are multiple. By creating a low-cost reinforced building material, a sustainable option when compared to costly synthetic fibre-reinforced concrete, opens the possibility for the widespread use of this new material. This innovation enables broader access to reinforced building materials, particularly in resource-limited regions, and promotes environmentally friendly construction practices by utilising waste materials like poultry feathers. The affordability and eco-conscious design make it a viable option for sustainable infrastructure development while reducing reliance on non-renewable, high-energy inputs such as synthetic fibres.

5.5.1.1 Improved Building Material

Overall, the outcomes of the experimental program have outlined a stronger building material. The most impressive improvements were noted in the reduction of early-stage and plastic cracking, as some mixes did not crack at all within the testing durations. Further improvements in compressive strength and ductility prove the potential for this building material to be compared to other materials on the market. While it was clear that there had been a reduction in the workability and fresh properties of the mixes, these can be overcome by opting for mixes with lower volume fractions, or by incorporating some mechanical vibration during the casting process. Additionally, the use of feather fibres has shown potential in enhancing the longevity and durability of concrete structures, suggesting significant long-term benefits.

5.5.1.2 Readiness of the Building Material based on TRL Scale

Following the intensive experimental program, the development and testing of the mixes has led to this material to be around 4-5 on the TRL (Technology Readiness Level) scale, as the material has been validated in a laboratory environment, using controlled testing to demonstrate its feasibility and potential. In fact, this building material is ready to be scaled up and tested on a larger scale, without needing to invest in any new equipment, thereby minimising the disruption and costs associated with adopting new technologies, apart from the possible development of a larger-scale shredder if shorter fibres are preferred, which may not be necessary for all applications.

Considering the availability and accessibility of the feather fibres, such scaling up should not be restricted to industrial projects but could also provide low-cost housing solutions in underdeveloped communities. This broad applicability underscores the material's versatility and potential to address housing shortages globally, particularly in areas where traditionally used fibre reinforcements are scarce or expensive.

5.5.1.3 Accessible Building Material

Given that chicken feather fibres are accessible on a global scale, the incorporation of such fibres as reinforcement allow for developing countries to have access to a suitable reinforcing material, which forgoes any limitations posed by closed markets or transportation difficulties.

The simple mechanical processing of the fibres also encourages the incorporation of this fibre material into the market, promising an easily attainable final product to be used in the construction industry. The overall simplicity and low cost of processing these fibres make them an attractive option for a wide range of construction projects, from small-scale residential buildings to large infrastructure developments.

5.5.1.4 Sustainable Building Material and Circular Economy

The replacement of synthetic fibres with natural fibres would ultimately reduce the carbon emissions associated with producing and processing synthetic fibres. The inevitable availability of chicken feathers as a by-product of the poultry industry means that the fibres would be generated without any additional manufacturing or processing.

Furthermore, using such fibres would contribute to reducing waste taken to landfills. As mentioned, this fibre is generated as an inevitable by-product, and there is no way to go about processing poultry without such fibre waste being generated. The reduction of waste being taken to the landfill is one side of the dual benefit of this project, as by reusing such waste in a value-added material, the construction industry subsequently would benefit from this, with improved construction materials.

This dual benefit contributes to the creation of a circular economy. By converting this waste product into a valuable construction resource, this project addresses both environmental and economic challenges, while linking two already highly wasteful industries. The integration of feather fibres into concrete mixes exemplifies how waste materials can be effectively repurposed, thereby promoting sustainability and resource efficiency. The successful implementation of this initiative could inspire similar efforts

across various industries, further advancing the principles of a circular economy and contributing to a more sustainable future.

5.5.2 Limitations of this Research

While the overall outcomes of the research were positive, there were obstacles, typically encountered in experimental research work, which may hinder the research outcomes. Addressing the limitations identified in this project is essential for advancing the understanding and application of feather fibre-reinforced concrete.

One of the significant limitations encountered by the researcher (myself) during this project was the physical challenge of handling materials with respect to the manual handling of loads (Directive 90/269/EEC). Raw materials and concrete samples should require lifting aid devices and laboratory support systems, which were unavailable. The inability to safely lift and manoeuvre heavy samples, requiring support and assistance, presented significant challenges in the research. Addressing such challenges aligns with the University of Malta's Gender+ Equity Plan (Univerisy of Malta, 2022), and promotes female participation in engineering and construction industries.

Maintaining controlled environmental conditions in the laboratory was critical for curing, shrinkage, early-stage cracking, and durability tests. These tests required additional effort to stabilise conditions, especially for shrinkage tests. Variations in environmental conditions were recorded during the experimental work and addressed in the analysis and discussion chapter.

Another limitation of the research concerns gaps in specific specialised equipment at the time of testing, or faults in the existing equipment beyond the control of the researcher. These issues were however mitigated through test repetition or, adaptations in the methodology, as seen with the flexural strength experiments.

Time constraints associated with the one-year Master's degree further limited the scope of the work. Despite these challenges, efforts were made to ensure the reliability

of the results. Addressing these limitations in further studies will improve testing conditions, data accuracy, and the overall quality of results.

5.6 Future Work

The promising results and insightful findings of this project have laid a strong foundation for future research and development in the field of feather fibre-reinforced concrete. However, numerous aspects merit further exploration and refinement to fully realise the potential of this innovative material. The following sections outline key areas for future work that can enhance the understanding, performance, and practical application of feather fibre-reinforced concrete.

One of the primary areas for future work involves the detailed characterisation of chicken feather fibres. Comprehensive studies are needed to understand the mechanical, thermal, and chemical properties of these fibres in greater depth. Advanced characterisation techniques such as scanning electron microscopy (SEM), Fourier-transform infrared spectroscopy (FTIR), and X-ray diffraction (XRD) can provide insights into the microstructure and composition of feather fibres. Understanding these properties is crucial for optimising their integration into concrete and predicting their long-term performance.

Another possibility to expand this work is by extensively testing a wide range of different constituent materials, mix designs, and additives, both synthetic and natural. These countless possibilities could potentially further improve the quality of the materials produced, and lead to more innovative building materials. In particular, it would be interesting to consider substituting the consistent materials with cheaper, local alternatives, such as local aggregates as opposed to dolomitic aggregates.

On another note, while this project intentionally avoided chemical treatments to keep the process accessible and cost-effective, future research could explore the benefits of various treatments to enhance fibre performance. Treatments such as alkali, silane, or enzymatic treatments could improve the adhesion between the fibres and the cement matrix, leading to better mechanical properties and durability. Investigating the

environmental impact and cost-effectiveness of these treatments will be essential to ensure that they align with the project's sustainability goals.

Another possibility for future work related to this project would be to focus on carrying out a more extensive range of testing, including larger sample sizes and under different curing conditions, or harsh environments such as marine or extreme temperatures, to further confirm or deny the properties found in this study. A further opportunity for further research is to consider long-term effects on the material to evaluate how the properties of feather fibres and the concrete matrix change over time, including monitoring for potential degradation of the fibres and its impact on the concrete's integrity.

Furthermore, based on the conclusions gathered from this study, the next logical step would be to evaluate the possibility of scaling up this project to be accessible to the construction industry. Implementing pilot projects in real-world construction scenarios to evaluate the feasibility and performance of feather fibre-reinforced concrete in various applications, such as pavements, structural elements, and non-structural components. By developing efficient manufacturing processes for integrating feather fibres into concrete mixes on a larger scale, this would serve as a step towards practical implementation. To facilitate the widespread adoption of feather fibre-reinforced concrete, it is also essential to develop standardised testing methods and guidelines.

While doing this, it would also be beneficial to assess the cost-benefit of using such materials. Analysing the cost-effectiveness of using feather fibres compared to conventional and synthetic fibres would include assessing the costs associated with fibre processing, treatment, and integration into concrete, as well as potential savings from improved material performance and reduced maintenance.

Overall, continued innovation and investment in this area will be essential to realise the full potential of feather fibre-reinforced concrete and continue to contribute to the development of more sustainable construction practices worldwide.

References and Bibliography

Abdilla, B. (2021). *Recycled Concrete Aggregates and Steel Waste Tyre Fibres for High-Performance Self-Compacting Concrete* (Issue July). University of Malta.

Abir, M. M. R., Kashif, S. M., & Razzak, M. A. (2015). Tensile and Statistical Analysis of Sisal Fibers for Natural Fiber Composite Manufacture. *Advanced Materials Research*, *1115*, 349–352. https://doi.org/10.4028/www.scientific.net/AMR.1115.349

Acda, M. N. (2009). Sustainable Use of Waste Chicken Feather for Durable and Low Cost Building Materials for Tropical Climates. *Sustainable Agriculture: Technology, Planning and Management*, 353–366.

Adesina, A., Bastani, A., Heydariha, J. Z., Das, S., & Lawn, D. (2020). Performance of basalt fibre-reinforced concrete for pavement and flooring applications. *Innovative Infrastructure Solutions*, *5*(3), 103. https://doi.org/10.1007/s41062-020-00359-y

Ajayi, S. O., Oyedele, L. O., Akinade, O. O., Bilal, M., Owolabi, H. A., Alaka, H. A., & Kadiri, K. O. (2016). Reducing waste to landfill: A need for cultural change in the UK construction industry. *Journal of Building Engineering*, *5*, 185–193. https://eprints.leedsbeckett.ac.uk/id/eprint/3220/

Akin, D. E. (2010). Flax – Structure, Chemistry, Retting and Processing. In *Industrial Applications of Natural Fibres* (pp. 87–108). John Wiley & Sons, Ltd. https://doi.org/https://doi.org/10.1002/9780470660324.ch4

Alonso, R. S., Sanches, R., & Marcicano, J. P. P. (2013). Chicken Feather - Study of physical properties of textile fibers for commercial use. *International Journal of Textile and Fashion Technology*, *3*(2).

Amaducci, S., & Gusovius, H.-J. (2010). Hemp – Cultivation, Extraction and Processing. In *Industrial Applications of Natural Fibres* (pp. 109–134). John Wiley & Sons, Ltd. https://doi.org/https://doi.org/10.1002/9780470660324.ch5

Amieva, E. J.-C., Velasco-Santos, C., Martínez-Hernández, A., Rivera-Armenta, J., Mendoza-Martínez, A., & Castaño, V. (2015). Composites from chicken feathers quill and recycled polypropylene. *Journal of Composite Materials*, *49*(3), 275–283. https://doi.org/10.1177/0021998313518359

Anandamurthy, A., Guna, V., Ilangovan, M., & Reddy, N. (2017). A review of fibrous reinforcements of concrete. *Journal of Reinforced Plastics and Composites*, *36*(7), 519–552. https://doi.org/10.1177/0731684416685168

Anandjiwala, R. D., & John, M. (2010). Sisal – Cultivation, Processing and Products. In *Industrial Applications of Natural Fibres* (pp. 181–195). John Wiley & Sons, Ltd. https://doi.org/https://doi.org/10.1002/9780470660324.ch8

Araya-Letelier, G., Gonzalez-Calderon, H., Kunze, S., Burbano-Garcia, C., Reidel, U., Sandoval, C., & Bas, F. (2020). Waste-based natural fiber reinforcement of adobe mixtures: Physical, mechanical, damage and durability performance assessment. *Journal of Cleaner Production*, *273*, 122806. https://doi.org/10.1016/j.jclepro.2020.122806

ASTM C1202-12. (2012). *Standard Test Method for Electrical Indication of Concrete's Ability to Resist Chloride Ion Penetration*. 1–8. https://doi.org/10.1520/C1202-12.2

ASTM C1579-06. (2006). *Standard Test Method for Evaluating Plastic Shrinkage Cracking of Restrained Fiber Reinforced Concrete (Using a Steel Form Insert)*. 7. https://doi.org/10.1520/C1579-06.2

ASTM C1581-04. (2004). *Standard Test Method for Determining Age at Cracking and Induced Tensile Stress Characteristics of Mortar and Concrete under Restrained Shrinkage*. 1–6. www.astm.org,

Baldacchino, O. (2014). *Mechanical and Shrinkage Properties of Recycled PET Fibre-Reinforced Concrete* (Issue June). University of Malta.

Baley, C. (2002). Analysis of the flax fibres tensile behaviour and analysis of the tensile stiffness increase. *Composites Part A: Applied Science and Manufacturing*, *33*(7), 939–948. https://doi.org/https://doi.org/10.1016/S1359-835X(02)00040-4

Bansal, G., Gope, P., Gupta, T., Singh, V. K., & Gope, P. C. (2017). Application and Properties of Chicken Feather Fiber (CFF) a Livestock Waste in Composite Material Development. In *Journal of Graphic Era University* (Vol. 5, pp. 16–24). https://www.researchgate.net/publication/311612937

Banthia, N., & Gupta, R. (2006). Influence of polypropylene fiber geometry on plastic shrinkage cracking in concrete. *Cement and Concrete Research*, *36*, 1263–1267. https://doi.org/10.1016/j.cemconres.2006.01.010

Basu, P., Kumar, R., & Das, M. (2023). Natural and manmade fibers as sustainable building materials. *Materials Today: Proceedings*. https://doi.org/10.1016/j.matpr.2023.07.222

Ben Hamad Bouhamed, S., & Kechaou, N. (2017). Kinetic study of sulphuric acid hydrolysis of protein feathers. *Bioprocess and Biosystems Engineering*, *40*(5), 715–721. https://doi.org/10.1007/s00449-017-1737-7

Bennenk, I. H. W. (2005). Self-compacting concrete-five years of experience with scc in the netherlands. *Proceedings of the 18th BIBM International Congress, Amsterdam*.

Bentur, A., & Mindess, S. (2006). *Fibre Reinforced Cementitious Composites* (Routledge (ed.)). CRC Press. https://doi.org/10.1201/9781482267747

Bhat, K. M. U. D., & Khan, M. Z. (2018). Effect of Steel Fibre Reinforcement on Early Strength of Concrete. *International Journal of Trend in Scientific Research and Development*, *Volume-2*(Issue-5), 198–225. https://doi.org/10.31142/ijtsrd15781

Bolat, H., Şimşek, O., Çullu, M., Durmuş, G., & Can, Ö. (2014). The effects of macro synthetic fiber reinforcement use on physical and mechanical properties of concrete. *Composites Part B: Engineering*, *61*, 191–198. https://doi.org/10.1016/j.compositesb.2014.01.043

Bonser, R. H. C., & Purslow, P. P. (1995). The Young's Modulus of Feather Keratin. *The Journal of Experimental Biology*, *198*, 1029–1033.

Borg, R. P., Baldacchino, O., & Ferrara, L. (2016). Early age performance and mechanical characteristics of recycled PET fibre reinforced concrete. *Construction and Building Materials*, *108*, 29–47. https://doi.org/10.1016/j.conbuildmat.2016.01.029

Brenner, M., & Weichold, O. (2021). Poultry feather waste as bio-based cross-linking additive for ethylene propylene diene rubber. *Polymers*, *13*(22). https://doi.org/10.3390/polym13223908

BS 812-109:1990. (1990). Testing aggregates - Part 109: Methods for determination of moisture content. *BSI Standards Publication*.

BS EN 1015-11:1999. (1999). Methods of Test for Mortar for Masonry — Part 11: Determination of Flexural and Compressive Strength of Hardened Mortar. *BSI Standards Publication*, *3*(1).

BS EN 1097-6:2000. (2000). Tests for mechanical and physical properties — Part 6: Determination of particle density and water absorption. *BSI Standards Publication*.

BS EN 12350-10:2010. (2010). Testing fresh concrete Part 10 : Self-compacting concrete — L-box test. *BSI Standards Publication*, *PART 10*.

BS EN 12350-2:2000. (2000). Testing Fresh Concrete — Part 2: Slump test. *BSI Standards Publication*, *04*, 1–6.

BS EN 12350-7:2009. (2019). Testing fresh concrete Part 8: Self-compacting concrete — Slumpflow test. *BSI Standards Publication*.

BS EN 12350-9:2010. (2010). Testing fresh concrete Part 9: Self-compacting concrete — V-funnel test. *BSI Standards Publication*.

BS EN 12390-2:2009. (2009). Testing hardened concrete — Part 2: Making and curing specimens for strength tests. *BSI Standards Publication*, *38*(10).

BS EN 12390-3:2009. (2009). Testing hardened concrete — Part 3: Compressive strength of test specimens. *BSI Standards Publication*, *38*(10).

BS EN 12390-6:2009. (2009). Testing hardened concrete — Part 6: Tensile splitting strength of test specimens. *BSI Standards Publication*, *38*(10).

BS EN 12390-7:2009. (2009). Testing hardened concrete Part 7: Density of hardened concrete. *Journal of Chemical Information and Modeling*, *53*(9), 1689–1699.

BS EN 12504-4:2004. (2004). Testing concrete — Part 4: Determination of ultrasonic pulse velocity. *BSI Standards Publication*, *3*(June).

BS EN 14651:2007. (2007). Test method for metallic fibered concrete - Measuring the flexural tensile strength (limit of proportionality (LOP), residual). *BSI Standards Publication*, 1–17.

BS EN 196-6:1989. (1992). British Standard Methods of testing cement — Part 6: Determination of fineness. *BSI Standards Publication*, *3*(August).

BS EN 934-2:2001. (2003). Admixtures for concrete, mortar and grout - Part 2: Concrete admixtures — Definitions, requirements, conformity, marking and labelling. *BSI Standards Publication*, 3–36. https://doi.org/10.1016/B978-075065686-3/50280-9

Calleja, A. (2023). *Bio-Based Fibres for use in Cement Composite Materials*. University of Malta.

Choudary, R. B., & Nehanth, R. (2019). Effects of fibre content on mechanical properties of chicken feather fibre/PP composites. *Materials Today: Proceedings*, *18*, 303–309. https://doi.org/10.1016/j.matpr.2019.06.305

Chukwunonso Ossai, I., Shahul Hamid, F., & Hassan, A. (2022). Valorisation of keratinous wastes: A sustainable approach towards a circular economy. *Waste Management*, *151*(February), 81–104. https://doi.org/10.1016/j.wasman.2022.07.021

Clark, I. A., Daly, C. A., Devenport, W., Alexander, W. N., Peake, N., Jaworski, J. W., & Glegg, S. (2016). Bio-inspired canopies for the reduction of roughness noise. *Journal of Sound and Vibration*, *385*, 33–54. https://doi.org/10.1016/j.jsv.2016.08.027

Cornejo, J., Pokrant, E., Carvallo, C., Maddaleno, A., & San Martín, B. (2018). Depletion of tylosin residues in feathers, muscle and liver from broiler chickens after completion of antimicrobial therapy. *Food Additives & Contaminants: Part A*, *35*(3), 448–457. https://doi.org/10.1080/19440049.2017.1401740

Cui, C., Sun, L., Chen, X., Zhu, Y., Zheng, Z., Mao, D., Li, M., Li, Y., Cao, Y., Feng, B., Wang, H., Wang, L., Zhao, F., Huang, Z., & Zhong, Z. (2023). Improving the biodegradation of chicken feathers by a Bacillus licheniformis ZSZ6 mutant and application of hydrolysate. *International Biodeterioration and Biodegradation*, *180*(October 2022), 105597. https://doi.org/10.1016/j.ibiod.2023.105597

Dalhat, M. A., Osman, S. A., Alhuraish, A. A. A., Almarshad, F. K., Qarwan, S. A., & Adesina, A. Y. (2020). Chicken Feather fiber modified hot mix asphalt concrete: Rutting performance, durability, mechanical and volumetric properties. *Construction and Building Materials*, *239*. https://doi.org/10.1016/j.conbuildmat.2019.117849

EFNARC. (1999). European Specification for Sprayed Concrete. *European Specification for Sprayed Concrete*, *44*(0), 35.

EFNARC. (2005). The European Guidelines for Self-Compacting Concrete. *The European Guidelines for Self Compacting Concrete*, *May*, 63. http://www.efnarc.org/pdf/SCCGuidelinesMay2005.pdf

EN 197-1:2011. (2011). Cement - Part 1: Composition, specifications and conformity criteria for common cements. *BSI Standards Publication*, *1*(I), 2–5.

European Commission. (2016). *Introduction to Circular Economy*.

European Commission. (2019). Lower CO2 emissions on the horizon for cement. *CORDIS*, 1–5.

European Commission. (2020). *Buildings and construction*. Directorate-General for Internal Market, Industry, Entrepreneurship and SMEs. https://single-market-economy.ec.europa.eu/industry/sustainability/buildings-and-construction_en

Evazynajad, A., Kar, A., Veluswamy, S., Mcbride, H., & George, B. R. (2002). *Production and Characterization of Yarns and Fabrics Utilizing Turkey Feather Fibers*.

Farzana, M., Maraz, K. M., Sonali, S., Hossain, M., Alom, M., & Khan, R. (2022). Properties and application of jute fiber reinforced polymer-based composites. *GSC Advanced Research and Reviews*, *11*, 84–94. https://doi.org/10.30574/gscarr.2022.11.1.0095

Felekoğlu, B., Türkel, S., & Baradan, B. (2007). Effect of water/cement ratio on the fresh and hardened properties of self-compacting concrete. *Building and Environment*, *42*(4), 1795–1802. https://doi.org/10.1016/j.buildenv.2006.01.012

Food and Agriculture Organization of the United Nations. (2013). *Global meat consumption, World, 1961 to 2050*. Our World in Data. https://ourworldindata.org/grapher/global-meat-projections-to-2050

Food and Agriculture Organization of the United Nations. (2023). *Poultry meat production*. Our World in Data. https://ourworldindata.org/grapher/poultry-production-tonnes

Fraser, R. D. B., & Parry, D. A. D. (2008). Molecular packing in the feather keratin filament. *Journal of Structural Biology*, *162*(1), 1–13. https://doi.org/10.1016/j.jsb.2008.01.011

Gaimster, R., & Dixon, N. (2003). Self-compacting. *Advanced Concrete Technology*, 1–1077.

Georgiadis, A. S., Sideris, K. K., & Anagnostopoulos, N. S. (2010). Properties of SCC Produced with Limestone Filler or Viscosity Modifying Admixture. *Journal of Materials in Civil Engineering*, *22*(4), 352–360. https://doi.org/10.1061/(ASCE)MT.1943-5533.0000030

German Instruments A/S. (2010). *Rheology using the ICAR Plus – An Introduction*. 1–10.

Ghaffar, I., Imtiaz, A., Hussain, A., Javid, A., Jabeen, F., Akmal, M., & Qazi, J. I. (2018). Microbial production and industrial applications of keratinases: an overview. *International Microbiology*, *21*(4), 163–174. https://doi.org/10.1007/s10123-018-0022-1

Ghanem, S. Y., Bowling, J., & Sun, Z. (2021). Mechanical Properties of Hybrid Synthetic Fiber Reinforced Self- Consolidating Concrete. *Composites Part C: Open Access*, *5*, 100154. https://doi.org/10.1016/j.jcomc.2021.100154

Glanville, T. D., Ahn, H. K., Richard, T. L., Shiers, L. E., & Harmon, J. D. (2009). Soil Contamination Caused by Emergency Bio-Reduction of Catastrophic Livestock Mortalities. *Water, Air, and Soil Pollution*, *198*(1), 285–295. https://doi.org/10.1007/s11270-008-9845-2

Gonzalez-Calderon, H., Araya-Letelier, G., Kunze, S., Burbano-Garcia, C., Reidel, Ú., Sandoval, C., Astroza, R., & Bas, F. (2020). Biopolymer-waste fiber reinforcement for earthen materials: Capillary, mechanical, impact, and abrasion performance. *Polymers*, *12*(8). https://doi.org/10.3390/polym12081819

Grünewald, S., & Walraven, J. C. (2001). Parameter-study on the influence of steel fibers and coarse aggregate content on the fresh properties of self-compacting concrete. *Cement and Concrete Research*, *31*(12), 1793–1798. https://doi.org/10.1016/S0008-8846(01)00555-5

Gupta, A. (2014). *Human hair "waste" and its utilization: gaps and possibilities. J Waste Manag*.

Gupta, R., & Ramnani, P. (2006). Microbial keratinases and their prospective applications: An overview. *Applied Microbiology and Biotechnology*, *70*(1), 21–33. https://doi.org/10.1007/s00253-005-0239-8

Hamoush, S. A., & El-Hawary, M. M. (1994). Feather Fiber Reinforced Concrete. *Concrete International*, 33–35. https://www.researchgate.net/publication/282407347

Hannant, D. . (2003). Fibre-reinforced concrete. *Advanced Concrete Technology*, *3*, 6.

Health and Safety Executive. (1992). Manual Handling Operations Regulations. *Managing Health and Safety at Work*, *3*(2), 55–56. https://doi.org/10.4324/9780080914695-18

Hill, C. A. S., Norton, A., & Newman, G. (2009). The water vapor sorption behavior of natural fibers. *Journal of Applied Polymer Science*, *112*(3), 1524–1537. https://doi.org/10.1002/app.29725

Hoseini, M., Bindiganavile, V., & Banthia, N. (2009). The effect of mechanical stress on permeability of concrete: A review. *Cement and Concrete Composites*, *31*(4), 213–220. https://doi.org/10.1016/j.cemconcomp.2009.02.003

Huda, M. S., Schmidt, W. F., Misra, M., & Drzal, L. T. (2013). Effect of fiber surface treatment of poultry feather fibers on the properties of their polymer matrix composites. *Journal of Applied Polymer Science*, *128*(2), 1117–1124. https://doi.org/10.1002/app.38306

Hwang, J. W., Cho, K., Park, C. E., & Huh, W. (1999). Phase separation behavior of cyanate ester resin/polysulfone blends. *Journal of Applied Polymer Science*, *74*(1), 33–45. https://doi.org/10.1002/(SICI)1097-4628(19991003)74:1<33::AID-APP4>3.0.CO;2-Q

Jaya, H., AbdulKadir, H. K., Noriman, N. Z., Omar, S. D., Mazelan, A. H., Latip, N. A., & Aini, A. K. (2018). The Influences of Chicken Feather Loading on Tensile and Physical Properties of R-Hdpe/Eva/Cff Composites. *IOP Conference Series: Materials Science and Engineering*, *454*, 012190. https://doi.org/10.1088/1757-899X/454/1/012190

Jayasekara, C., & Amarasinghe, N. (2010). Coir – Coconut Cultivation, Extraction and Processing of Coir. In *Industrial Applications of Natural Fibres* (pp. 197–217). John Wiley & Sons, Ltd. https://doi.org/https://doi.org/10.1002/9780470660324.ch9

Johannes, L. P., Minh, T. T. N., & Xuan, T. D. (2024). Elephant Grass (Pennisetum purpureum): A Bioenergy Resource Overview. *Biomass*, *4*(3), 625–646. https://doi.org/10.3390/biomass4030034

Johnston, C. D. (2014). *Fiber-Reinforced Cements and Concretes*. CRC Press. https://doi.org/10.1201/9781482298154

JSCE-SF4. (2005). *Test method for bending strength and bending toughness of steel fiber reinforced concrete. Standard Specification for Concrete Structures, Test Methods and Specifications* (pp. 58–61).

Khan, A. A., Parikh, H., & Qureshi, M. R. N. (2022). A Review on Chicken Feather Fiber (CFF) and its application in Composites. In *Journal of Natural Fibers*. Taylor and Francis Ltd. https://doi.org/10.1080/15440478.2022.2073495

Khayat, K., & Guizani, Z. (1997). Use of viscosity-modifying admixture to enhance stability of fluid concrete. *ACI Materials Journal*, *94*, 332–340.

Khoury, G. A. (2008). Polypropylene fibres in heated concrete. Part 2: Pressure relief mechanisms and modelling criteria. *Magazine of Concrete Research*, *60*(3), 189–204. https://doi.org/10.1680/macr.2007.00042

Kodak, S., Gharge, T., Chavan, V., & G, S. (2019). Microbial Degradation of Poultry Feather Wastes under the Influence of Temperature and pH – A Review. *International Journal of Environmental Sciences & Natural Resources*, *21*(3). https://doi.org/10.19080/IJESNR.2019.21.556063

Kraai, P. P. (1985). Proposed Test To Determine the Cracking Potential Due To Drying Shrinkage of Concrete. *Concrete Construction - World of Concrete*, *30*(9), 775–778.

Kumar, T. N., Muralidharan, K., Pradhan, R., & Suresh, M. (2020). *Study of flexural strength and flexural modulus on chicken feather fiber used fiber reinforced polyester composite*. 020079. https://doi.org/10.1063/5.0025083

Lau, A. K. T., & Cheung, K. H. Y. (2017). Natural fiber-reinforced polymer-based composites. In *Natural Fiber-Reinforced Biodegradable and Bioresorbable Polymer Composites* (pp. 1–18). Elsevier Inc. https://doi.org/10.1016/B978-0-08-100656-6.00001-7

Leung, H., & Balendran, R. V. (2003). Properties of Fresh Polypropylene Fibre Reinforced Concrete under the Influence of Pozzolans. *Journal of Civil Engineering and Management*, *9*(4), 271–279. https://doi.org/10.1080/13923730.2003.10531339

Majumdar, A. J., & Nurse, R. W. (1974). Glass fibre reinforced cement. *Materials Science and Engineering*, *15*(2–3), 107–127. https://doi.org/10.1016/0025-5416(74)90043-3

Marculescu, C., & Stan, C. (2011). Poultry processing industry waste to energy conversion. *Energy Procedia*, *6*, 550–557. https://doi.org/https://doi.org/10.1016/j.egypro.2011.05.063

Martínez-Hernández, A. L., Velasco-Santos, C., De-Icaza, M., & Castaño, V. M. (2007). Dynamical–mechanical and thermal analysis of polymeric composites reinforced with keratin biofibers from chicken feathers. *Composites Part B: Engineering*, *38*(3), 405–410. https://doi.org/10.1016/j.compositesb.2006.06.013

Martínez-Hernández, A. L., Velasco-Santos, C., De Icaza, M., & Castaño, V. M. (2005). Microstructural characterisation of keratin fibres from chicken feathers. *International Journal of Environment and Pollution*, *23*(2), 162–178. https://doi.org/10.1504/ijep.2005.006858

MCST. (2024). *Research Excellence Programme Funded Projects*. https://mcst.gov.mt/research-excellence-programme-funded-projects/

Mendoza, R. C., Grande, J. O., & Acda, M. N. (2021). Effect of Keratin Fibers on Setting and Hydration Characteristics of Portland Cement. *Journal of Natural Fibers*, *18*(11), 1801–1808. https://doi.org/10.1080/15440478.2019.1701604

Mohanty, A. K., Misra, M., & Drzal, L. T. (Eds.). (2005). *Natural Fibers, Biopolymers, and Biocomposites*. CRC Press. https://doi.org/10.1201/9780203508206

Molins, G., Garrido, N., Macanás, J., & Carrillo, F. (2012). *Chicken Feathers Based Composites: a Life Cycle Assessment*. *June*, 24–28.

Moravvej, M., & Rashidi, M. (2020). Structural performance of self-compacting concrete. In *Self-Compacting Concrete: Materials, Properties and Applications* (pp. 371–387). Elsevier. https://doi.org/10.1016/B978-0-12-817369-5.00013-1

Morton, W. E., & Hearle, J. W. S. (2008). Physical Properties of Textile Fibres: Fourth Edition. In *Physical Properties of Textile Fibres: Fourth Edition*. https://doi.org/10.1533/9781845694425

Naaman, A. E. (2003). Engineered Steel Fibers with Optimal Properties for Reinforcement of Cement Composites. *Journal of Advanced Concrete Technology*, *1*(3), 241–252. https://doi.org/10.3151/jact.1.241

Nagaraju, A. (2020). Effect Of Binder Content on Super Plasticizer Dosage for Self-Compacting Concrete. *JOURNAL OF MECHANICS OF CONTINUA AND MATHEMATICAL SCIENCES*, *15*(4). https://doi.org/10.26782/jmcms.2020.04.00004

Neville, A. M. (1973). *Properties of concrete.* (2nd ed.). Pitman.

Ng, P.-L., Rudžionis, Ž., Ng, I. Y.-T., & Kwan, A. K.-H. (2018). Development of Sustainable High-Strength Self-Consolidating Concrete Utilising Fly Ash, Shale Ash and Microsilica. In *Sustainable Buildings - Interaction Between a Holistic Conceptual Act and Materials Properties*. InTech. https://doi.org/10.5772/intechopen.75508

Okamura, H., & Ouchi, M. (2003). Self-Compacting Concrete. *Journal of Advanced Concrete Technology*, *1*(1), 5–15. https://doi.org/10.3151/jact.1.5

Oladele, I. O. (2016). Assessment of Thermo-Mechanically Treated Chicken Feather Fibre Reinforced Epoxy Composites for Automobile Application. *American Journal of Materials Science and Technology*. https://doi.org/10.7726/ajmst.2016.1001

Oladele, I. O., Okoro, A. M., Omotoyinbo, J. A., & Khoathane, M. C. (2018). Evaluation of the mechanical properties of chemically modified chicken feather fibres reinforced high density polyethylene composites. *Journal of Taibah University for Science*, *12*(1), 56–63. https://doi.org/10.1080/16583655.2018.1451103

Ozawa, K. (1989). High performance concrete based on the durability design of concrete structures. *The Second East Asia-Pasific Conference on Structural Engineering \& Construction*.

Papadopoulos, M. C. (1985). Processed chicken feathers as feedstuff for poultry and swine. A review. *Agricultural Wastes*, *14*(4), 275–290. https://doi.org/https://doi.org/10.1016/S0141-4607(85)80009-3

Perța-Crișan, S., Ursachi, C. Ștefan, Gavrilaș, S., Oancea, F., & Munteanu, F.-D. (2021). Closing the Loop with Keratin-Rich Fibrous Materials. *Polymers*, *13*(11). https://doi.org/10.3390/polym13111896

Ragavendra, S., Reddy, P. I., & Dongre, A. (2017). Fibre Reinforced Concrete- A Case Study. *33rd National Convention of Architectural Engineers and National Seminar on "Architectural Engineering Aspect for Sustainable Building Envelopes" ArchEn-BuildEn-2017, Hyderabad, India, December*, 1–16.

Rahman, M. S. (2010). Jute – A Versatile Natural Fibre. Cultivation, Extraction and Processing. In *Industrial Applications of Natural Fibres* (pp. 135–161). John Wiley & Sons, Ltd. https://doi.org/https://doi.org/10.1002/9780470660324.ch6

Ramos, E., Dj, H.-M., Camacho-Pérez, & Cruz, Q. (2019). *Degradation of Chicken Feathers: A Review*.

Reddy, N., & Yang, Y. (2007). Structure and properties of chicken feather barbs as natural protein fibers. *Journal of Polymers and the Environment*, *15*(2), 81–87. https://doi.org/10.1007/s10924-007-0054-7

Reddy, N., & Yang, Y. (2010). Light-weight polypropylene composites reinforced with whole chicken feathers. *Journal of Applied Polymer Science*, *116*(6), 3668–3675. https://doi.org/10.1002/app.31931

Rossi, P., & Chanvillard, G. (2000). *PRO 15: 5th RILEM Symposium on Fibre-Reinforced Concretes (FRC) - BEFIB' 2000*. RILEM Publications. https://books.google.com.mt/books?id=q0RkTDNDdR0C

Roulac, J. W. (1997). *Hemp horizons: the comeback of the world's most promising plant.* https://api.semanticscholar.org/CorpusID:107799708

Sahmaran, M., Yurtseven, A., & Ozgur Yaman, I. (2005). Workability of hybrid fiber reinforced self-compacting concrete. *Building and Environment*, *40*(12), 1672–1677. https://doi.org/10.1016/j.buildenv.2004.12.014

Saieh, N. (2009). *Sodra Lanken _ Rotstein Arkitekter*. ArchDaily. https://www.archdaily.com/24252/sodra-lanken-rotstein-arkitekter

Sakudo, A. (2020). Inactivation Methods for Prions. *Current Issues in Molecular Biology*, 23–32. https://doi.org/10.21775/cimb.036.023

Sapuan, S. M., Ismail, H., & Zainudin, E. S. (2018). *Natural Fibre Reinforced Vinyl Ester and Vinyl Polymer Composites*. Elsevier. https://doi.org/10.1016/C2016-0-03362-4

Selmi. (2014). Steel Fiber Curvature in Concrete Composites: Modulus Predictions Using Effective Steel Fiber Properties. *American Journal of Applied Sciences*, *11*(1), 145–151. https://doi.org/10.3844/ajassp.2014.145.151

Shafei, B., Kazemian, M., Dopko, M., & Najimi, M. (2021). State-of-the-Art Review of Capabilities and Limitations of Polymer and Glass Fibers Used for Fiber-Reinforced Concrete. *Materials*, *14*(2), 409. https://doi.org/10.3390/ma14020409

Shestakova, A., Timorshina, S., & Osmolovskiy, A. (2021). Biodegradation of Keratin-Rich Husbandry Waste as a Path to Sustainable Agriculture. *Sustainability*, *13*(16). https://doi.org/10.3390/su13168691

Stingone, J. A., & Wing, S. (2011). Poultry Litter Incineration as a Source of Energy: Reviewing the Potential for Impacts on Environmental Health and Justice. *NEW SOLUTIONS: A Journal of Environmental and Occupational Health Policy*, *21*(1), 27–42. https://doi.org/10.2190/NS.21.1.g

Sustainable Development Goals. (2015). https://sustainabledevelopment.gov.mt/sustainable-development-goals/

Sutarno, S., Rahmawati, D., Masvika, H., & Strength, F. (2021). *The Effect of Chicken Feather Waste on the Concrete Mixture on Compressive Strength and Flexural Strength*. 162–172.

Sutoyo, Subandi, Ardyati, T., & Suharjono. (2019). Screening of Keratinolytic Fungi for Biodegradation Agent of Keratin from Chicken Feather Waste. *IOP Conference Series: Earth and Environmental Science*, *391*(1). https://doi.org/10.1088/1755-1315/391/1/012027

Suttie, J. M., & Food and Agriculture Organization of the United Nations. (2000). *Hay and Straw Conservation: For Small-scale Farming and Pastoral Conditions*. Food and Agriculture Organization of the United Nations. https://books.google.com.mt/books?id=ZYcDhblVEssC

Tamreihao, K., Mukherjee, S., Khunjamayum, R., Devi, L. J., Asem, R. S., & Ningthoujam, D. S. (2019). Feather degradation by keratinolytic bacteria and biofertilizing potential for sustainable agricultural production. *Journal of Basic Microbiology*, *59*(1), 4–13. https://doi.org/10.1002/jobm.201800434

Tesfaye, T., Sithole, B., & Ramjugernath, D. (2017). Valorisation of chicken feathers: a review on recycling and recovery route—current status and future prospects. *Clean Technologies and Environmental Policy*, *19*(10), 2363–2378. https://doi.org/10.1007/s10098-017-1443-9

Tesfaye, T., Sithole, B., Ramjugernath, D., & Mokhothu, T. (2018). Valorisation of chicken feathers: Characterisation of thermal, mechanical and electrical properties. *Sustainable Chemistry and Pharmacy*, *9*, 27–34. https://doi.org/10.1016/j.scp.2018.05.003

The Concrete Society. (2013). Concrete industrial ground floors. In *Concrete Society Technical Report* (Vol. 29, Issue 1).

Ullah, A., Vasanthan, T., Bressler, D., Elias, A. L., & Wu, J. (2011). Bioplastics from feather quill. *Biomacromolecules*, *12*(10), 3826–3832. https://doi.org/10.1021/bm201112n

United Nations. (2020). Goals @ Sdgs.Un.Org. In *United Nations Sustainable Development Goals*. https://sdgs.un.org/goals

Univerisy of Malta. (2022). *Gender+ Equity Plan Action plan for equity , diversity and inclusion at UM*. https://www.um.edu.mt/media/um/docs/about/equity/GenderEquityPlan-UM.pdf

Vella, A. (2018). *The Fresh Properties and Early Age Performance of Waste-Tyre Fibre Reinforced Self-Compacting Concrete* (Issue January). University of Malta.

Vineis, C., Varesano, A., Varchi, G., & Aluigi, A. (2019). Extraction and Characterization of Keratin from Different Biomasses. In S. Sharma & A. Kumar (Eds.), *Keratin as a Protein Biopolymer: Extraction from Waste Biomass and Applications* (pp. 35–76). Springer International Publishing. https://doi.org/10.1007/978-3-030-02901-2_3

Vinodh Kumar, S., Prasanth, K., Prashanth, M., Prithivirajan, S., & Anil Kumar, P. (2021). Investigation on mechanical properties of chicken feather fibers reinforced polymeric composites. *Materials Today: Proceedings*, *37*, 3767–3770. https://doi.org/10.1016/j.matpr.2020.10.877

Wahab, E. S. A., & Osmi, S. F. C. (2012). Mechanical properties of concrete added with chicken rachis as reinforcement. *Applied Mechanics and Materials*, *147*, 37–41. https://doi.org/10.4028/www.scientific.net/AMM.147.37

Wang, Z. Z., & Supartono, F. X. (2011). Defects of Conventional Concrete and Developments of Self Compacting Concrete along with its Applications. *Advanced Materials Research*, *250–253*, 761–764. https://doi.org/10.4028/www.scientific.net/AMR.250-253.761

Wehbe, N., & Stripling, C. (2009). *Structural Performance of Prestressed Self-Consolidating Concrete Bridge Girders Made with Limestone Aggregates*. *October*.

Yurugi, M., Sakata, N., Iwai, M., & Sakai, G. (2000). Mix proportion for highly workable concrete. *Proceedings of Concrete*, 579–589.

Zhan, M., & Wool, R. P. (2011). Mechanical properties of chicken feather fibers. *Polymer Composites*, *32*(6), 937–944. https://doi.org/10.1002/pc.21112

Zhang, N., Zuo, W., Xu, W., & Song, S. (2020). A New Approach for Designing Fluid Concrete with Low Cement Content: Optimization of Packing Density of Aggregates. *Materials*, *13*(18), 4082. https://doi.org/10.3390/ma13184082

Zheng, Z., & Feldman, D. (1995). Synthetic fibre-reinforced concrete. *Progress in Polymer Science*, *20*(2), 185–210. https://doi.org/10.1016/0079-6700(94)00030-6

Appendix A

Poultry Production Process

The Poultry Production Process

***Content Warning**: This text includes an in-depth description of the slaughtering and processing of chickens.*

The information for this report was gathered during a site visit and interview with Mr Paul Spiteri on site on the 2nd of February, 2023. Mr Spiteri noted that SMINA Poultry Products Ltd produces around 55-65% of poultry produced in Malta.

SMINA Poultry Products Ltd is a local poultry processing plant in Fawwara (Siġġiewi), Malta, which slaughters around 7,000 chickens per night, 5 nights a week[1]. The company employs around 60 people and is run by the Spiteri family, and there is always a veterinary doctor present on site during hours of processing, monitoring quality of chickens and the processing. The plant receives live chickens at around 6pm, begin their slaughter at 7pm and continue overnight until around 11am the next morning, where the plant is thoroughly cleaned and disinfected for the next slaughter. The process is mostly done using modern equipment and machinery, which is organised in Table 1, taken from the record files at SMINA referenced in Figure 1.

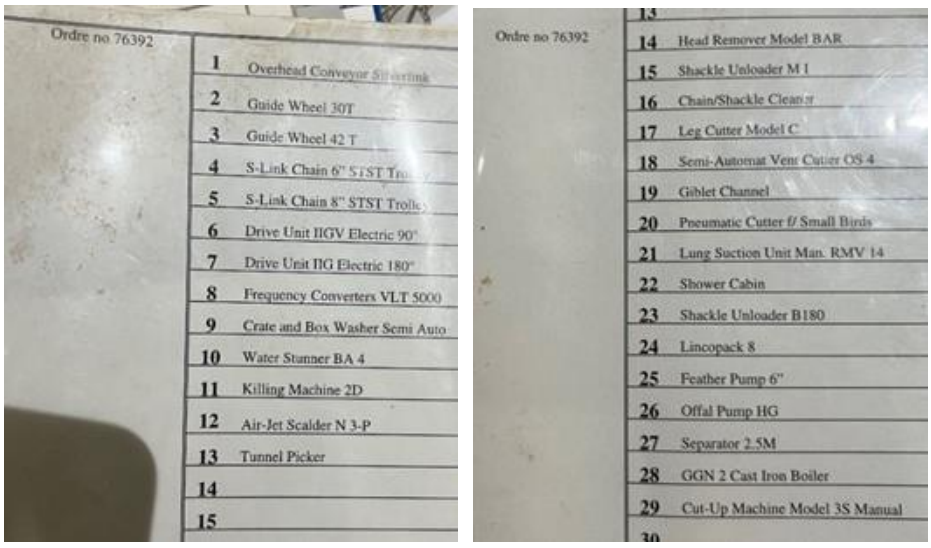

Figure 1 - List of machinery being used at the processing plant.

[1] Legal Notice 260 of 2003 outlines the "Animal Slaughter or Killing (Protection) Regulations" as a Subsidiary Legislation 439.03 (of the Animal Welfare Act).

Table 1 - List of equipment and machinery at SMINA.

#	*Name*	*Processing Process*
1.	Overhead Conveyor Silverlink	
2.	Guide Wheel 30 T	
3.	Guide Wheel 42 T	
4.	S-Link Chain 6" STST Trolley	To operate the chain belt throughout the plant.
5.	S-Link Chain 8" STST Trolley	
6.	Drive Unit IIGV Electric 90°	
7.	Drive Unit IIG Electric 180°	
8.	Frequency Converters VLT 5000	
9.	Crate and Box Washer Semi Auto	To wash used crates and boxes.
10.	Water Stunner BA 4	To stun live chickens before slaughter.
11.	Killing Machine 2D	To cut the throats to slaughter the chicken.
12.	Air-Jet Scalder N 3-P	To facilitate the process of feather removal.
13.	Tunnel Picker	To remove feathers without damaging skin.
14.	Head Remover Model BAR	To remove the heads.
15.	Shackle Unloader M I	To remove the chickens from the chain.
16.	Chain/Shackle Cleaner	To clean the chain and shackles.
17.	Leg Cutter Model C	To cut the chicken feet off.
18.	Semi-Automat Vent Cutter OS 4	To remove the cloaca of the chicken.
19.	Giblet Channel	To remove the giblets.
20.	Pneumatic Cutter f/ Small Birds	To cut the chicken necks off.
21.	Lung Suction Unit Man. RMV 14	To remove the lungs.
22.	Shower Cabin	To wash and refrigerate the chickens.
23.	Shackle Unloader B 180	To remove the chickens from the chain.

24.	Lincopack 8	To pack and seal chickens or chicken parts.
25.	Feather Pump 6"	To separate solid waste from wastewater.
26.	Offal Pump HG	To transport offal to the separator.
27.	Separator 2.5M	To separate solid waste from wastewater.
28.	GGN 2 Cast Iron Boiler	To heat the water for the scalder.
29.	Cut-Up Machine Model 3S Manual	To cut and portion chickens and parts.

The chickens arrive in crates which usually hold exactly ten chickens, each as can be seen in Figure 2, unless they are particularly large, where they can only hold eight chickens.

Figure 2 - Chickens ready for slaughter as they arrive in blue crates.

The chickens are unloaded from the crated and hung upside-down, by hand, on a motorised chain which will take them into the processing plant. The chain (Figure 3) runs through the entire plant and is motorised by two separate motors. Both motors each have a 1HP electric engine. Once they are hung, they begin their journey through the plant.

Figure 3 - Chain where chickens are hung upside-down to enter the plant.

Once they enter the processing plant, the chickens pass through the first machine where are given a small electric shock to stun them, shown in Figure 4. The shock given is small enough to stun them, but weak enough so that the chicken can wake up and walk around within 30 seconds. This is done in order to conform to Halal meat processing standards. The shock is said to confuse the chickens for when their necks are slit, to ensure a more humane slaughter.

Figure 4 - Water Stunner BA4 where the chickens are stunned.

Once they receive the electric shock, their throats are then slit in order to begin draining their blood. The blood is collected in a through beneath the chain, until the blood is completely drained from the chicken. The troughs which collect the blood are shown in Figure 5.

Figure 5 - Stainless steel troughs where blood is collected.

In order to remove the feathers from the chicken without damaging the skin or extremities, the feather removal process is done in two parts. The first part consists of passing the chickens along hot water jets, where water at 50°C-60°C scalds the chicken, allowing for easier and faster feather removal. This machine is shown in Figure 6. The next machine consists of rotating machine heads with rubber fingers, shown in Figure 6, which turn and defeathers the chickens as they pass through.

Figure 6 - (right) Scalder to facilitate feather removal (left) Tunnel picker to remove the feathers.

The defeathered chickens then continue along the chain where their heads are pulled for removal. There is a steel hoop, shown in Figure 7, is mounted below the chain where the hung chicken will pass, allowing the head to be removed. The heads are then transported outside for disposal.

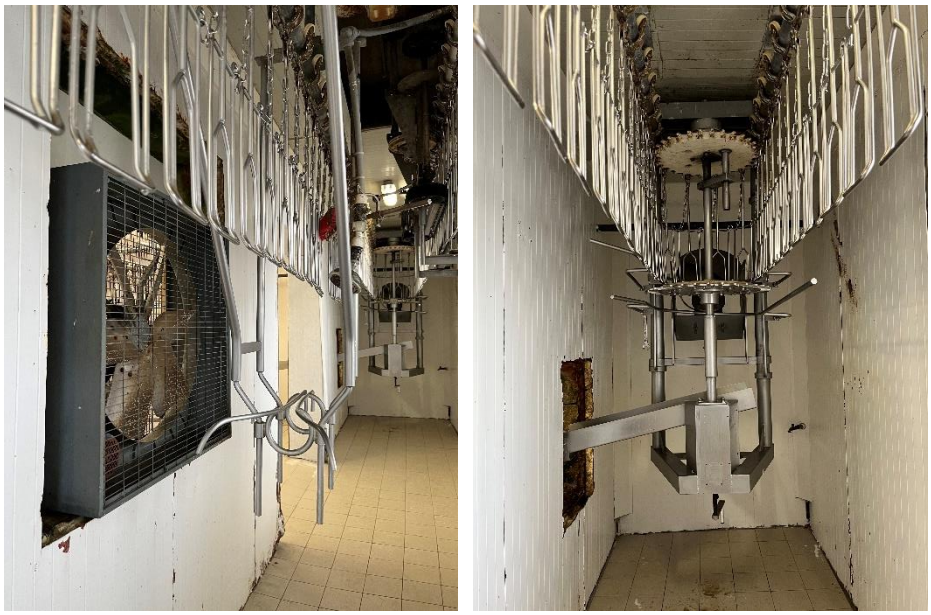

Figure 7 - (right) Suspended head remover (left) Leg cutter.

Following the removal of the heads, the feet are then removed mechanically. The chickens pass through a suspended cutter, shown in Figure 7, where blades slice the feet from the rest of the chicken. The feet are then transported outside for disposal.

The chain continues to the next room where the necks are cut manually using a cutter with a pneumatic mechanism. The necks are sometimes sold, usually during winter, as they are used to make broth, but in summer, due to lack of consumer demand, they are often disposed of with the rest of the waste material.

Once the extremities are removed from the chicken, the remaining parts to be removed are the organs. These are removed using a series of machinery, shown in Figure 8, to remove the lungs, intestines, and the heart. The giblets (hearts and livers) are sometimes sold, but not always, depending on consumer demand. The rest of the intestines are also transported out of the plant for disposal. This part of the plant involves the most human labour, and plans to introduce automatic machinery are being considered, however, due to their costly nature (approx. €500,000) these will not be upgraded for the time being.

Figure 8 - Removal of internal organs, mostly manually operated.

At this point, all that is left is a whole chicken which is washed and passed along a conveyor chain, shown in Figure 9, to a refrigerator room for 1 hour and 15 minutes at

4°C, shown in Figure 9, to ensure all bacteria is dormant before beginning the packaging process. This process is necessary to maintain proper health and safety standards. Once the chickens have spent the allocated time in the refrigerator room, they then exit the room on the same chain where they are then sorted for processing.

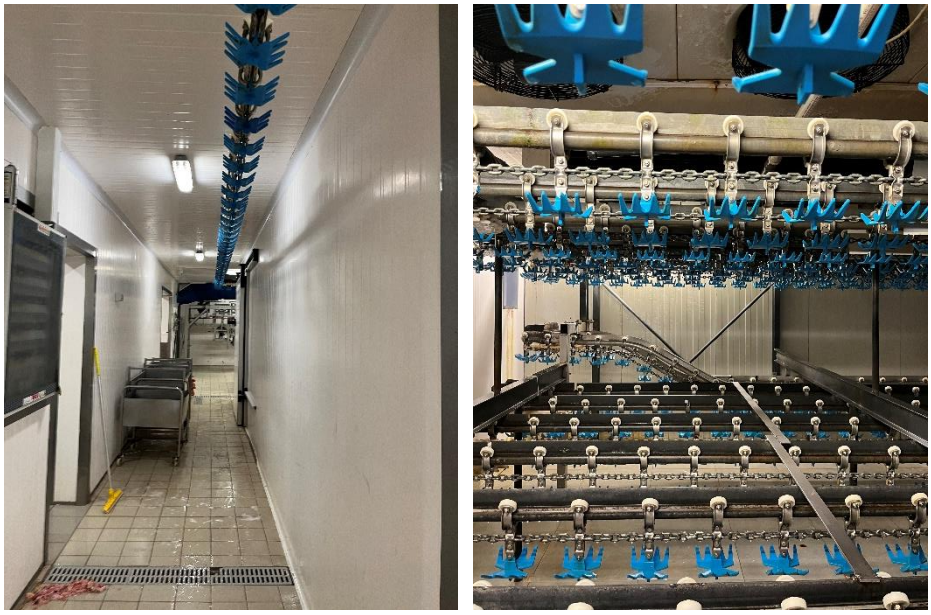

Figure 9 - (right) Conveyer chain to the refrigerator room (left) Refrigerator room where the chickens spend 1h 15min to chill at 4°C.

The sorting of chickens is the step where the chickens are then divided into those which will be sold as whole chickens, and those which will be cut into parts (breasts, legs, drumsticks, wings, or thighs). The amount of each is dependent on the orders received for the next day.

There are two dedicated machines at this stage, the first of which, shown in Figure 10, is used to sort the chickens to be sold as whole chickens by their weight. The chickens pass over a conveyer belt which has been calibrated to sort the chickens by size in four separate bins, depending on the orders for the morning. The second machine, shown in Figure 10, is used to cut the chicken into pieces which are then transported to be packed, again depending on the orders for the following morning.

Figure 10 - (right) Conveyer belt which sorts the chicken by weight into four bins (left) Machine which cuts the chicken into parts by order.

Once the poultry has been produced according to the orders, they are packed in order to be sent out for delivery. Packaging is mostly done manually, and is done in a dedicated room until they are loaded into trucks for delivery.

Figure 11 - (right) Collected waste is pumped up to the drum (left) Drum which empties solids into the large plastic bin.

On the back end, the waste accumulated from the process is collected outside and then pumped into a large drum. The pump is the largest engine on the facility, rating at 15HP and shown in Figure 3.6. The drum, also shown in Figure 3.6, is used to separate the solids from the wastewater and is powered by an engine with a rating of approximately 1.1-1.2HP. The wastewater is treated and disposed, while the mixed waste solids are dumped into large reusable plastic bins, which are transported to the WasteServ Thermal Treatment Facility (TTF) in Marsa. The TTF is 8.6km away, and each truck can carry up to six bins. Approximating from the receipt given by WasteServ, shown in Figure 1.4, each delivery contains between 3,500-4,500 tonnes of waste.

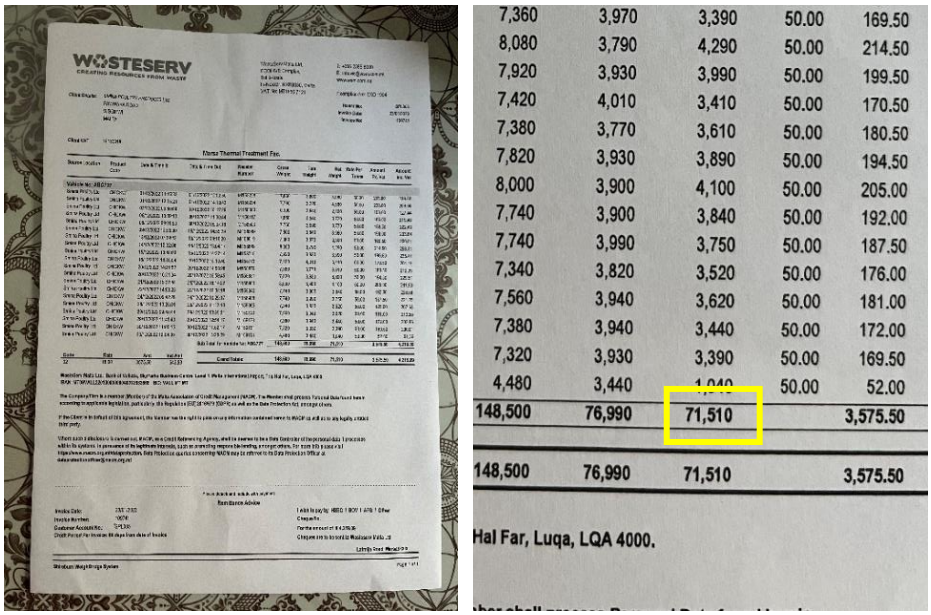

Figure 12 - Receipt from WasteServ for December 2022.

Appendix B

Risk Assessment

Occupational Health and Safety Risk Assessment

Location:

Rural Sciences Farmhouse, CP6

Built Environment Laboratory

Process:

Handling of feathers and mix with cement and other additives

UNIVERSITY OF MALTA

OCCUPATIONAL
HEALTH & SAFETY SERVICES

Office 4/5,
Porta Cabins B,
CP6, Msida MSD2080
Tel: 2340 2993
Email:
louis.coleiro@um.edu.mt

Preface

This report is compiled on good faith that the relevant and correct information was forwarded to the undersigned. The assessor disassociates himself from any risks that may arise from any information about any work or situation that was concealed and not forwarded during this assessment.

In compiling this report the assessor has relied on information provided for its accuracy and completeness in forming an opinion and has taken steps to verify it, were possible.

This report gives an opinion in respect to certain potential risk exposures, the quality of the control measures in place and also makes recommendations to minimise the risks. While implementing these recommendations will reduce the risk, an element of residual risk shall remain and therefore other actions through Task risk assessments or Method Statements may still be necessary as this is a generic risk assessment report.

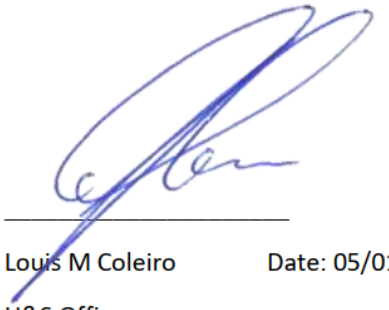

Louis M Coleiro Date: 05/01/2023

H&S Officer

Louis M. Coleiro Email: louis.coleiro@um.edu.mt Mob: +356 79711262

Risk Assessments & Method Statements

It is the responsibility of the Researchers to carry out suitable and sufficient risk assessments of all the occupational hazards which may arise at due to the work / research activity and place of work.

Such assessments shall consider the risks to the health and safety of the hands on person/s who are exposed whilst on the job, as well as to the health and safety of those persons who may be affected due to the works being carried out.

The researchers shall ensure that this risk assessment is kept updated to reflect the current state of the work. Whenever changes to the work activities and equipment occur, or whenever there are sufficient reasons to declare that the risks assessment is no longer relevant, it has to be reviewed and updated. It is the responsibility of the Researchers to consider and implement all recommendations and to prepare specific standard operational procedure/s as necessary.

The findings and observations are based on the requirements of current legislation and good practise. It is imperative that there is identification of the hazards and actions are taken accordingly by the establishment executing the work to mitigate the arising risks.

Definitions

Hazards: anything arising out of an activity/work that can cause harm

Systematic: following a logical and defined methodology.

Sufficient: develop prioritised measures to improve the occupational conditions according to the hierarchy of prevention

Suitable: taking in consideration the severity of the hazards well known in the respective area of work activities

Louis M. Coleiro Email: louis.coleiro@um.edu.mt Mob: +356 79711262

General Overview

The process being assessed undertakes the following steps:

1. Handling of feathers originating from a disease free facility, in double bags for transportation
2. The amounts that are handle are in low quantities since these are for research purposes
3. Storage in a purposely built freezer until used
4. Disinfected further within a laminar flow cabinet
5. Use of chemicals to carry out disinfection or disinfectant with water according to requirements
6. Dried in a ventilated oven at 80°C when disinfected with disinfectant and water
7. Air dried when chemically disinfected within the laminar flow cabinet.
8. Handled to mix with cement and its additives
9. Use of concrete mixer for the final mix with concrete mix
10. Through the whole process gloves, respiratory and eye protection and laboratory coat are being used.

Overview of Risk

The process is of very low risk nature once the required precautions are taken.

Louis M. Coleiro Email: louis.coleiro@um.edu.mt Mob: +356 79711262

Risk Assessment

Risk Rating

LIKELIHOOD	
FREQUENT	**Occurs frequently (repeatedly) due to process or activity, can be expected to happen**
LIKELY	**Can happen due to nature of work if the right measures are not taken**
OCCASIONAL	**Can happen possible**
UNLIKELY	**Unlikely to happen once the right procedures are followed**
VERY UNLIKELY	**Based on control, it is unlikely that it may occur**

CONSEQUENCE	
CATASTROPHE	**Life threatening bodily damages, loss of life, explosion, fire. Loss of property leading to liquidation**
MAJOR	**Amputations, major fractures, internal organs damage, multiple injuries**
MODERATE	**Lacerations, burns, concussion, serious sprains, minor fractures, hearing damage, skin conditions, ill health, small fire, property damage**
MINOR	**Slight property damage, minor injuries that keep a worker out of work for a minimum of 3 working days.**
INSIGNIFICANT	**Superficial injuries, minor cuts etc… nuisance, discomfort, minimal property damage**

Louis M. Coleiro Email: louis.coleiro@um.edu.mt Mob: +356 79711262

Risk Evaluation Matrix						
SEVERITY	Catastrophe 5	5	10	15	20	25
	Major 4	4	8	12	16	20
	Moderate 3	3	6	9	12	15
	Minor 2	2	4	6	8	10
	Insignificant 1	1	2	3	4	5
	VERY HIGH	1	2	3	4	5
	HIGH	VERY UNLIKELY	UNLIKELY	OCCASIONAL	LIKELY	FREQUENT
	MEDIUM	LIKELIHOOD				
	LOW					
	VERY LOW					

RISK LEVEL	
VERY HIGH	Work should not be started or continued as the risk cannot be reduced to acceptable levels or eliminated, even if considerable resources are spent.
HIGH	Work should not be started until the risk is mitigated. Considerable amount of resources may have to be used to reduce the risk
MEDIUM	Urgently needs attention to reduce risk as can become more serious if unattended within a specified time.
LOW	The risk can be reduced by means of a safe system of work as well as implementing a set of controls. Monitoring required.
VERY LOW	The risk can be mitigated by means of administrative measures and the use of PPE. Minimal action required that can be included in the work procedure

Louis M. Coleiro Email: louis.coleiro@um.edu.mt Mob: +356 79711262

No	Activity	Hazard	Result	Findings	likelihood	Severity	Risk level	Measures to be adopted
01	Handling of feathers	Feathers	Skin, eye and respiratory sensitization	Feathers originating from chicken that are certified disease free before being processed. The feathers that are already treated at the originating facility are double bagged for transportation. During disinfection treatment eye, skin and respiratory protection are used.	1	1	1 VL	It is important that during the disinfection and drying processes the presently used protective equipment is used. Additionally all surfaces are to be cleaned once the process is over.
02	Disinfection process	Chemicals	Skin, eye & respiratory irritation	The chemicals used for disinfection are the following: • Regular off the shelf disinfectant • Ethanol (70%) • Hypochlorite (10%) The required PPE is available	2	2	4 L	To enforce the use of the required PPE.
03	Disinfection process	Electricity / inefficient laminar flow cabinet	Electric shock / eye, skin & respiratory irritation	The laminar flow cabinet was checked with an anemometer and the results produced were well over 0.5m/s (air speed) i.e. Average of 0.76m/s.	2	2	4 L	Always keep filters up to date.

Louis M. Coleiro Email: louis.coleiro@um.edu.mt Mob: +356 79711262

No	Activity	Hazard	Result	Findings	likelihood	Severity	Risk level	Measures to be adopted
04	Drying - Use of ventilated oven	Electricity / hot surfaces	Electric shock / skin burn	The ventilated oven being used visibly is in good condition.	1	3	3 VL	Make sure that user carry out a visual inspection before use. Make sure that all the required signs are in place indicating the hot surfaces.
05	Mixing with cement and additives	Air borne cement dust and other additives	Respiratory and eye irritation / skin irritation	The required PPE is available	2	2	4 L	Enforce the use of the required PPE
06	Use of concrete mixer	Rotating parts	Entanglement	The mixer being used is visibly in good condition and well maintained.	2	3	6 L	Important the lab officer is always supervising the student/ researcher whilst using this equipment.
07	Process is over	Residue	Skin irritation	Cleaning after use of surfaces with disinfectant	1	2	2 VL	Enforce that such action is taken all the times; benches or any other surface require such procedure.

Safety data sheets are to be available on location where chemicals are used.

Louis M. Coleiro Email: louis.coleiro@um.edu.mt Mob: +356 79711262

Appendix C

Data Collection

Fibre Characterisation and Statistical Analysis

Sample	Length	Ø 1	Ø 2	Ø 3	Average Ø
#	*mm*	*mm*	*mm*	*mm*	*mm*
1	152.00	2.42	1.20	0.23	1.28
20	99.00	1.19	0.75	0.06	0.67
40	78.00	0.88	0.43	0.05	0.45
60	70.00	0.64	0.17	0.03	0.28
80	66.00	0.66	0.22	0.06	0.31
100	63.00	0.42	0.11	0.07	0.20
120	60.00	0.24	0.11	0.11	0.15
140	56.00	0.55	0.18	0.03	0.25
160	55.00	0.60	0.17	0.06	0.28
180	54.00	0.33	0.10	0.06	0.16
200	50.00	0.92	0.11	0.06	0.36
220	45.00	0.51	0.19	0.03	0.24
240	43.00	0.36	0.13	0.05	0.18
260	39.00	0.24	0.17	0.10	0.17
280	35.00	0.63	0.16	0.06	0.28
300	34.00	0.02	0.01	0.01	0.01
320	31.00	0.25	0.11	0.02	0.13
340	30.00	0.28	0.10	0.04	0.14
360	28.00	0.43	0.09	0.02	0.18
380	23.00	0.46	0.25	0.06	0.26
400	12.00	0.14	0.06	0.05	0.08

Statistical Analysis on 2 sets of 200 Feather Fibres at Different Ages (36 days and 41 days)

Group Statistics

	Days	N	Mean	Std. Deviation	Std. Error Mean
Length	36 days	200	62.7800	23.93084	1.69217
	41 days	200	51.7315	25.30456	1.78930

Group Statistics

				Bootstrap [a]			
					Std.	95% Confidence Interval	
	Days		Statistic	Bias	Error	Lower	Upper
Length	36 days	N	200				
		Mean	62.7800	-.0888	1.6922	59.3026	66.1815
		Std. Deviation	23.93084	-.11517	1.79266	20.22166	27.10505
		Std. Error Mean	1.69217				
	41 days	N	200				
		Mean	51.7315	-.0049	1.9022	48.1639	55.5101
		Std. Deviation	25.30456	-.18122	2.44208	20.73709	29.98623
		Std. Error Mean	1.78930				

a. Unless otherwise noted, bootstrap results are based on 400 bootstrap samples

Bootstrap Specifications

Sampling Method	Simple
Number of Samples	400
Confidence Interval Level	95.0%
Confidence Interval Type	Percentile

Group Statistics

	Days	N	Mean	Std. Deviation	Std. Error Mean
Length	36 days	200	62.7800	23.93084	1.69217
	41 days	200	51.7315	25.30456	1.78930
Thickness 1 (mm)	36 days	200	.7491	.46789	.03308
	41 days	200	.5586	.42160	.02981
Thickness 2 (mm)	36 days	200	.2445	.23488	.01661
	41 days	200	.1996	.21149	.01495
Thickness 3 (mm)	36 days	200	.0865	.08486	.00600
	41 days	200	.0506	.04318	.00305
Average Thickness (mm)	36 days	200	.3603	.24634	.01742
	41 days	200	.2694	.21697	.01534

Independent Samples Effect Sizes

				95% Confidence Interval	
		Standardizer [a]	Point Estimate	Lower	Upper
Length	Cohen's d	24.62728	.449	.250	.647
	Hedges' correction	24.67381	.448	.249	.646
	Glass's delta	25.30456	.437	.235	.637

a. The denominator used in estimating the effect sizes.

Cohen's d uses the pooled standard deviation.

Hedges' correction uses the pooled standard deviation, plus a correction factor.

Glass's delta uses the sample standard deviation of the control group.

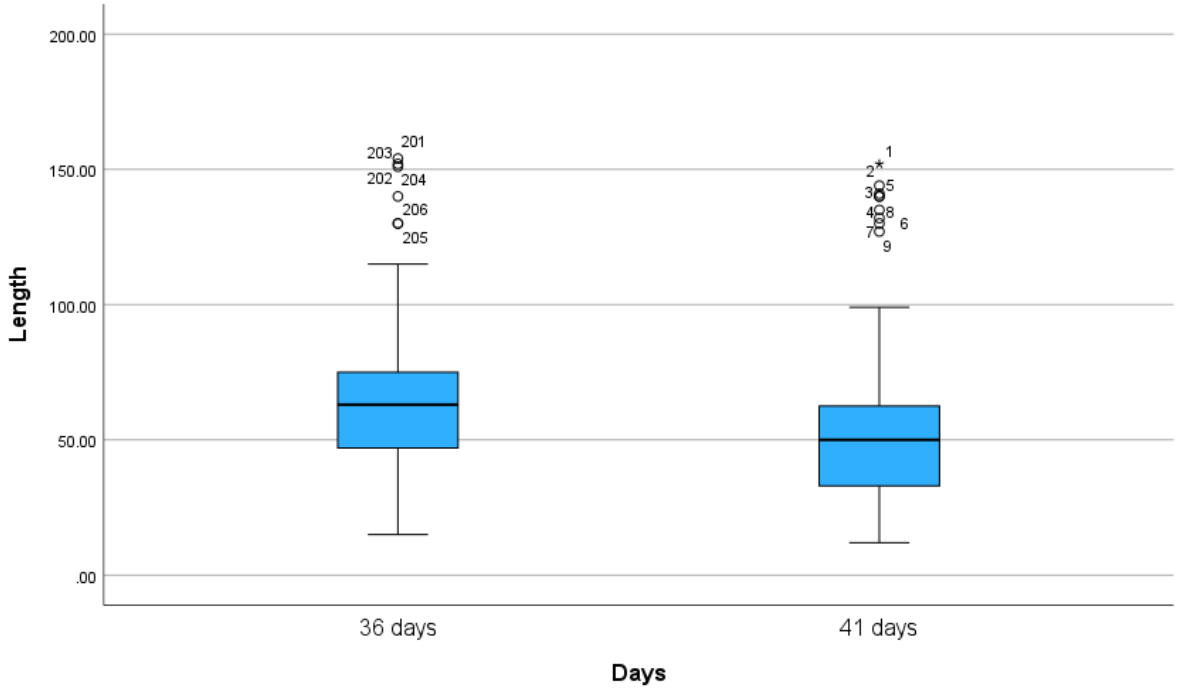
200.00
150.00
100.00
50.00
.00
Length
36 days
41 days
Days

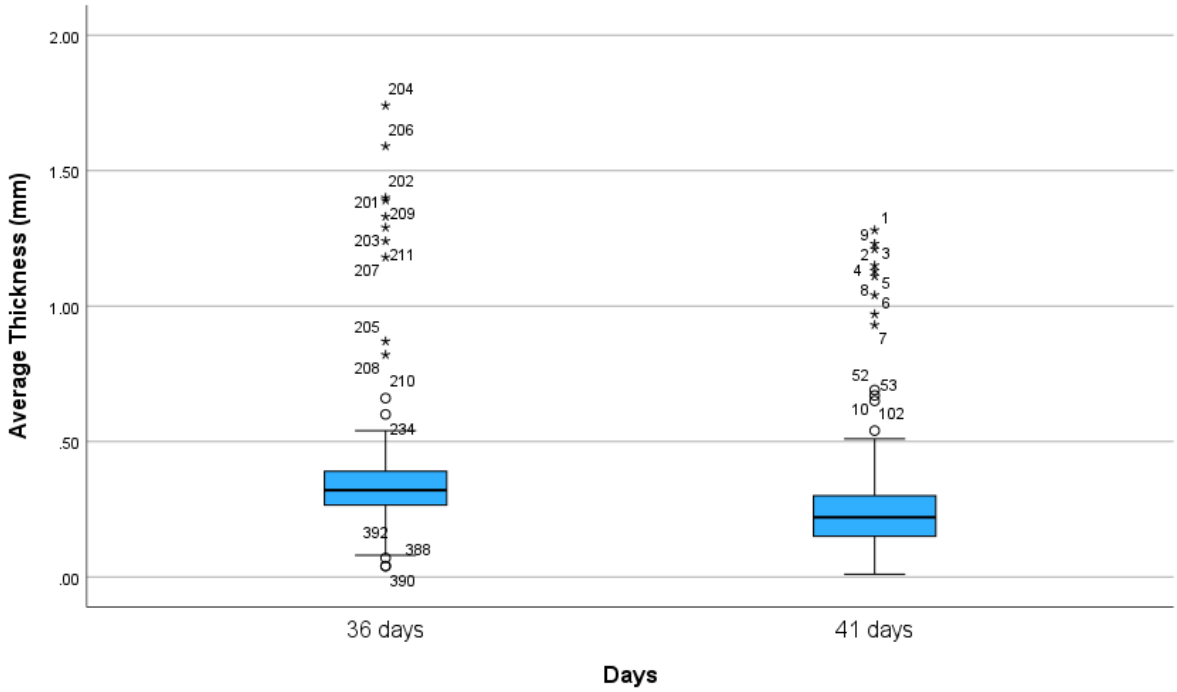
2.00
1.50
1.00
.50
.00
Average Thickness (mm)
36 days
41 days
Days

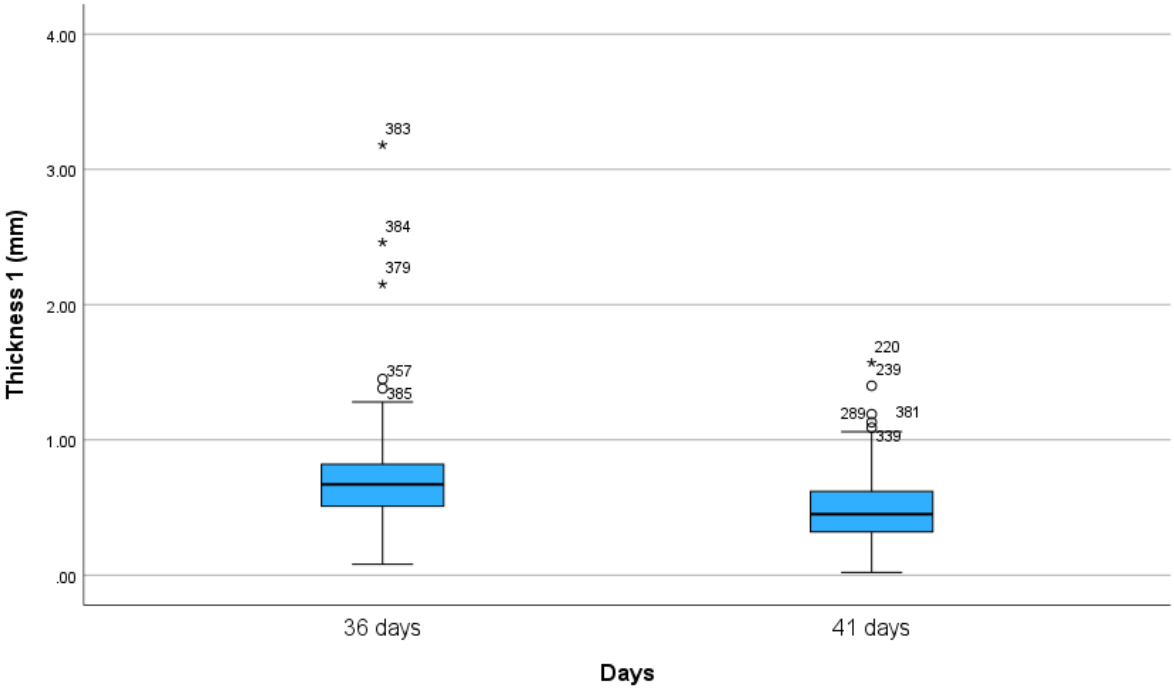
Thickness 1 (mm)
4.00
3.00
2.00
1.00
.00
383
384
379
357
385
220
239
289
381
339
36 days
41 days
Days

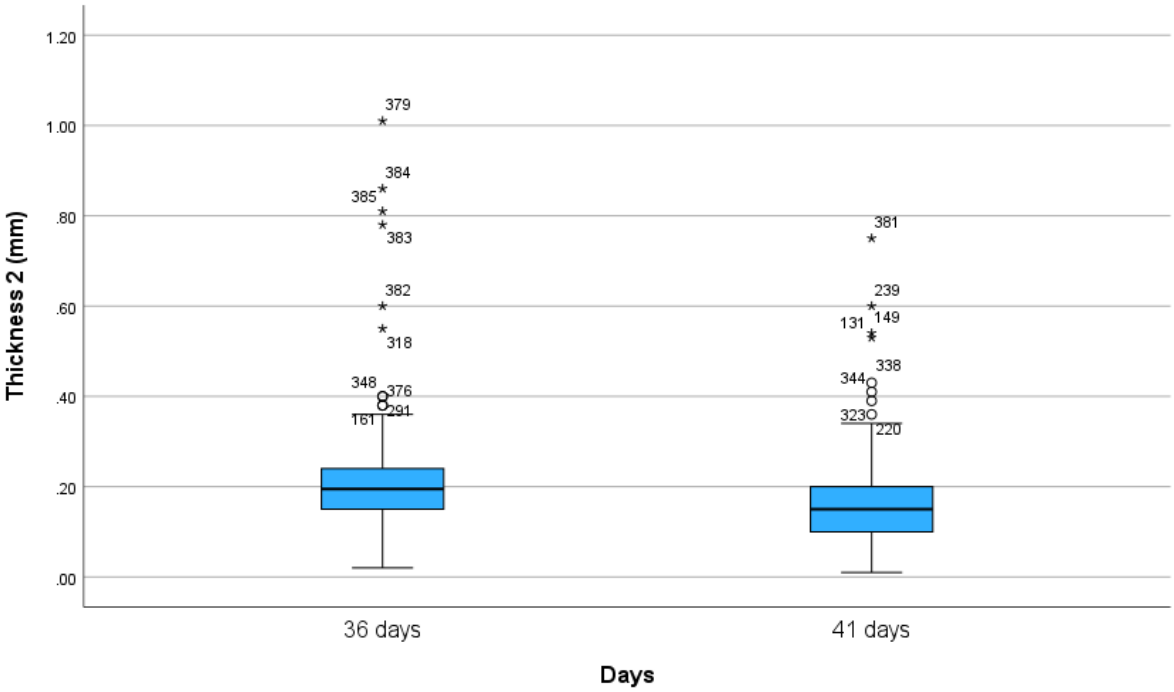
Thickness 2 (mm)
1.20
1.00
.80
.60
.40
.20
.00
379
384
385
383
382
318
348
376
291
161
381
239
131
149
338
344
323
220
36 days
41 days
Days

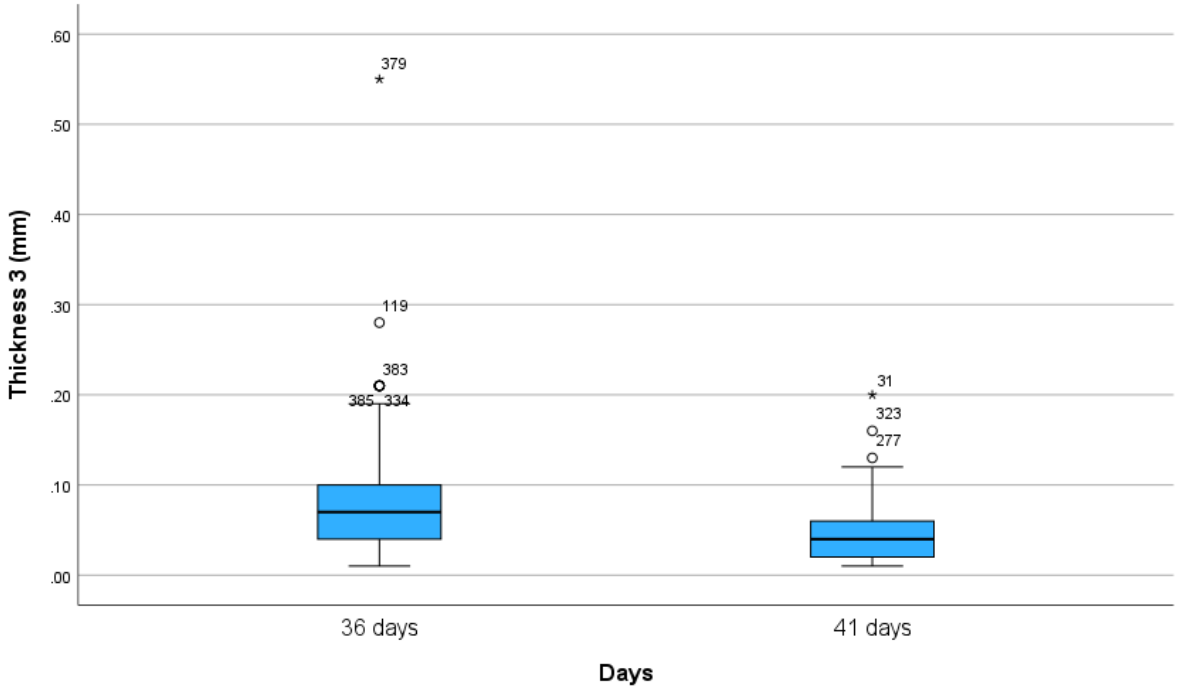

Case Processing Summary

		Cases					
		Valid		Missing		Total	
	Days	N	Percent	N	Percent	N	Percent
Length	36 days	200	100.0%	0	0.0%	200	100.0%
	41 days	200	100.0%	0	0.0%	200	100.0%
Average Thickness (mm)	36 days	200	100.0%	0	0.0%	200	100.0%
	41 days	200	100.0%	0	0.0%	200	100.0%

Correlations

		Length 36 days	Length 41 days
Length 36 days	Pearson Correlation	1	.978**
	Sig. (2-tailed)		<.001
	N	200	200
Length 41 days	Pearson Correlation	.978**	1
	Sig. (2-tailed)	<.001	
	N	200	200

**. Correlation is significant at the 0.01 level (2-tailed).

Correlations

			Length 36 days	Length 41 days
Kendall's tau_b	Length 36 days	Correlation Coefficient	1.000	.985**
		Sig. (2-tailed)	.	<.001
		N	200	200
	Length 41 days	Correlation Coefficient	.985**	1.000
		Sig. (2-tailed)	<.001	.
		N	200	200
Spearman's rho	Length 36 days	Correlation Coefficient	1.000	.998**
		Sig. (2-tailed)	.	<.001
		N	200	200
	Length 41 days	Correlation Coefficient	.998**	1.000
		Sig. (2-tailed)	<.001	.
		N	200	200

**. Correlation is significant at the 0.01 level (2-tailed).

Descriptives

	Days			Statistic	Std. Error
Length	36 days	Mean		62.7800	1.69217
		95% Confidence Interval for Mean	Lower Bound	59.4431	
			Upper Bound	66.1169	
		5% Trimmed Mean		61.3611	
		Median		63.0000	
		Variance		572.685	
		Std. Deviation		23.93084	
		Minimum		15.00	
		Maximum		154.00	
		Range		139.00	
		Interquartile Range		28.00	
		Skewness		.950	.172
		Kurtosis		2.510	.342
	41 days	Mean		51.7315	1.78930
		95% Confidence Interval for Mean	Lower Bound	48.2030	
			Upper Bound	55.2599	
		5% Trimmed Mean		49.0738	
		Median		50.0000	
		Variance		640.321	
		Std. Deviation		25.30456	
		Minimum		12.00	
		Maximum		152.00	
		Range		140.00	
		Interquartile Range		29.75	
		Skewness		1.681	.172
		Kurtosis		4.031	.342

Descriptives

	Days			Statistic	Std. Error
Average Thickness (mm)	36 days	Mean		.3603	.01742
		95% Confidence Interval for Mean	Lower Bound	.3259	
			Upper Bound	.3946	
		5% Trimmed Mean		.3241	
		Median		.3200	
		Variance		.061	
		Std. Deviation		.24634	
		Minimum		.04	
		Maximum		1.74	
		Range		1.70	
		Interquartile Range		.13	
		Skewness		3.227	.172
		Kurtosis		12.601	.342
	41 days	Mean		.2694	.01534
		95% Confidence Interval for Mean	Lower Bound	.2391	
			Upper Bound	.2997	
		5% Trimmed Mean		.2370	
		Median		.2200	
		Variance		.047	
		Std. Deviation		.21697	
		Minimum		.01	
		Maximum		1.28	
		Range		1.27	
		Interquartile Range		.15	
		Skewness		2.868	.172
		Kurtosis		9.241	.342

Extreme Values

	Days			Case Number	Value
Length	36 days	Highest	1	201	154.00
			2	202	152.00
			3	203	151.00
			4	204	140.00
			5	205	130.00[a]
		Lowest	1	400	15.00
			2	399	18.00
			3	398	19.00
			4	397	20.00
			5	396	20.00
	41 days	Highest	1	1	152.00
			2	2	144.00
			3	3	141.00
			4	4	140.00
			5	5	140.00
		Lowest	1	200	12.00
			2	199	15.00
			3	198	15.00
			4	197	16.00
			5	196	18.00[b]

a. Only a partial list of cases with the value 130.00 are shown in the table of upper extremes.

b. Only a partial list of cases with the value 18.00 are shown in the table of lower extremes.

Extreme Values

	Days			Case Number	Value
Average Thickness (mm)	36 days	Highest	1	204	1.74
			2	206	1.59
			3	202	1.40
			4	209	1.39
			5	201	1.33
		Lowest	1	390	.04
			2	388	.04
			3	392	.07
			4	375	.08
			5	373	.09
	41 days	Highest	1	1	1.28
			2	2	1.23
			3	9	1.21
			4	3	1.15
			5	4	1.13
		Lowest	1	149	.01
			2	174	.02
			3	193	.03
			4	199	.05
			5	197	.05

Statistical Analysis on 400 measured Feather Fibre Lengths

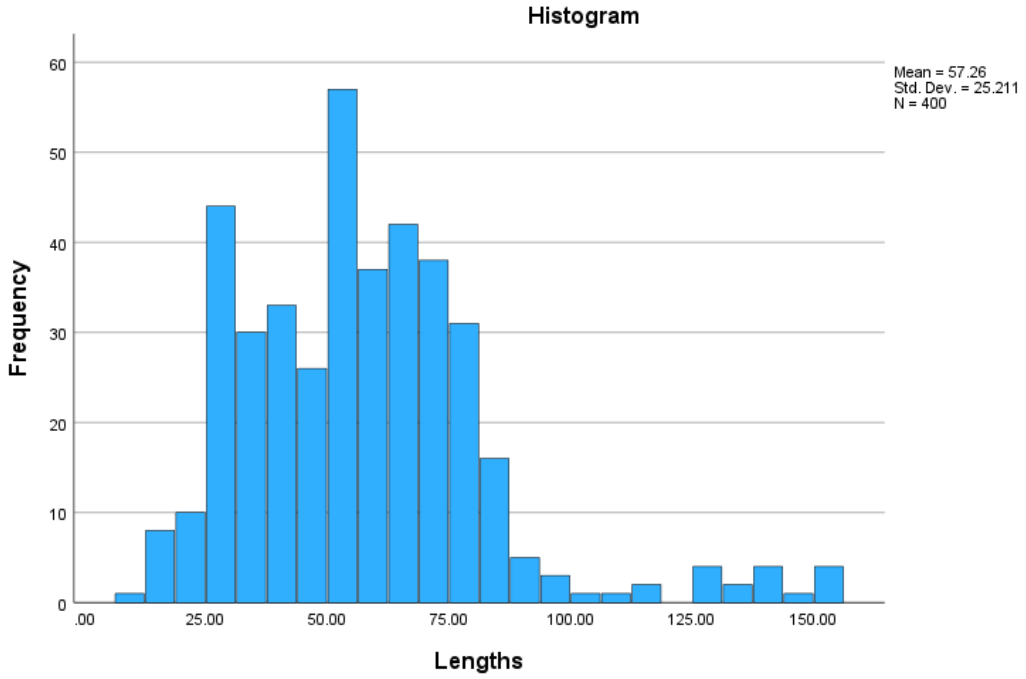

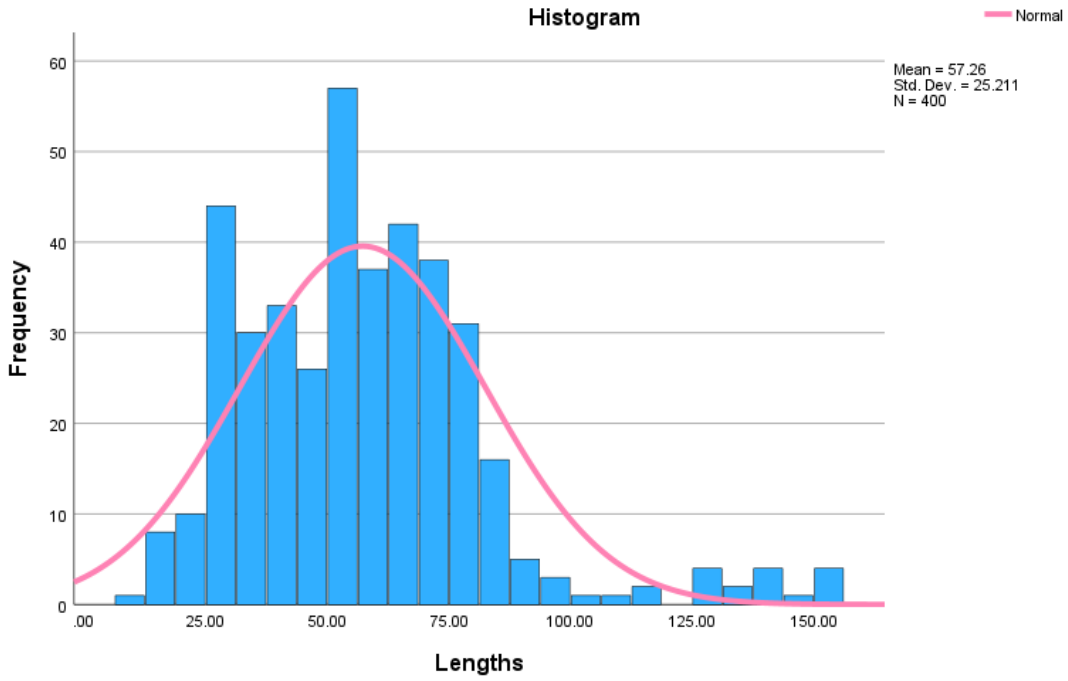

Descriptives

			Statistic	Std. Error
Lengths	Mean		57.2557	1.26053
	95% Confidence Interval for Mean	Lower Bound	54.7776	
		Upper Bound	59.7338	
	5% Trimmed Mean		55.2369	
	Median		55.0000	
	Variance		635.577	
	Std. Deviation		25.21065	
	Minimum		12.00	
	Maximum		154.00	
	Range		142.00	
	Interquartile Range		30.00	
	Skewness		1.211	.122
	Kurtosis		2.613	.243

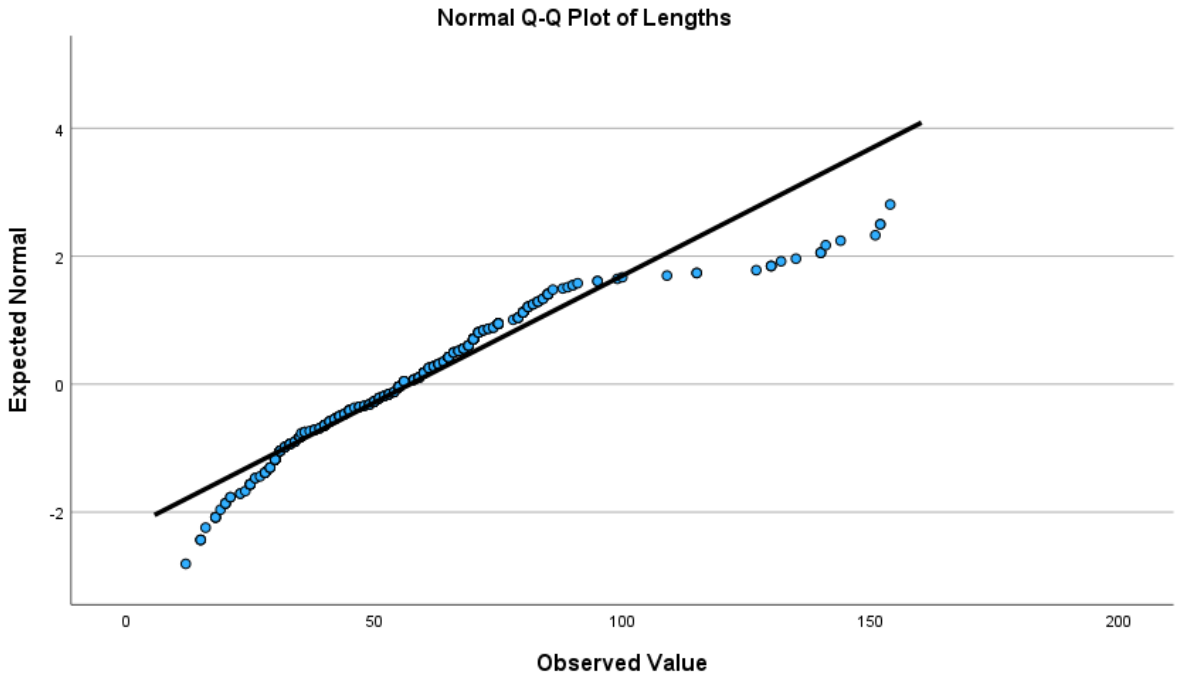

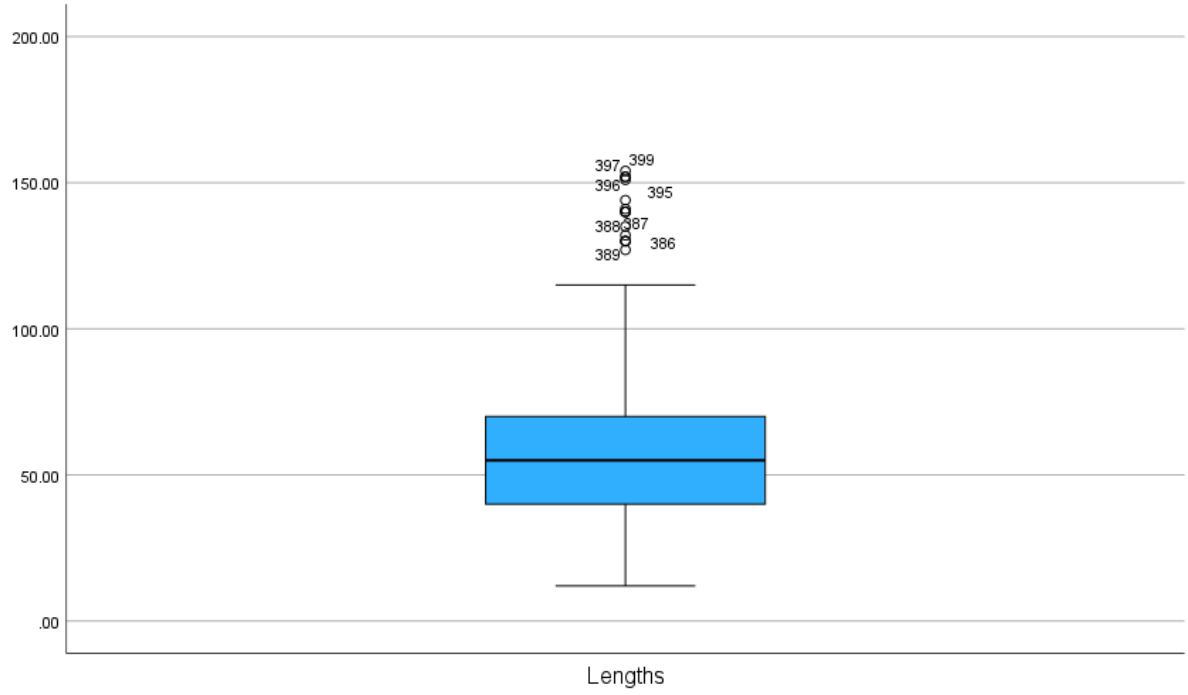

One-Sample Kolmogorov-Smirnov Test

			Lengths
N			400
Normal Parameters [a, b]	Mean		57.2557
	Std. Deviation		25.21065
Most Extreme Differences	Absolute		.092
	Positive		.092
	Negative		-.053
Test Statistic			.092
Asymp. Sig. (2-tailed) [c]			<.001
Monte Carlo Sig. (2-tailed) [d]	Sig.		<.001
	99% Confidence Interval	Lower Bound	.000
		Upper Bound	.000

a. Test distribution is Normal.

b. Calculated from data.

c. Lilliefors Significance Correction.

d. Lilliefors' method based on 400 Monte Carlo samples with starting seed 299883525.

Tests of Normality

	Kolmogorov-Smirnova			Shapiro-Wilk		
	Statistic	df	Sig.	Statistic	df	Sig.
Lengths	.092	400	<.001	.916	400	<.001

a. Lilliefors Significance Correction

Descriptive Statistics

						Percentiles	
	N	Mean	Std. Deviation	Minimum	Maximum	25th	50th (Median)	75th
Lengths	400	57.2557	25.21065	12.00	154.00	40.0000	55.0000	70.0000

Statistical Analysis on 400 Feather Fibre Lengths and Thicknesses

Correlations

		Length	Thickness 1 (mm)	Thickness 2 (mm)	Thickness 3 (mm)	Average Thickness (mm)
Length	Pearson Correlation	1	.803**	.772**	.527**	.813**
	Sig. (2-tailed)		<.001	<.001	<.001	<.001
	N	400	400	400	400	400
Thickness 1 (mm)	Pearson Correlation	.803**	1	.867**	.636**	.980**
	Sig. (2-tailed)	<.001		<.001	<.001	<.001
	N	400	400	400	400	400
Thickness 2 (mm)	Pearson Correlation	.772**	.867**	1	.703**	.943**
	Sig. (2-tailed)	<.001	<.001		<.001	<.001
	N	400	400	400	400	400
Thickness 3 (mm)	Pearson Correlation	.527**	.636**	.703**	1	.730**
	Sig. (2-tailed)	<.001	<.001	<.001		<.001
	N	400	400	400	400	400
Average Thickness (mm)	Pearson Correlation	.813**	.980**	.943**	.730**	1
	Sig. (2-tailed)	<.001	<.001	<.001	<.001	
	N	400	400	400	400	400

**. Correlation is significant at the 0.01 level (2-tailed).

Independent Samples Test (Part A)

		Levene's Test for Equality of Variances	
		F	Sig.
Length	Equal variances assumed	.116	.734
	Equal variances not assumed		
Thickness 1 (mm)	Equal variances assumed	.366	.545
	Equal variances not assumed		
Thickness 2 (mm)	Equal variances assumed	.000	.992
	Equal variances not assumed		
Thickness 3 (mm)	Equal variances assumed	9.646	.002
	Equal variances not assumed		
Average Thickness (mm)	Equal variances assumed	.117	.732
	Equal variances not assumed		

Independent Samples Test (Part B)

t-test for Equality of Means							
		Significance				95% Confidence Interval of the Difference	
t	df	One-Sided p	Two-Sided p	Mean Difference	Std. Error Difference	Lower	Upper
4.486	398	<.001	<.001	11.04855	2.46273	6.20697	15.89013
4.486	396.766	<.001	<.001	11.04855	2.46273	6.20692	15.89018
4.276	398	<.001	<.001	.19045	.04453	.10290	.27800
4.276	393.757	<.001	<.001	.19045	.04453	.10289	.27801
2.013	398	.022	.045	.04500	.02235	.00106	.08894
2.013	393.699	.022	.045	.04500	.02235	.00106	.08894
5.325	398	<.001	<.001	.03585	.00673	.02261	.04909
5.325	295.563	<.001	<.001	.03585	.00673	.02260	.04910
3.914	398	<.001	<.001	.09085	.02321	.04522	.13648
3.914	391.753	<.001	<.001	.09085	.02321	.04521	.13649

Independent Samples Effect Sizes

			Point	95% Confidence Interval	
		Standardizer [a]	Estimate	Lower	Upper
Length	Cohen's d	24.62728	.449	.250	.647
	Hedges' correction	24.67381	.448	.249	.646
	Glass's delta	25.30456	.437	.235	.637
Thickness 1 (mm)	Cohen's d	.44535	.428	.229	.626
	Hedges' correction	.44619	.427	.229	.624
	Glass's delta	.42160	.452	.250	.652
Thickness 2 (mm)	Cohen's d	.22349	.201	.005	.398
	Hedges' correction	.22391	.201	.005	.397
	Glass's delta	.21149	.213	.015	.410
Thickness 3 (mm)	Cohen's d	.06733	.532	.333	.732
	Hedges' correction	.06746	.531	.332	.730
	Glass's delta	.04318	.830	.617	1.042
Average Thickness (mm)	Cohen's d	.23212	.391	.193	.589
	Hedges' correction	.23256	.391	.193	.588
	Glass's delta	.21697	.419	.218	.618

a. The denominator used in estimating the effect sizes.

Cohen's d uses the pooled standard deviation.

Hedges' correction uses the pooled standard deviation, plus a correction factor.

Glass's delta uses the sample standard deviation of the control group.

Descriptives

			Statistic	Std. Error
Thickness 1 (mm)	Mean		.6538	.02274
	95% Confidence Interval for Mean	Lower Bound	.6091	
		Upper Bound	.6985	
	5% Trimmed Mean		.5959	
	Median		.5700	
	Variance		.207	
	Std. Deviation		.45489	
	Minimum		.02	
	Maximum		3.18	
	Range		3.16	
	Interquartile Range		.39	
	Skewness		2.435	.122
	Kurtosis		7.951	.243
Thickness 2 (mm)	Mean		.2220	.01122
	95% Confidence Interval for Mean	Lower Bound	.2000	
		Upper Bound	.2441	
	5% Trimmed Mean		.1846	
	Median		.1700	
	Variance		.050	
	Std. Deviation		.22435	
	Minimum		.01	
	Maximum		1.61	
	Range		1.60	
	Interquartile Range		.12	
	Skewness		3.704	.122
	Kurtosis		15.628	.243

			Statistic	Std. Error
Thickness 3 (mm)	Mean		.0686	.00348
	95% Confidence Interval for Mean	Lower Bound	.0617	
		Upper Bound	.0754	
	5% Trimmed Mean		.0600	
	Median		.0600	
	Variance		.005	
	Std. Deviation		.06960	
	Minimum		.01	
	Maximum		.75	
	Range		.74	
	Interquartile Range		.06	
	Skewness		5.034	.122
	Kurtosis		39.085	.243

Extreme Values

			Case Number	Value
Thickness 1 (mm)	Highest	1	209	3.18
		2	204	2.97
		3	202	2.53
		4	203	2.46
		5	207	2.46
	Lowest	1	149	.02
		2	174	.04
		3	193	.05
		4	390	.08
		5	388	.08
Thickness 2 (mm)	Highest	1	204	1.61
		2	206	1.57
		3	202	1.53
		4	201	1.41
		5	8	1.24
	Lowest	1	187	.01
		2	174	.01
		3	173	.01
		4	149	.01
		5	388	.02
Thickness 3 (mm)	Highest	1	206	.75
		2	204	.64
		3	211	.55
		4	9	.28
		5	360	.28
	Lowest	1	397	.01
		2	393	.01
		3	390	.01
		4	387	.01
		5	372	.01

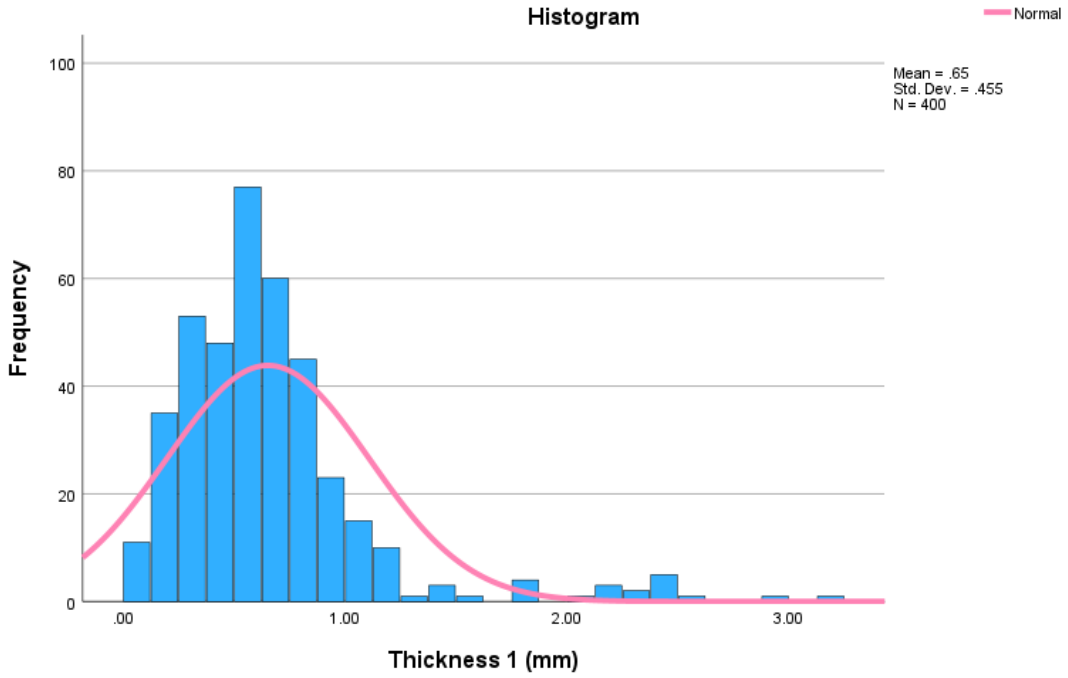
Histogram
Normal
Mean = .65
Std. Dev. = .455
N = 400
Frequency
100
80
60
40
20
0
.00
1.00
2.00
3.00
Thickness 1 (mm)

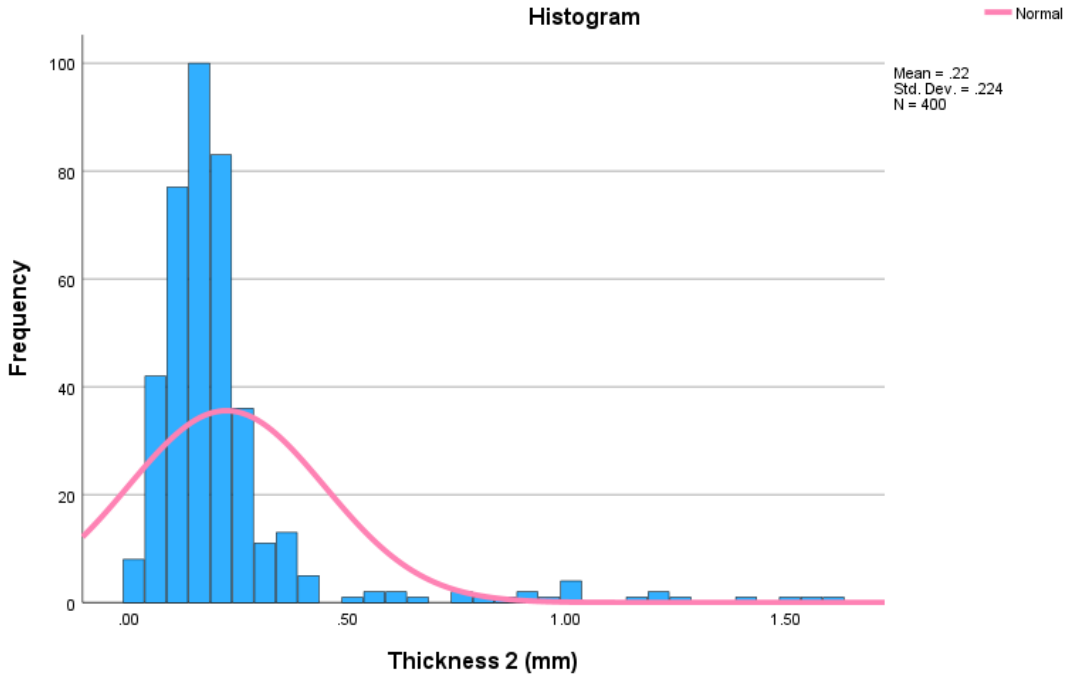
Histogram
Normal
Mean = .22
Std. Dev. = .224
N = 400
Frequency
100
80
60
40
20
0
.00
.50
1.00
1.50
Thickness 2 (mm)

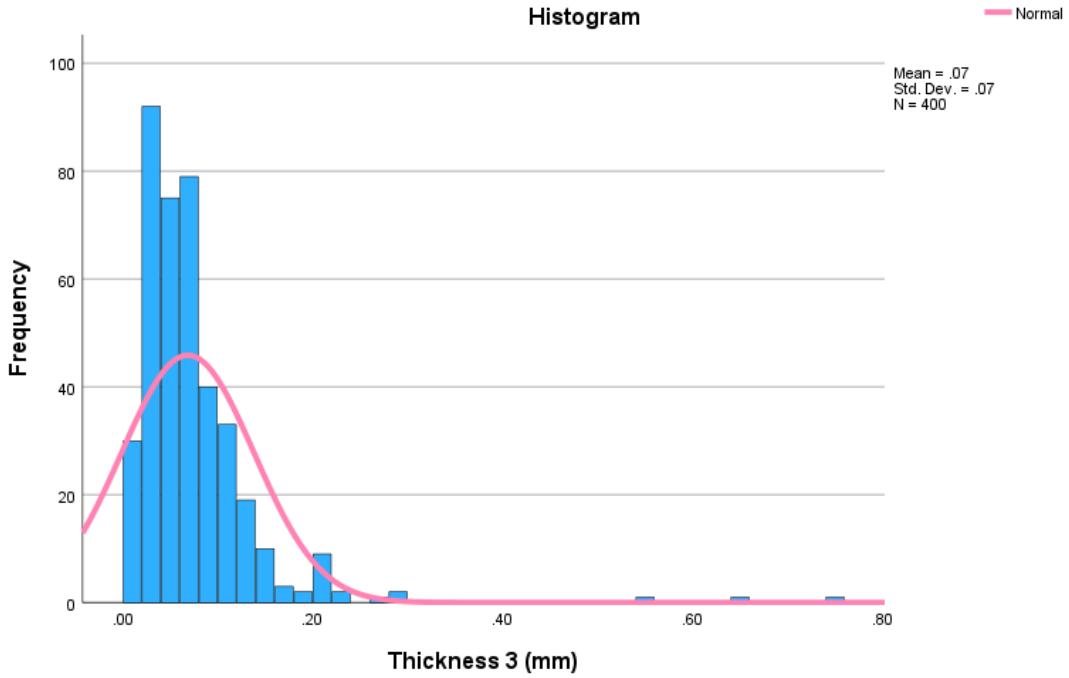
Histogram
Normal
Mean = .07
Std. Dev. = .07
N = 400
Frequency
100
80
60
40
20
0
.00
.20
.40
.60
.80
Thickness 3 (mm)

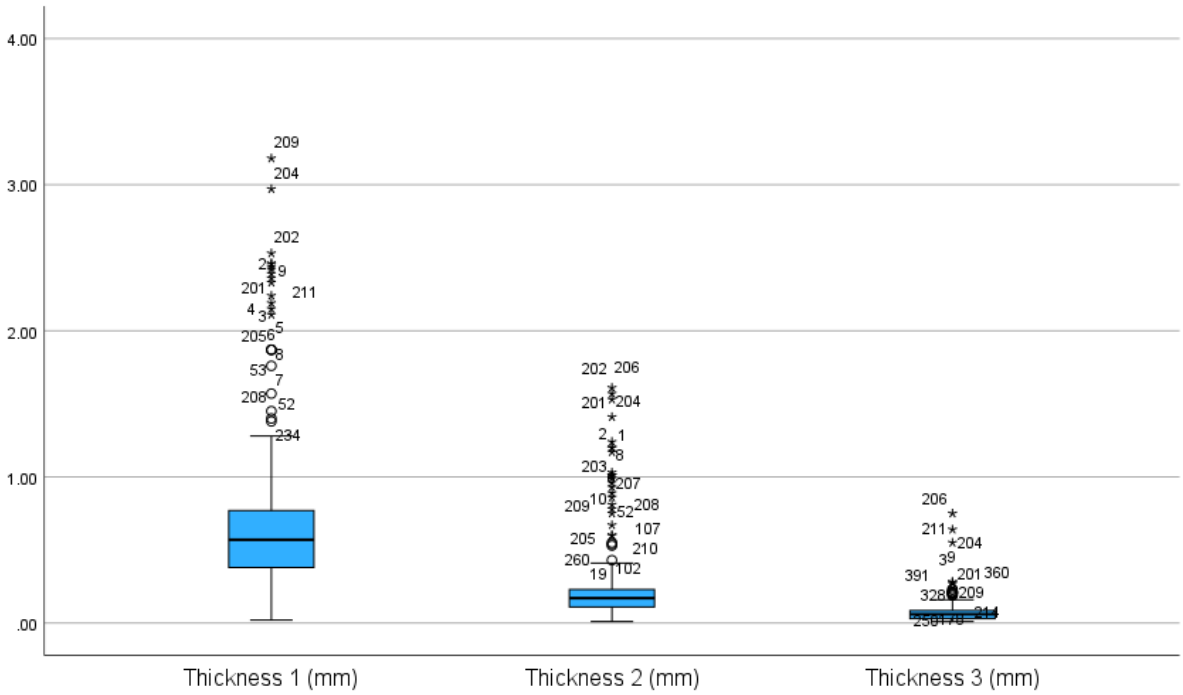
4.00
3.00
2.00
1.00
.00
Thickness 1 (mm)
Thickness 2 (mm)
Thickness 3 (mm)

Statistical Analysis of Shredded and Unshredded Fibres

Shredded	Unshredded
mm	*mm*
7	30
9	30
10	34
15	35
25	35
25	40
25	40
25	41
30	43
30	43
35	45
35	45
35	49
35	50
35	50
35	50
35	60
40	62
40	68
40	68
43	70
45	70
45	75
55	75
56	75

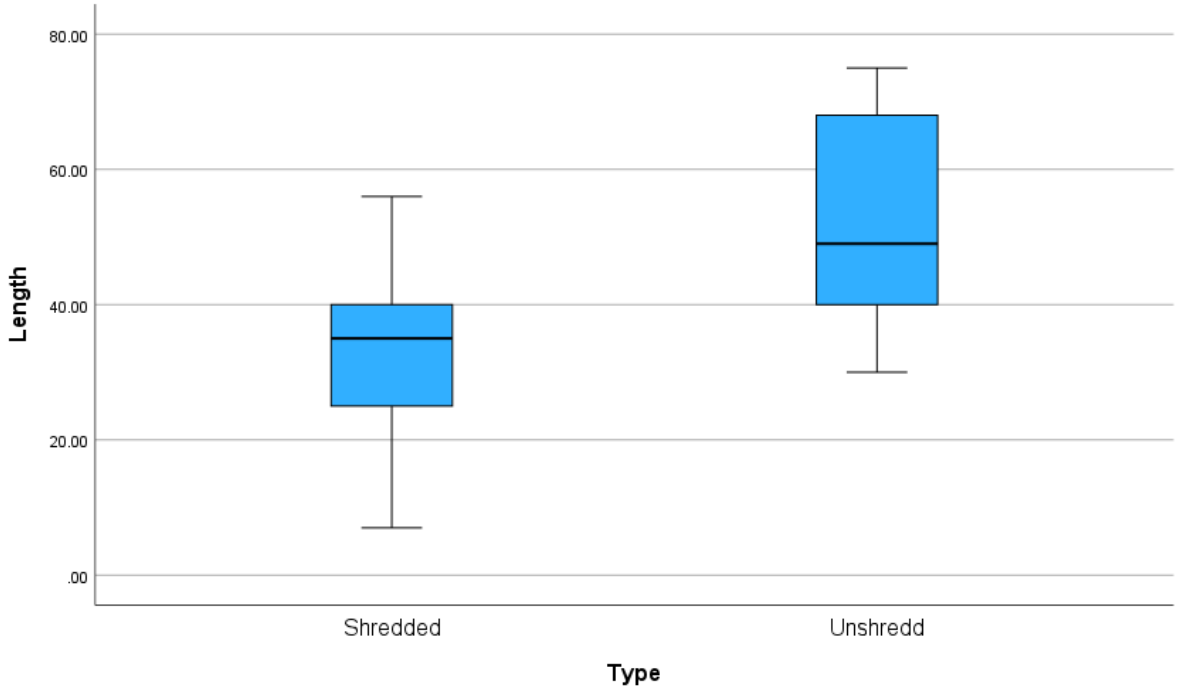

Group Statistics

	Fibre	N	Mean	Std. Deviation	Std. Error Mean
Length	Shredded	25	32.4000	12.82251	2.56450
	Unshredded	25	51.3200	15.08233	3.01647

Independent Samples Effect Sizes

				95% Confidence Interval	
		Standardizer [a]	Point Estimate	Lower	Upper
Length	Cohen's d	13.99810	-1.352	-1.962	-.729
	Hedges' correction	14.22167	-1.330	-1.931	-.718
	Glass's delta	15.08233	-1.254	-1.902	-.588

a. The denominator used in estimating the effect sizes.

Cohen's d uses the pooled standard deviation.

Hedges' correction uses the pooled standard deviation, plus a correction factor.

Glass's delta uses the sample standard deviation of the control group.

Descriptives

	Type			Statistic	Std. Error
Length	Shredded	Mean		32.4000	2.56450
		95% Confidence Interval for Mean	Lower Bound	27.1071	
			Upper Bound	37.6929	
		5% Trimmed Mean		32.4889	
		Median		35.0000	
		Variance		164.417	
		Std. Deviation		12.82251	
		Minimum		7.00	
		Maximum		56.00	
		Range		49.00	
		Interquartile Range		15.00	
		Skewness		-.345	.464
		Kurtosis		-.017	.902
	Unshredded	Mean		51.3200	3.01647
		95% Confidence Interval for Mean	Lower Bound	45.0943	
			Upper Bound	57.5457	
		5% Trimmed Mean		51.1889	
		Median		49.0000	
		Variance		227.477	
		Std. Deviation		15.08233	
		Minimum		30.00	
		Maximum		75.00	
		Range		45.00	
		Interquartile Range		28.00	
		Skewness		.331	.464
		Kurtosis		-1.282	.902

Independent Samples Test (Part A)

		Levene's Test for Equality of Variances	
		F	Sig.
Length	Equal variances assumed	1.971	.167
	Equal variances not assumed		

Independent Samples Test (Part B)

				t-test for Equality of Means			
		Significance				95% Confidence Interval of the Difference	
t	df	One-Sided p	Two-Sided p	Mean Difference	Std. Error Difference	Lower	Upper
-4.779	48	<.001	<.001	-18.92000	3.95926	-26.88062	-10.95938
-4.779	46.789	<.001	<.001	-18.92000	3.95926	-26.88595	-10.95405

Density of Fibres Calculation

	Sample A	*Sample B*	
P_L	0.9971	0.9971	g/cm^3
W_3	3585.96	3597.48	g
W_4	43.57	26.52	g
W_5	3569.24	3595.99	g
Empty	1189.99	1201.75	g
P	0.72	0.94	g/cm^3
Average	1.664/2=		
P	**0.832**		$\boldsymbol{g/cm^3}$

Mix Design for Fibre-Reinforced Mortar

Self-Compacting Mortar Mix Design per **Unit Volume** for all % Variables						
Mix Proportions			**Control**	**0.125%**	**0.25%**	**0.5%**
Cement	*CEM II/A-LL 42.5 R*	*kg*	495	495	495	495
Water		*kg*	247.50	247.50	247.50	247.50
Fine Aggregate	*Dolomitic, <4mm*	*kg*	1728	1728	1725	1723
Superplasticiser	*MasterGlenium SKY 698, 1.2%*	*kg*	5.94	5.94	5.94	5.94
Water Absorption		*kg*	5.18	5.18	5.18	5.17
W/C Ratio			0.50	0.50	0.50	0.50
Fibres Volume Fraction		*%*	0.00	0.25	0.25	0.50
Fibre Mass	*Density = 800kg/m³*	*kg*	0.00	2.00	2.00	4.00

Mix Design for Fibre-Reinforced Concrete

Self-Compacting Concrete Mix Design per **Unit Volume** for all % Variables						
Mix Proportions			**Control**	**0.125%**	**0.25%**	**0.50%**
Cement	*CEM II/A-LL 42.5 R*	*kg*	495	495	495	495
Water		*kg*	222.75	222.75	222.75	222.75
Fine Aggregate	*Dolomitic, <4mm*	*kg*	1080	1080	1080	1080
Coarse Aggregate	*Dolomitic, <10mm*	*kg*	648.0	645.5	643.0	638.0
Superplasticiser	*MasterGlenium SKY 698, 1.2%*	*kg*	5.94	5.94	5.94	5.94
Water Absorption		*kg*	5.18	5.18	5.17	5.15
W/C Ratio			0.45	0.45	0.45	0.45
Fibres Volume Fraction		*%*	0.00	0.125	0.25	0.50
Fibre Mass	*Density = 800kg/m³*	*kg*	0.00	1.00	2.00	4.00

Mix Code	**Fibre %**	**Fibre Length Range**
C0	-	-
C0.125S	0.125%	5 - 42mm
C0.125L	0.125%	30 - 75mm
C0.25S	0.25%	5 - 42mm
C0.25L	0.25%	30 - 75mm
C0.5S	0.50%	5 - 42mm
C0.5L	0.50%	30 - 75mm

Fresh Properties: Empirical Tests and Rheology

Slump Flow					
Mix Code		**d_1**	**d_2**	**d_3**	**Avg. d**
	Time	*mm*	*mm*	*mm*	*mm*
Mix C0	t_0	590	610	630	610
	t_{15}	560	560	560	560
	t_{30}	560	550	540	550
Mix C0.125S	t_0	690	690	690	690
	t_{15}	700	690	690	693
	t_{30}	690	690	690	690
Mix C0.125L	t_0	610	620	630	620
	t_{15}	530	530	530	530
	t_{30}	500	500	500	500
Mix C0.25S	t_0	480	500	490	490
	t_{15}	480	480	490	483
	t_{30}	420	420	410	417
Mix C0.25L	t_0	600	590	590	593
	t_{15}	550	550	550	550
	t_{30}	520	520	520	520
Mix C0.5S	t_0	-	-	-	-
	t_{15}	-	-	-	-
	t_{30}	-	-	-	-
Mix C0.5L	t_0	-	-	-	-
	t_{15}	-	-	-	-
	t_{30}	-	-	-	-

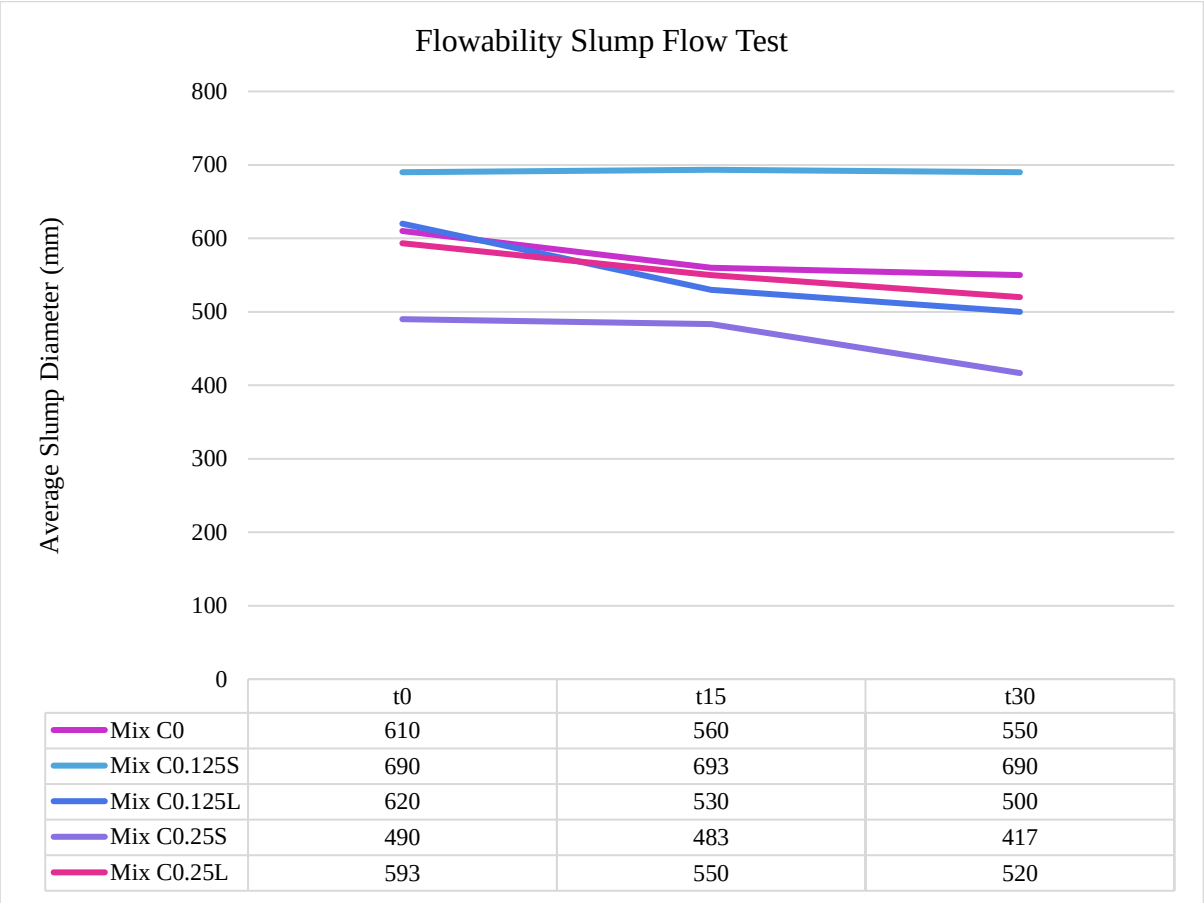

	t0	t15	t30
Mix C0	610	560	550
Mix C0.125S	690	693	690
Mix C0.125L	620	530	500
Mix C0.25S	490	483	417
Mix C0.25L	593	550	520

T_{500}			
Mix Code		**Time**	**Classification**
	Time	*s*	*EFNARC*
Mix C0	t_0	3	VS2
	t_{15}	4	VS2
	t_{30}	4	VS2
Mix C0.125S	t_0	1.5	VS1
	t_{15}	2	VS1
	t_{30}	3	VS2
Mix C0.125L	t_0	2.5	VS2
	t_{15}	2.5	VS2
	t_{30}	2.5	VS2
Mix C0.25S	t_0	9	VS2
	t_{15}	9	VS2
	t_{30}	-	VS2
Mix C0.25L	t_0	3	VS2
	t_{15}	3	VS2
	t_{30}	7	VS2
Mix C0.5S	t_0	-	-
	t_{15}	-	-
	t_{30}	-	-
Mix C0.5L	t_0	-	-
	t_{15}	-	-
	t_{30}	-	-

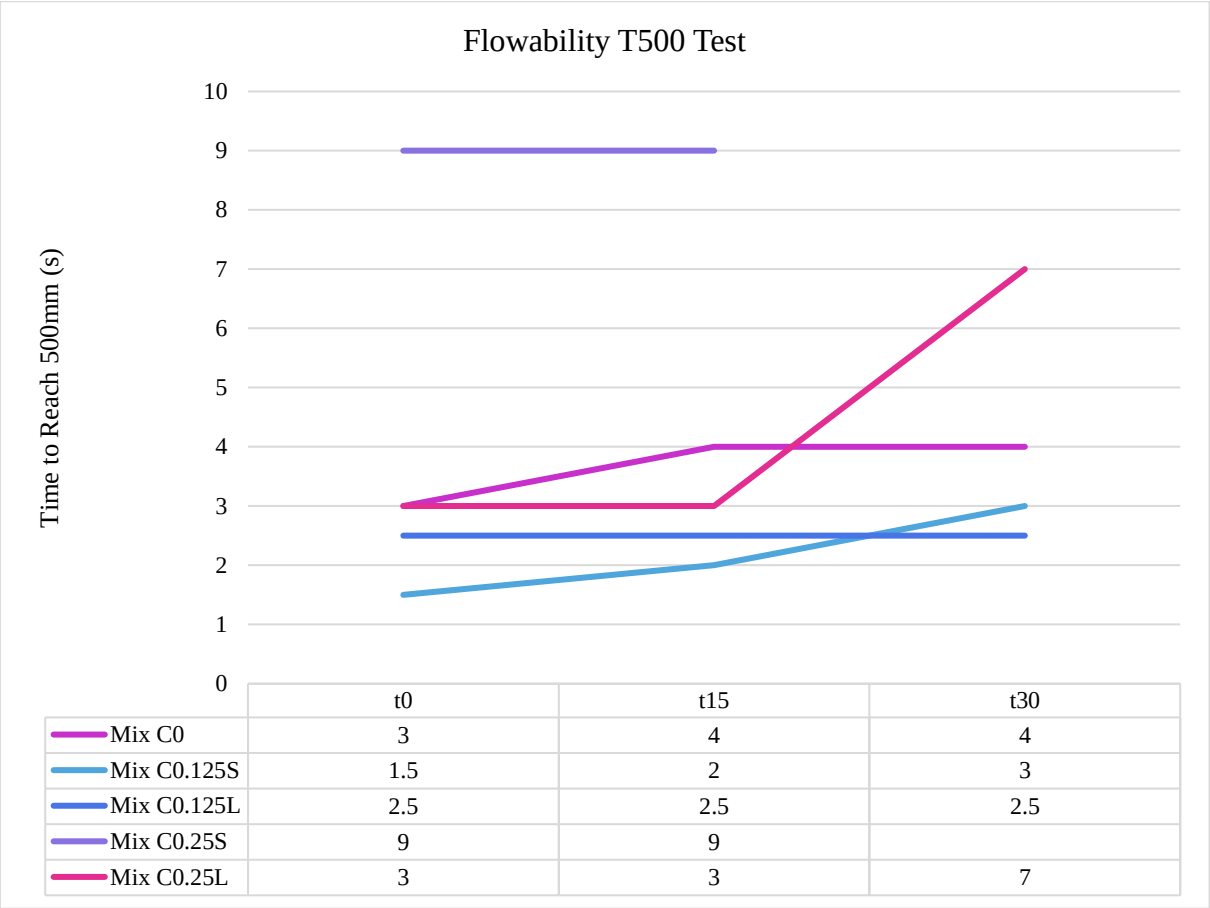

	t0	t15	t30
Mix C0	3	4	4
Mix C0.125S	1.5	2	3
Mix C0.125L	2.5	2.5	2.5
Mix C0.25S	9	9	
Mix C0.25L	3	3	7

L-Box					
Mix Code		**Distance**	**h_1**	**h_2**	**PL**
	Time	*mm*	*mm*	*mm*	*h2/h1*
Mix C0	t_0	550	190	65	0.342
	t_{15}	550	170	82	0.482
	t_{30}	550	180	76.75	0.426
Mix C0.125S	t_0	550	210	67.5	0.321
	t_{15}	550	180	73.75	0.410
	t_{30}	550	170	66.25	0.390
Mix C0.125L	t_0	550	350	37.5	0.107
	t_{15}	550	150	70	0.467
	t_{30}	550	150	65	0.433
Mix C0.25S	t_0	360	480	30	0.063
	t_{15}	550	380	33.75	0.089
	t_{30}	515	300	48.75	0.163
Mix C0.25L	t_0	540	440	23.75	0.054
	t_{15}	550	350	43.75	0.125
	t_{30}	550	310	45	0.145
Mix C0.5S	t_0	-	-	-	-
	t_{15}	-	-	-	-
	t_{30}	-	-	-	-
Mix C0.5L	t_0	-	-	-	-
	t_{15}	-	-	-	-
	t_{30}	-	-	-	-

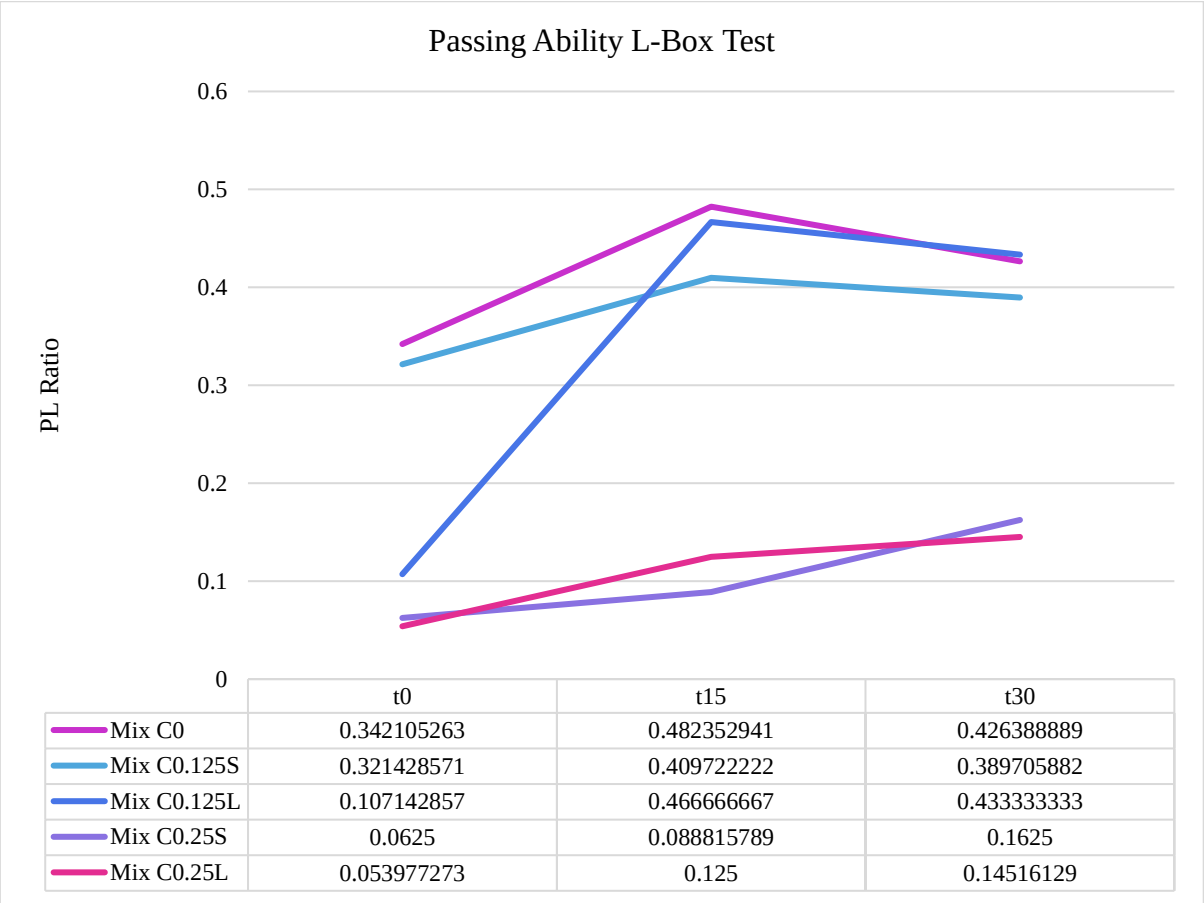

	t0	t15	t30
Mix C0	0.342105263	0.482352941	0.426388889
Mix C0.125S	0.321428571	0.409722222	0.389705882
Mix C0.125L	0.107142857	0.466666667	0.433333333
Mix C0.25S	0.0625	0.088815789	0.1625
Mix C0.25L	0.053977273	0.125	0.14516129

V-Funnel			
Mix Code		**Time**	**Classification**
	Time	*s*	*EFNARC*
Mix C0	t_0	7	VF1
	t_{15}	9	VF2
	t_{30}	7	VF1
Mix C0.125S	t_0	12	VF2
	t_{15}	15	VF2
	t_{30}	15	VF2
Mix C0.125L	t_0	9	VF2
	t_{15}	6	VF1
	t_{30}	6	VF1
Mix C0.25S	t_0	34	VF2
	t_{15}	41	VF2
	t_{30}	21	VF2
Mix C0.25L	t_0	17	VF2
	t_{15}	18	VF2
	t_{30}	18	VF2
Mix C0.5S	t_0	-	-
	t_{15}	-	-
	t_{30}	-	-
Mix C0.5L	t_0	-	-
	t_{15}	-	-
	t_{30}	-	-

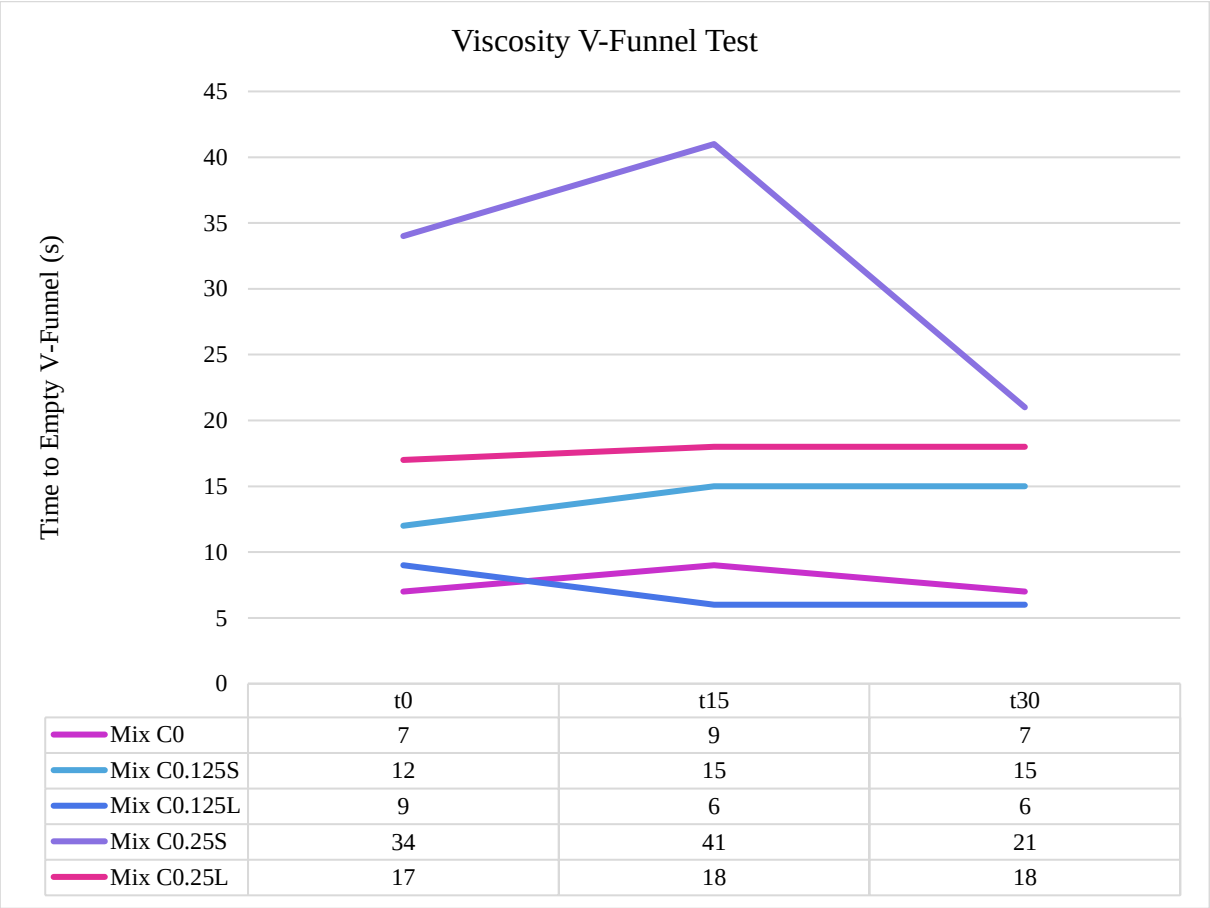

	t0	t15	t30
Mix C0	7	9	7
Mix C0.125S	12	15	15
Mix C0.125L	9	6	6
Mix C0.25S	34	41	21
Mix C0.25L	17	18	18

Rheology: Stress Strain data from Bingham Parameters				
Mix C0	*Y-Intercept*	Yield Stress (T_0)	*Pa*	82.37
	Gradient	Plastic Viscosity (μ)	*Pa/s*	10.33
	Line Equation		$Y = mx + c$	Y = 10.33x + 82.37
Mix C0.125S	*Y-Intercept*	Yield Stress (T_0)	*Pa*	42.69
	Gradient	Plastic Viscosity (μ)	*Pa/s*	34.99
	Line Equation		$Y = mx + c$	Y = 34.99x + 42.69
Mix C0.125L	*Y-Intercept*	Yield Stress (T_0)	*Pa*	48.32
	Gradient	Plastic Viscosity (μ)	*Pa/s*	32.60
	Line Equation		$Y = mx + c$	Y = 32.60x + 48.32
Mix C0.25S	*Y-Intercept*	Yield Stress (T_0)	*Pa*	115.78
	Gradient	Plastic Viscosity (μ)	*Pa/s*	20.46
	Line Equation		$Y = mx + c$	Y = 20.46x + 115.78
Mix C0.25L	*Y-Intercept*	Yield Stress (T_0)	*Pa*	43.93
	Gradient	Plastic Viscosity (μ)	*Pa/s*	42.58
	Line Equation		$Y = mx + c$	Y = 42.58x + 43.93

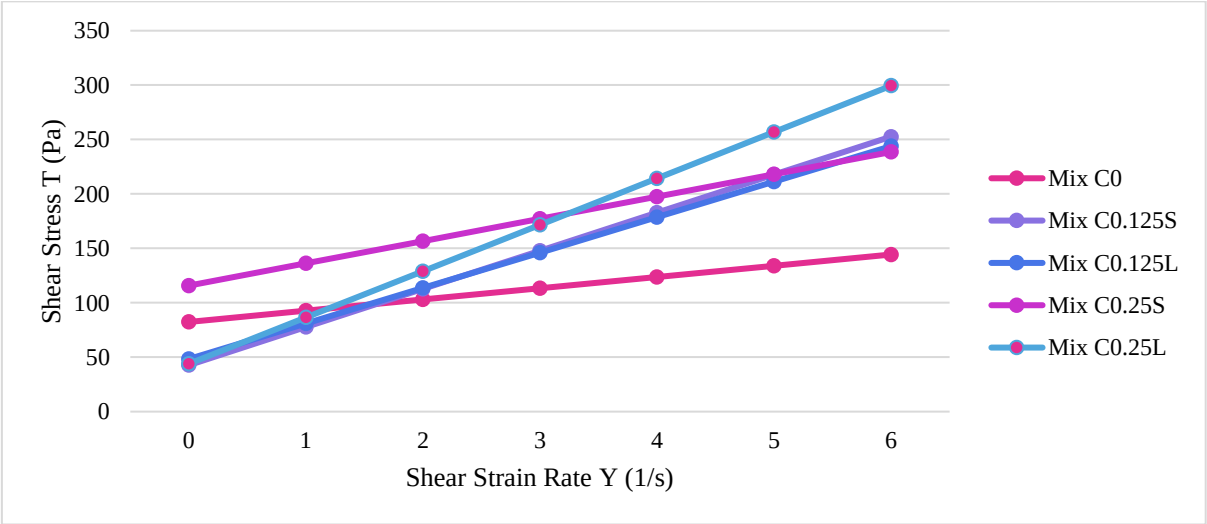

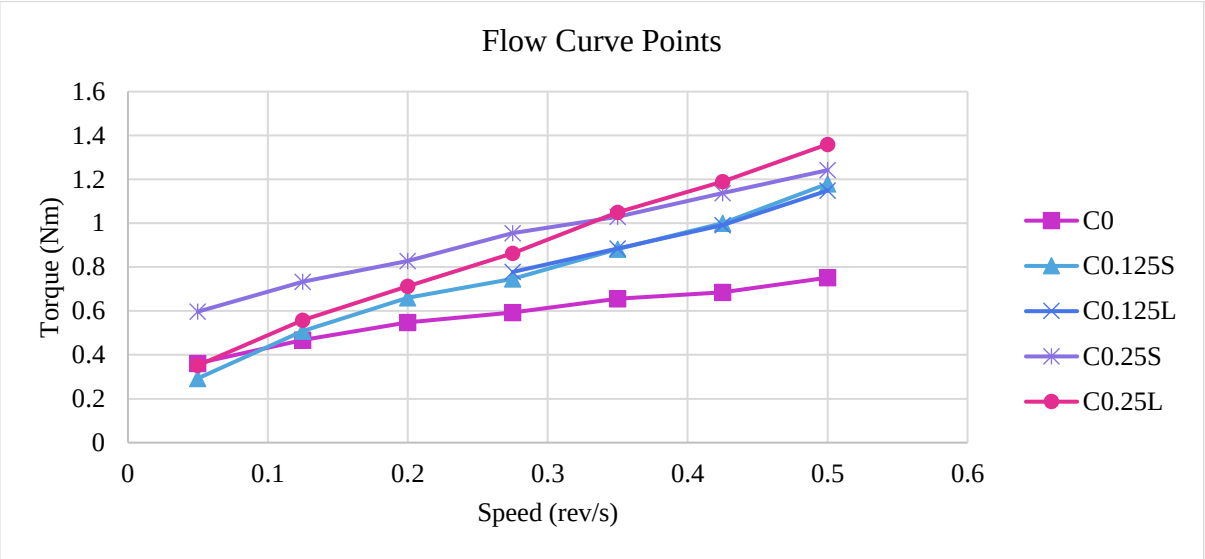
Flow Curve Points
Torque (Nm)
1.6
1.4
1.2
1
0.8
0.6
0.4
0.2
0
0
0.1
0.2
0.3
0.4
0.5
0.6
Speed (rev/s)
C0
C0.125S
C0.125L
C0.25S
C0.25L

Early-Stage Cracking Behaviour

Environmental Chamber Test		
	Time of First Crack Development	**Average Crack Width**
Mix Code	*hours*	*mm*
Mix C0	1.75	0.454
Mix C0.125S	2	0.325
Mix C0.125L	2.5	0.035
Mix C0.25S	0	0.000
Mix C0.25L	2.5	0.704
Mix C0.5S	2.75	0.278
Mix C0.5L	3.5	0.094

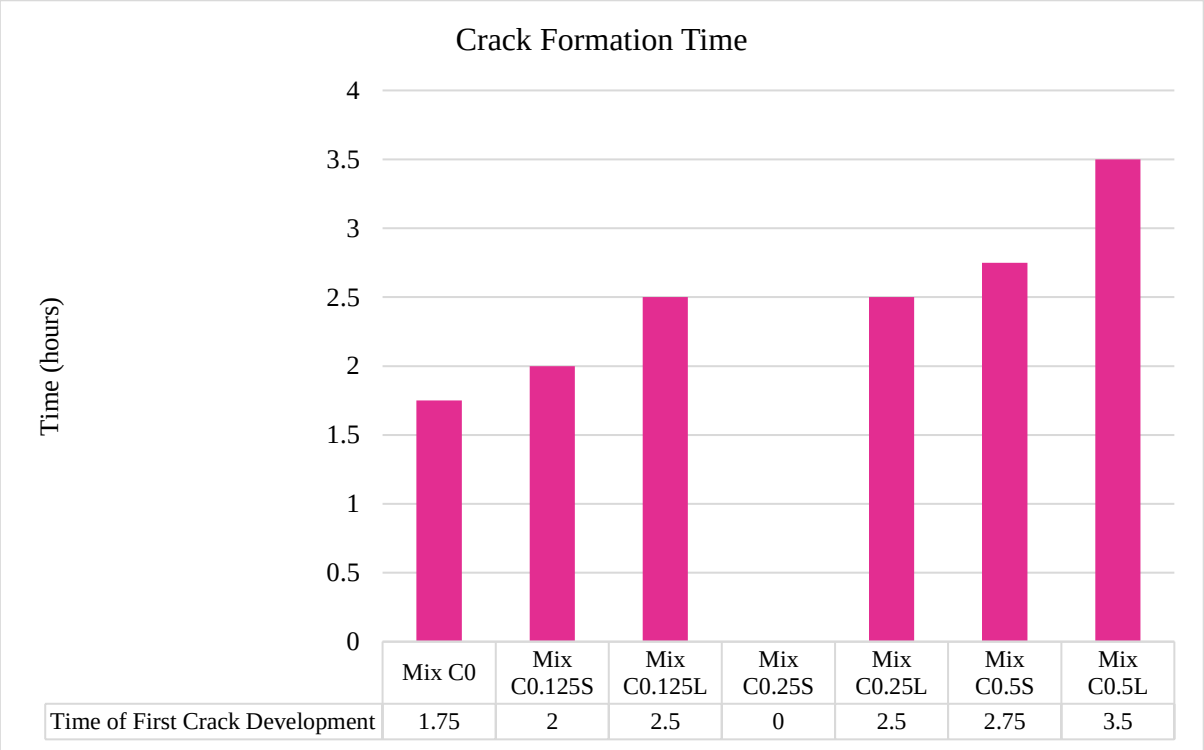

Environmental Chamber Test						
Mix Code	C0					
Date	14-Jul					
Crack Time	1.75	hours				
Crack Type	Continuous					
Time	Ambient Temperature	Concrete Temperature	Chamber Temperature	Mass of Water Evaporated	Water Evaporation Rate	
Hours	*°C*	*°C*	*°C*	*g*	*kg/m²/hr*	Crack Width *mm*
0.5	21.350	26.951	23.677	986.5	29.4	0.60
1	21.724	28.063	22.840	980.0	29.4	0.45
1.5	21.990	28.617	22.529	973.5	29.4	0.55
2	22.551	29.405	22.684	966.5	29.4	0.20
2.5	22.803	30.215	22.932	960.0	29.4	0.60
3	23.035	30.914	23.361	953.5	29.4	0.65
3.5	23.377	31.543	23.954	946.5	29.4	0.45
4	23.927	32.388	24.632	939.5	29.4	0.50
4.5	23.843	33.183	25.764	932.5	29.4	0.30
5	24.355	33.528	26.847	925.5	29.4	0.25
5.5	24.091	34.881	28.099	918.5	29.4	0.75
6	24.108	34.825	29.293	911.5	29.4	0.15

Environmental Chamber Test						
Mix Code	C0-125S					
Date	27-Jul					
Crack Time	2	hours				
Crack Type	Continuous					
Time	Ambient Temperature	Concrete Temperature	Chamber Temperature	Mass of Water Evaporated	Water Evaporation Rate	
Hours	*°C*	*°C*	*°C*	*g*	*kg/m²/hr*	Crack Width *mm*
0.5	22.627	28.827	22.077	994.0	29.4	0.75
1	23.354	30.754	24.603	987.0	29.4	0.45
1.5	23.631	31.425	25.262	984.0	29.4	0.40
2	24.006	32.827	26.129	979.0	29.4	0.30
2.5	24.373	34.140	27.389	974.5	29.4	0.25
3	24.434	35.116	28.445	971.0	29.4	0.50
3.5	24.496	35.503	29.501	966.5	29.4	0.35
4	24.557	35.889	30.557	965.5	29.4	0.05
4.5	24.619	36.275	31.613	960.0	29.4	0.30
5	24.681	36.634	32.669	960.0	29.4	0.25
5.5	24.655	36.865	35.533	956.0	29.4	0.20
6	24.830	37.569	36.694	951.0	29.4	0.10

Environmental Chamber Test						
Mix Code	C0-125L					
Date	20-Jul					
Crack Time	2.5	hours				
Crack Type	Short, Shallow, only on Sides					
Time	Ambient Temperature	Concrete Temperature	Chamber Temperature	Mass of Water Evaporated	Water Evaporation Rate	
Hours	*°C*	*°C*	*°C*	*g*	*kg/m²/hr*	Crack Width *mm*
0.5	22.479	31.347	23.837	990.5	29.4	0.05
1	22.755	32.920	24.645	986.5	29.4	0.05
1.5	22.996	34.360	25.698	981.0	29.4	0.03
2	24.055	35.718	27.325	974.5	29.4	0.03
2.5	24.442	36.214	29.052	968.5	29.4	0.03
3	24.674	37.066	30.513	962.5	29.4	0.03
3.5	24.876	36.959	31.847	952.5	29.4	0.03
4	25.076	37.848	33.058	944.5	29.4	0.03
4.5	24.971	36.617	34.130	939.5	29.4	0.03
5	25.038	38.723	35.087	935.5	29.4	0.05
5.5	25.643	39.148	35.941	917.5	29.4	0.08
6	25.713	39.774	36.740	904.5	29.4	0.03

Environmental Chamber Test						
Mix Code	C0-25S					
Date	18-Jul					
Crack Time	-	hours				
Crack Type	No Crack Formed					
Time	Ambient Temperature	Concrete Temperature	Chamber Temperature	Mass of Water Evaporated	Water Evaporation Rate	
Hours	*°C*	*°C*	*°C*	*g*	*kg/m²/hr*	Crack Width *mm*
0.5	21.428	21.977	29.485	986.0	29.4	0.00
1	21.949	25.062	30.726	985.0	29.4	0.00
1.5	22.488	26.001	32.208	978.5	29.4	0.00
2	22.625	27.023	32.358	977.5	29.4	0.00
2.5	23.087	28.750	33.001	976.5	29.4	0.00
3	23.559	30.568	34.203	976.5	29.4	0.00
3.5	23.686	32.083	34.610	976.5	29.4	0.00
4	23.802	33.346	34.648	972.5	29.4	0.00
4.5	23.915	34.454	35.175	968.5	29.4	0.00
5	24.327	35.499	35.750	967.0	29.4	0.00
5.5	24.464	36.373	36.075	967.0	29.4	0.00
6	25.428	37.279	36.973	960.5	29.4	0.00

Environmental Chamber Test						
Mix Code	C0-25L					
Date	20-Jul					
Crack Time	2.5	hours				
Crack Type	Continuous					
Time	Ambient Temperature	Concrete Temperature	Chamber Temperature	Mass of Water Evaporated	Water Evaporation Rate	
Hours	*°C*	*°C*	*°C*	*g*	*kg/m²/hr*	Crack Width *mm*
0.5	24.321	31.835	24.537	984.5	29.4	0.90
1	24.492	31.901	25.719	982	29.4	0.55
1.5	24.708	32.897	27.013	978	29.4	0.50
2	24.920	33.198	27.852	975.5	29.4	0.60
2.5	25.282	33.405	28.440	972.5	29.4	0.80
3	25.241	33.758	29.325	968	29.4	0.50
3.5	25.427	34.062	31.188	965.5	29.4	1.90
4	25.769	34.595	32.554	964	29.4	0.55
4.5	25.918	34.970	33.124	958	29.4	1.00
5	26.118	35.362	34.247	956.5	29.4	0.43
5.5	26.318	35.754	35.323	953.5	29.4	0.48
6	26.517	36.145	36.400	936	29.4	0.25

Environmental Chamber Test						
Mix Code	C0-5S					
Date						
Crack Time	2.75	hours				
Crack Type	Continuous					
Time	Ambient Temperature	Concrete Temperature	Chamber Temperature	Mass of Water Evaporated	Water Evaporation Rate	
Hours	*°C*	*°C*	*°C*	*g*	*kg/m²/hr*	Crack Width *mm*
0.5	20.966	24.050	23.437	1003.5	29.4	0.25
1	21.876	30.469	22.900	995.0	29.4	0.19
1.5	22.538	31.915	23.753	987.5	29.4	0.13
2	22.126	31.602	24.944	980.0	29.4	0.45
2.5	22.545	33.331	26.175	974.5	29.4	0.35
3	23.465	35.030	29.104	972.5	29.4	0.25
3.5	23.335	34.761	29.989	966.5	29.4	0.30
4	23.503	35.558	30.812	957.0	29.4	0.50
4.5	23.685	36.007	31.888	953.0	29.4	0.23
5	24.017	36.759	33.098	948.5	29.4	0.45
5.5	24.235	37.559	34.164	944.5	29.4	0.15
6	24.509	37.528	35.237	941.5	29.4	0.10

Environmental Chamber Test						
Mix Code	C0-5L					
Date						
Crack Time	3.5	hours				
Crack Type	Not Continuous					
Time	Ambient Temperature	Concrete Temperature	Chamber Temperature	Mass of Water Evaporated	Water Evaporation Rate	
Hours	*°C*	*°C*	*°C*	*g*	*kg/m²/hr*	Crack Width *mm*
0.5	21.068	27.299	22.335	984.5	29.4	0.10
1	21.409	28.164	22.183	981.5	29.4	0.08
1.5	21.534	30.079	22.388	978.0	29.4	0.10
2	21.959	31.108	22.931	975.0	29.4	0.08
2.5	21.957	32.150	23.866	972.5	29.4	0.00
3	22.210	32.511	25.020	968.0	29.4	0.13
3.5	22.762	33.073	26.422	965.5	29.4	0.15
4	23.287	34.011	27.659	964.0	29.4	0.13
4.5	23.425	34.719	28.826	958.0	29.4	0.00
5	23.708	34.914	29.952	956.5	29.4	0.18
5.5	24.104	35.341	30.925	953.5	29.4	0.10
6	24.076	35.692	31.967	950.0	29.4	0.10

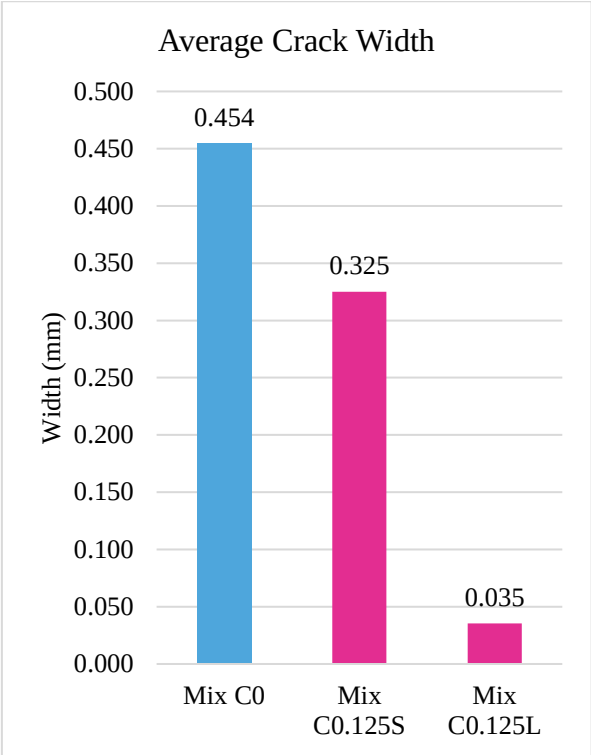
Average Crack Width
0.500
0.450
0.400
0.350
0.300
0.250
0.200
0.150
0.100
0.050
0.000
Width (mm)
0.454
0.325
0.035
Mix C0
Mix C0.125S
Mix C0.125L

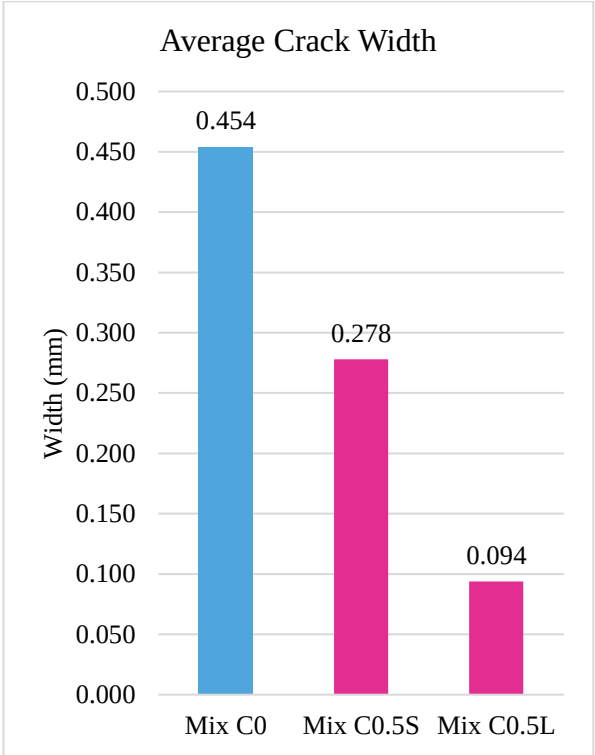
Average Crack Width
0.500
0.450
0.400
0.350
0.300
0.250
0.200
0.150
0.100
0.050
0.000
Width (mm)
0.454
0.278
0.094
Mix C0
Mix C0.5S
Mix C0.5L

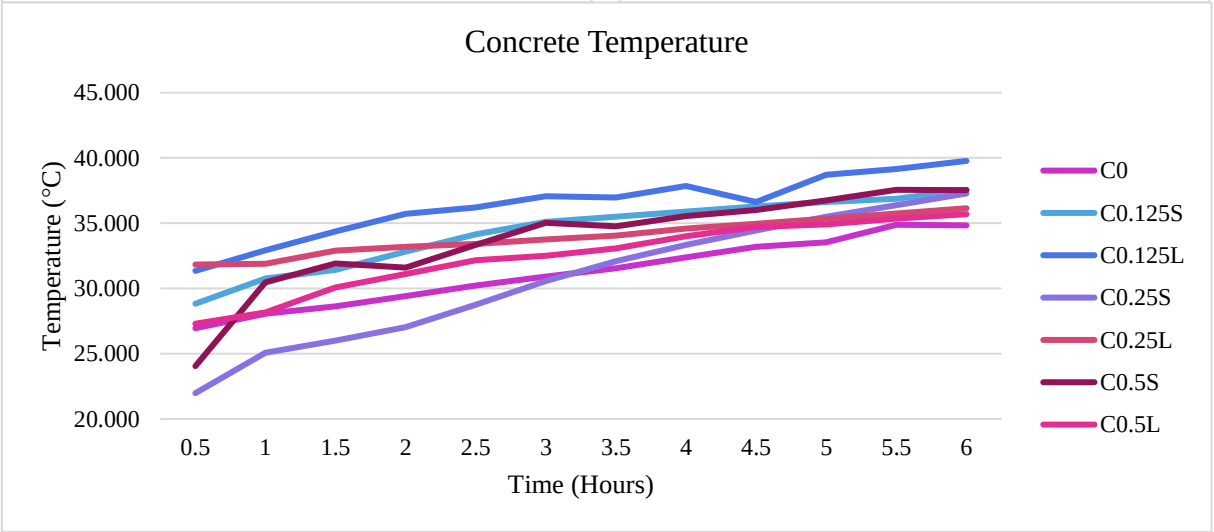
Concrete Temperature
45.000
40.000
35.000
30.000
25.000
20.000
Temperature (°C)
0.5
1
1.5
2
2.5
3
3.5
4
4.5
5
5.5
6
Time (Hours)
C0
C0.125S
C0.125L
C0.25S
C0.25L
C0.5S
C0.5L

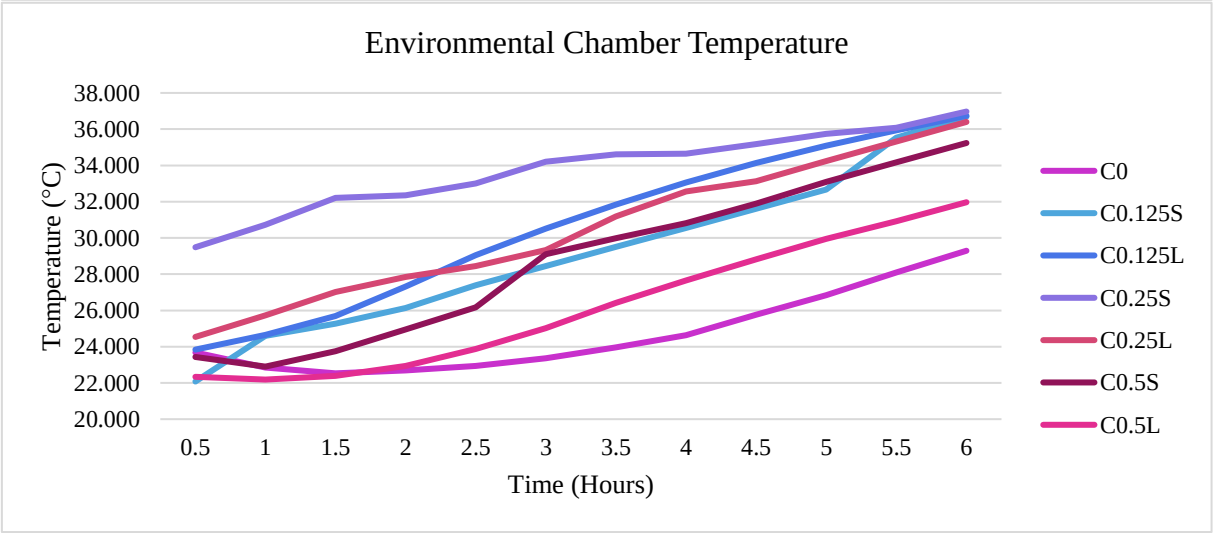
Environmental Chamber Temperature
38.000
36.000
34.000
32.000
30.000
28.000
26.000
24.000
22.000
20.000
Temperature (°C)
0.5
1
1.5
2
2.5
3
3.5
4
4.5
5
5.5
6
Time (Hours)
C0
C0.125S
C0.125L
C0.25S
C0.25L
C0.5S
C0.5L

Mix Code	Time of Crack Formation	Crack Weighting
	hours	*mm²*
M0	5	30
M0.125S	-	-
M0.25S	-	-
M0.5S	-	-

M0 – Crack Formation

M0.125S – No Crack Formed

M0.25S – No Crack Formed

M0.5S – No Crack Formed

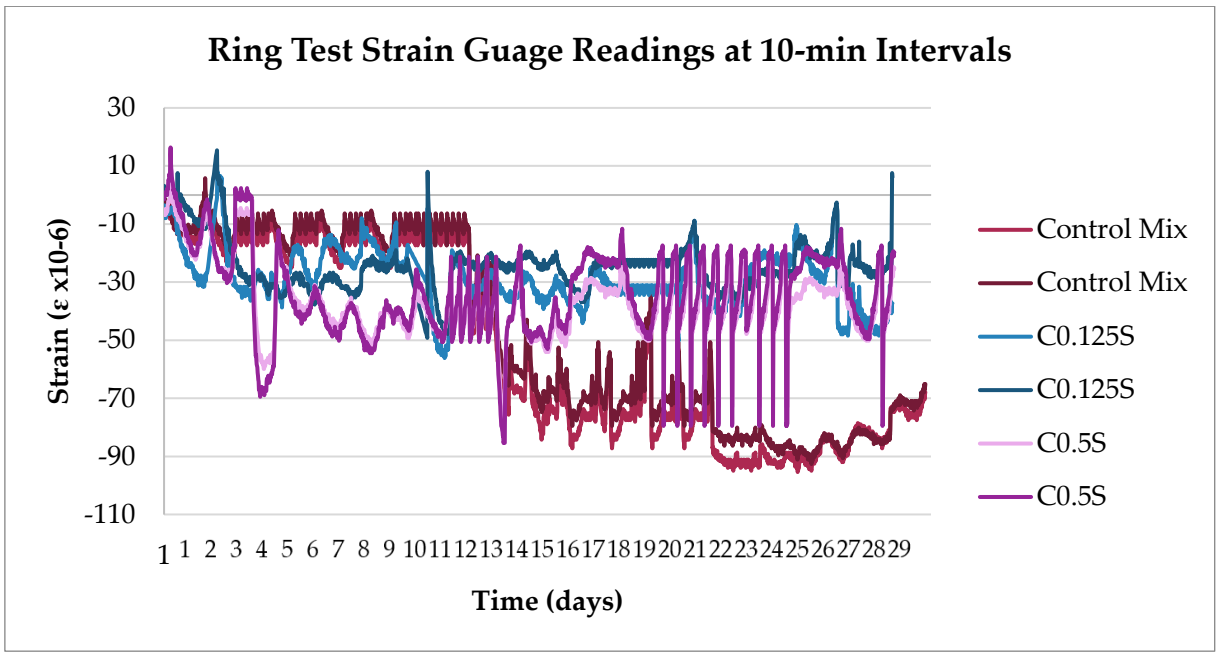
Ring Test Strain Guage Readings at 10-min Intervals
Strain (ε x10-6)
30
10
-10
-30
-50
-70
-90
-110
1 1 2 3 4 5 6 7 8 9 10 11 12 13 14 15 16 17 18 19 20 21 22 23 24 25 26 27 28 29
Time (days)
Control Mix
Control Mix
C0.125S
C0.125S
C0.5S
C0.5S

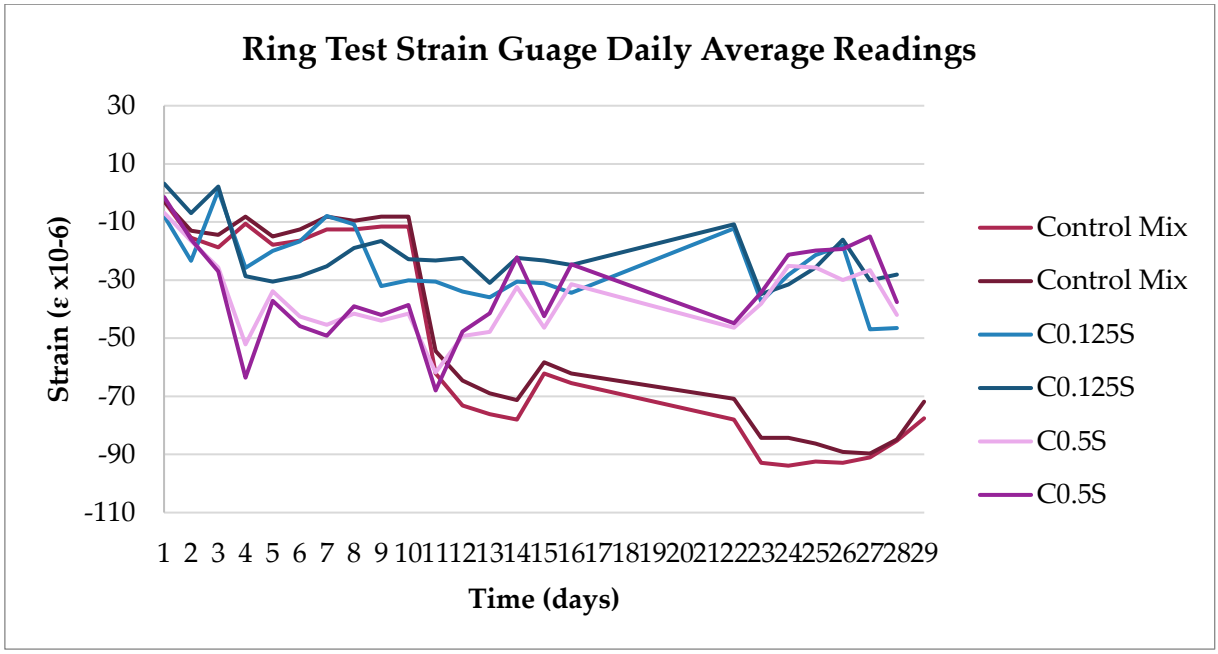
Ring Test Strain Guage Daily Average Readings
Strain (ε x10-6)
30
10
-10
-30
-50
-70
-90
-110
1 2 3 4 5 6 7 8 9 10 11 12 13 14 15 16 17 18 19 20 21 22 23 24 25 26 27 28 29
Time (days)
Control Mix
Control Mix
C0.125S
C0.125S
C0.5S
C0.5S

Mortar Mechanical Properties

	Density			UPV		
	kg/m³	*kg/m³*	*kg/m³*	*μs*	*μs*	*μs*
Mix Code	**3 days**	**7 days**	**28 days**	**3 days**	**7 days**	**28 days**
M0	2.0731	2.12831	2.20419	39.5	37.8	35
M15-0.25	2.29062	2.30253	2.30679	35.7	34.8	33.3
M25-0.25	2.23272	2.23921	2.23233	37.7	36.8	34.8
M35-0.25	2.26223	2.27364	2.20084	37.7	35.2	35.8
M50-0.25	2.21173	2.28788	2.23785	37.8	34.9	33.5
M15-0.50	2.23095	2.28339	2.282	35.9	34.9	33.5
M25-0.50	2.33748	2.36223	2.3647	35.2	34.3	32.4
M35-0.50	2.30999	2.30507	2.33709	34.9	33.4	33.4
M50-0.50	2.29452	2.3676	2.30562	36.2	34.4	33.7
M15-0.75	2.30048	2.32548	2.33264	34.8	34.2	33.8
M25-0.75	2.21757	2.24351	2.26141	36.7	35.7	34.6
M35-0.75	2.26717	2.22151	2.28088	37	36.6	34.2
M50-0.75	2.28282	2.25038	2.27961	37	36.3	34.8
M15-1	2.3386	2.28496	2.35036	36.1	35.7	33.7
M25-1	2.23371	2.21523	2.31162	38.2	36.9	33.8
M35-1	2.2266	2.1826	2.17935	39.8	37.4	35.6
M50-1	2.17889	2.16761	2.16548	38.3	39.3	36.4

	Flexural Strength			Compressive Strength		
	MPa	*MPa*	*MPa*	*MPa*	*MPa*	*MPa*
Mix Code	**3 days**	**7 days**	**28 days**	**3 days**	**7 days**	**28 days**
M0	5.72097	6.72842	8.61819	23.3438	36.4313	45.8150
M15-0.25	6.81014	6.59856	7.31176	32.2406	36.2969	43.1969
M25-0.25	6.33467	5.81905	7.55390	28.6531	35.5938	40.4469
M35-0.25	6.88337	7.47891	7.46822	31.1250	38.0188	40.0938
M50-0.25	6.60423	7.13851	7.99461	29.1938	37.7250	45.2313
M15-0.50	7.30352	7.76691	9.80816	36.6563	41.9250	48.1969
M25-0.50	7.39706	7.07888	9.62131	36.2719	41.3156	47.3313
M35-0.50	7.38606	7.72054	8.11904	37.2125	41.7156	43.1406
M50-0.50	5.93914	6.42728	7.44626	30.2563	38.4250	40.2781
M15-0.75	7.80780	6.73244	8.44506	40.5906	43.7875	50.9625
M25-0.75	7.09000	7.03679	8.99317	32.8875	38.6250	41.6188
M35-0.75	6.97479	7.28447	8.60196	32.6344	36.3438	43.9531
M50-0.75	6.80890	7.29536	8.49443	31.2656	36.6969	42.0531
M15-1	8.05051	7.66733	8.53635	32.9156	42.0594	49.1063
M25-1	6.79234	6.89048	8.02404	33.6438	38.6906	40.6188
M35-1	6.36306	6.61905	7.50236	24.4906	28.9063	33.8031
M50-1	6.54289	6.51000	6.40521	20.8000	29.5406	28.9594

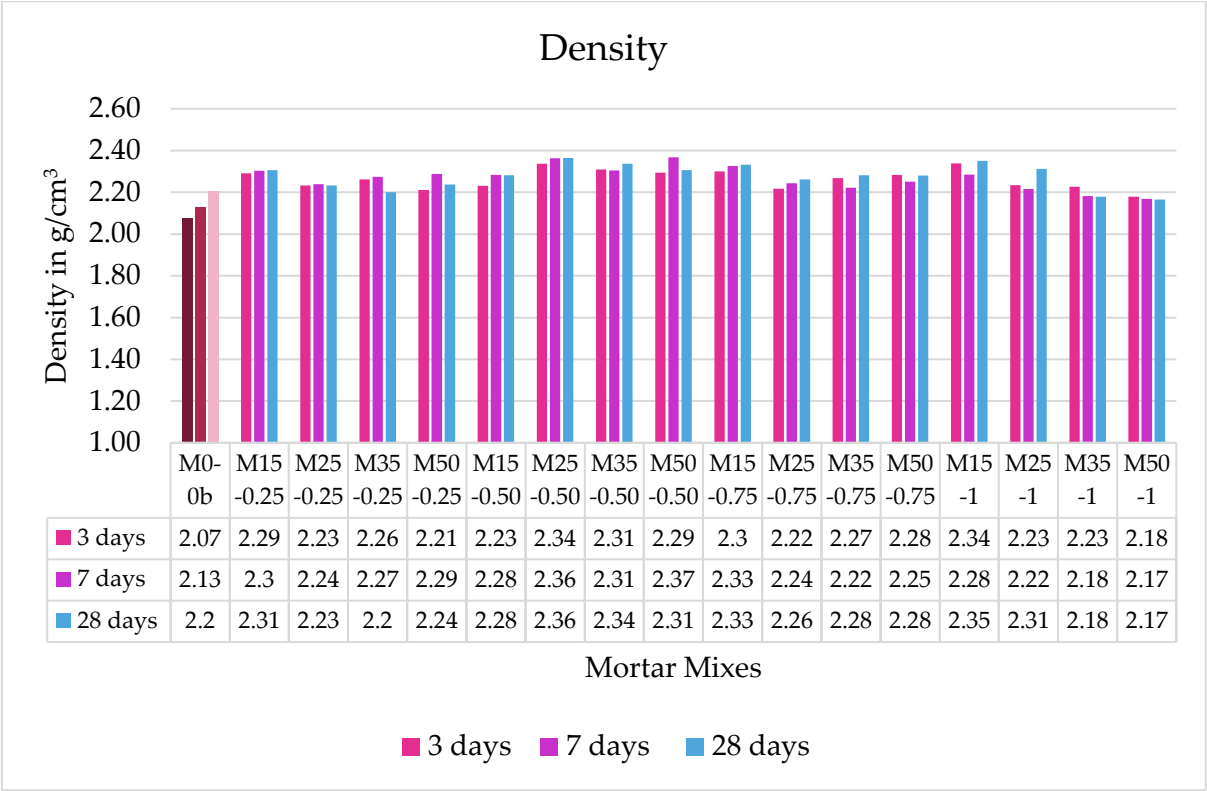

	M0-0b	M15-0.25	M25-0.25	M35-0.25	M50-0.25	M15-0.50	M25-0.50	M35-0.50	M50-0.50	M15-0.75	M25-0.75	M35-0.75	M50-0.75	M15-1	M25-1	M35-1	M50-1
3 days	2.07	2.29	2.23	2.26	2.21	2.23	2.34	2.31	2.29	2.3	2.22	2.27	2.28	2.34	2.23	2.23	2.18
7 days	2.13	2.3	2.24	2.27	2.29	2.28	2.36	2.31	2.37	2.33	2.24	2.22	2.25	2.28	2.22	2.18	2.17
28 days	2.2	2.31	2.23	2.2	2.24	2.28	2.36	2.34	2.31	2.33	2.26	2.28	2.28	2.35	2.31	2.18	2.17

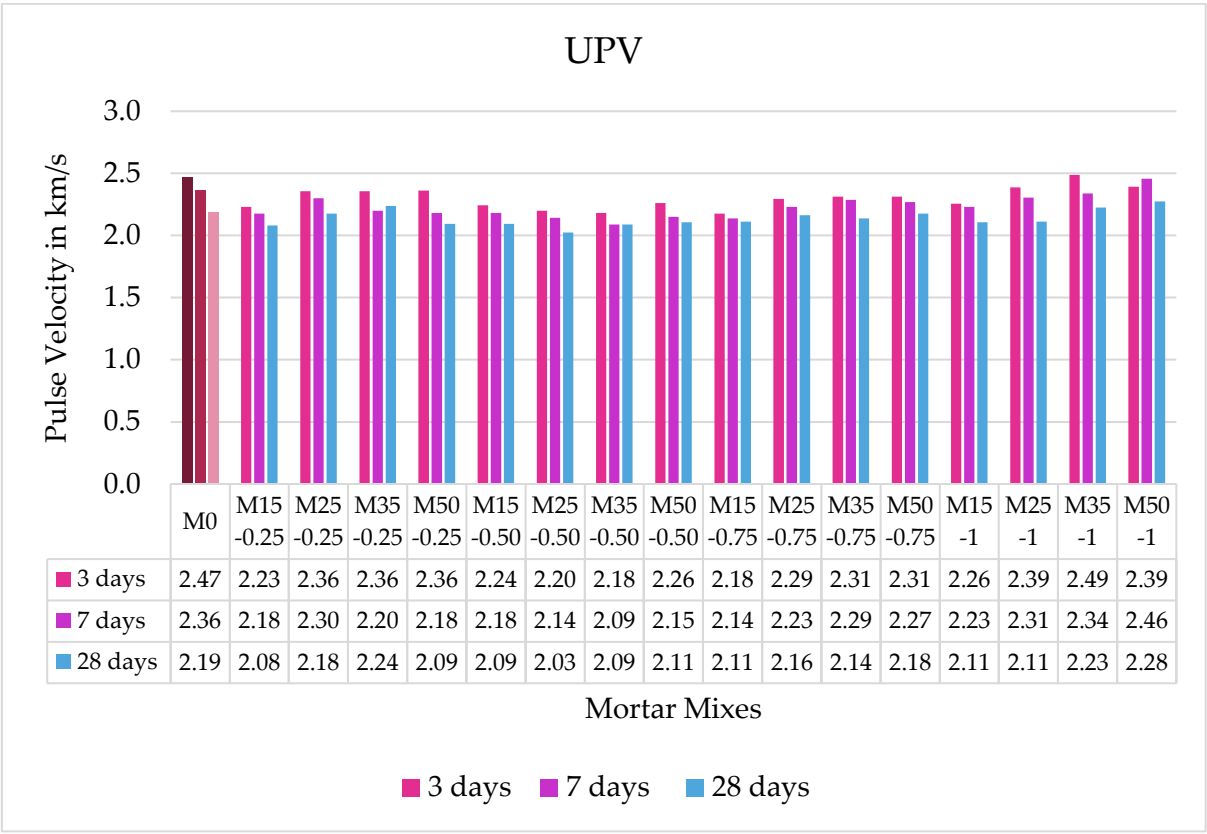

	M0	M15-0.25	M25-0.25	M35-0.25	M50-0.25	M15-0.50	M25-0.50	M35-0.50	M50-0.50	M15-0.75	M25-0.75	M35-0.75	M50-0.75	M15-1	M25-1	M35-1	M50-1
3 days	2.47	2.23	2.36	2.36	2.36	2.24	2.20	2.18	2.26	2.18	2.29	2.31	2.31	2.26	2.39	2.49	2.39
7 days	2.36	2.18	2.30	2.20	2.18	2.18	2.14	2.09	2.15	2.14	2.23	2.29	2.27	2.23	2.31	2.34	2.46
28 days	2.19	2.08	2.18	2.24	2.09	2.09	2.03	2.09	2.11	2.11	2.16	2.14	2.18	2.11	2.11	2.23	2.28

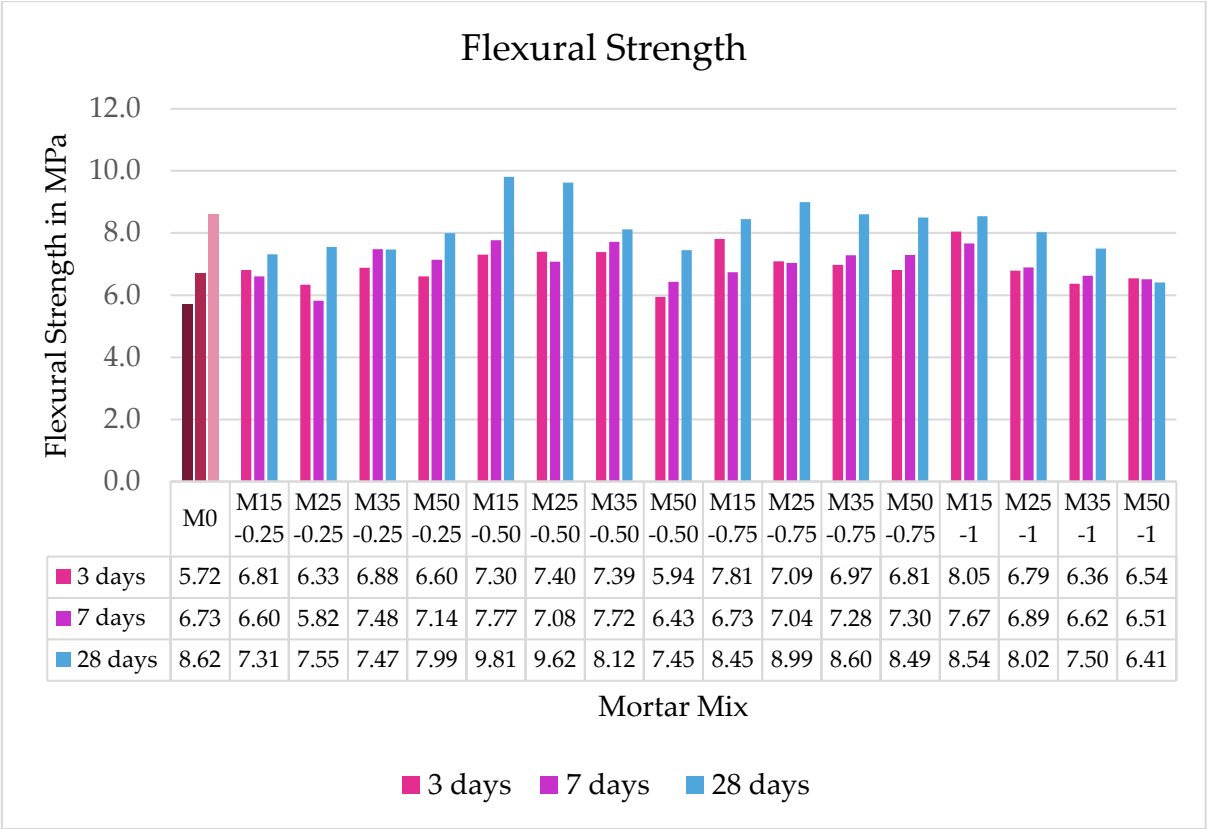

	M0	M15 -0.25	M25 -0.25	M35 -0.25	M50 -0.25	M15 -0.50	M25 -0.50	M35 -0.50	M50 -0.50	M15 -0.75	M25 -0.75	M35 -0.75	M50 -0.75	M15 -1	M25 -1	M35 -1	M50 -1
3 days	5.72	6.81	6.33	6.88	6.60	7.30	7.40	7.39	5.94	7.81	7.09	6.97	6.81	8.05	6.79	6.36	6.54
7 days	6.73	6.60	5.82	7.48	7.14	7.77	7.08	7.72	6.43	6.73	7.04	7.28	7.30	7.67	6.89	6.62	6.51
28 days	8.62	7.31	7.55	7.47	7.99	9.81	9.62	8.12	7.45	8.45	8.99	8.60	8.49	8.54	8.02	7.50	6.41

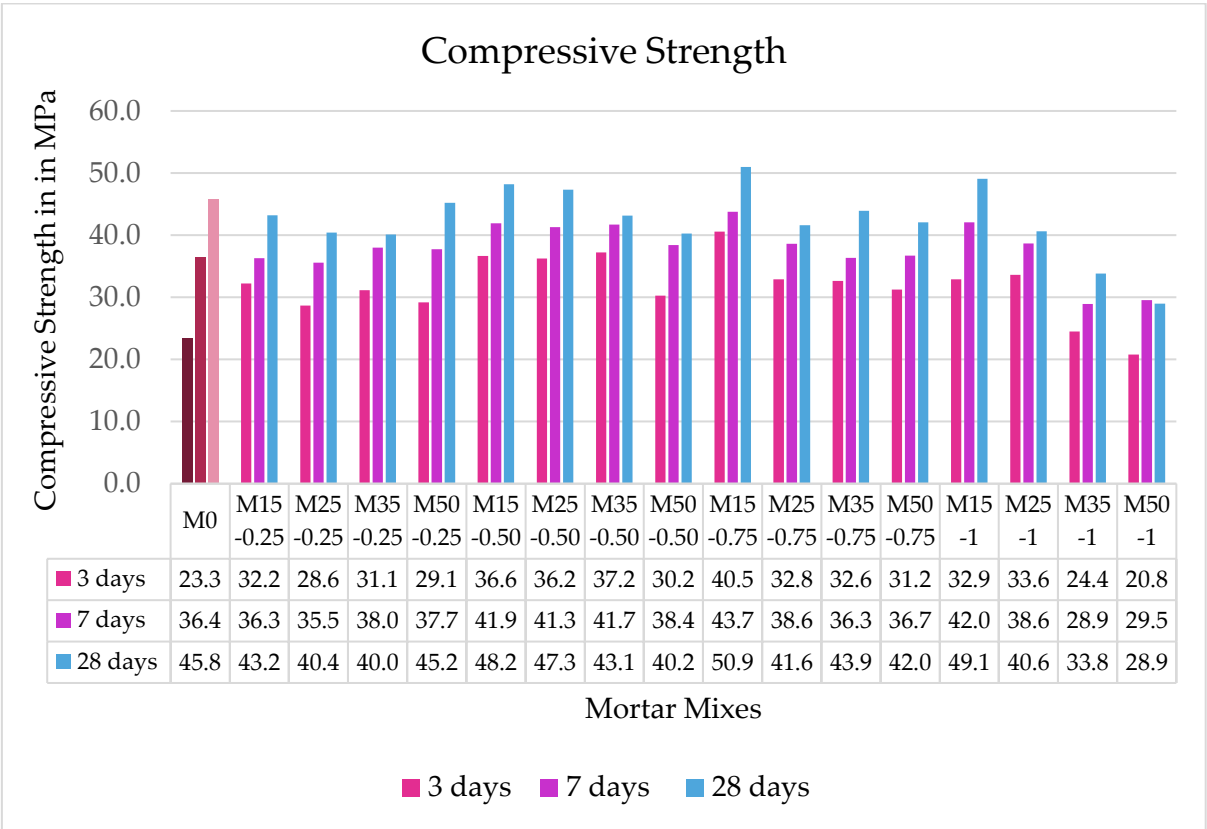

	M0	M15 -0.25	M25 -0.25	M35 -0.25	M50 -0.25	M15 -0.50	M25 -0.50	M35 -0.50	M50 -0.50	M15 -0.75	M25 -0.75	M35 -0.75	M50 -0.75	M15 -1	M25 -1	M35 -1	M50 -1
3 days	23.3	32.2	28.6	31.1	29.1	36.6	36.2	37.2	30.2	40.5	32.8	32.6	31.2	32.9	33.6	24.4	20.8
7 days	36.4	36.3	35.5	38.0	37.7	41.9	41.3	41.7	38.4	43.7	38.6	36.3	36.7	42.0	38.6	28.9	29.5
28 days	45.8	43.2	40.4	40.0	45.2	48.2	47.3	43.1	40.2	50.9	41.6	43.9	42.0	49.1	40.6	33.8	28.9

Mechanical Concrete Properties

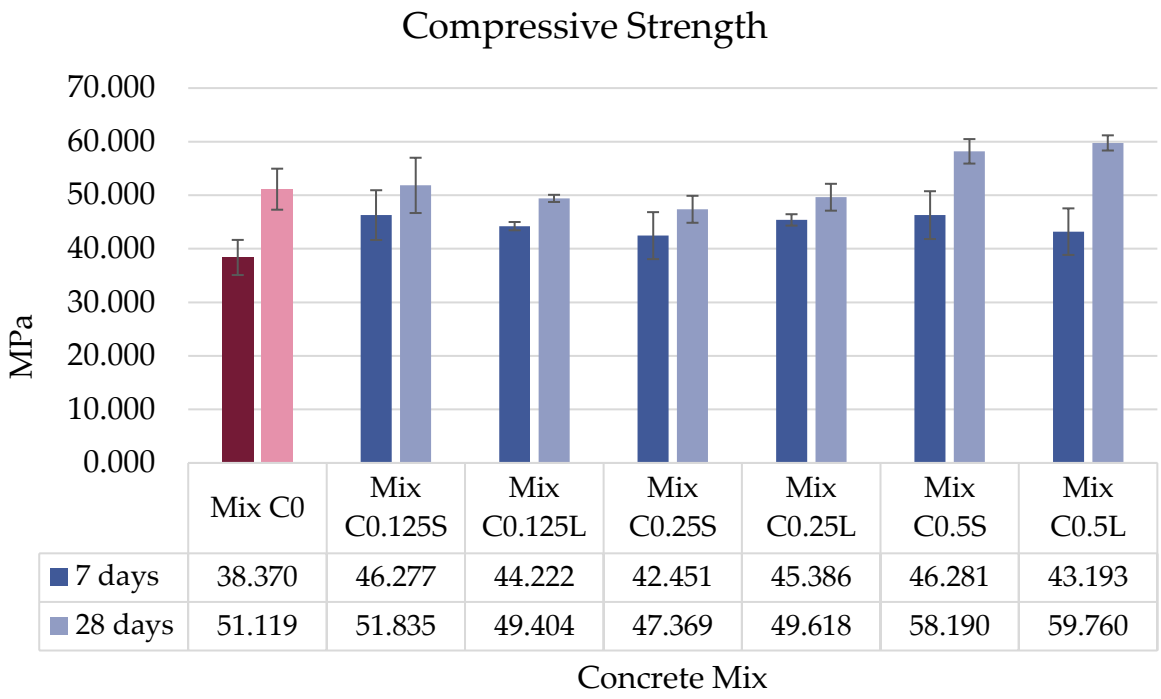

	Mix C0	Mix C0.125S	Mix C0.125L	Mix C0.25S	Mix C0.25L	Mix C0.5S	Mix C0.5L
7 days	38.370	46.277	44.222	42.451	45.386	46.281	43.193
28 days	51.119	51.835	49.404	47.369	49.618	58.190	59.760

Compressive Tests 7 days												
	#	L *mm*	B *mm*	H *mm*	Volume mm^3	Mass (air) *g*	Mass (water) *g*	Density g/cm^3	Density kg/m^3	Max Load *kN*	N/mm²	**AVERAGE** **N/mm^2**
Mix C0	A	101.84	100.37	100.59	1028198.872	2371.69	-	2.3066	2.3066	410.8	40.689	**38.370**
	B	102.97	100.45	100.21	1036505.751	2386.62	-	2.3026	2.3026	362.9	36.052	
Mix C0.125S	A	100.13	100.14	101.84	1021151.533	2518.96	1021.46	2.4668	2.466784	454.7	44.586	**46.277**
	B	100.21	100.16	100.96	1013338.912	2494.18	1014.56	2.4613	2.461348	431.9	42.711	
	C	100.04	99.88	100.56	1004795.037	2484.12	1011.54	2.4723	2.472265	517.6	51.534	
Mix C0.125L	A	100.18	100.28	100.25	1007116.553	2323.93	1016.11	2.4668	2.4668	450.7	44.832	**44.222**
	B	100.2	100.32	100.13	1006513.168	2321.84	1012.98	2.4613	2.4613	435.5	43.355	
	C	101.61	101.84	100.25	1037383.231	2386.3	1018.37	2.4723	2.4723	454.1	44.478	
Mix C0.25S	A	101.46	100.14	99.93	1015309.226	2347.41	1013.68	2.3075	2.3075	388.6	38.833	**42.421**
	B	100.04	97.18	100.71	979091.260	2378.04	980.58	2.3068	2.3068	463	47.308	
	C	98.7	100.68	101.23	1005934.253	2317.95	1003.41	2.3003	2.3003	419.1	41.121	
Mix C0.25L	A	100.17	96.63	100.56	973363.189	2379.84	983.56	2.3939	2.3939	452.2	46.536	**45.386**
	B	100.27	99.14	100.08	994872.041	2428.63	1000.97	2.4080	2.4080	440.9	44.437	
	C	99.94	100.63	100.11	1006802.486	2464.42	1017.48	2.3363	2.3363	455.2	45.185	
Mix C0.5S	A	98.13	100.23	100.05	984048.768	2409.63	992.37	2.4450	2.4450	309.3	30.844	**46.281**
	B	100.35	100.2	100.07	1006210.855	2442.87	1000.56	2.4411	2.4411	223.7	22.310	
	C	100.15	100.06	99.71	999194.807	2436.74	999.38	2.4478	2.4478	256.3	25.689	
Mix C0.5L	A	100.38	99.85	99.78	1000089.253	2473.53	1008.7	2.4272	2.4272	445.1	44.675	**43.193**
	B	100.14	100.08	99.98	1002000.680	2403.81	991.67	2.4277	2.4277	383.2	38.297	
	C	100.37	100.22	99.34	999269.146	2422.89	994.42	2.4490	2.4490	464	46.606	

Compressive Tests 28 days												
	#	L *mm*	B *mm*	H *mm*	Volume mm^3	Mass (air) *g*	Mass (water) *g*	Density g/cm^3	Density kg/m^3	Max Load *kN*	N/mm^2	**AVERAGE** N/mm^2
Mix C0	A	100.25	99.84	100.18	1002697.613	2385.25	1005.25	2.3788	2.3788	484.2	48.410	**51.119**
	B	100.36	100.38	99.94	1006809.232	2411.12	1011.46	2.3948	2.3948	540.0	53.828	
Mix C0.125S	A	100.32	100.46	101.28	1020714.748	2514.50	1017.13	2.4635	2.4635	566.3	55.658	**51.835**
	B	100.12	99.98	100.46	1005604.359	2434.69	997.46	2.4211	2.4211	541.2	53.883	
	C	100.48	100.62	99.96	1010625.348	2464.45	1012.25	2.4385	2.4385	462.3	45.964	
Mix C0.125L	A	100.23	100.18	100.32	1007317.273	2336.39	1003.02	2.3194	2.3194	489.7	48.726	**49.404**
	B	100.06	101.24	100.39	1016958.169	2381.00	1018.37	2.3413	2.3413	508.8	50.062	
	C	100.18	101.65	100.24	1020773.691	2430.46	1026.08	2.3810	2.3810	503.6	49.424	
Mix C0.25S	A	100.05	100.72	99.9	1006695.896	2345.13	1012.12	2.3295	2.3295	382.1	37.975	**37.537**
	B	100.04	100.15	100.08	1002702.120	2458.47	1008.92	2.4518	2.4518	399.0	39.808	
	C	99.82	99.55	100.14	995099.291	2429.13	996.21	2.4411	2.4411	347.2	34.828	
Mix C0.25L	A	100.15	100.08	99.88	1001098.439	2472.14	1047.48	2.4694	2.4694	468.6	46.879	**49.618**
	B	100.08	100.04	99.45	995693.718	2369.30	1006.88	2.3795	2.3795	499.2	50.176	
	C	100.42	100.44	99.62	1004785.730	2425.78	999.84	2.4142	2.4142	518.3	51.800	
Mix C0.5S	A	100.15	100.44	98.89	994741.037	2447.95	990.34	2.4609	2.4609	593.5	59.753	**58.190**
	B	100.28	100.52	100.64	1014465.853	2474.29	1013.00	2.4390	2.4390	599.4	59.251	
	C	100.02	100.18	100.26	1004605.561	2430.34	998.50	2.4192	2.4192	558.1	55.565	
Mix C0.5L	A	98.67	100.14	100.08	988871.845	2425.77	994.08	2.4531	2.4531	602.9	60.158	**59.760**
	B	100.12	100.07	100.02	1002101.220	2468.59	1008.85	2.4634	2.4634	582.4	58.188	
	C	99.52	100.24	100.16	999184.622	2431.62	996.28	2.4336	2.4336	611.8	60.936	

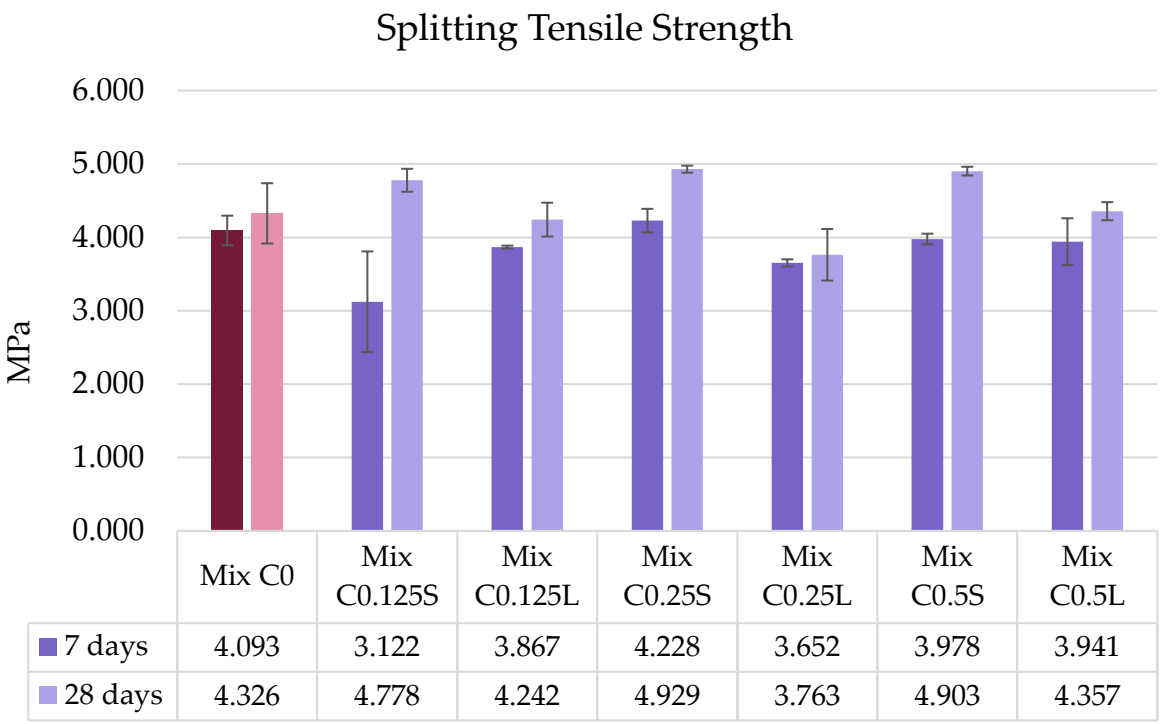

	Mix C0	Mix C0.125S	Mix C0.125L	Mix C0.25S	Mix C0.25L	Mix C0.5S	Mix C0.5L
7 days	4.093	3.122	3.867	4.228	3.652	3.978	3.941
28 days	4.326	4.778	4.242	4.929	3.763	4.903	4.357

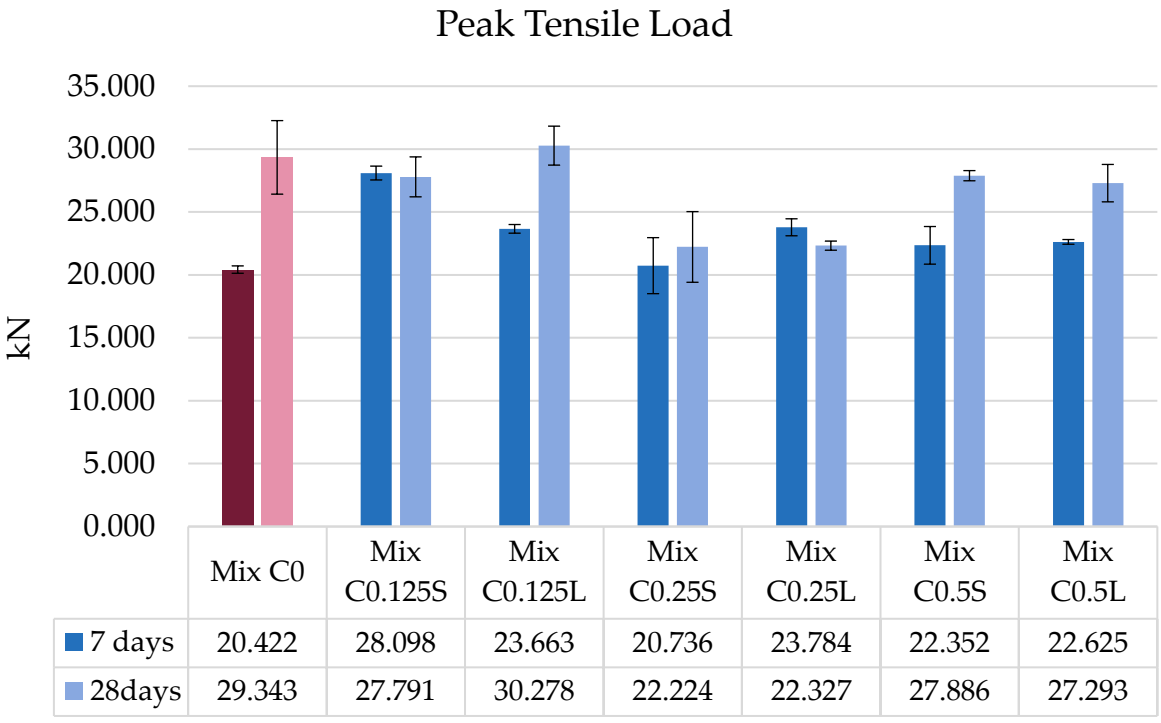

	Mix C0	Mix C0.125S	Mix C0.125L	Mix C0.25S	Mix C0.25L	Mix C0.5S	Mix C0.5L
7 days	20.422	28.098	23.663	20.736	23.784	22.352	22.625
28days	29.343	27.791	30.278	22.224	22.327	27.886	27.293

Splitting Tensile Tests 7 days										
	#	D	H	Volume	Mass (air)	Density	Max Load		Calculation	**AVERAGE**
		mm	*mm*	mm^3	*g*	g/cm^3	*kN*	*MPa*		***MPa***
Mix C0	A	152.2	305.7	5561790	13055	2.3473	288.7	4.08	3.950179362	**4.093**
	B	152.6	302.8	5538024	12990	2.3456	307.5	4.35	4.23657441	
Mix C0.125S	A	153.28	300.35	5542280	13355	2.4097	190.7	2.7	2.637045893	**3.122**
	B	152.36	299.62	5462640	13400	2.4530	258.7	3.66	3.607736315	
Mix C0.125L	A	153.19	300.27	5534299	12800	2.3128	278.4	3.94	3.85307084	**3.867**
	B	151.97	305.73	5545538	12895	2.3253	283.3	4.01	3.881778745	
Mix C0.25S	A	152.8	290	5317832	12990	2.4427	302.2	4.28	4.341634212	**4.228**
	B	152.1	300.1	5452734	13005	2.3850	295	4.17	4.114403962	
Mix C0.25L	A	152.32	300.8	5481275	13050	2.3808	265.3	3.75	3.686231534	**3.652**
	B	152.43	301.85	5508355	13100	2.3782	261.4	3.7	3.616796522	
Mix C0.5S	A	152.72	300.78	5509734	13365	2.4257	283.3	4.01	3.926285057	**3.978**
	B	151.79	301.57	5457130	13475	2.4692	289.7	4.1	4.029000499	
Mix C0.5L	A	150.22	298.84	5296441	13005	2.4554	293.8	4.16	4.166442849	**3.941**
	B	152.38	302.68	5519879	13580	2.4602	269.2	3.81	3.715724311	

Splitting Tensile Tests 28 days										
	#	D	H	Volume	Mass (air)	Density	Max Load		Calculation	**AVERAGE**
		mm	*mm*	*mm³*	*g*	*g/cm³*	*kN*	*MPa*		***MPa***
Mix C0	A	151.25	309.86	5567320	13255	2.3809	339.9	4.81	4.617112	**4.326**
	B	152.32	307.05	5595164	13220	2.3628	296.5	4.19	4.035885	
Mix C0.125S	A	152.03	301.35	5470407	13595	2.4852	351.8	4.98	4.888498	**4.778**
	B	151.76	302.87	5478489	13575	2.4779	337	4.77	4.66763	
Mix C0.125L	A	152.11	301.47	5478347	12970	2.3675	293.8	4.16	4.078778	**4.242**
	B	151.37	300.96	5415995	12690	2.3431	315.2	4.46	4.404714	
Mix C0.25S	A	151.72	296.42	5358991	13215	2.4659	350.6	4.96	4.962971	**4.929**
	B	152.68	297.86	5453388	13300	2.4389	349.7	4.95	4.895324	
Mix C0.25L	A	152.34	300.14	5470684	13415	2.4522	252.4	3.57	3.514242	**3.763**
	B	151.82	301.48	5457659	13420	2.4589	288.4	4.08	4.011325	
Mix C0.5S	A	151.11	295.65	5302176	13215	2.4659	347	4.91	4.944684	**4.903**
	B	152.69	302.09	5531557	13300	2.4389	352.2	4.98	4.860965	
Mix C0.5L	A	152.44	301.47	5502143	13555	2.4636	308.2	4.36	4.269428	**4.357**
	B	151.32	302.46	5439394	13555	2.4920	319.5	4.52	4.444129	

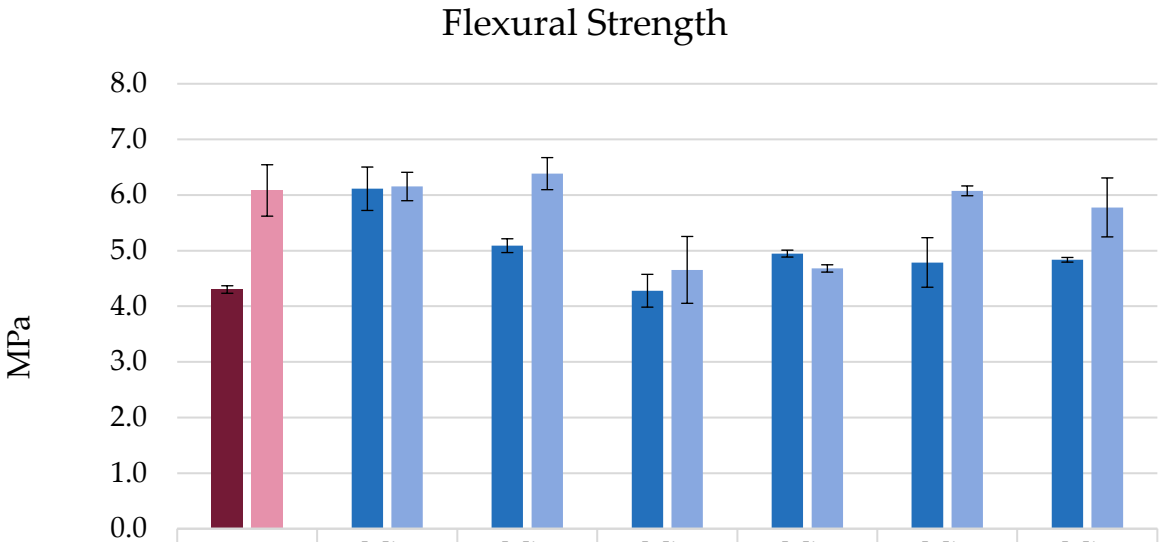

	Mix C0	Mix C0.125S	Mix C0.125L	Mix C0.25S	Mix C0.25L	Mix C0.5S	Mix C0.5L
7 days	4.301	6.113	5.089	4.279	4.947	4.787	4.835
28 days	6.082	6.153	6.384	4.654	4.680	6.075	5.776

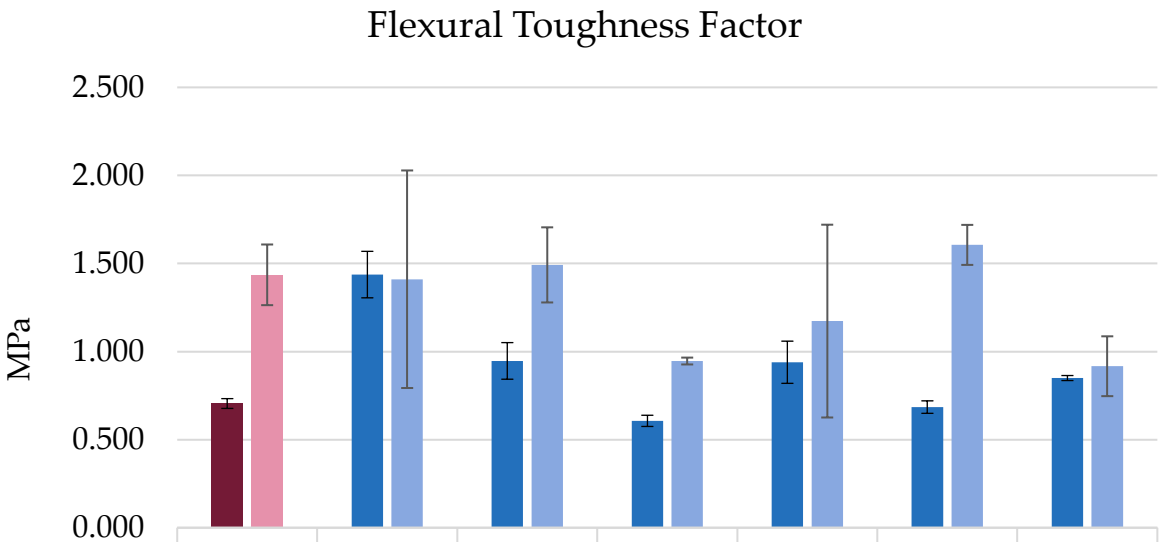

	Mix C0	Mix C0.125S	Mix C0.125L	Mix C0.25S	Mix C0.25L	Mix C0.5S	Mix C0.5L
7 days	0.705	1.437	0.947	0.607	0.939	0.685	0.850
28 days	1.436	1.411	1.492	0.946	1.173	1.606	0.917

Flexural Strength Tests 7 days								
	#	L mm	B mm	H mm	Volume mm^3	Max Load kN	Strength N/mm^2	**AVG** ***N/mm²***
Mix C0	A	554.1	154.1	152.1	12987333.8	20.2157	4.252934275	**4.301**
	B	554.9	151.2	153.4	12870394.99	20.6291	4.348498204	
Mix C0.125S	A	553.2	151.57	153.26	12850624.79	27.7069	5.836853232	**6.113**
	B	554.1	151.17	148.73	12458115.16	28.4884	6.389486063	
Mix C0.125L	A	554.5	149.97	151.97	12637576.73	23.9056	5.176546244	**5.089**
	B	554.1	148.96	153.55	12673822.91	23.4199	5.001227475	
Mix C0.25S	A	554.5	149.75	158.2	13070563.1	22.3106	4.487175157	**4.279**
	B	553.7	148.10	154.4	12661258.57	19.1619	4.070519205	
Mix C0.25L	A	551.3	148.14	153.76	12557514.93	23.3067	4.990937836	**4.947**
	B	550.5	157.05	153.72	13290020.16	24.2616	4.903232267	
Mix C0.5S	A	551.3	149.97	151.47	13325492.16	23.4081	5.102352419	**4.787**
	B	550.1	151.54	153.51	12769907.26	21.2951	4.472402776	
Mix C0.5L	A	545	153.5	151.22	3517816.555	22.4929	4.80596519	**4.835**
	B	547	153.42	151.22	12690494.3	22.7565	4.864813877	

Flexural Strength Toughness Tests 28 days								
	#	L mm	B mm	H mm	Volume mm^3	Max Load kN	Strength N/mm^2	**AVG** ***N/mm²***
Mix C0	A	556.2	156.15	153.43	13325492.16	31.4095	6.408553997	**6.082**
	B	553.1	149.97	153.95	12769907.26	27.2769	5.755615836	
Mix C0.125S	A	553.5	146.15	151.38	12245737.5	26.6686	5.972072054	**6.153**
	B	548.7	145.09	153.62	12229823.85	28.9138	6.333346789	
Mix C0.125L	A	548.1	151.46	152.91	12693858.21	29.1837	6.180609926	**6.384**
	B	551.5	152.03	153.27	12850853.41	31.3724	6.588170935	
Mix C0.25S	A	554.2	151.25	153.75	12887747.81	24.2100	5.078441026	**4.654**
	B	553.1	152.66	153.34	12947453.96	20.2380	4.228565096	
Mix C0.25L	A	552.1	148.14	153.76	12575737.33	22.0702	4.726156576	**4.680**
	B	548.1	154.64	153.75	13031570.79	22.5838	4.633464747	
Mix C0.5S	A	555	151	151	12654555	28.1723	6.13694578	**6.075**
	B	555	151	151	12654555	27.5999	6.012264368	
Mix C0.5L	A	554	147.66	152.99	12515138.88	28.3451	6.151059352	**5.776**
	B	556	154.09	153.77	13174097.13	26.2411	5.401648338	

Flexural Toughness Factor Calculations 7 days																
		Graph Width	Graph Height	Area Under Graph	Length of Beam	dtb	l	b	h	h^2	Tb/dtb	bh^2	l/bh^2	**σb**		**AVG**
	#	*m*	*kN*		*m*		*m*	*m*	*m*	m^2					*MPa*	***MPa***
Mix C0	A	1.889	20.216	19.089	0.554	0.004	0.500	0.154	0.152	0.023	5167.597	0.004	140.252	724765.540	0.725	**0.705**
	B	1.749	20.629	18.043	0.555	0.004	0.500	0.151	0.153	0.024	4877.399	0.004	140.529	685418.458	0.685	
Mix C0.125S	A	2.901	27.707	40.191	0.553	0.004	0.500	0.152	0.153	0.023	10897.791	0.004	140.443	1530514.971	1.531	**1.437**
	B	2.331	28.488	33.199	0.554	0.004	0.500	0.151	0.149	0.022	8987.239	0.003	149.523	1343796.544	1.344	
Mix C0.125L	A	2.186	23.906	26.134	0.555	0.004	0.500	0.150	0.152	0.023	7069.593	0.003	144.361	1020573.473	1.021	**0.947**
	B	1.936	23.420	22.668	0.554	0.004	0.500	0.149	0.154	0.024	6136.557	0.004	142.364	873625.900	0.874	
Mix C0.25S	A	1.444	22.311	16.109	0.555	0.004	0.500	0.149	0.158	0.025	4357.608	0.004	134.082	584277.181	0.584	**0.607**
	B	1.712	19.162	16.401	0.554	0.004	0.500	0.148	0.154	0.024	4443.000	0.004	141.619	629211.498	0.629	
Mix C0.25L	A	1.888	23.307	22.007	0.551	0.004	0.500	0.148	0.154	0.024	5987.652	0.004	142.761	854805.889	0.855	**0.939**
	B	2.300	24.262	27.897	0.551	0.004	0.500	0.157	0.154	0.024	7601.467	0.004	134.732	1024162.162	1.024	
Mix C0.5S	A	1.426	23.408	16.689	0.551	0.004	0.500	0.150	0.151	0.023	4540.911	0.003	145.316	659865.333	0.660	**0.685**
	B	1.746	21.295	18.592	0.550	0.004	0.500	0.152	0.154	0.024	5069.552	0.004	140.013	709804.909	0.710	
Mix C0.5L	A	1.905	22.493	21.419	0.545	0.004	0.500	0.154	0.151	0.023	5895.189	0.004	142.444	839732.298	0.840	**0.850**
	B	1.934	22.756	22.004	0.547	0.004	0.500	0.153	0.151	0.023	6034.094	0.004	142.518	859966.676	0.860	

Flexural Toughness Factor Calculations 28 days																
		Graph Width	Graph Height	Area Under Graph	Length of Beam	dtb	l	b	h	h^2	Tb/dtb	bh^2	l/bh^2	**σb**		**AVG**
	#	*m*	*kN*		*m*		*m*	*m*	*m*	m^2					*MPa*	***MPa***
Mix C0	A	2.431	31.410	38.172	0.556	0.004	0.500	0.156	0.153	0.024	10294.459	0.004	151.310	1557657.512	1.558	**1.436**
	B	2.283	27.277	31.139	0.553	0.004	0.500	0.150	0.154	0.024	8444.886	0.004	155.611	1314115.917	1.314	
Mix C0.125S	A	1.631	26.669	21.748	0.554	0.004	0.500	0.146	0.151	0.023	5893.866	0.003	165.265	974051.861	0.974	**1.411**
	B	2.917	28.914	42.171	0.549	0.004	0.500	0.145	0.154	0.024	11528.336	0.003	160.251	1847432.451	1.847	
Mix C0.125L	A	2.658	29.184	38.790	0.548	0.004	0.500	0.151	0.153	0.023	10615.705	0.004	154.771	1643005.151	1.643	**1.492**
	B	2.036	31.372	31.938	0.552	0.004	0.500	0.152	0.153	0.023	8686.638	0.004	154.419	1341385.493	1.341	
Mix C0.25S	A	1.891	24.210	22.888	0.554	0.004	0.500	0.151	0.154	0.024	6194.838	0.004	155.003	960220.268	0.960	**0.946**
	B	2.206	20.238	22.318	0.553	0.004	0.500	0.153	0.153	0.024	6052.675	0.004	154.088	932641.737	0.933	
Mix C0.25L	A	3.301	22.070	36.427	0.552	0.004	0.500	0.148	0.154	0.024	9896.746	0.004	157.637	1560095.102	1.560	**1.173**
	B	1.697	22.584	19.160	0.548	0.004	0.500	0.155	0.154	0.024	5243.479	0.004	149.937	786189.561	0.786	
Mix C0.5S	A	2.486	28.172	35.015	0.555	0.004	0.500	0.151	0.151	0.023	9463.468	0.003	161.199	1525500.932	1.526	**1.606**
	B	2.804	27.600	38.702	0.555	0.004	0.500	0.151	0.151	0.023	10459.873	0.003	161.199	1686120.292	1.686	
Mix C0.5L	A	1.295	28.345	18.358	0.148	0.001	0.500	0.148	0.153	0.023	18649.006	0.003	42.724	796763.822	0.797	**0.917**
	B	1.920	26.241	25.189	0.556	0.004	0.500	0.154	0.154	0.024	6795.471	0.004	152.601	1036994.946	1.037	

Pull-Out Test Data and Images

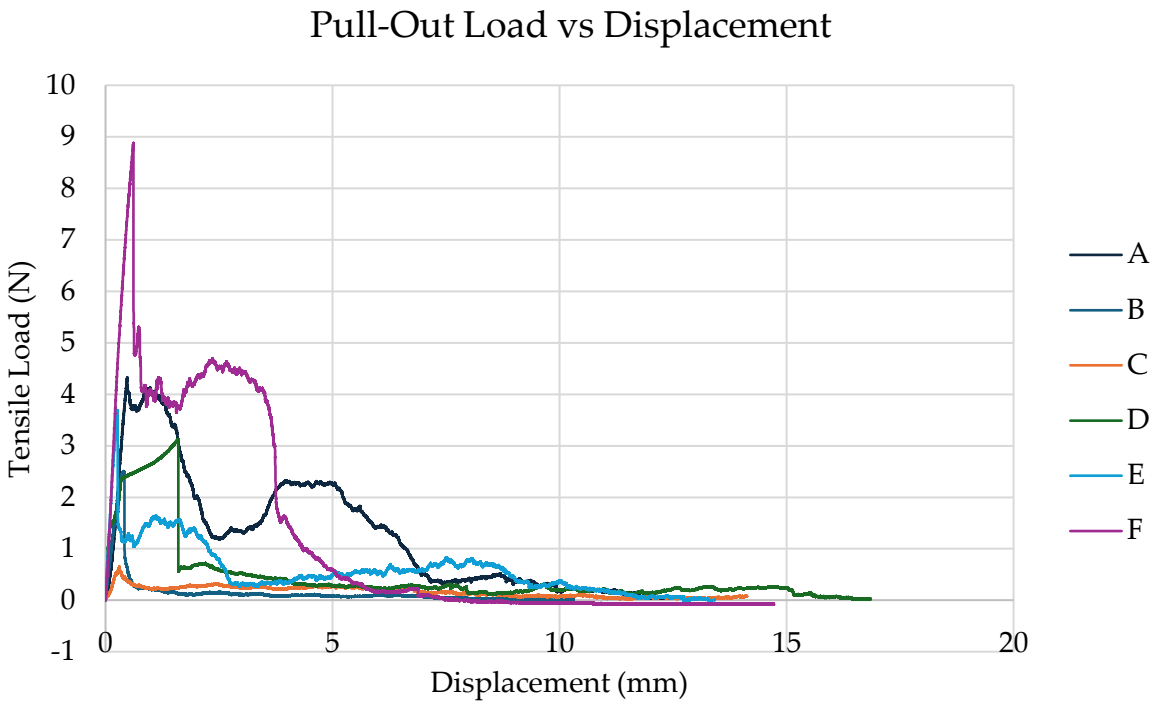

Image Series from Test A:

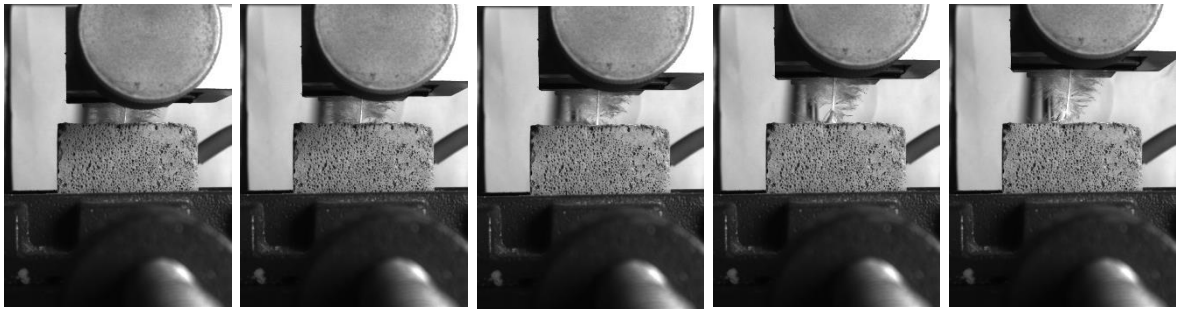

Image Series from Test B:

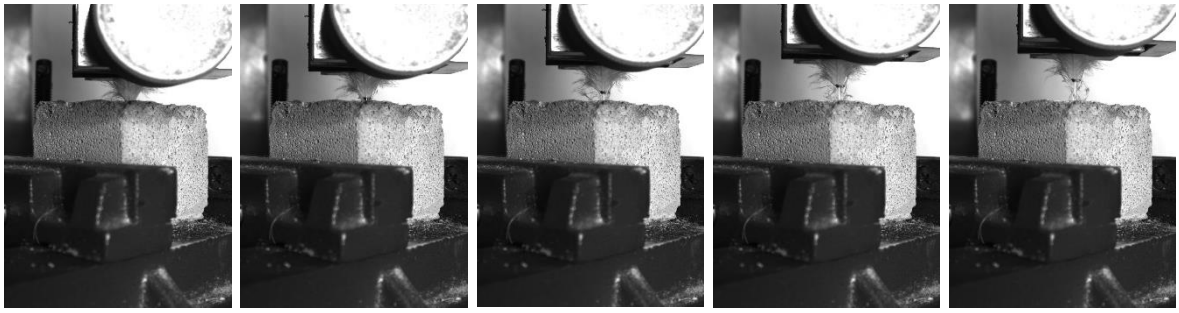

Image Series from Test C:

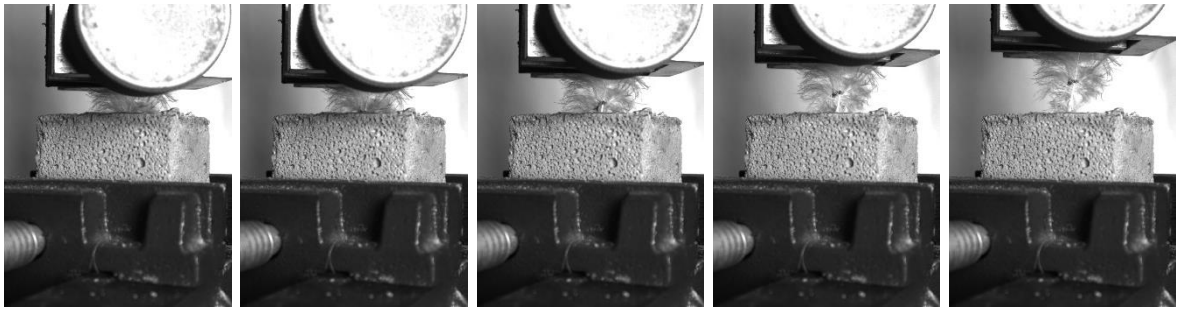

Image Series from Test D:

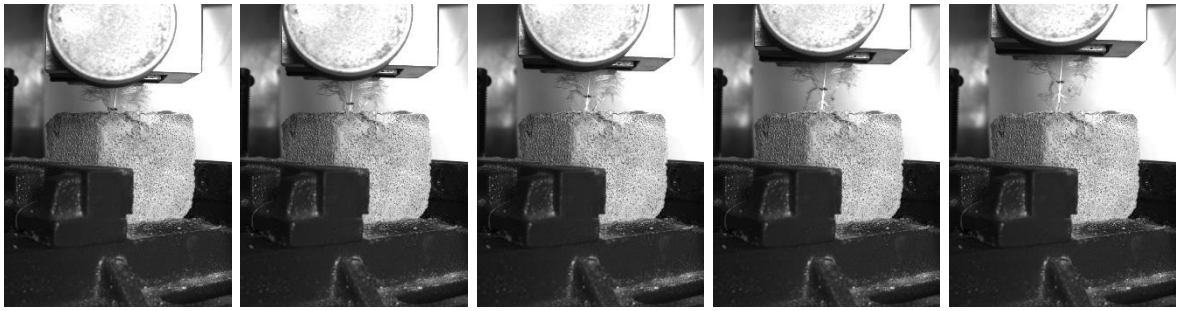

Image Series from Test E:

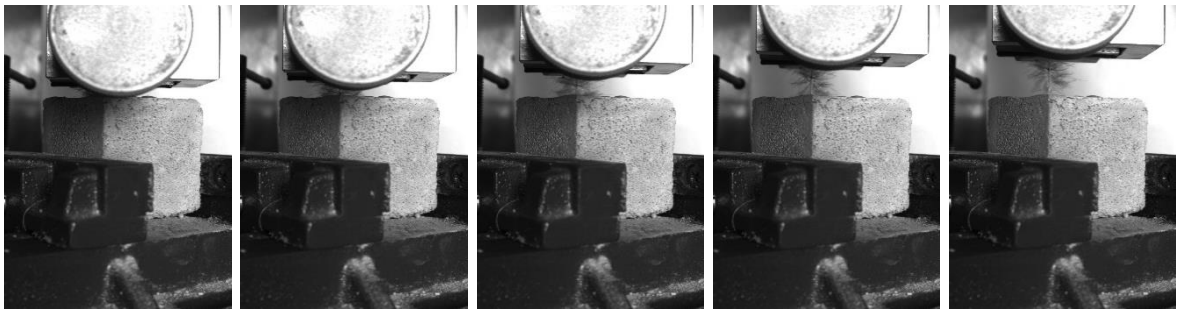

Image Series from Test F:

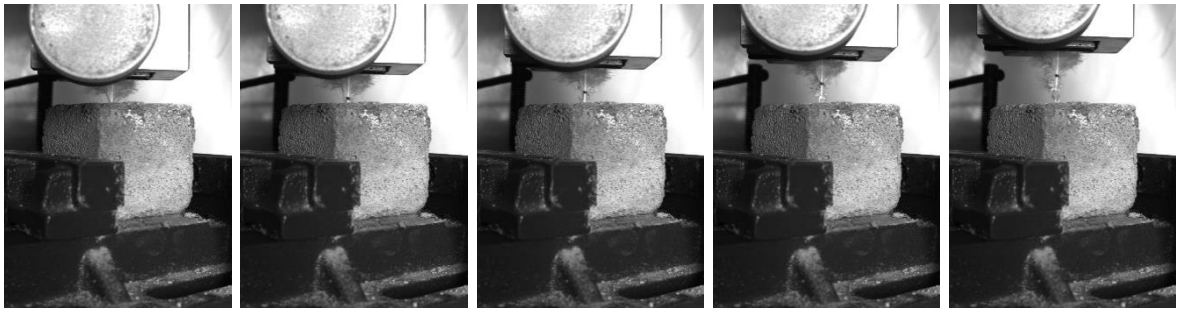

Concrete Durability Properties

Vacuum Saturation Porosity Results						
Mix	*grams*	*grams*	*grams*	*grams*	*grams*	*grams*
Control	*Wet 0 hrs*	*Stirrup Only*	*Wet 0 hrs Difference*	*Dry 0 hrs*	*Dry 24 hrs*	*Dry 48 hrs*
Sample A	413.84	1000.33	586.49	986.50	950.92	939.94
Sample B	418.12	972.70	554.58	959.42	924.58	914.14
C0.125S	*Wet 0 hrs*	*Stirrup Only*	*Wet 0 hrs Difference*	*Dry 0 hrs*	*Dry 24 hrs*	*Dry 48 hrs*
Sample A	368.72	969.58	600.86	956.39	927.78	916.06
Sample B	398.89	953.96	555.07	939.99	912.05	900.28
C0.125L	*Wet 0 hrs*	*Stirrup Only*	*Wet 0 hrs Difference*	*Dry 0 hrs*	*Dry 24 hrs*	*Dry 48 hrs*
Sample A	399.55	900.91	501.36	887.39	861.87	826.06
Sample B	397.93	924.53	526.60	910.97	890.28	845.33
C0.25S	*Wet 0 hrs*	*Stirrup Only*	*Wet 0 hrs Difference*	*Dry 0 hrs*	*Dry 24 hrs*	*Dry 48 hrs*
Sample A	376.88	935.34	558.46	922.11	891.63	870.56
Sample B	402.72	977.35	574.63	963.63	933.52	918.28
C0.25L	*Wet 0 hrs*	*Stirrup Only*	*Wet 0 hrs Difference*	*Dry 0 hrs*	*Dry 24 hrs*	*Dry 48 hrs*
Sample A	414.45	1003.40	588.95	990.82	958.13	936.51
Sample B	420.56	1017.82	597.26	1003.24	967.34	947.87
C0.5S	*Wet 0 hrs*	*Stirrup Only*	*Wet 0 hrs Difference*	*Dry 0 hrs*	*Dry 24 hrs*	*Dry 48 hrs*
Sample A	413.35	1000.89	587.54	986.25	955.42	942.36
Sample B	422.65	1022.56	599.91	1008.60	976.55	963.70
C0.5L	*Wet 0 hrs*	*Stirrup Only*	*Wet 0 hrs Difference*	*Dry 0 hrs*	*Dry 24 hrs*	*Dry 48 hrs*
Sample A	410.22	995.90	585.68	983.70	947.26	927.12
Sample B	405.93	992.22	586.29	979.32	946.14	927.56

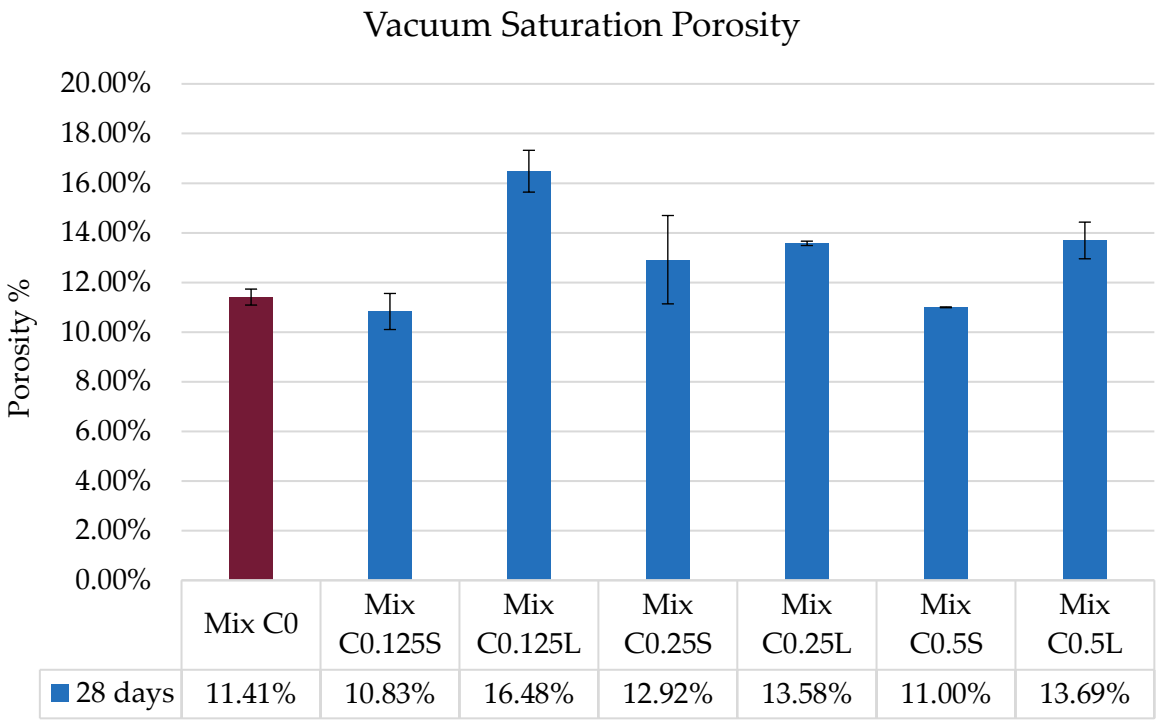
Vacuum Saturation Porosity
Porosity %
20.00%
18.00%
16.00%
14.00%
12.00%
10.00%
8.00%
6.00%
4.00%
2.00%
0.00%
Mix C0
Mix C0.125S
Mix C0.125L
Mix C0.25S
Mix C0.25L
Mix C0.5S
Mix C0.5L
28 days
11.41%
10.83%
16.48%
12.92%
13.58%
11.00%
13.69%

Ability to Resist Chloride Ion Penetration				
Mix C0	**Sample 1**		**Sample 2**	
Hour	**Current**	**Temperature**	**Current**	**Temperature**
	mA	*°C*	*mA*	*°C*
0	158	21.3	159.4	21.2
0.5	171.8	24.1	181.2	28.3
1	180.7	26.8	183.1	33.1
1.5	189	30.1	191.2	36.6
2	195.8	32.4	199.3	40.1
2.5	203.3	35.2	207.5	43.3
3	211.6	37.3	214.2	45.6
3.5	218.2	39.1	223.4	49.1
4	224.4	39.9	231.4	51.4
4.5	231.8	42.2	239.5	53.2
5	238.7	44.3	241.9	55.2
5.5	245.7	45.2	249.9	57.1
6	249.9	46.9	256.9	58.6

Ability to Resist Chloride Ion Penetration				
Mix C0.125S	**Sample 1**		**Sample 2**	
Hour	**Current**	**Temperature**	**Current**	**Temperature**
	mA	*°C*	*mA*	*°C*
0	149	21.9	141.3	22.1
0.5	162	24.3	151.98	24.2
1	172	27.2	162.39	26.9
1.5	185	29.9	173.83	29.0
2	198	33.7	183.78	31.5
2.5	214	36.1	191.14	33.7
3	225	38.5	199.05	35.3
3.5	235	40.2	209	37.6
4	245	42.1	218	38.4
4.5	252	43.2	226	39.1
5	257	44.3	234	40.2
5.5	262	45.2	240	41.2
6	266	45.8	245	41.8

Ability to Resist Chloride Ion Penetration				
C0.125L	**Sample 1**		**Sample 2**	
Hour	**Current**	**Temperature**	**Current**	**Temperature**
	mA	*°C*	*mA*	*°C*
0	135	22.3	143.25	22.4
0.5	149	24.6	161.72	24.9
1	163	27.1	175.39	27.5
1.5	176	28.8	186.21	29.6
2	192	31.3	201	32.5
2.5	204	33.9	214	34.2
3	214	36.3	224	36.1
3.5	227	37.7	229	37.2
4	236	39.0	236	39.3
4.5	242	39.9	245	40.0
5	247	41.2	251	41.3
5.5	252	42.0	258	42.0
6	256	42.6	263	42.8

Ability to Resist Chloride Ion Penetration				
C0.25S	**Sample 1**		**Sample 2**	
Hour	**Current**	**Temperature**	**Current**	**Temperature**
	mA	*°C*	*mA*	*°C*
0	111.3	20.2	130.7	19.1
0.5	125.6	22.0	148.6	22.5
1	134.8	24.1	160	24.4
1.5	142.5	26.9	170.1	27.0
2	149.9	29.3	179.8	29.1
2.5	156.7	30.6	188.4	31.3
3	162.3	32.2	196.4	32.9
3.5	167.9	34.1	203.6	35.0
4	173.4	35.4	210.7	37.1
4.5	177.7	37.1	217.2	39.3
5	184	38.0	223.5	40.0
5.5	188.9	39.2	229.3	42.1
6	193.3	40.1	234.9	43.2

Ability to Resist Chloride Ion Penetration				
C0.25L	**Sample 1**		**Sample 2**	
Hour	**Current**	**Temperature**	**Current**	**Temperature**
	mA	*℃*	*mA*	*℃*
0	116.3	20.3	112.1	20.1
0.5	129.2	22.1	124.2	22.3
1	137.3	24.9	131.9	24.1
1.5	144.8	27.1	139.3	27.0
2	152.1	29.0	146.4	28.4
2.5	159.1	31.2	153	29.9
3	165.6	32.1	159.1	32.2
3.5	171.5	34.4	164.5	33.4
4	177	35.2	169.3	35.1
4.5	182	36.9	174.1	36.0
5	186.7	38.2	178.3	37.2
5.5	191.1	39.0	181.4	37.8
6	195	40.1	184.6	39.2

Ability to Resist Chloride Ion Penetration				
C0.5S	**Sample 1**		**Sample 2**	
Hour	**Current**	**Temperature**	**Current**	**Temperature**
	mA	*℃*	*mA*	*℃*
0	143.4	22.0	112.38	23.2
0.5	160.9	25.2	126.14	24.4
1	173.1	27.7	135.02	25.6
1.5	182.9	30.8	144.97	27.9
2	192.9	32.1	150.05	30.3
2.5	199.96	34.6	157.28	31.1
3	196.7	36.5	162.24	33.6
3.5	210	38.8	165.46	34.4
4	237	40.5	168.72	35.2
4.5	245	42.2	174.07	36.6
5	249	43.4	176.26	37.1
5.5	256	44.7	178.71	38.2
6	262	46.2	180.82	39.5

Ability to Resist Chloride Ion Penetration				
C0.5L	**Sample 1**		**Sample 2**	
Hour	**Current**	**Temperature**	**Current**	**Temperature**
	mA	*°C*	*mA*	*°C*
0	110.1	21.9	122.48	22.6
0.5	120.2	23.9	135.85	24.2
1	127.3	26.8	143.24	26.9
1.5	134.5	28.3	150.36	29.2
2	138.1	29.4	153.92	30.1
2.5	143.4	31.5	159.31	30.7
3	148.1	32.8	163.79	33.1
3.5	153.2	34.6	168.87	34.3
4	155.1	35.1	170.87	35.3
4.5	160.3	36.8	175.54	37.3
5	163.7	37.7	177.94	38.1
5.5	165.3	37.6	178.85	38.2
6	168.1	38.1	180.75	38.7

	Charge Passed	**Chloride Ion Penetrability**
Mix Code	*Coulombs*	
Mix C0	4632.075	Very High
Mix C0.125S	4497.138	Very High
Mix C0.125L	4573.751	Very High
Mix C0.25S	3803.760	High
Mix C0.25L	3439.710	High
Mix C0.5S	3628.512	High
Mix C0.5L	3310.610	High

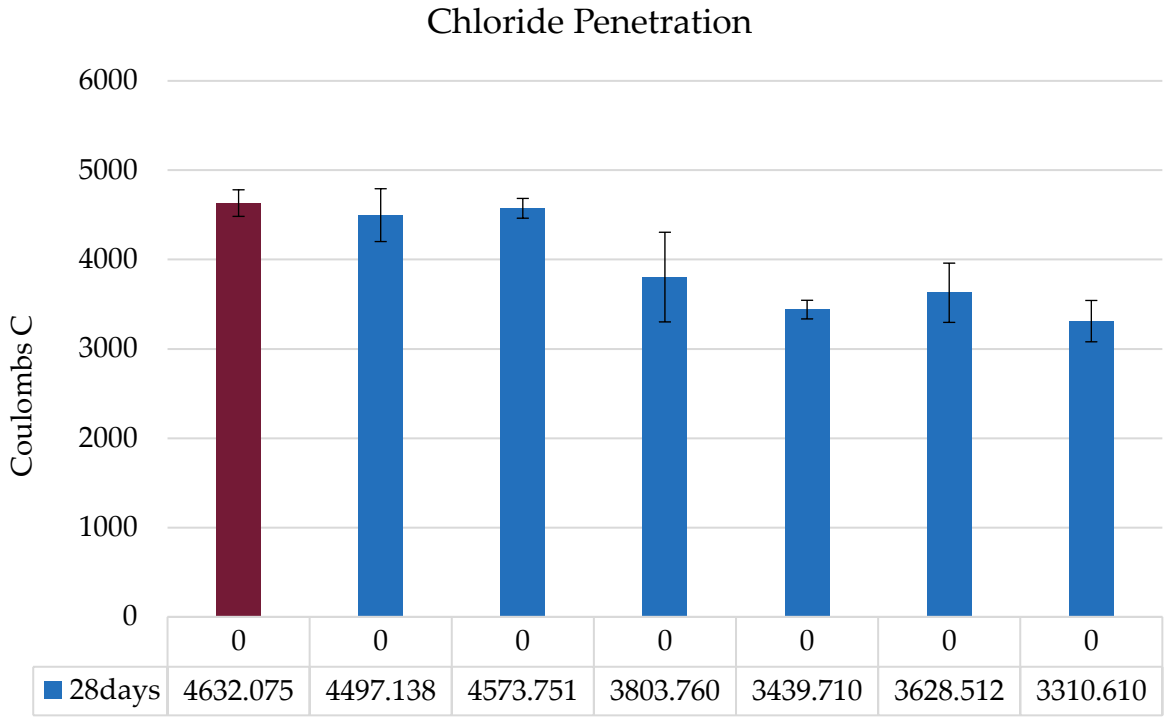
Chloride Penetration
Coulombs C
6000
5000
4000
3000
2000
1000
0
0 0 0 0 0 0 0
28days 4632.075 4497.138 4573.751 3803.760 3439.710 3628.512 3310.610

Appendix D

Material Datasheets

COLACEM
forte • sostenibile
Ragusa Cementi S.p.A. Gruppo Colacem

Technical data sheet CEMENT

26/04/2023
page 1 of 1

CEM II/A-LL 42,5 R
Portland-limestone cement
Ragusa Plant (Italy)
Cement loaded: *MT 2600*
Vessel's name: *M/V NS Holland – v.313*
Loading port: *Pozzallo Italy*
B/L date: *23/03/2023*
Discharge port: *La Valletta - Malta*

Cement provided with:
- Certificate of constancy of performance 0970-CPR-0243/CE/0202 in accordance with EN 197-1 Standard
- Evaluation Document 0011/CR/19 in compliance with the Ministerial Decrees dated 10/05/2004 and 17/02/2005 (water-soluble chromium (VI) content of cement ≤ 2 ppm)

Chemical features

	unit	average ship	requirement in EN 197-1	method
Sulfate content (as SO_3)	%	**3,08**	≤ 4,00	EN 196-2
Chloride content (Cl^-)	%	**0,05**	≤ 0,10	EN 196-2

Physical features

	unit	average ship	requirement in EN 197-1	method
Initial setting time	min	**141**	≥ 60	EN 196-3
Soundness (expansion)	min	**0**	≤ 10	EN 196-3
Fineness (as Blaine specific surface)	cm^2/g	**3819**	n.a.	EN 196-6
Residue on 63 µm	%	**2,3**	n.a.	EN 196-3

Mechanical compressive strength

	unit	average ship	requirement in EN 197-1	method
Early strength at 2 days	MPa	**29,0**	≥ 20,0	EN 196-1
Std strength at 28 days	MPa	**51,7**	≥ 42,5 e ≤ 62,5 MPa	EN 196-1

Notes

1) Data sheet issued by the Quality Assurance Department in accordance with the company procedures and using the test results carried out by the Factory Laboratory.
2) For technical-commercial information: +39 075 924 00 24 assistenzaclienti@colacem.it

Plant Manager
(Mr. Nunzio TUMINO)
(Signature)

www.colacem.it

solidbase LABORATORY LTD.

ISO 17025 ACCREDITED TESTING NAB- MALTA Nº 008

Test for the Determination of Cement Strength to MSA EN 196-1:2016

Client Information

Client	Central Cement Ltd	Client tel. No.	21232282	Certificate date	2023-04-25
Client Address	Cem House	Client fax No.	21221659	Certificate No.	2881
	National Road	Client ref No.	138239	Logbook ID	23/00642523/006425
	Blata-l-Bajda HMR 9011	Attn.	Sammut John Mr	Project	Central Cement Ltd - J064 - Cement: 23/006425

General Information

Shipment ID / Location	Holland 313	Shipment date	2023-03-27	Country of origin	N.A.
Truck No.	JBW 451	Delivery note No.	138239	Cement type	CEM II / A-LL 42.5R
Date received sample	2023-03-27	Date / time prisms cast	2023-03-28 07:00	Quantity of prisms	9
Compressive strength pace rate (N/s)	2400	Flexural pace rate (N/s)	50	Mix Ratio (H_2O : Cement : Sand)	0.5:1:3
No. of layers	2	Jolts per layer	60	Laboratory temp. (°C)	20

Test Results

	Prisms Pre-Test Data					Flexural Strength Test					Compressive Strength Test				
Sample No.	L (mm)	B (mm)	H (mm)	Weight (g)	Flatness	Test Date / Time	Age (Days)	Ft (N)	l (mm)	Rt (N/mm^2)	Plattens (mm^2)	F_C Part A (N)	R_C Part A (N/mm^2)	F_C Part B (N)	R_C Part B (N/mm^2)
M23/00549	160	40	40	602	good	2023-04-25 07:00	28	3850	100	9.0	1600	83360	52.1	83300	52.1
M23/00548	160	40	40	600	good	2023-04-25 07:00	28	3940	100	9.2	1600	83790	52.4	84940	53.1
M23/00547	160	40	40	601	good	2023-04-25 07:00	28	3960	100	9.3	1600	83730	52.3	85180	53.2
M23/00546	160	40	40	599	good	2023-04-04 07:00	7	3360	100	7.9	1600	63240	39.5	61370	38.4
M23/00545	160	40	40	601	good	2023-04-04 07:00	7	3160	100	7.4	1600	61760	38.6	62680	39.2
M23/00544	160	40	40	601	good	2023-04-04 07:00	7	3160	100	7.4	1600	63970	40.0	61270	38.3
M23/00543	160	40	40	595	good	2023-03-30 07:00	2	2970	100	7.0	1600	48420	30.3	49070	30.7
M23/00542	160	40	40	598	good	2023-03-30 07:00	2	2780	100	6.5	1600	44810	28.0	47050	29.4
M23/00541	160	40	40	597	good	2023-03-30 07:00	2	2730	100	6.4	1600	48010	30.0	45690	28.6

F_t	Load applied to the middle of the prism at fracture
l	Span-rods
R_t	Flexural strength
F_C - Part A	Failure load for compression test of first part of prism
R_C - Part A	Compressive strength of first part of prism
F_C - Part B	Failure load for compression test of second part of prism
R_C - Part B	Compressive strength of second part of prism

Blaine Fineness Test (cm^2/g): 4491.48

Initial setting time: Final setting time:

NB: An NAB-MALTA accredited Testing Laboratory Reg. No. 008
Accreditation applies to the Compressive and Machine operations.

Deviations from standard None

Comments None

Darmanin Gilbert
Laboratory Manager

Tal-Handaq Industrial Estate, N/S in Handaq Road, Qormi, QRM 4000, Malta.
T: (356) 2149 2807/8
F: (356) 2149 2810
E: info@solidbasemalta.com
W: www.solidbasemalta.com
Co. No.: C 33162
VAT No.: MT 1695 3537

The expanded level of uncertainty is less than 0.1%. The uncertainty evaluation has been carried out in accordance with NAB-Malta requirements.

solidbase LABORATORY LTD.

NAB- MALTA ISO/IEC 170 ACCREDITE TESTIN Nº 008

Aggregate Test Report

Client Name:	Central Cement Ltd		
Client Address:	Cem House	Certificate Date:	2023-02-24
	National Road	Certificate No:	2869
	Blata-l-Bajda HMR 9011	Client Ref:	
Client Tel No:	21232282	Logbook ID	23/003228
Client Fax No:	21221659	Project:	Central Cement Ltd - J064
Attn:	Sammut John Mr		

Sampling

Test carried out to EN 932-1:1997

Supplier	Central Cement Ltd	Location of sampling	Moon 3
Date sampled	2023-02-21	Sampled by	
Material type	0-4mm	Date received	2023-02-21
Material description	Dolomite Sand		
Comments	Receipt No.: 138226, Truck No.: JBW 451		
Deviations	Sampled by client		

Particle Size Distribution

Test carried out to EN 933-1:2012

Sieve Size (mm)	Passing %	Upper Limit	Lower Limit
8.0	100.0	0.0	0.0
6.3	100.0	0.0	0.0
4.0	94.0	0.0	0.0
2.0	66.0	0.0	0.0
1.0	41.0	0.0	0.0
0.25	18.0	0.0	0.0
0.063	10.0	0.0	0.0

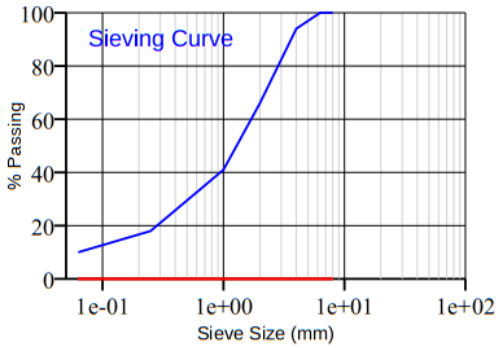

Fines content	10.3%
Fineness modulus	2.7
Method of analysis	wet sieving
Comment	None
Deviation	None

Moisture Content

Test carried out to EN 1097-5:2008

Moisture content	0.83%		
Technician	Camilleri Nathan	Date tested	2023-02-23
Comments	None		
Deviation	None		

Tal-Handaq Industrial Estate,
N/S in Handaq Road,
Qormi, QRM 4000, Malta.

T: (356) 2149 2807/8
F: (356) 2149 2810
E: info@solidbasemalta.com
W: www.solidbasemalta.com

Co. No.: C 33162
VAT No.: MT 1695 3537

solidbase LABORATORY LTD.

ISO/IEC 17025 ACCREDITED TESTING NAB- MALTA Nº 008

Relative Density

Test carried out to EN 1097-6:2022

Method used		Pyknometer method pass 4mm, retain 63µm	
Mass of dry portion (g)		390.21	
Apparent particle density (ρ_{a}) (Mg/m^3)*		2.77	
Oven dry particle density (ρ_{rd}) (Mg/m^3)*		2.75	
Saturated surface-dried particle density (ρ_{ssd}) (Mg/m^3)*		2.76	
Water absorption (WA_{24}) (%)		0.3	
Technician	Atif Hanif	Date tested	2023-02-24
Comments	None		
Deviation	None		

Darmanin Gilbert
Laboratory Manager

Tal-Handaq Industrial Estate,
N/S in Handaq Road,
Qormi, QRM 4000, Malta.

T: (356) 2149 2807/8
F: (356) 2149 2810
E: info@solidbasemalta.com
W: www.solidbasemalta.com

Co. No.: C 33162
VAT No.: MT 1695 3537

solidbase LABORATORY LTD.

ISO/IEC 17025 ACCREDITED TESTING NAB- MALTA Nº 008

Aggregate Test Report

Client Name:	Central Cement Ltd		
Client Address:	Cem House	Certificate Date:	2023-02-24
	National Road	Certificate No:	2870
	Blata-l-Bajda HMR 9011	Client Ref:	
Client Tel No:	21232282	Logbook ID	23/003229
Client Fax No:	21221659	Project:	Central Cement Ltd - J064
Attn:	Sammut John Mr		

Sampling

Test carried out to EN 932-1:1997

Supplier	Central Cement Ltd	Location of sampling	Moon 3
Date sampled	2023-02-21	Sampled by	
Material type	4-10mm	Date received	2023-02-21
Material description	Dolomite Gravel		
Comments	Receipt No.: 138227, Truck No.: JBW 451		
Deviations	Sampled by client		

Particle Size Distribution

Test carried out to EN 933-1:2012

Sieve Size (mm)	Passing %	Upper Limit	Lower Limit
20.0	100.0	0.0	0.0
14.0	100.0	0.0	0.0
10.0	100.0	0.0	0.0
8.0	65.0	0.0	0.0
4.0	10.0	0.0	0.0
2.0	4.0	0.0	0.0
0.063	2.0	0.0	0.0

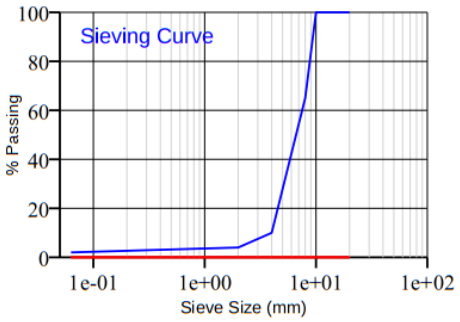

Fines content	2.3%
Fineness modulus	3.2
Method of analysis	wet sieving
Comment	None
Deviation	None

Moisture Content

Test carried out to EN 1097-5:2008

Moisture content	0.66%		
Technician	Camilleri Nathan	Date tested	2023-02-23
Comments	None		
Deviation	None		

Tal-Handaq Industrial Estate,
N/S in Handaq Road,
Qormi, QRM 4000, Malta.

T: (356) 2149 2807/8
F: (356) 2149 2810
E: info@solidbasemalta.com
W: www.solidbasemalta.com

Co. No.: C 33162
VAT No.: MT 1695 3537

solidbase LABORATORY LTD.

ISO/IEC 17025 ACCREDITED TESTING NAB- MALTA Nº 008

Relative Density

Test carried out to EN 1097-6:2022

Method used		Pyknometer method pass 31.5mm, retain 4mm	
Mass of dry portion (g)		1444.57	
Apparent particle density ($\rho\eta o_a$) (Mg/m^3)*		2.84	
Oven dry particle density (ρ_{rd}) (Mg/m^3)*		2.83	
Saturated surface-dried particle density (ρ_{ssd}) (Mg/m^3)*		2.83	
Water absorption (WA_{24}) (%)		0.2	
Technician	Atif Hanif	Date tested	2023-02-24
Comments	None		
Deviation	None		

Aggregate Abrasion Value by Los Angeles

Test carried out to EN 1097-2:2020

No. of balls used in charge		9	
Size fraction of test portions		6.3 - 10mm : 100.0%	
Los Angeles Coefficient (LA)		17.8	
Technician	Atif Hanif	Date tested	2023-02-24
Comments	None		
Deviation	None		

Darmanin Gilbert
Laboratory Manager

Tal-Handaq Industrial Estate,
N/S in Handaq Road,
Qormi, QRM 4000, Malta.

T: (356) 2149 2807/8
F: (356) 2149 2810
E: info@solidbasemalta.com
W: www.solidbasemalta.com

Co. No.: C 33162
VAT No.: MT 1695 3537

MasterGlenium SKY 698

Second generation high range water reducing polycarboxylate ether admixture for ready-mix concrete with high slump retention and a low W/C. It is suitable for hot weather conditions.

MATERIAL DESCRIPTION

MasterGlenium SKY 698 is an innovative second generation superplasticizer of polycarboxylic ether (PCE) polymers. It is derived directly from the Total Performance Control™ concept.

MasterGlenium SKY 698 is specially engineered for ready-mix Rheoplastic concrete having fluid consistence and self-compacting concrete, having a very high workability retention (> 90 minutes), especially under hot weather conditions. The fresh concrete shows no segregation and at the same time has a low water cement ratio and, consequently, high early and long term strengths as per EN 206-1 standards.

MasterGlenium SKY 698 may be used also to produce Rheodynamic concrete, capable of self compaction, even in the presence of dense reinforcement, without the aid of vibration.

MasterGlenium SKY 698 is chloride free, meets EN 934-2, and it is compatible with all cements meeting the EN 197-1 standards.

TOTAL PERFORMANCE CONTROL ™

The Total Performance Control™ concept ensures that ready-mix producers, contractors and engineers get a concrete that is of the same high quality as originally specified; starting from production at the batching plant, to the delivery and placing into the formworks and followed by its hardening process. Utilizing Rheodynamic™ concrete technology it provides a concrete mix with exceptional placing characteristics and accelerated cement hydration for early strength development and high-quality concrete.

THE CHEMISTRY OF MASTERGLENIUM SKY

The Total Performance Control™ concept is the result of years of study of an in-house expertise in nanotechnology. This allows Master Builders Solutions to control the chemical and physical behaviour of polymers and their interactions with cement. MasterGlenium SKY 698 is an innovative second generation superplasticiser of polycarboxylic ether (PCE) polymers.

The dispersion effect of superplasticizers is based on the adsorption of molecules on cement particles, imparting a negative charge that causes electrostatic repulsion and steric hindrance between them and, therefore, causing dispersion.

The hydration, and particularly the ettringite formation, works against the superplasticiser.

The molecules already adsorbed are covered by the ettringite lawn and thus are ineffective.

The particular configuration of the MasterGlenium SKY molecules allows its delayed adsorption onto the cement particles and disperses them efficiently over a long period of time. The molecular structure is essential for the early development of strength. With superplasticizers based on conventional polycarboxylate ether, the molecules cover the entire surface of the cement grain and build a barrier against contact with water. Therefore, the hydration process takes place slowly. The MasterGlenium SKY molecules on the other hand leave sufficient surface of the cement exposed to allow contact with water for a rapid hydration reaction which results in high early strength development.

BENEFITS FOR READY-MIX PRODUCER

Total Performance Control and the use of MasterGlenium SKY 698 offers the following benefit to the ready-mix concrete producer:

- Reduction the water content with respect to the state of the art polycarboxylate based superplasticisers.
- Production of Rheoplastic and Rheodynamic concrete having a very low W/C.
- Workability retention for a longer period especially in hot weather conditions avoiding the problem of re-tempering with water before the pouring operation.
- Improvement of the rheology even in concrete mixes having a low fines content.
- Optimization of the production of durable concrete as per the EN 206-1 and UNI 11104 standards.
- As compared to the traditional superplasticisers, the engineering properties such as early and ultimate compressive and flexural strengths, bond to steel, and modulus of elasticity, shrinkage, creep, and impermeability are improved

MasterGlenium SKY 698

Second generation high range water reducing polycarboxylate ether admixture for ready-mix concrete with high slump retention and a low W/C. It is suitable for hot weather conditions.

COMPATIBILITY

In order to optimise some special properties of the concrete, use of the following complementary admixtures is suggested:

- air entraining agent MasterAir to improve freeze thaw resistance (exposure class XF1 to XF4, EN 206-1);
- silica fume, MasterLife MS 610, for high performance concrete and to improve the durability in chemical aggressive environments (exposure class XA1 to XA3, EN 206-1)
- synthetic micro-fibres MasterFiber to prevent cracks due to plastic shrinkage;
- curing agent MasterKure for sealing the surface of freshly finished concrete against rapid evaporation of water which may cause plastic shrinkage cracking.
- demoulding agent MasterFinish for good surface appearance.

In compliance with the European Regulation (EU No 305/2011 and EU No. 574/2014) the product is provided with the CE marking according to UNI EN 934-2 and the relative DoP (Declaration of Performance).

CE
1305
EN 934-2 **Table 11.1-11.2** Set retarding/high range water reducing/superplasticizing admixtures

DOSAGE

MasterGlenium SKY 698 The recommended dosage can range from 0.8 to 1.6 litres per 100 kg of binder.
Other dosages may be recommended in special cases according to specific job site conditions.
In such cases please consult our Technical Service Department for advice.

PACKAGING AND STORAGE

MasterGlenium SKY 698 is available in 10 litre cans, 1.000 litre container or in bulk.
MasterGlenium SKY 698 must be stored in a place where the temperature does not drop below 5 °C. In case of freezing, warm up and homogenise the admixture solution before using.

DIRECTIONS FOR USE

MasterGlenium SKY 698 is a liquid admixture to be added to the concrete during the mixing process:

- mix cement and secondary binders, sand, coarse aggregates and the mix water until a stiff, yet homogeneous, mixture is obtained;
- optimal mixing water reduction is obtained if MasterGlenium SKY 698 is mixed into the concrete right after the addition of the initial 80-90% of the total water;
- avoid adding the admixture to the dry aggregates;
- add MasterGlenium SKY 698 admixture and mix again for to 60 seconds in order to disperse it homogeneously;
- continue mixing until required workability is obtained, with addition of the remaining water.

COMPATIBILITY

MasterGlenium SKY 698 is not compatible with all admixtures of MasterRheobuild series.

SAFETY INFORMATION

For information on the correct and safe use, transport, storage and disposal of the product, consult the most recent Safety Data Sheet.

MasterGlenium SKY 698

Second generation high range water reducing polycarboxylate ether admixture for ready-mix concrete with high slump retention and a low W/C. It is suitable for hot weather conditions.

Technical Information	
Form	Liquid
Relative density (g/cc at 20°C)	1.082 – 1.112
Essential characteristic in accordance to EN 934-2	**Performance**
Chloride ion content	≤ 0,1% by mass
Alkali content (Na_2O equivalent)	≤ 5.0%
Corrosion behaviour	Contains component only from EN 934-1: 2008 Annex A.1
Compressive strength	Equal consistence: 7 days ≥ 100%; 28 days ≥ 115% Equal w/c ratio: 28 days ≥ 90%
Air content	Equal consistence: ≤ 2,0 % Equal w/c ratio: ≤ 2,0 %
Water reduction	≥ 12%
Setting time	Initial: test mix ≥ control mix + 90 min Final: test mix ≤ control mix + 360 min
Consistency	Retention: comply 11.2 (1)

OTHER SERVICES

For price analysis, specifications, supplementary brochures, references, reports and technical assistance, visit the website www.master-builders-solutions.com/it-it or contact infomac@mbcc-group.com.

Scan the QR code to visit the product page and download the latest version of this datasheet

Since 16/12/1992, Master Builders Solutions Italia Spa has been operating under a Certified Quality System compliant with the UNI EN ISO 9001 Standard. Furthermore, the Environmental Management System is certified according to the UNI EN ISO 14001 Standard and the Safety Management System is certified according to the UNI ISO 45001 Standard.

Master Builders Solutions Italia Spa
Via Vicinale delle Corti, 21 – 31100 Treviso – Italia
T +39 0422 429200 F +39 0422 421802
www.master-builders-solutions.com/it-it
e-mail: infomac@mbcc-group.com

Procter&Gamble

PROFESSIONAL

Fairy Professional Original Washing Up Liquid 750ml

Safety Data Sheet

according to Regulation (EC) No. 453/2010

Date of issue: 17/11/2011 Revision date: Version: 1.0

SECTION 1: Identification of the substance/mixture and of the company/undertaking

1.1. Product identifier

Chemical type : Mixture

Trade name : Fairy Professional Original Washing Up Liquid 750ml

Product code : PA00175440

1.2. Relevant identified uses of the substance or mixture and uses advised against

1.2.1. Relevant identified uses

Function or use category : Cleaning/washing agents and additives

1.2.2. Uses advised against

No additional information available

1.3. Details of the supplier of the safety data sheet

To be completed by Shipper / Person responsible for placing the product on the market

1.4. Emergency telephone number

Emergency number To be completed by Shipper / Person responsible for placing the product on the market

SECTION 2: Hazards identification

2.1. Classification of the substance or mixture

Classification according to Directive 67/548/EEC or 1999/45/EC

Xi; R41
Xi; R38

Full text of R-phrases: see section 16.

Adverse physicochemical, human health and environmental effects

No additional information available

2.2. Label elements

Labelling according to Directive 67/548/EEC or 1999/45/EC

Hazard symbols :

Xi - Irritant

R-phrases : R38 - Irritating to skin.
R41 - Risk of serious damage to eyes.

S-phrases : S26 - In case of contact with eyes, rinse immediately with plenty of water and seek medical advice.
S25 - Avoid contact with eyes.
S39 - Wear eye/face protection.
S46 - If swallowed, seek medical advice immediately and show this container or label.

2.3. Other hazards

No additional information available

SECTION 3: Composition/information on ingredients

3.1. Substances

Not applicable

3.2. Mixtures

Name	Product identifier	%	Classification according to Directive 67/548/EEC
Sodium Laureth Sulfate	(CAS No.) 68585-34-2 (EC no) 500-223-8	20 - 30	Xi; R41 Xi; R38
Lauramine Oxide	(CAS No.) 70592-80-2 (EC no) 274-687-2	5 - 10	Xi; R41 Xi; R38 N; R50

Name	Product identifier	%	Classification according to Regulation (EC) No. 1272/2008 [CLP]
Sodium Laureth Sulfate	(CAS No.) 68585-34-2 (EC no) 500-223-8	20 - 30	Skin Irrit. 2, H315 Eye Dam. 1, H318
Lauramine Oxide	(CAS No.) 70592-80-2 (EC no) 274-687-2	5 - 10	Skin Irrit. 2, H315 Eye Dam. 1, H318 Aquatic Acute 1, H400

Full text of R-, H- and EUH-phrases: see section 16.

SECTION 4: First aid measures

4.1. Description of first aid measures

First-aid measures after inhalation : When symptoms occur: go into open air and ventilate suspected area. Respiratory problems: consult a doctor/medical service.

First-aid measures after skin contact : Rinse immediately with plenty of water for 15 minutes. Take victim to a doctor if irritation persists. Remove contaminated clothing immediately.

First-aid measures after eye contact : Rinse immediately with plenty of water for 15 minutes. Take victim to a doctor if irritation persists.

First-aid measures after ingestion : Give nothing or a little water to drink. Do not induce vomiting. Consult a doctor/medical service.

4.2. Most important symptoms and effects, both acute and delayed

Symptoms/injuries after inhalation : May cause irritation or asthma-like symptoms.

Symptoms/injuries after skin contact : May cause moderate irritation.

Symptoms/injuries after eye contact : May cause severe irritation.

Symptoms/injuries after ingestion : Gastrointestinal complaints.

4.3. Indication of any immediate medical attention and special treatment needed

Refer to section 4.1.

SECTION 5: Firefighting measures

5.1. Extinguishing media

Suitable extinguishing media : Dry chemical powder, alcohol-resistant foam, carbon dioxide (CO2).

5.2. Special hazards arising from the substance or mixture

Fire hazard : No fire hazard. Non combustible.

Explosion hazard : Product is not explosive.

Reactivity : No dangerous reactions known.

5.3. Advice for firefighters

Firefighting instructions : No specific firefighting instructions required.

Protection during firefighting : In case of inadequate ventilation wear respiratory protection.

SECTION 6: Accidental release measures

6.1. Personal precautions, protective equipment and emergency procedures

6.1.1. For non-emergency personnel

Protective equipment : Wear suitable gloves and eye/face protection.

6.1.2. For emergency responders

Protective equipment : Wear suitable gloves and eye/face protection.

6.2. Environmental precautions

Consumer products ending up down the drain after use. Prevent soil and water pollution. Prevent spreading in sewers.

6.3. Methods and material for containment and cleaning up

For containment : Scoop absorbed substance into closing containers.

Methods for cleaning up : Small quantities of liquid spill: take up in non-combustible absorbent material and shovel into container for disposal. Large spills: contain released substance, pump into suitable containers. This material and its container must be disposed of in a safe way, and as per local legislation.

6.4. Reference to other sections

Refer to Sections 8 and 13.

SECTION 7: Handling and storage

7.1. Precautions for safe handling

Precautions for safe handling : Avoid contact with skin. Avoid contact with eyes. Use personal protective equipment as required. Do not eat, drink or smoke when using this product. Do not handle until all safety precautions have been read and understood.

7.2. Conditions for safe storage, including any incompatibilities

Storage conditions : Store in original container. Refer to section 10.

Incompatible products	: Refer to section 10.
Incompatible materials	: Not applicable.
Prohibitions on mixed storage	: Not applicable.
Storage area	: Store in a cool area. Store in a dry area.

7.3. Specific end use(s)

Cleaning/washing agents and additives.

SECTION 8: Exposure controls/personal protection

8.1. Control parameters

No additional information available

8.2. Exposure controls

Personal protective equipment	: Wear eye/face protection.
Hand protection	: Not applicable.
Eye protection	: Safety glasses.
Skin and body protection	: Not applicable.
Respiratory protection	: Not applicable.

SECTION 9: Physical and chemical properties

9.1. Information on basic physical and chemical properties

Physical state	: Liquid
Appearance	: Liquid.
Colour	: Coloured.
Odour	: pleasant (perfume).
Odour threshold	: No data available
pH	: 9
pH solution	: 10 %
Melting point	: Not measured.
Solidification point	: No data available
Boiling point	: Not measured.
Flash point	: < 60 °C but not sustaining combustion
Relative evaporation rate (butylacetate=1)	: Not measured.
Flammability (solid, gas)	: Not flammable.
Explosive limits	: Product is not explosive
Vapour pressure	: Not measured.
Relative vapour density at 20 °C	: Not measured.
Relative density	: No data available
Density	: 1026 g/l
Solubility	: Soluble in water.
Log Pow	: No data available
Self ignition temperature	: Not measured.
Decomposition temperature	: Not measured.
Viscosity	: 500 - 800 cP

9.2. Other information

No additional information available

SECTION 10: Stability and reactivity

10.1. Reactivity

No dangerous reactions known.

10.2. Chemical stability

Stable under normal conditions.

10.3. Possibility of hazardous reactions

Refer to section 10.1 on Reactivity.

10.4. Conditions to avoid

Not required for normal conditions of use.

10.5. Incompatible materials

Not applicable.

10.6. Hazardous decomposition products

None under normal use.

SECTION 11: Toxicological information

11.1. Information on toxicological effects

Irritation : Irritating to skin. Risk of serious damage to eyes.

Potential Adverse human health effects and symptoms : Acute Toxicity: based upon available data of the substances, classification criteria are not met. Carcinogenicity: based upon available data of the substances, classification criteria are not met. Corrosivity: based upon available data of the substances, classification criteria are not met. Irritation: moderately irritating to skin. Irritation: severly irritant to eyes. Mutagenicity: based upon available data of the substances, classification criteria are not met. Repeated Dose Toxicity: based upon available data of the substances, classification criteria are not met. Sensitization: based upon available data of the substances, classification criteria are not met. Toxicity for Reproduction: based upon available data of the substances, classification criteria are not met.

Other information : Likely routes of exposure: ingestion, skin and eye. Information on Effects: refer to section 4.

SECTION 12: Ecological information

12.1. Toxicity

Ecology - general : No known adverse effects on the functioning of water treatment plants under normal use conditions as recommended. The product is not considered harmful to aquatic organisms nor to cause long-term adverse effects in the environment.

12.2. Persistence and degradability

No additional information available

12.3. Bioaccumulative potential

No additional information available

12.4. Mobility in soil

No additional information available

12.5. Results of PBT and vPvB assessment

PGP HDW UK 28.1% Lightning 2 London production	
Results of PBT assessment	No presence of PBT and vPvB ingredients

12.6. Other adverse effects

Other information : No other effects known.

SECTION 13: Disposal considerations

13.1. Waste treatment methods

Regional legislation (waste) : Disposal must be done according to official regulations.

SECTION 14: Transport information

14.1. UN number

Not applicable

14.2. UN proper shipping name

Not applicable

14.3. Transport hazard class(es)

Not applicable

14.4. Packing group

Not applicable

14.5. Environmental hazards

Not applicable

14.6. Special precautions for user

Not applicable

14.7. Transport in bulk according to Annex II of MARPOL 73/78 and the IBC Code

Not applicable

SECTION 15: Regulatory information

Ingredient label : 15-30% Anionic surfactants; 5-15% Non-ionic surfactants; Methylisothiazolinone, Phenoxyethanol, Perfumes.

15.1. Safety, health and environmental regulations/legislation specific for the substance or mixture

15.1.1. EU-Regulations

No additional information available

15.1.2. National regulations

EURAL code : 20 01 29*

CESIO recommendations : The surfactant(s) contained in this preparation complies(comply) with the biodegradability criteria as laid down in Regulation (EC) No.648/2004 on detergents. Data to support this assertion are held at the disposal of the competent authorities of the Member States and will be made available to them, at their direct request or at the request of a detergent manufacturer.

15.2. Chemical safety assessment

Not available.

SECTION 16: Other information

Training advice : Normal use of this product shall imply use in accordance with the instructions on the packaging.

Salts listed in Section 3 without a REACh Registration number are exempt, based on Annex V

Full text of R-, H- and EUH-phrases:

Aquatic Acute 1	Hazardous to the aquatic environment - Acute Hazard Category 1
Eye Dam. 1	Serious eye damage/eye irritation Category 1
Skin Irrit. 2	skin corrosion/irritation Category 2
H315	Causes skin irritation
H318	Causes serious eye damage
H400	Very toxic to aquatic life
R38	Irritating to skin.
R41	Risk of serious damage to eyes.
R50	Very toxic to aquatic organisms.

This information is based on our current knowledge and is intended to describe the product for the purposes of health, safety and environmental requirements only. It should not therefore be construed as guaranteeing any specific property of the product.

Honeywell Fluka™

Sodium chloride

31434-1KG

Version 1.5 Revision Date 04.06.2024

SECTION 1: Identification of the substance/mixture and of the company/undertaking

1.1. Product identifier

Product name	:	Sodium chloride
SDS-number	:	000000020255
Type of product	:	Substance
Remarks	:	Document according to Art. 32 of Regulation (EC) 1907/2006.
Chemical name	:	Sodium chloride
CAS-No.	:	7647-14-5
REACH Registration Number	:	no data available

1.2. Relevant identified uses of the substance or mixture and uses advised against

Use of the Substance/Mixture	:	Laboratory chemicals
Uses advised against	:	none

1.3. Details of the supplier of the safety data sheet

Company	:	Honeywell Specialty Chemicals Seelze GmbH Wunstorfer Straße 40 30926 Seelze Germany	Honeywell International, Inc. 115 Tabor Road Morris Plains, NJ 07950-2546 USA
Telephone	:	(49) 5137-999 0	
For further information, please contact:	:	SafetyDataSheet@Honeywell.com	

1.4. Emergency telephone number

Emergency telephone number	:	+1-703-527-3887 (ChemTrec-Transport) +1-303-389-1414 (Medical)

: Poison Control Center:
United Kingdom: (+44) 844 892 0111

SECTION 2: Hazards identification

2.1. Classification of the substance or mixture

REGULATION (EC) No 1272/2008

Not a hazardous substance or mixture according to Regulation (EC) No. 1272/2008.

2.2. Label elements

REGULATION (EC) No 1272/2008

Not a hazardous substance or mixture according to Regulation (EC) No. 1272/2008.

2.3. Other hazards

None known. The substance/mixture does not contain components considered to have endocrine disrupting properties according to REACH Article 57(f) or Commission Delegated regulation (EU) 2017/2100 or Commission Regulation (EU) 2018/605 at levels of 0.1% or higher. This substance/mixture contains no components considered to be either persistent, bioaccumulative and toxic (PBT), or very persistent and very bioaccumulative (vPvB) at levels of 0.1% or higher.

SECTION 3: Composition/information on ingredients

3.1. Substances

Chemical name	CAS-No. Index-No. REACH Registration Number EC-No.	Classification 1272/2008	Concentration	Remarks
Sodium chloride	7647-14-5 231-598-3		100 %	N.C.*

N.C.* - Non-hazardous substance - for information only

3.2. Mixtures
Not applicable

Occupational Exposure Limit(s), if available, are listed in Section 8.
For the full text of the H-Statements mentioned in this Section, see Section 16.

SECTION 4: First aid measures

4.1 Description of first aid measures

General advice:
First aider needs to protect himself.

Inhalation:
Remove to fresh air. If breathing is difficult, give oxygen. Use oxygen as required, provided a qualified operator is present. Call a physician.

Skin contact:
Wash off with plenty of water. Remove and wash contaminated clothing before re-use. Call a physician if irritation develops or persists.

Eye contact:
Rinse immediately with plenty of water, also under the eyelids, for at least 15 minutes. Call a physician if irritation develops or persists.

Ingestion:
Do not induce vomiting without medical advice. Never give anything by mouth to an unconscious person. If victim is fully conscious, give a cupful of water. Call a physician.

4.2. Most important symptoms and effects, both acute and delayed

No data available

4.3. Indication of any immediate medical attention and special treatment needed

Treat symptomatically.

See Section 11 for more detailed information on health effects and symptoms. :

SECTION 5: Firefighting measures

5.1. Extinguishing media

Suitable extinguishing media:
Water spray
Foam
Carbon dioxide (CO2)
Dry powder

Extinguishing media which shall not be used for safety reasons:
High volume water jet

5.2. Special hazards arising from the substance or mixture

The product is not flammable.

5.3. Advice for firefighters

Wear self-contained breathing apparatus and protective suit.
Use extinguishing measures that are appropriate to local circumstances and the surrounding environment.

SECTION 6: Accidental release measures

6.1. Personal precautions, protective equipment and emergency procedures

Wear personal protective equipment. Evacuate personnel to safe areas. Ensure adequate ventilation. Avoid dust formation. Avoid breathing dust. Avoid contact with skin, eyes and clothing.

6.2. Environmental precautions

Prevent further leakage or spillage if safe to do so. Discharge into the environment must be avoided. Do not flush into surface water or sanitary sewer system.

6.3. Methods and materials for containment and cleaning up

Use mechanical handling equipment.
Pick for disposal in tightly closed containers

6.4. Reference to other sections

For personal protection see section 8.

SECTION 7: Handling and storage

7.1. Precautions for safe handling

Advice on safe handling:
Wear personal protective equipment. Use only in well-ventilated areas. Avoid dust formation. Avoid breathing dust.

Advice on protection against fire and explosion:
Normal measures for preventive fire protection.

Hygiene measures:
When using, do not eat, drink or smoke. Wash hands before breaks and at the end of workday. Keep working clothes separately. Remove and wash contaminated clothing before re-use.

7.2. Conditions for safe storage, including any incompatibilities

Further information on storage conditions:
Store in original container. Keep in a dry place.

7.3. Specific end use(s)

no additional data available

SECTION 8: Exposure controls/personal protection

8.1. Control parameters

Components with workplace control parameters

Contains no substances with occupational exposure limit values.

DNEL/ PNEC-Values

Component	End-use/impact	Exposure duration	Value	Exposure routes	Remarks
Sodium chloride	Workers /		2068,62	Inhalation	

	Long-term systemic effects		mg/m3		
Sodium chloride	Workers / Acute systemic effects		2068,62 mg/m3	Inhalation	
Sodium chloride	Workers / Long-term systemic effects		295,52mg/kg bw/d	Skin contact	
Sodium chloride	Workers / Acute systemic effects		295,52mg/kg bw/d	Skin contact	
Sodium chloride	Consumers / Long-term systemic effects		443,28 mg/m3	Inhalation	
Sodium chloride	Consumers / Acute systemic effects		443,28 mg/m3	Inhalation	
Sodium chloride	Consumers / Long-term systemic effects		126,65mg/kg bw/d	Skin contact	
Sodium chloride	Consumers / Acute systemic effects		126,65mg/kg bw/d	Skin contact	
Sodium chloride	Consumers / Long-term systemic effects		126,65mg/kg bw/d	Ingestion	
Sodium chloride	Consumers / Acute systemic effects		126,65mg/kg bw/d	Ingestion	

Component	Environmental compartment / Value	Remarks
Sodium chloride	Fresh water: 5 mg/l	Assessment factor: 50
Sodium chloride	Sewage treatment plant: 500 mg/l	Assessment factor: 10
Sodium chloride	Soil: 4,86 mg/kg dw	Assessment factor: 50

8.2. Exposure controls

Occupational exposure controls

The Personal Protective Equipment must be in accordance with EN standards:respirator EN 136, 140, 149; safety glasses EN 166; protective suit: EN 340, 463, 468, 943-1, 943-2; gloves EN 374, 511; safety shoes EN-ISO 20345.

Personal protective equipment
Respiratory protection:
Recommended Filter type:
P1
In the case of dust or aerosol formation use respirator with an approved filter.
Recommended Filter type:
Particulates type

Hand protection:
Glove material: Natural Latex
Break through time: > 480 min
Glove thickness: 0,6 mm
Lapren®706
Gloves must be inspected prior to use.
Replace when worn.

Remarks:Supplementary note: The specifications are based on information and tests from similar substances by analogy.
Due to varying conditions (e.g.temperature or other strains) it must be considered that the usage of a chemical protective glove in practice may be much shorter than the permeation time determined in accordance with EN 374.
Since actual conditions of practical use often deviate from standardised conditions according EN 374 the glove manufacturer reccomends to use the chemical protective glove in practice not longer than 50% of the recomended permeation time.
Manufacturer´s directions for use should be observed because of great diversity of types .
Suitable gloves tested according EN 374 are supplied e.g. from KCL GmbH, D-36124 Eichenzell, Vertrieb@kcl.de

Eye protection:
Safety glasses with side-shields

Skin and body protection:
Lightweight protective clothing

Environmental exposure controls

Handle in accordance with local environmental regulations and good industrial practices.

SECTION 9: Physical and chemical properties

9.1. Information on basic physical and chemical properties

(a) Physical state	:	solid
(b) Colour	:	colourless
(c) Odour	:	odourless
(d) Melting point/freezing point	:	800 °C
(e) Boiling point/boiling range	:	1.465 °C at 1.013 hPa
(f) Flammability	:	The product is not flammable.
(g) Lower and upper explosion limit	:	Lower explosion limit Not applicable

	:	Upper explosion limit Not applicable
(h) Flash point	:	Not applicable
(i) Auto-ignition temperature	:	Not applicable not auto-flammable
(j) Decomposition temperature	:	No decomposition if used as directed.
(k) pH	:	7,0 at 20 °C
(l) Viscosity, kinematic	:	No data available
(m) Solubility(ies)	:	Water solubility: 358 g/l at 20 °C
(n) Partition coefficient: n-octanol/water	:	No data available
(o) Vapour pressure	:	No data available
(p) Density and / or relative density	:	ca. 2,160 g/cm3 at 20 °C
(q) Bulk density	:	ca. 1.260 kg/m3
(q) Relative vapour density	:	No data available
(r) Particle characteristics	:	No data available

9.2 Other Information

Oxidizing properties	:	The substance or mixture is not classified as oxidizing.
Evaporation rate	:	No data available

Viscosity, dynamic : No data available

SECTION 10: Stability and reactivity

10.1. Reactivity

Stable under normal conditions.

10.2. Chemical stability

No decomposition if used as directed.

10.3. Possibility of hazardous reactions

Hazardous polymerisation does not occur.

10.4. Conditions to avoid

Protect from atmospheric moisture and water.

10.5. Incompatible materials

None.

10.6. Hazardous decomposition products

None known.

SECTION 11: Toxicological information

11.1. Information on hazard classes as defined in Regulation (EC) No 1272/2008

(a) Acute toxicity

Acute oral toxicity:
LD50
Species: Rat
Value: 3.550 mg/kg

Acute dermal toxicity:
No data available

Acute inhalation toxicity:
No data available

Acute toxicity (other routes of administration):
No data available

(b) Skin corrosion/irritation:
Species: Rabbit
Result: No skin irritation

(c) Serious eye damage/eye irritation:
No data available

(d) Respiratory or skin sensitisation:
No data available

(h) STOT-single exposure:
Assessment: The substance or mixture is not classified as specific target organ toxicant, single exposure.

(i) STOT - repeated exposure:
No data available
STOT - repeated exposure:
Assessment: The substance or mixture is not classified as specific target organ toxicant, repeated exposure.

(j) Aspiration hazard:
No data available

11.2. Information on other hazards

Endocrine disrupting properties
The substance/mixture does not contain components considered to have endocrine disrupting properties according to REACH Article 57(f) or Commission Delegated regulation (EU) 2017/2100 or Commission Regulation (EU) 2018/605 at levels of 0.1% or higher.

Other information:
No data available

SECTION 12: Ecological information

12.1. Toxicity

Toxicity to fish:
LC50
flow-through test
Species: Lepomis macrochirus (Bluegill sunfish)
Value: 5.840 mg/l
Exposure time: 96 h

NOEC
flow-through test
Species: Pimephales promelas (fathead minnow)
Value: 252 mg/l
Exposure time: 33 d
Method: OECD

Toxicity to aquatic plants:
EC50
Species: Algae
Value: 2.430 mg/l
Exposure time: 120 h
Method: OECD Test Guideline 201

Toxicity to aquatic invertebrates:
LC50
static test
Species: Daphnia magna (Water flea)
Value: 4.136 mg/l
Exposure time: 48 h
Method: OECD Test Guideline 202

Chronic toxicity to aquatic invertebrates:
NOEC
semi-static test
Species: Daphnia pulex (Water flea)
Value: 314 mg/l
Exposure time: 21 d
Method: OECD Test Guideline 211

12.2. Persistence and degradability

Biodegradability:
The methods for determining biodegradability are not applicable to inorganic substances.

12.3. Bioaccumulative potential

No data available

12.4. Mobility in soil

No data available

12.5. Results of PBT and vPvB assessment

Substance is not persistent, bioaccumulative, and toxic (PBT).
Substance is not very persistent and very bioaccumulative (vPvB).

12.6. Endocrine disrupting properties

The substance/mixture does not contain components considered to have endocrine disrupting properties according to REACH Article 57(f) or Commission Delegated regulation (EU) 2017/2100 or Commission Regulation (EU) 2018/605 at levels of 0.1% or higher.

12.7. Other adverse effects

No data available

SECTION 13: Disposal considerations

13.1. Waste treatment methods

Product:
Dispose according to legal requirements.

Packaging:
Legal requirements are to be considered in regard of reuse or disposal of used packaging materials

Further information:
Provisions relating to waste:
EC Directive 2006/12/EC; 2008/98/EEC
Regulation No. 1013/2006
For personal protection see section 8.

SECTION 14: Transport information

14.1 UN number or ID number

ADR/RID:Not dangerous goods IMDG:Not dangerous goods IATA:Not dangerous goods

14.2 UN proper shipping name
ADR/RID:Not dangerous goods
IMDG:Not dangerous goods
IATA:Not dangerous goods

14.3 Transport hazard class(es)
No data available

14.4 Packaging group
No data available

14.5 Environmental hazards
ADR/RID:no Marine pollutant: no

14.6 Special precautions for user
No data available

14.7 Maritime transport in bulk according to IMO instruments
No data available

SECTION 15: Regulatory information

15.1 Safety, health and environmental regulations/legislation specific for the substance or mixture

Basis	Value	Remarks
Directive 2012/18/EC SEVESO III		Not applicable
Substances of very high concern (SVHC)		This product does not contain substances of very high concern according to Regulation (EC) No Article 57 above the respective regulatory 1907/2006 (REACH), concentration limit of ≥ 0.1 % (w/w).

Other inventory information

USA. List of Active Substances on the Toxic Substances Control Act (TSCA) Chemical Substances Inventory, as amended

On TSCA Inventory

Australia. Inventory of Industrial Chemicals (AIIC), as amended
On the inventory, or in compliance with the inventory

Canada. Domestic Substances List (DSL), as amended
All components of this product are on the Canadian DSL

Japan. Kashin-Hou Law List
On the inventory, or in compliance with the inventory

Korea. Existing Chemicals Inventory (KECI)
On the inventory, or in compliance with the inventory

Philippines. Inventory of Chemicals and Chemical Substances (PICCS)
On the inventory, or in compliance with the inventory

China. Inventory of Existing Chemical Substances (IECSC)
On the inventory, or in compliance with the inventory

New Zealand. Inventory of Chemicals (NZIoC), as published by ERMA New Zealand
On the inventory, or in compliance with the inventory

Taiwan Chemical Substance Inventory (TCSI)
On the inventory, or in compliance with the inventory

15.2 Chemical safety assessment

A Chemical Safety Assessment has not been carried out.

SECTION 16: Other information

Further information

All directives and regulations refer to amended versions.
Vertical lines in the left hand margin indicate a relevant amendment from the previous version.

Abbreviations:
EC European Community
CAS Chemical Abstracts Service
DNEL Derived no effect level
PNEC Predicted no effect level

vPvB Very persistent and very biaccumulative substance
PBT Persistent, bioaccmulative und toxic substance

The information provided in this Safety Data Sheet is correct to the best of our knowledge, information and belief at the date of its publication. The information given is designed only as a guidance for safe handling, use, processing, storage, transportation, disposal and release and is not to be considered a warranty or quality specification. The information relates only to the specific material designated and may not be valid for such material used in combination with any other materials or in any process, unless specified in the text. Final determination of suitability of any material is the sole responsibility of the user.
This information should not constitute a guarantee for any specific product properties.

Honeywell Fluka™

Sodium hydroxide

30620-1KG

Version 1.6 Revision Date 12.11.2023

SECTION 1: Identification of the substance/mixture and of the company/undertaking

1.1. Product identifier

Product name	:	Sodium hydroxide
SDS-number	:	000000020688
Type of product	:	Substance
Remarks	:	SDS according to Art. 31 of Regulation (EC) 1907/2006.
Chemical name	:	Sodium hydroxide
Index-No.	:	011-002-00-6
REACH Registration Number	:	no data available

1.2. Relevant identified uses of the substance or mixture and uses advised against

Use of the Substance/Mixture	:	Laboratory chemicals
Uses advised against	:	none

1.3. Details of the supplier of the safety data sheet

Company	:	Honeywell Specialty Chemicals Seelze GmbH Wunstorfer Straße 40 30926 Seelze Germany	Honeywell International, Inc. 115 Tabor Road Morris Plains, NJ 07950-2546 USA
Telephone	:	(49) 5137-999 0	
For further information, please contact:	:	PMTEU Product Stewardship: SafetyDataSheet@Honeywell.com	

1.4. Emergency telephone number

Emergency telephone number	:	+1-703-527-3887 (ChemTrec-Transport) +1-303-389-1414 (Medical)

: Poison Control Center:
United Kingdom: (+44) 844 892 0111

SECTION 2: Hazards identification

2.1. Classification of the substance or mixture

REGULATION (EC) No 1272/2008

Corrosive to metals Category 1
H290 May be corrosive to metals.
Skin corrosion Category 1A
H314 Causes severe skin burns and eye damage.

2.2. Label elements

REGULATION (EC) No 1272/2008

Hazard pictograms :

Signal word : Danger

Hazard statements :	H290	May be corrosive to metals.
	H314	Causes severe skin burns and eye damage.
Precautionary statements :	P260	Do not breathe dust/ fume/ gas/ mist/ vapours/ spray.
	P280	Wear protective gloves/protective clothing/eye protection/face protection.
	P301 + P330 + P331	IF SWALLOWED: Rinse mouth. Do NOT induce vomiting.
	P302 + P352	IF ON SKIN: Wash with plenty of water.
	P304 + P340	IF INHALED: Remove person to fresh air and keep comfortable for breathing.
	P305 + P351 + P338	IF IN EYES: Rinse cautiously with water for several minutes. Remove contact lenses, if present and easy to do. Continue rinsing.
	P308 + P313	IF exposed or concerned: Get medical advice/ attention.

2.3. Other hazards

Extremely corrosive and destructive to tissue. Results of PBT and vPvB assessment, see chapter 12.5. The substance/mixture does not contain components considered to have endocrine disrupting properties according to REACH Article 57(f) or Commission Delegated regulation (EU) 2017/2100 or Commission Regulation (EU) 2018/605 at levels of 0.1% or higher.

SECTION 3: Composition/information on ingredients

3.1. Substances

Chemical name	CAS-No. Index-No. REACH Registration Number EC-No.	Classification 1272/2008	Concentration	Remarks
Sodium hydroxide	1310-73-2 011-002-00-6 215-185-5	Met. Corr. 1; H290 Skin Corr. 1A; H314	100 %	Skin Corr. 1A; H314:>= 5 % Skin Corr. 1B; H314:2 - < 5 % Eye Irrit. 2; H319:0,5 - < 2 % Skin Irrit. 2; H315:0,5 - < 2 %

3.2. Mixtures
Not applicable

Occupational Exposure Limit(s), if available, are listed in Section 8.
For the full text of the H-Statements mentioned in this Section, see Section 16.

SECTION 4: First aid measures

4.1 Description of first aid measures

General advice:
First aider needs to protect himself. Take off all contaminated clothing immediately.

Inhalation:
Remove to fresh air. If breathing is difficult, give oxygen. Use oxygen as required, provided a qualified operator is present. Call a physician immediately.

Skin contact:
Wash off immediately with plenty of water for at least 15 minutes. Take off contaminated clothing and shoes immediately. Wash contaminated clothing before re-use. Call a physician immediately.

Eye contact:
Rinse immediately with plenty of water, also under the eyelids, for at least 15 minutes. Protect unharmed eye. Call a physician immediately.

Ingestion:
When swallowed, allow water to be drunk. Do NOT induce vomiting. Call a physician immediately.

4.2. Most important symptoms and effects, both acute and delayed

No data available

4.3. Indication of any immediate medical attention and special treatment needed

Treat symptomatically.

See Section 11 for more detailed information on health effects and symptoms. :

SECTION 5: Firefighting measures

5.1. Extinguishing media

Suitable extinguishing media:
Water spray
Foam
Carbon dioxide (CO2)
Dry powder

Extinguishing media which shall not be used for safety reasons:
High volume water jet

5.2. Special hazards arising from the substance or mixture

The product is not flammable.
Contact with metals liberates hydrogen gas.
Fire may cause evolution of:
Sodium oxides

5.3. Advice for firefighters

Wear self-contained breathing apparatus and protective suit.
Use extinguishing measures that are appropriate to local circumstances and the surrounding environment.In wet solutions watch out for etching influence.The product itself does not burn.

SECTION 6: Accidental release measures

6.1. Personal precautions, protective equipment and emergency procedures

Wear personal protective equipment. Unprotected persons must be kept away. Evacuate personnel to safe areas. Keep people away from and upwind of spill/leak. Ensure adequate ventilation. Do not get in eyes, on skin, or on clothing.

6.2. Environmental precautions

Prevent further leakage or spillage if safe to do so. Discharge into the environment must be avoided. Do not flush into surface water or sanitary sewer system. Do not allow run-off from fire fighting to enter drains or water courses.

6.3. Methods and materials for containment and cleaning up

Use mechanical handling equipment.
Pick for disposal in tightly closed containers
Personal protection through wearing a tightly closed chemical protection suit and a self-contained breathing apparatus.

6.4. Reference to other sections

For personal protection see section 8.

SECTION 7: Handling and storage

7.1. Precautions for safe handling

Advice on safe handling:
Exhaust ventilation at the object is necessary. Wear personal protective equipment. Use only alkali-proof equipment. When diluting, always stir product into water.

Advice on protection against fire and explosion:
Normal measures for preventive fire protection.

Hygiene measures:
Take off all contaminated clothing immediately. Remove and wash contaminated clothing before re-use. Keep working clothes separately. When using, do not eat, drink or smoke. Wash hands before breaks and immediately after handling the product.

7.2. Conditions for safe storage, including any incompatibilities

Further information on storage conditions:
Store in original container. Keep containers tightly closed in a dry, cool and well-ventilated place. Protect from atmospheric moisture and water. Product is hygroscopic.

7.3. Specific end use(s)

no additional data available

SECTION 8: Exposure controls/personal protection

8.1. Control parameters

Occupational exposure limits:

Components	Basis / Value type	Value / Form of exposure	Exceeding Factor	Remarks
Sodium hydroxide	EH40 WEL STEL	2 mg/m3		
Sodium hydroxide	EH40 WEL			Listed

EH40 WEL - UK. EH40 Workplace Exposure Limits (WELs), as amended
STEL - Short term exposure limit
EH40 WEL - UK. EH40 Workplace Exposure Limits (WELs), as amended
-

DNEL/ PNEC-Values

Component	End-use/impact	Exposure duration	Value	Exposure routes	Remarks
Sodium hydroxide	Workers / Long-term local effects		1 mg/m3	Inhalation	
Sodium hydroxide	Consumers / Long-term local effects		1 mg/m3	Inhalation	

No PNEC data available.

8.2. Exposure controls

Occupational exposure controls

The Personal Protective Equipment must be in accordance with EN standards:respirator EN 136, 140, 149; safety glasses EN 166; protective suit: EN 340, 463, 468, 943-1, 943-2; gloves EN 374, 511; safety shoes EN-ISO 20345.
Do not breathe dust.

Engineering measures
Use with local exhaust ventilation.
Emergency sprinkling nozzle

Personal protective equipment
Respiratory protection:
In the case of dust or aerosol formation use respirator with an approved filter.

Hand protection:
Glove material: Natural Latex
Break through time: > 480 min
Glove thickness: 0,6 mm
Lapren®706
Gloves must be inspected prior to use.
Replace when worn.
Remarks:Supplementary note: The specifications are based on information and tests from similar substances by analogy.
Due to varying conditions (e.g.temperature or other strains) it must be considered that the usage of a chemical protective glove in practice may be much shorter than the permeation time determined in accordance with EN 374.
Since actual conditions of practical use often deviate from standardised conditions according EN 374 the glove manufacturer reccomends to use the chemical protective glove in practice not longer than 50% of the recomended permeation time.
Manufacturer´s directions for use should be observed because of great diversity of types .
Suitable gloves tested according EN 374 are supplied e.g. from KCL GmbH, D-36124 Eichenzell, Vertrieb@kcl.de

Eye protection:
Safety goggles
Face-shield

Skin and body protection:
Complete suit protecting against chemicals

Environmental exposure controls

Handle in accordance with local environmental regulations and good industrial practices.

SECTION 9: Physical and chemical properties

9.1. Information on basic physical and chemical properties

(a) Physical state	:	solid
(b) Colour	:	colourless
(c) Odour	:	odourless
(d) Melting point/freezing point	:	319 °C
(e) Boiling point/boiling range	:	1.390 °C at 1.013 hPa
(f) Flammability	:	The product is not flammable.
(g) Lower and upper explosion limit	:	Lower explosion limit Not applicable
	:	Upper explosion limit Not applicable
(h) Flash point	:	Not applicable
(i) Auto-ignition temperature	:	Not applicable
(j) Decomposition temperature	:	No decomposition if used as directed.
(k) pH	:	alkaline
(l) Viscosity, kinematic	:	No data available
(m) Solubility(ies)	:	Water solubility: completely soluble

		Solubility in other solvents: No data available
(n) Partition coefficient: n-octanol/water	:	No data available
(o) Vapour pressure	:	No data available
(p) Density and / or relative density	:	2,13 g/cm3 at 20 °C
(q) Bulk density	:	No data available
(q) Relative vapour density	:	No data available
(r) Particle characteristics	:	No data available

9.2 Other Information

Oxidizing properties	:	The substance or mixture is not classified as oxidizing.
Corrosive to metals	:	Corrosive to metals
Evaporation rate	:	No data available
Viscosity, dynamic	:	No data available

SECTION 10: Stability and reactivity

10.1. Reactivity

Stable under normal conditions.

10.2. Chemical stability

No decomposition if used as directed.

10.3. Possibility of hazardous reactions

Possible incompatibility with alkali sensitive materials.
With acid and aluminium.
Reacts violently with water.
Corrosive in contact with metals

10.4. Conditions to avoid

Corrodes metals in the presence of water or moisture.
Protect from moisture.

10.5. Incompatible materials

Zinc
Aluminium
Tin
Gives off hydrogen by reaction with metals.
Exothermic reaction with water.
Exothermic reaction with strong acids.

10.6. Hazardous decomposition products

Sodium oxides

SECTION 11: Toxicological information

11.1. Information on hazard classes as defined in Regulation (EC) No 1272/2008

(a) Acute toxicity

Acute oral toxicity:
Toxicity is determined by the corrosivity of the product.

Acute dermal toxicity:
Toxicity is determined by the corrosivity of the product.

Acute inhalation toxicity:
Toxicity is determined by the corrosivity of the product.

Acute toxicity (other routes of administration):
No data available

(b) Skin corrosion/irritation:

Classification based on Annex VI of regulation 1272/2008/EC.

(c) Serious eye damage/eye irritation:
Classification based on Annex VI of regulation 1272/2008/EC.

(d) Respiratory or skin sensitisation:
Species: human
Classification: non-sensitizing

(e) Germ cell mutagenicity:
Note: No data available

(f) Carcinogenicity:
Species: not specified
Note: No data available

(g) Reproductive toxicity:
Species: not specified
Remarks: No data available

(h) STOT-single exposure:
Remarks: No data available

(i) STOT - repeated exposure:
Note: No data available
STOT - repeated exposure:
Remarks: No data available

(j) Aspiration hazard:
No data available

11.2. Information on other hazards

Endocrine disrupting properties
The substance/mixture does not contain components considered to have endocrine disrupting properties according to REACH Article 57(f) or Commission Delegated regulation (EU) 2017/2100 or Commission Regulation (EU) 2018/605 at levels of 0.1% or higher.

Other information:
No data available

SECTION 12: Ecological information

12.1. Toxicity

Toxicity to fish:
No data available

Toxicity to aquatic plants:
No data available

Toxicity to aquatic invertebrates:
EC50
Immobilization
Species: Ceriodaphnia spec
Value: 40,4 mg/l
Exposure time: 48 h

12.2. Persistence and degradability

Biodegradability:
The methods for determining the biological degradability are not applicable to inorganic substances.

12.3. Bioaccumulative potential

No data available

12.4. Mobility in soil

No data available

12.5. Results of PBT and vPvB assessment

No data available

12.6. Endocrine disrupting properties

The substance/mixture does not contain components considered to have endocrine disrupting properties according to REACH Article 57(f) or Commission Delegated regulation (EU) 2017/2100 or Commission Regulation (EU) 2018/605 at levels of 0.1% or higher.

12.7. Other adverse effects

Should not be released into the environment.
If it is not neutralised, observe pH value.
Neutralisation will reduce ecotoxic effects.

SECTION 13: Disposal considerations

13.1. Waste treatment methods

Product:
Dispose according to legal requirements.

Packaging:
Legal requirements are to be considered in regard of reuse or disposal of used packaging materials

Further information:
Provisions relating to waste:
EC Directive 2006/12/EC; 2008/98/EEC
Regulation No. 1013/2006
For personal protection see section 8.

SECTION 14: Transport information

14.1 UN number or ID number
ADR/RID:1823 IMDG:1823 IATA:1823

14.2 UN proper shipping name
ADR/RID:SODIUM HYDROXIDE, SOLID
IMDG:SODIUM HYDROXIDE, SOLID
IATA:Sodium hydroxide, solid

14.3 Transport hazard class(es)
ADR/RID:8 IMDG: 8 IATA: 8

14.4 Packaging group
ADR/RID:II IMDG: II IATA: II

14.5 Environmental hazards
ADR/RID:no Marine pollutant: no

14.6 Special precautions for user
IMDG Code segregation group (SGG18) – ALKALIS,

14.7 Maritime transport in bulk according to IMO instruments
No data available

SECTION 15: Regulatory information

15.1 Safety, health and environmental regulations/legislation specific for the substance or mixture

Basis	Value	Remarks
Directive 2012/18/EC		Not applicable
Substances of very high concern (SVHC)		This product does not contain substances of very high concern according to Regulation (EC) No Article 57 above the respective regulatory 1907/2006 (REACH), concentration limit of ≥ 0.1 % (w/w).
Regulation (EC) No. 1907/2006, Annex XIV		Not listed

Other inventory information

US. Toxic Substances Control Act
On TSCA Inventory

Australia. Inventory of Industrial Chemicals (AIIC), as amended
On the inventory, or in compliance with the inventory

Canada. Canadian Environmental Protection Act (CEPA). Domestic Substances List (DSL)
All components of this product are on the Canadian DSL

Japan. Kashin-Hou Law List
On the inventory, or in compliance with the inventory

Korea. Existing Chemicals Inventory (KECI)
On the inventory, or in compliance with the inventory

Philippines. Inventory of Chemicals and Chemical Substances (PICCS)
On the inventory, or in compliance with the inventory

China. Inventory of Existing Chemical Substances (IECSC)
On the inventory, or in compliance with the inventory

New Zealand. Inventory of Chemicals (NZIoC), as published by ERMA New Zealand
On the inventory, or in compliance with the inventory

Taiwan Chemical Substance Inventory (TCSI)
On the inventory, or in compliance with the inventory

15.2 Chemical safety assessment

A Chemical Safety Assessment has not been carried out.

SECTION 16: Other information

Text of H-statements referred to under heading 3

Sodium hydroxide	:	H290	May be corrosive to metals.
		H314	Causes severe skin burns and eye damage.

Further information

All directives and regulations refer to amended versions.
Vertical lines in the left hand margin indicate a relevant amendment from the previous version.

Abbreviations:
EC European Community
CAS Chemical Abstracts Service
DNEL Derived no effect level
PNEC Predicted no effect level
vPvB Very persistent and very biaccumulative substance
PBT Persistent, bioaccmulative und toxic substance

The information provided in this Safety Data Sheet is correct to the best of our knowledge, information and belief at the date of its publication. The information given is designed only as a guidance for safe handling, use, processing, storage, transportation, disposal and release and is not to be considered a warranty or quality specification. The information relates only to the specific material designated and may not be valid for such material used in combination with any other

materials or in any process, unless specified in the text. Final determination of suitability of any material is the sole responsibility of the user.
This information should not constitute a guarantee for any specific product properties.

Appendix E

Conference Presentations

This work was previously presented and well received at the following international fora:

i. American Society of Civil Engineers ASCE Engineering Mechanics Institute EMI 2023 International Conference, Palermo, Italy, 27th - 30th August, 2023.
ii. CircularB European Project Workshop COST Action: CA21103 - Implementation of Circular Economy in the Built Environment, Córdoba, Spain, 12th - 14th September, 2023.
iii. Concrete Sustainability: Materials and Structures International Concrete Conference - Structures of Tomorrow, Valletta Campus of the University of Malta, 21st November, 2023.

The work was also presented on the Sunday Times of Malta, and on a local radio station, *Radju Malta*.

iv. Sunday Times of Malta article "Creating a circular economy in construction and agriculture" published on 1st October, 2023. (Online Version: https://timesofmalta.com/article/creating-circular-economy-construction-agriculture.1058067). Accessed on 5th April, 2024.
v. Radio Mocha Malta radio programme, aired on 12th October at 2:30 pm on *Radju Malta*.